2004

Monitored natural attenuation at a coal-tar impacted aquifer in Northwestern Iowa: coupled biogeochemical and molecular microbiological approaches for establishing secondary and tertiary lines of evidence

Shane William Rogers

Iowa State University

Monitored natural attenuation at a coal-tar impacted aquifer in Northwestern Iowa:

coupled biogeochemical and molecular microbiological approaches for establishing

secondary and tertiary lines of evidence

by

Shane William Rogers

A dissertation submitted to the graduate faculty

in partial fulfillment of the requirements for the degree of

DOCTOR OF PHILOSOPHY

Major: Civil Engineering (Environmental Engineering)

Program of Study Committee:
Say Kee Ong, Co-Major Professor
Bruce Kjartanson, Co-Major Professor
Thomas Moorman
Johanshir Golchin
Jiasong Fang

Iowa State University
Ames, Iowa
2004

UMI Number: 3145679

INFORMATION TO USERS

The quality of this reproduction is dependent upon the quality of the copy submitted. Broken or indistinct print, colored or poor quality illustrations and photographs, print bleed-through, substandard margins, and improper alignment can adversely affect reproduction.

In the unlikely event that the author did not send a complete manuscript and there are missing pages, these will be noted. Also, if unauthorized copyright material had to be removed, a note will indicate the deletion.

UMI®

UMI Microform 3145679

Copyright 2004 by ProQuest Information and Learning Company.

All rights reserved. This microform edition is protected against unauthorized copying under Title 17, United States Code.

Graduate College
Iowa State University

This is to certify that the doctoral dissertation of

Shane William Rogers

has met the dissertation requirements of Iowa State University

Signature was redacted for privacy.

Co-Major Professor

Signature was redacted for privacy.

Co-Major Professor

Signature was redacted for privacy.

For the Major Program

For my partner in life, JoAnn, who amazes me with her love and support
My oldest son, Jordan, for saving me countless times and pretending like it wasn't a big deal
My little buddy, Nathaniel, for your tears when you missed me and your hugs when I came home
And my little princess, Cassie, for the songs you sang to me on my morning rides to school

TABLE OF CONTENTS

LIST OF FIGURES

LIST OF TABLES

ACKNOWLEDGEMENTS

There are several people to whom I owe a debt of gratitude for this work. First and foremost is Dr. Say Kee Ong, who invested an incredible amount of time and effort into providing me a unique and rewarding graduate experience. He challenged me to think critically, maintained faith in my abilities, allowed me to work outside the box, and inspired me to continually reach for higher goals. Second is Dr. Thomas Moorman, who opened his laboratory and offered his expertise to a strange engineer with big ideas about microbiology. This work would be entirely impossible without his invaluable guidance. I would also like to thank Elizabeth Douglass, who taught me more about proper laboratory practices and microbiological techniques than any graduate course could ever hope to. I will always remember her warm heart and her ability to make long days in the laboratory bearable. I look forward to the long and lasting friendships I will have with these people.

I relied heavily on the use of several laboratory facilities to complete this work. Jen Anhalt, Sheri Steadham, Dr. Cherie Ziemer, and Dr. Steve Trabue at the USDA-ARS Swine Research Center provided free and virtually unlimited access to their facilities including endless hours on their fluorescence microscope and the key to their digital imaging software. Tracey Pepper, Randall Den Adel, and Dr. Harry Horner of the Bessey Microscopy Facility provided support for the microautoradiography work including access to a very dark room, a fluorescence microscope, and digital imaging software. Most of the laboratory work was performed at the USDA-ARS National Soil Tilth Laboratory. The scientists and support staff at this facility took me in and made me one of their own during my doctoral research. No matter how busy these people were, they always made time to give me help when I needed it and made sure I never had a need go unanswered. All of the people at these three laboratories provided valuable techniques and guidance for strengthening my work, moral support in my research seminars, advice in my job search process, and dear friendships. I find the willingness of these scientists to open their facilities and their hearts to young researchers amazing.

I also feel grateful to have had the opportunity to work alongside several outstanding graduate students, professors, and post-doctoral researchers within my research group. I appreciate the support I received from Dr. Bruce Kjartanson and Dr. Johanshir Golchin, who worked hard to maintain funding from several energy companies for my project and never questioned my requests for additional supplies or equipment. Although I was their student, they always made me feel like a colleague. I could always rely on Dr. Greg Stenback for help in data analysis, modeling, and providing a quick and thorough review of my work. I enjoyed working on manuscripts with him and mutually challenging each other to achieve a higher level of understanding. I met several outstanding

graduate students during my tenure and was blessed to make friends with people from almost every continent. Among my most memorable experiences are freezing my tail off trying to thaw water lines while groundwater sampling in the dead of the Iowa winter, playing cribbage at the bar in Dubuque with Nick Miller in the evenings on sampling events, cursing groundwater models late at night with Rahul Biyani, monitoring well 2B (which always had a wasp nest in the summer), setting up endless bioassays with Insoo Joo, working glorious 36 hour shifts in the lab with Angie Kolz, and lighting contaminated groundwater bailed from monitoring well PMW2 on fire.

ABSTRACT

Coal-tar contamination resulting from former manufactured gas plant (FMGP) operations pervades the shallow aquifer underlying a small area south of downtown Cherokee, Iowa. Monitored natural attenuation (MNA) is of interest for remediating this contaminated aquifer system. However, it is a complex process to identify intrinsic biodegradation of specific polycyclic aromatic hydrocarbons (PAHs) at contaminated FMGP sites because several hundred potential substrates comprise coal-tar mixtures. Microbial activity on non-PAH carbon sources may give rise to plume-scale biogeochemical responses that indicate biodegradation activity. Incubations with site sediments may poorly reflect intrinsic conditions. Molecular microbiological techniques coupling whole-cell hybridizations and microautoradiography (MICRO-FISH) are used to identify PAH-degrading bacteria in the coal-tar impacted site sediments and ascertain their intrinsic activity. These techniques are used to provide a link between plume-scale biogeochemical monitoring, fate and transport modeling, incubations with site sediments, and molecular characterizations of the intrinsic microbial community structure. Through this innovative approach, the potential for natural attenuation of specific PAHs in the contaminated aquifer are explored.

A superposition of 2-D reactive transport analytical solutions was used to estimate the best-fit first-order degradation rate coefficients for benzene (0.0084 d^{-1}), ethylbenzene (0.0076 d^{-1}), xylenes (0.0057 d^{-1}), naphthalene (0.0058 d^{-1}), 1-methylnaphthalene (0.0042 d^{-1}), acenaphthene (0.0011 d^{-1}), acenaphthylene (0.00069 d^{-1}), and fluorene (0.0058 d^{-1}). Contaminant mass transformation rates based on analytical modeling compared favorably to estimates based on depletion of terminal electron accepting compounds using a geochemical mass balance approach. Total DAPI-detected cell counts in the coal-tar source region reached 1.45 x 10^7 organisms per gram sediments, three orders of magnitude greater than that of non-affected sediments, suggesting active growth on the coal-tar constituents in situ. Whole-cell hybridizations with site sediments indicated that *Actinobacteria, γ-Proteobacteria, Bacteriodetes*, and *β-Proteobacteria* dominated the aerobic (>1 mg/L) in-situ microbial community structure. Sulfate-reducing bacteria were enriched in anaerobic environments exhibiting hydrogen sulfide production and oxidation-reduction potentials as low as -247 mV.

Mineralization of [UL-^{14}C]naphthalene in anaerobic nitrate- and sulfate-amended laboratory-scale incubations was observed in sediments corresponding to nitrate and sulfate-reducing aqueous geochemical environments exhibited in situ. Mineralization of [UL-^{14}C]naphthalene and [9-^{14}C]phenanthrene in anaerobic iron-amended incubations was also observed, but did not correlate well to aqueous geochemical indicators of iron-reduction. Aerobic incubations resulted in up to 61% mineralization of naphthalene and 42% mineralization of phenanthrene. Enrichment of *β-* and *γ-*

Proteobacteria in aerobic incubations implicated the activity of these phylotypes in PAH degradation. MICRO-FISH methods to track substrate uptake to specific microbial cell types were adapted for PAH uptake in coal-tar DNAPL contaminated sediments. MICRO-FISH confirmed the activity of β- and γ-*Proteobacteria* in aerobic incubations, but indicated that *Actinobacteria* were also active in the uptake of [9-^{14}C]phenanthrene, even though their populations declined in the microbial community.

MICRO-FISH was applied to several sediments from the coal-tar impacted aquifer, and established the activity of β-*Proteobacteria*, γ-*Proteobacteria*, and *Actinobacteria* in growth on both [9-^{14}C]phenanthrene and [UL-^{14}C]naphthalene. The presence of the β-*Proteobacteria* in the in situ microbial community structure was overshadowed by that of the *Actinobacteria* and γ-*Proteobacteria* indicating that the later two were the primary degraders of naphthalene and phenanthrene in situ. Cell-specific PAH biodegradation rates were calculated based on active bacterial populations (comprising less than 5% of the microbial community) and liquid scintillation counting of the washed biomass. Cell-specific naphthalene biodegradation rates based on MICRO-FISH (4.7 to 97 pg·active cell^{-1}·d^{-1}) compared favorably to estimates using the first-order degradation rate coefficient presented above (0.7 to 19 pg·active cell^{-1}·d^{-1}). Cell-specific phenanthrene biodegradation rates based on MICRO-FISH were between one and two orders of magnitude greater than model predicted values. Discrepancies in the biodegradation rates for phenanthrene may have resulted from fitting limited data in analytical models and/or dosing large masses of readily available ^{14}C-PAH in order to elicit an autoradiographic response for MICRO-FISH.

These studies suggest that enrichment of specific microbial phylotypes associated with coal-tar pollution relative to nearby pristine conditions may not be a reliable marker for PAH-degrading microbes. Similarly, enrichment of microbial phylotypes in laboratory-scale incubations may not reflect uptake of specific PAH compounds identified by MICRO-FISH. The results of this study support active natural attenuation of PAH compounds in this coal-tar polluted aquifer, and suggest that direct evidence of intrinsic degradation of PAH pollutants such as that presented in this work is necessary to effectively demonstrate natural attenuation at complex PAH contaminated sites. Based on these results, the MICRO-FISH technique may be an effective tool for establishing tertiary lines of evidence that can be used to support intrinsic bioremediation of at least low-ring coal-tar PAHs.

1. INTRODUCTION

1.1 History of manufactured gas and coal-tar pollution

From the turn of the 19th century to the middle of the 20th century, manufactured gas dominated the energy industry. Manufactured gas was produced locally and piped to municipalities, businesses, and homes primarily for heating, lamp light, and cooking purposes. Manufactured gas was initially made from coal feedstock by heating the coal in the absence of oxygen in vessels called retorts. This process converted approximately 40% of the coal to gaseous products, which cooled in the hydraulic main and condenser, precipitating water and coal tar byproducts. By the late 1800's the carbureted water-gas process gained popularity due to a superior gas with a higher BTU value and increased efficiency in gas manufacture. This processes passed stream through an incandescent mass of coke feedstock to produce water gas, which was passed through a carburetor in which light gas oil was sprayed into the gas stream. This light gas oil and water gas mixture was heated to thermally crack the oil vapors fixing them into the gas. Tar byproducts were removed from the gas stream in a series of tar separators and condensing units. Coal-tars were collected as byproducts at several locations in manufactured gas facilities, commonly precipitated from ammoniacal or oil liquors or gravity-separated from scrubbing waters. These liquor byproducts and separated tars were generated at the rate of hundreds to thousands of gallons per day.

The carbureted water gas process enabled many medium to small-size towns to operate manufactured gas facilities. Brown's Directory of North American Gas Plants listed 1,500 primary gas producing facilities in operation by 1887 based on membership in gas associations. Vast quantities of byproducts were produced from the gas manufacturing process providing cheap materials for product manufacture and driving invention in the industrial age. In 1874 Alexander Findlay wrote a book titled The Treasures of Coal Tar, touting the beneficial uses of coal-tar compounds, particularly in the chemical industry. Notable innovations for coal-tar byproducts include the use of naphtha for processing raw rubber for commercial products (~1820), the first successful synthesized dyes (anilines) used heavily in the textile industry (~1850), and the first the plastic, bakelite (1907). Other products derived from coal-tars included explosives, medicines, fertilizers, perfumes, flavors, food preservatives, and photographic materials.

Many disadvantages of the manufactured gas process and its byproducts were also well known during its use. Prior to the widespread manufacture of gas in the United States, there were reports of scrotal cancer in chimney sweeps linked to exposure to coal tars in Britain. By the mid 1850's deaths to aquatic life, crop damage, drinking water contamination, and health problems were

all attributed to the discharge of gas works residuals. Unfortunately, the large volumes of hazardous byproducts generated on a daily basis and limited storage forced plant operators to make choices regarding the disposition of low commercial value wastes. Commonly, this involved depositing wastes in on-site dumps or transporting to nearby waste dumps. Nuisance lawsuits against gas works to recover damages caused by dumping their waste byproducts were widespread by the late 1800's. By the early 1900's shortages in light fuel oils due to the emerging automotive industry and coke byproducts forced many carbureted water gas plants to operate with inferior coals as reactor feedstock and to carburet with heavier oils leading to higher water content tar byproducts of low commercial value, increasing waste byproducts. With increased litigation and awareness of the impacts of environmental pollution, states began enacting environmental regulations limiting discharge of gas works wastes to rivers and streams between the early and mid 1900's. By the mid 1960's the last of the town gas works were closed, primarily due to competition from cleaner and more efficient natural gas. Contamination resulting from poor waste disposal practices at these facilities is vast and persists today.

1.2 Modern environmental concerns regarding coal-tar pollution

Finding coal tar at a former manufactured gas facility during a site investigation is not like finding buried treasure. Coal-tars are hydrophobic and denser than water. In the subsurface, they migrate downward, coating soils surfaces and pooling on impermeable layers deep in aquifer systems making free product recovery difficult. Residual coal-tar DNAPLs solubilize slowly, providing a long-term source for groundwater contamination. Due to their hydrophobic properties and low volatility, off the shelf remediation technologies relying on physical removal mechanisms such as pump and treat, soil venting, or air sparging are relatively ineffective for coal-tar removal. These factors greatly increase the costs and uncertainty associated with remediation of former manufactured gas plant sites.

Because of the difficulties associated with removing all residual coal tars from contaminated soils and aquifer sediments, there is intense interest in the potential for the intrinsic system to assimilate and detoxify residual coal-tar contamination. Of primary concern at coal-tar impacted sites are the polycyclic aromatic hydrocarbons (PAHs), which may cause toxic and or carcinogenic effects in exposed individuals. All 16 U.S. EPA Priority PAH pollutants have been shown to be susceptible to aerobic biodegradation in laboratory studies, and many PAH-contaminated sites exhibit changes in geochemical environments commonly associated with increased microbial activity and intrinsic

bioremediation. However, coal-tars contain hundreds of compounds, any of which may elicit hydrogeochemical responses, leading to misinterpretation of the measured geochemical data relative to coal-tar PAH contamination. There remains ambiguity about the specific activity of PAH-degrading organisms in-situ necessary to verify intrinsic bioremediation of PAH pollutants. Many PAH compounds are sparingly soluble, typically exhibiting sorption nonlinearities, source materials phase change and unique dissolution characteristics, and complex biodegradation patterns limited by the bioavailability of sorbed contaminant mass and complicated by the inhibitory and/or cometabolic effects of co-contaminating compounds in contaminated soils and sediments. Uncertainty regarding these factors limits interpretation of groundwater monitoring data at coal-tar impacted sites. The low concentrations of PAH compounds relative to analytical detection limits at contaminated sites also make fate and transport modeling particularly sensitive to estimates of key hydrodynamic parameters and model assumptions such as lateral and transverse dispersivity and linear and reversible sorption. Considering these issues, a recent report by the National Research Council (2000) on MNA ranked the current understanding of the fate and transport of PAH compounds at contaminated sites as "moderate" and thus the likelihood of successful application of natural attenuation technology as "low". Based on these findings, acceptance of monitored natural attenuation at PAH contaminated sites will require a much greater level of evidence and increased monitoring efforts to support intrinsic degradation potential than more traditional applications of this technology at fuel release sites.

Following the recommendations of the U.S. EPA, a three-tiered approach may be used to evaluate natural attenuation as a remedial mechanism at contaminated sites. This approach is primarily weighted on historical data displaying a clear and meaningful trend of decreasing contaminant mass (1st line of evidence), which is supported by *indirect* measures of intrinsic remediation such as changes in the geochemical environment potentially related to biodegradation of pollutants coupled with modeling approaches to estimate the rate at which the pollutants will be reduced to required levels (2nd line of evidence). For particularly challenging cases such as PAH pollution, the U.S. EPA suggests tertiary lines of evidence based on field or microcosm studies that *directly* demonstrate microbial activity in the aquifer material and its ability to transform the contaminants of concern. However, laboratory-scale assays with contaminated site media typically result in an altered (enriched) microbial communities that may not accurately reflect in-situ conditions. Therefore a gap exists between interpreting microcosm study results as related to field-scale processes. In these cases, linking microcosm studies to the site condition is of great importance as regulatory acceptance of in situ bioremediation efforts hinge on the ability to definitively attribute

decreasing hydrocarbon concentrations measured in situ to microbial degradation, as opposed to abiotic processes that may lend to similar plume-scale behavior such as non-linear sorption, dispersion, and volatilization. For natural attenuation to become a viable remedial option at coal-tar impacted sites, a better understanding of the capacity of indigenous microbial consortia to transform PAHs into innocuous byproducts must be realized.

1.3 Specific objectives and approach

This work stems from expedited site characterization activities and groundwater monitoring performed at a former manufactured gas plant site in Cherokee, Iowa between August 2001 and March 2003. The manufactured gas plant operated from 1905 to 1936 using the carbureted water gas process. Site investigations prior to those above indicated extensive coal-tar contamination. This led to the excavation and removal of contaminated soil to a maximum depth of 2.4 m or the water table. Groundwater monitoring data prior to 2001 indicated that the contaminant plume emanating from the coal-tar source was of limited aerial extent. However, hydraulic irregularities in groundwater flow complicated modeling efforts to estimate intrinsic degradation potential. Due to the difficulties associated with complete removal of free-phase coal-tar materials, the limited extent of plume migration, and limited routes of exposure to the contaminants by potential receptors, monitored natural attenuation as a "polishing step" was of interest at this site.

The primary objectives of expedited site characterizations were to obtain data to construct a realistic site conceptual hydrologic model, characterize the aqueous geochemical environment, and identify whether or not PAH compounds were biodegrading in situ. Based on groundwater monitoring well data prior to August 2001, there was evidence that contaminant concentrations were declining with time following source removal action (1st line of evidence). However, there was ambiguity regarding the reason for the declining concentrations, whether due to reduction of source mass and decreased leaching and/or through biological action. The work presented herein addresses the latter two of the primary objectives and considers both the three tiered approach suggested by the U.S. EPA for exploring monitored natural attenuation as a remedial mechanism and the need to better link the in situ condition to laboratory-scale studies to provide more weight to the argument for intrinsic degradation of coal-tar PAHs.

The innovative approach taken in this study involves integrating plume-scale aqueous geochemical monitoring, fate and transport modeling, and molecular characterizations of the intrinsic microbial community structure with novel molecular microbiological techniques modified in this

study for tracking uptake of individual PAHs to specific cell types in the coal-tar impacted sediments. The unique data sets provided by these techniques may yield a link between tertiary lines of evidence of natural attenuation such as laboratory-scale incubations and secondary lines of evidence such as plume-scale modeling and monitoring data. Through this approach, the presence of PAH-degrading microbial phylotypes can be identified in-situ as a portion of the intrinsic microbial community. Cell-specific biodegradation rates in short-term laboratory incubations can be compared to model estimates of PAH degradation, better linking laboratory-scale assays to the in-situ condition.

The specific objectives of this work were to:

1. Apply coupled analytical fate and transport solutions and lumped-hydrocarbon geochemical mass balance approaches to investigate intrinsic biodegradation of coal-tar impacted systems and estimate pollutant mass degradation rates in the aquifer underlying the Cherokee FMGP site (2nd line of evidence)

2. Determine whether the spatial heterogeneity in the in-situ microbial community structure as related to known PAH-degrading microbial phylotypes reflect the heterogeneity in the aqueous geochemistry and pollutant concentrations observed in groundwater measurements in situ

3. Identify whether the aqueous geochemical environments exhibited in-situ are related to the degradation of U.S. EPA priority PAH compounds based on laboratory incubations with contaminated site sediments (3rd line of evidence)

4. Determine whether the relative enrichment of specific microbial phylotypes observed in situ as described in objective 2 correlate to the enrichment of specific microbial phylotypes observed in laboratory incubations of objective 3, further supporting in-situ microbial growth on priority PAH pollutants

5. Develop procedures and address potential interferences for coupling whole-cell hybridization and microautoradiography to track uptake of select PAH compounds to specific microbial types in the microbial communities populating coal-tar impacted sediments

6. Apply combined whole-cell hybridization and microautoradiography techniques to identify the spatial heterogeneity in microbial cell types growing on naphthalene and phenanthrene in polluted sediments from the coal-tar impacted aquifer underlying the Cherokee FMGP site and identify relationships between the degrading microbial community structure and the overall microbial community structure identified in objective 2.

7.   Compare and contrast estimates of the in-situ biodegradation rates of naphthalene and phenanthrene based on molecular microbiological measurements with the whole-cell hybridization and microautoradiographic techniques to those of plume-scale analytical modeling approaches in objective 1 in order to evaluate the potential for molecular microbiological tools to tie secondary lines of evidence of natural attenuation to tertiary lines of evidence better supporting natural attenuation investigations

The application of these seven objectives towards the goal of displaying intrinsic remediation potential at the Cherokee FMGP site and implications for future investigations of natural attenuation at PAH-contaminated sites are the focus of the work presented herein.

1.4 Dissertation Organization

This dissertation describes a unique approach taken to evaluate the potential of the intrinsic microbial community populating coal-tar impacted aquifer sediments underlying a former manufactured gas plant site in Cherokee, Iowa to assimilate and detoxify polycyclic aromatic hydrocarbons (PAHs). It is organized into a total of seven chapters and two appendices. Chapter 1 introduces the research presented in the proceeding chapters, placing the work into an historical and environmental context. Chapter 2 presents a summary of literature reviewed encompassing published works essential to providing a fundamental basis for the work performed herein. Much of Chapter 2 was published as a critical review of PAH-contaminated sites in the ASCE Practice Periodical of Hazardous, Toxic, and Radioactive Waste Management. Chapter 3 is an article submitted to the Journal of Contaminant Hydrology. This chapter summarizes the Cherokee FMGP site conceptual model and presents estimates of the intrinsic biodegradation of PAH pollutants based on both a simplified lumped-hydrocarbon geochemical mass balance approach and analytical plume-scale modeling. Results of the two models are compared to identify variability and limitations of plume-scale modeling of coal-tar impacted sites. Chapter 4 is an article to be submitted to Applied and Environmental Microbiology. This chapter explores PAH biodegradation in the contaminated aquifer sediments underlying the Cherokee FMGP site based on an integrated biogeochemical and molecular microbiological approach. Perturbation of microbial community structures of contaminated versus nearby pristine sediments are investigated spatially relative to the aqueous geochemical environments exhibited in situ, and are compared to the mineralization of select PAH compounds in aerobic and anaerobic incubations. Enrichment of select microbial phylotypes in laboratory-scale incubations are

compared and contrasted to the intrinsic microbial community structure. Promises and pitfalls of these types of molecular microbiological approaches for supporting investigations of intrinsic bioremediation are discussed considering the uptake of phenanthrene by specific bacteria identified with whole-cell hybridizations and microautoradiography. Chapter 5 is an article to be submitted to the Journal of Microbiological Methods. It describes detailed procedures for properly interfacing whole-cell hybridizations and microautoradiography (MICRO-FISH) for tracking the uptake of polycyclic aromatic hydrocarbons to specific microbial cell types in sediments contaminated with coal-tar DNAPLs. Several interferences are addressed including autofluorescence from soils and DNAPL residuals, autoradiographic false-positives from sorption of hydrophobic radioisotopes to bacterial cell surfaces, and the effects of incubation time on autoradiographic detection and perturbation from the initial microbial community structure. Application of MICRO-FISH to contaminated site sediments of several locations in the coal-tar source region and resulting plume is presented in Chapter 6. The spatial heterogeneity in bacterial phylotypes growing on naphthalene and phenanthrene are linked to the intrinsic microbial community structure. Cell-specific uptake and mineralization rates of naphthalene and phenanthrene based on MICRO-FISH results are compared to estimates of the plume-scale first-order degradation rate coefficients presented in Chapter 3. The results of this study are used to better identify intrinsic bioremediation potential of these compounds at the Cherokee FMGP site. Chapter 6 will be submitted to Environmental Science and Technology. Chapter 7 provides a summary of the work presented in Chapters 3 through 6, and includes recommendations for future study related to this work. Appendix A summarizes aqueous geochemical properties and PAH concentrations measured in groundwater at the Cherokee FMGP site. Appendix B summarizes the methods used for groundwater sampling.

Advisors and coworkers in the natural attenuation research group at Iowa State University included Dr. Bruce H. Kjartanson, Dr. Johanshir Golchin, and Dr. Greg A. Stenback, who provided valuable input for writing and revising both the critical review published from portions of Chapter 2 as well as technical guidance in the modeling work presented in Chapter 3. As such, their names were included as co-authors on the final manuscripts for these chapters. Dr. Thomas Moorman provided input and technical guidance in all of the microbiological work performed, edited and revised manuscripts, and made available laboratory space in the USDA's National Soil Tilth Laboratory in Ames Iowa. He is included as a co-author on the manuscripts for Chapters 4, 5, and 6. Dr. Say Kee Ong was listed as a co-author on all manuscripts. He served as the primary research professor for all the work performed herein, providing technical guidance in every aspect of the work and in editing and revising all manuscripts.

2. LITERATURE REVIEW

Adapted from a paper published in the Practice Periodical of Hazardous, Toxic, and Radioactive Waste Management entitled "Natural Attenuation of PAH Contaminated Sites: A Review"

Shane W. Rogers, Say Kee Ong, Bruce H. Kjartanson, Johanshir Golchin, and Greg A. Stenback

2.1 Abstract

Natural attenuation is currently being applied as a remedial technology at many petroleum hydrocarbon and chlorinated compound sites. Although information on the use of natural attenuation at these sites is abundant, information on sites contaminated with polycyclic aromatic hydrocarbons (PAH) is limited. An assessment report by the National Research Council on natural attenuation indicates that the current understanding of fate and transport of PAH compounds at contaminated sites is "moderate" and the likelihood of success in the application of natural attenuation at these sites is expected to be "low" given the current level of understanding. The purpose of this paper is to review documented work on natural attenuation of PAH-contaminated sites and summarize information to improve our level of understanding and address important issues for the implementation of natural attenuation at these sites. The main processes affecting the attenuation of PAH compounds are sorption and biodegradation. The relative contribution of each of the two attenuation processes is unclear. The few studies available tend to focus on the degradation of low molecular weight PAHs such as naphthalene, acenaphthylene, and phenanthrene. The estimated first-order decay rates of naphthalene, acenaphthylene, and phenanthrene from the various studies were 0.00057 to 0.0063 d^{-1}, 0.00027 d^{-1}, and 0.000027 to 0.063 d^{-1}, respectively. Some of the issues that need further investigation include: the lack of understanding of the solubility and dissolution of PAH NAPLs; the interactions and effects of the more soluble low molecular weight PAHs on the sparingly soluble high molecular weight PAHs; and the utilization of electron acceptors other than oxygen during microbial degradation of PAHs under complex mixture conditions. As significant variability in monitoring data exist at many PAH contaminated sites, extended monitoring efforts and tertiary lines of evidence may be necessary for effective evaluation of the potential of select sites for intrinsic degradation. Emerging molecular microbiological approaches may be particularly well suited for these investigations and may result in more effective monitoring efforts. Overall, the natural attenuation of low molecular weight PAHs appears to be promising for the sites investigated.

2.2 Introduction

Over the last decade, there has been an increase in the application of natural attenuation as a remedial alternative for the cleanup of contaminated groundwater. The increase is generally in response to the high capital and operating costs and technical limitations of some of the engineered cleanup technologies for the remediation of these contaminated sites. A survey of state underground storage tank programs indicates that as many as 15,780 sites are applying monitored natural attenuation as a remedial technology (MacDonald, 2000). Correspondingly, the number of publications appearing on this subject has increased recently with several noteworthy publications such as that of Wiedemeier et al. (1999). However, most of the literature is centered on two of the more commonly found classes of contaminants, petroleum hydrocarbons and chlorinated compounds. Nevertheless, there are several completed studies and some that are in progress in extending the concept of natural attenuation to other pollutants such as heavy metals and polycyclic aromatic compounds (PAHs). PAH compounds are common byproducts of petroleum and chemical industries and are the third most commonly found class of contaminants at Superfund sites (US EPA, 2000). A recent assessment of natural attenuation indicates that current understanding of fate and transport of PAH compounds at contaminated sites is "moderate" and that the likelihood of success in the application of natural attenuation at these sites is expected to be "low" given the current level of understanding (NRC, 2000). With that in mind, this article reviews the current literature on natural attenuation of sites contaminated with PAHs and highlights some of the issues involved in implementing natural attenuation as a remedial technology at PAH-contaminated sites.

2.3 PAH-Contaminated Sites

PAH-contaminated sites are generally associated with industrial activities such as wood preservation, petroleum refining, transportation, former manufactured gas plants (FMGPs), lignite pyrolysis sites, military installations, and municipal and hazardous waste landfills. In many cases, PAHs at these sites are found with other contaminants such as heterocyclic compounds, monoaromatic compounds, cyanides, pesticides, pentachlorophenol, and arsenic-based wood preservatives. Of the 1,226 sites currently registered on the Superfund National Priority List (NPL), 598 are contaminated with PAH compounds (48.8%). The number of Superfund sites with PAHs as contaminants is only surpassed by sites containing volatile organic compounds, which include

chlorinated solvents, benzene, toluene, ethylbenzene and xylenes (BTEX) (849 sites (69.2%)), and metals (794 sites (64.8%)) (US EPA, 2000).

Although there are many PAH-contaminated sites with different sources of contamination, much remedial work has been placed on sites originating from creosote works, wood treatment industries, coking industries, and FMGPs, as they comprise the largest fraction of PAH-contaminated sites. Burton et al. (1988) reported that there were approximately 700 sites in the United States alone where wood preservation is currently conducted or has been conducted in the past. The number of creosote-contaminated sites was estimated to be approximately 700 by Mueller et al. (1989). In 1984, Edison Electric Institute estimated that the number of FMGP sites that pose an environmental threat was approximately 1,500 (Edison Electric Institute, 1984). In 1997 Larsen indicated that there may be more than 5000 former MGP sites in the United States, with many requiring some form of remedial action. According to Hatheway (1997), this estimate was conservative, as it did not include potentially contaminated FMGP sites. Hatheway asserted that the number of contaminated FMGP sites in North America alone may reach beyond 32,000, considering that there were similar gas manufacturing facilities located at rail yards, military posts, arsenals, institutes, and large residential estates that were not reported. Creosote and coal tar compounds have been cited as a widespread problem in nearly all industrialized countries (Broholm et al., 1999). According to Delorme and Carlier (1998), the French National Gas Company alone owns 467 FMGP plants. In Germany, the total number of FMGP sites is estimated to reach about 1,000 (Knopp et al., 2000), and in Denmark, Arvin and Flyvbjerg (1992) estimated that there are 35 – 45 creosote waste sites per million people.

Contamination at these sites has resulted from leaking tanks and pipe networks, incomplete separation of tar from aqueous liquids, drippings from treated lumber (wood treatment facilities), spills, decommissioning activities, and leachate from unlined storage ponds or shallow wells. In any case, the nonaqueous phase liquids (NAPLs) released from sites that contained these compounds tend to be denser than water and usually migrate downward and laterally into the subsurface by gravity and capillary forces. In many of these sites, the NAPLs may pool on the confining layer of the aquifer and move along its geologic gradient. Given the physical-chemical properties of PAH compounds, they can be very challenging to remediate.

2.4 Monitored Natural Attenuation: Regulatory Concerns

The problem of environmental PAH contamination is a global issue. Based on their chemical properties, conventional physical/chemical remediation techniques may not be completely effective in

removing PAH compounds from the subsurface. However, those same properties lend to strong partitioning to soils and sediments resulting in low potential for contaminant migration. Combined with their potential to biodegrade to innocuous byproducts, the prospect for intrinsic systems to stabilize and cleanse themselves of residual PAH contamination is of intense interest. The following discussion of regulatory concerns provides the basis for evaluating PAH compounds in terms of their potential for undergoing natural attenuation in polluted environments.

The U.S EPA has established guidelines for implementing and demonstrating monitored natural attenuation (MNA) at contaminated sites (EPA, 1999). In general, they suggest the use of appropriate active (engineered) source control measures or active remedial measures combined with or followed by MNA. Monitoring efforts should be used for detailed site characterization and to compare actual (long-term) site conditions with expectations based on numerical and/or analytical modeling approaches. The EPA prefers processes that (1) remove and treat free-phase NAPLs and source materials, and (2) degrade or destroy contaminants rather than stabilize (physically) or dilute them. In evaluating whether or not MNA is appropriate for a given site, the EPA will be primarily interested in strong evidence of specific natural attenuation processes and their action on the contaminants, a stable or shrinking groundwater contaminant plume with limited migration, and no unacceptable risks to human health or environmental resources posed by the contaminants over the MNA remedial period. As it is not uncommon to observe at PAH contaminated sites free-phase coal-tar or creosote contamination originating from operations of over a century past, it is highly unlikely that MNA of PAH contaminated sites will succeed without implementation of active source control and/or removal measures.

A three tiered approach to documenting the potential for MNA at contaminated sites is suggested by the U.S. EPA (1999). This approach centers about an effective monitoring program that yields site-specific data of sufficient quality to estimate with an acceptable level of confidence both the rate of contaminant attenuation based on specific attenuation processes and the timeframe for achieving remediation objectives. Specifically, for MNA to be acceptable, the EPA suggest that historical data display a clear and meaningful trend of decreasing contaminant mass at appropriate monitoring points. This should be supported by indirect measures of intrinsic remediation such as changes in the aqueous geochemical environment potentially related to biodegradation of pollutants (consumption of potential terminal electron accepting compounds or production of reduced species associated with specific terminal electron accepting processes) coupled with modeling approaches to estimate the rate at which the pollutants will be reduced to required levels (U.S. EPA, 1999). In the case of PAH compounds, which may be particularly challenging to establish clear trends with a high

degree of confidence, tertiary lines of evidence based on field or microcosm studies that directly demonstrate intrinsic microbial activity and biological degradation of the PAH compounds to innocuous byproducts may be necessary (U.S.EPA, 1999).

2.5 PAH Compounds of Concern

PAHs are defined as compounds consisting of carbon and hydrogen in the form of two or more fused aromatic rings forming planar structures with resonating *pi* bonds. They are classified as unsaturated hydrocarbons, yet tend to have low reactivity compared to other unsaturated hydrocarbons (alkenes and alkynes) as their *pi* electrons are stabilized through delocalization of the *pi* orbitals (Brown et al., 1994).

Of the many PAH compounds, the U.S. EPA has identified 16 PAH compounds as priority pollutants that are of environmental concern. Figure 2.1 shows the structure of the 16 PAH compounds. A summary of their physical and chemical properties is provided in Table 2.1. As can be seen from Table 2.1, some of these compounds have very low water solubility and are solid at most temperatures found in the environment. These compounds tend to have a moderate to low volatility that decreases with increasing molar mass (Brown et al., 1994). Furthermore, PAH compounds have a high adsorption tendency (due to their non-polar nature), and moderate to low biodegradability, which again is directly related to the molecular size and shape of the compounds. The solid-water partition coefficients of the 16 priority PAH pollutants are also given in Table 2.1. Because of these properties, PAH compounds tend to be relatively immobile and persistent in soil.

The hydrophobic nature of these compounds lends to rapid partitioning onto particulate matter or tissue suggesting bioaccumulation potential (LaGrega et al., 1994). Some PAH compounds have been shown to be acutely toxic to aquatic organisms at concentrations ranging from 0.2 mg/L to 10 mg/L, with acute toxicity increasing with increasing molecular weight to a point at which compound solubilities become too low to elicit a response (Neff, 1985). Table 2.2 lists the critical toxic (non-carcinogenic) effects that may result from oral exposure to select PAH compounds based on animal studies. Toxic responses from exposure to PAH compounds may include atrophy of the hematopoietic elements leading to progressive anemia and agranulocytosis (deficiency in white blood cells), shrinkage of lymphoid organs and lymphopenia, damage to epithelial cells, and reproductive disorders such as the destruction of the spermatogonia and resting spermatocytes in males and the primary oocytes in females (RAIS, 2004; IRIS, 2004). Metabolites of PAH compounds, which are more water soluble and reactive than their respective parent compounds, may bind to protein, DNA,

and other macromolecules leading to cell damage, mutagenesis, or possible cancers of the stomach, lung, or skin (LaGrega et al., 1994). PAH compounds related to carcinogenicity tend to induce immunosuppression in laboratory animals, whereas noncarcinogenic PAHs do not (Dean et al., 1986). Benz(a)anthracene, benzo(b)fluoranthene, benzo(k)fluoranthene, benzo(a)pyrene, benzo(g,h,i)perylene, chrysene, dibenz(a,h)anthracene, and indeno(1,2,3-cd)pyrene have been identified by the U.S. EPA as probable human carcinogens. U.S. EPA drinking water standards and risk-based factors for corrective action based on toxicity and carcinogenicity are listed in Table 2.2. Of the 16 U.S. EPA priority PAH pollutants, benzo(a)pyrene is the only pollutant with an established maximum contaminant level (MCL) in drinking water.

2.6 Environmental PAH Contamination

PAH compounds at contaminated sites are likely to be found in complex mixtures that vary in composition with depth and distance from the source region. Novotny et al. (1981) studied the composition of several coal tar samples derived from coals of different geographical origin and determined that the major constituents were similar. Priddle and MacQuarrie (1994), however, compared the chemical composition of four creosote samples and one coal tar sample and found that they all varied significantly. Barbé et al. (1998) studied PAH concentration profiles with depth at a former coke plant and determined that lighter PAH compounds were typically present in shallower depths with heavier compounds (for example, benzo(a)pyrene) becoming increasingly predominant at greater depths in the unsaturated zone and into the saturated region of the subsurface. Delorme and Carlier (1998) studied several former manufactured gas plant sites in France and determined that in the majority of cases, silts and clays tend to be more polluted at these sites than the coarser sands. Furthermore, they determined that the presence of coal tars tended to decrease soil permeability, and that many PAH components in residues showed little mobility and were naturally stabilized in soil.

In complex mixtures, PAH compounds may exhibit properties that differ from their pure phase properties. For example, Bayard et al. (1998) studied the influence of PAH compounds in aqueous and NAPL phases on naphthalene sorption to soil organic matter. Aqueous phase PAH compounds had no effect on naphthalene sorption due to their low solubilities and thereby insignificant competition. However, when coal tar was added to the soil system, soil sorption of naphthalene dropped significantly as the naphthalene preferably partitioned onto the coal tar NAPL in lieu of the natural organic matter.

In addition to changes in their sorptive behavior, it is expected that the solubility of PAHs in liquid mixtures of organic compounds will be much different from the solubilities expressed in their natural solid form. Raoult's law has been shown to adequately predict equilibrium PAH solubilities (within a factor of two to four) in complex organic mixtures such as diesel fuel, gasoline, coal tar, and creosote (Lee et al., 1992a; 1992b; Cline et al., 1991; King and Barker, 1999). Based on this, a comparison of the pure aqueous solubility of the 16 priority PAH compounds and the effective solubilities calculated with Raoult's law for two coal tar mixtures and a coal tar creosote are shown in Table 2.3. It is interesting to note that the effective solubility of a compound expressed in mixed liquid state may not necessarily be lower than its solubility in pure solid form (as in anthracene and chrysene). Effective solubilities of PAH compounds based upon Raoult's law have been used in numerical models to simulate steady-state PAH dissolution from complex mixtures of nonaqueous phase liquids (NAPLs) over time with some success (King and Barker, 1999). However, Priddle and MacQuarrie (1994) studied the efficacy of such models in columns of glass beads and determined that these models predicted the trends in dissolution but over-predicted aqueous concentrations by factors ranging from 1.5 to 8. These researchers suggested using a reduction factor as an extra model fitting parameter to account for the lower observed aqueous concentrations. Because of the uncertainty in PAH solubilities in the presence of complex mixtures and NAPLs, model prediction on the fate and transport of PAHs in the presence of NAPLs should be carefully evaluated.

2.7 Abiotic Attenuation of PAH Compounds

Abiotic processes that may influence the fate of hydrocarbons in the subsurface include dilution, dispersion, volatilization, hydrolysis, and sorption. Although dilution and dispersion may influence plume geometry and migration of PAHs in the environment, these processes do not result in attenuation of PAH compounds as they do not destroy, stabilize, or remove PAHs from a contaminated system. Volatilization losses in the vadose zone and at the capillary fringe of the subsurface environment may be one of the attenuation processes for low molecular weight PAH compounds such as naphthalene. Bioremediation studies conducted by Bossert and Bartha (1986) and Park et al. (1990) indicated that 2- and 3-ring PAH compounds may be lost from soil samples through volatilization. No significant volatilization losses were found for PAH compounds containing more than three benzene rings. An inverse correlation between the number of rings in PAHs and their volatilization losses is generally assumed. However, quantification of losses of PAHs by volatilization from the subsurface environment under field conditions is not available.

PAHs are chemically stable and are not hydrolyzed by reactive groups under subsurface environmental conditions. Therefore, hydrolysis does not contribute to the abiotic change in the PAHs (Radding et al., 1976; Howard et al., 1991). PAHs can be photodegraded but this effect is minimal in a subsurface environment (Sims and Overcash, 1983).

Sorption of PAH compounds is an area of intense research. As indicated earlier in Table 2.1, sorption onto the organic matter and mineral surfaces of soils may be one of the major attenuation processes for PAH compounds in the subsurface. For example, the log K_{oc} value for naphthalene, the most soluble of the 16 priority PAHs, is approximately two times larger than that of benzene. Although the K_{oc} values may provide a basis for comparison, several researchers have shown that specific subsurface geosorbents such as natural organic matter (NOM), soot and mineral surfaces have very different affinities for PAH. In fact, the equilibrium partitioning coefficients may vary as much as several orders of magnitude in materials such as soot, NAPLs, bacterial biomass, mineral surfaces, recent amorphous NOM that is relatively more oxidized, and aged, increasingly condensed, highly microcrystalline, and relatively more reduced NOM (Xia and Ball, 2000; Chiou et al., 2000; Bayard et al., 2000; Huang and Weber, 1997; Leuking et al., 2000; Weber et al., 1998; Ghosh et al, 2000; Young and Weber, 1995; Jonker and Smedes, 2000; Stringfellow and Alvarez-Cohen, 1999; Karapanagioti et al., 2000). Furthermore, the location of sorption sites may have an impact on the desorption of PAH compounds in the aqueous-soil environment as diffusion from micropores and intraorganic matter may strongly influence contaminant mass transfer to the aqueous phase (Luthy et al., 1997; Brusseau et al., 1991). For these reasons, PAH sorption exhibits strong isotherm nonlinearities and hysteresis that become more prominent with the age of contamination (Hatzinger and Alexander, 1995; MacLeod and Semple, 2000; Carmichael et al., 1997). These nonlinearities lend to abiotic stabilization of PAHs in the environment and are of benefit to natural attenuation efforts. Consequently, the use of linear and reversible sorption models with lumped distribution coefficients may not be suitable for modeling sorption of individual PAHs to the subsurface media.

2.8 Biological Attenuation of PAH Compounds

Biological action may result in the complete conversion of PAH compounds to innocuous byproducts in the environment. As such, it may be the most important attenuation mechanism for displaying natural attenuation at PAH-contaminated sites (EPA, 1999). PAH compounds are ubiquitous in the environment at low concentrations, thus the presence of organisms capable of degrading these compounds may be ubiquitous as well. Padmanabhan et al. (2003) identified

naphthalene-degrading *Acinetobacter* spp., *Variovorax* spp., and *Pseudomonas* spp. in uncontaminated soils from the Agricultural Experimental Station in Ithaca, New York. Monna et al. (1993) isolated *Terrabacter* sp. strain DBF63 on fluorene from uncontaminated eastern Japanese soils. Daane et al. (2001) identified *Paenibacillus naphthalenovorans* SA-N1 as a degrader of naphthalene in uncontaminated plant root rhizosphere soils from Marine Station Lewes, Delaware. Eriksson et al. (2003) identified two *Acidovorax* spp. associated with the degradation of a PAH mixture in laboratory incubations with uncontaminated arctic soil from Vancouver, Canada. The ubiquity of PAH-degrading organisms in the environment lends strong support to bioattenuation potential of PAH-contaminated sites. Several researchers have even noted that PAHs may form the basis of complex food webs in polluted systems (Ghiorse et al., 1995; Carman et al, 1995; Langworthy et al., 1998).

2.8.1 Aerobic PAH biodegradation

Many bacterial, fungal and algal strains have been shown to biodegrade PAHs pollutants in laboratory incubations with contaminated soils and sediments. In several studies, 2- to 3-ring PAH compounds were readily removed by microorganisms as a sole source of carbon and energy (Heitkamp and Cerniglia 1989; Mueller et al., 1989; Weissenfels et al., 1990; Davis and Evans, 1964; Dean-Raymond and Bartha, 1975). Park et al. (1990) showed that the mineralization of 2-ring PAHs in sandy soils was extensive with half-lives of approximately two days. In comparison, the half-lives for the 3-ring PAHs anthracene and phenanthrene were 16 and 134 days, respectively. The work of Heitkamp and Cerniglia (1987) showed similar results for PAH degradation in sediment/water microcosms. McGinnis et al. (1988) conducted laboratory treatability studies on creosote-contaminated soils from wood treatment sites and found that PAHs with two rings generally exhibited half-lives of less than 10 days and PAHs with three rings had half-lives of less than 100 days. 4-, 5-, and 6-ring PAHs tend to be recalcitrant with reported half-lives greater than 200 days. However, researchers have characterized microorganisms capable of using 4-ring PAHs as their sole carbon and energy sources from contaminated soils (Mueller et al., 1990; Walter et al., 1991; Weissenfels et al., 1991). The half-lives and the aerobic degradation rates of the 16 U.S. EPA Priority PAH Pollutants in situ and in laboratory incubations with contaminated soils and sediments are summarized in Table 2.4. The half-lives and first-order degradation rates presented are only representative and should be used with care as the estimated degradation rates in these studies may be different from the environmental conditions (e.g., electron acceptors, nutrient, etc.) present at a given site.

A partial list of PAH-degrading microorganisms (bacteria, algae, and fungi) that have been isolated from contaminated soils and sediments is presented in Table 2.5. In general, it has been observed that an organism capable of degrading a higher-ring PAH compound has the ability to degrade PAHs with fewer rings. However, microbial mineralization of PAHs with four or more rings has generally been reported to occur via cometabolism (Bouchez et al., 1995; Ye et al., 1996; Aitken et al., 1998). This cometabolic process may be stimulated by the presence of lower molecular weight PAH compounds or their intermediates of biodegradation such as salicylate (Keck et al, 1989; Kanaly et al., 1997; Chen and Aitken, 1999). At PAH-contaminated sites, there is no clear indication of how the presence of low molecular weight PAHs influence the biodegradation of higher molecular weight PAHs or vice versa.

Aerobic metabolism of PAH compounds by bacteria and some green algae commonly involves the initial oxidation of an aromatic ring by dioxygenases such as naphthalene dioxygenase or phenanthrene dioxygenase to produce cis-dihydrodiols (Wilson et al., 1999; Laurie and Lloyd-Jones, 2000; Dean-Ross and Cerniglia, 1996; Heitkamp et al., 1988b; Walter et al., 1991; Weissenfels et al., 1991). Commonly, these dihydroxylated intermediates are further metabolized through an ortho- or meta-cleavage type pathway leading to protocatechuates and catechols, which are subsequently converted to tricarboxylic acid cycle intermediates. Initial activation of PAH compounds by monooxygenases of many bacteria may result in production of trans-dihydrodiols and phenols. Cytochrome P450 monooxygenases of fungi and some bacteria also produce arene oxides which can be subsequently converted by the enzyme epoxide hydrolase to a trans-dihydrodiol or non-ezymatically to phenols. The lignin-degrading enzymes of white-rot fungi such as lignin peroxidase or manganese peroxidase may produce quinones which can be subsequently mineralized by the fungus or commensal bacteria (Prince and Drake, 1999). Table 2.5 lists the primary sites of aerobic enzymatic attack on several PAH compounds.

Following isolation and characterization of several PAH-degrading bacteria from creosote contaminated soils in the United States, Norway, and Germany, Mueller et al. (1997) determined that PAH-degrading capabilities appeared to be associated with members of certain taxa such as Sphingomonas spp. and Burkholderia spp., independent the origin of the soils from which the bacteria were isolated. Later, it was noted by Bastiens et al. (2000) that the use of different isolation techniques influenced the selective growth of PAH-degrading bacteria. These researchers noted that relatively slow growing gram positive bacteria such as Mycobacterium spp. were more likely to be isolated with PAH-sorbing carriers whereas more opportunistic bacteria such as Pseudomonas spp., Sphingomonas spp., and Burkholderia spp. are more likely to be identified using liquid media. In a

later study, Johnsen et al. (2002) noted that PAH mineralization in soils and sediments is dominated by bacteria that belong to a limited number of taxonomic groups including *Nocardioforms*, *Sphingomonas*, *Burkholderia*, *Pseudomonas*, and *Mycobacterium*. A review of several studies does reveal phylotypic clustering of PAH-degrading bacteria isolated from soils and sediments globally (see Table 2.6). This is interesting because most known specific genetic elements related to PAH degradation (such as those exhibiting classical *nah*-like (*nah, ndo, pah*, and *dox*) sequences or *phn*-sequences) are plasmidborne and thus transposable. This may suggest that other phenotypic characteristics such as cell hydrophobicity, the ability to conjugate, and/or the ability to produce biosurfactants may be equally important to displaying the PAH-degrading phenotype as the availability of specific genetic elements the environment. However, it may also be that specific phenotypic characteristics lead to cultivability, by which most PAH-degrading bacteria are characterized. Culture techniques may not fully capture the suite of organisms capable of degrading PAH compounds in the environment. The use of emerging molecular techniques may play an important role in identifying new PAH-degrading bacteria (and potentially novel catabolic genetic elements) that have resisted cultivation to date.

2.8.2 Anaerobic PAH Biodegradation

Most works on PAH biodegradation have focused on aerobic conditions. However, bioenergetic growth modeling of heterotrophic metabolism of PAH compounds shows potential for several compounds such as naphthalene, anthracene, phenanthrene, and pyrene to mineralize using nitrate, ferric iron, manganese (IV), sulfate, and carbon dioxide as terminal electron acceptors (McFarland and Sims, 1991). Large microbial growth yields were predicted for the reduction of free metal species during PAH oxidation, and suggest the ability to degrade PAH compounds in these redox environments may even pose a selective advantage. There also exists strong field evidence that the anaerobic biodegradation of PAH compounds may be significant for attenuation of at least low molecular weight PAH compounds. Many PAH-polluted sites exhibit changes in aqueous geochemistry relative to nearby pristine conditions commonly associated with increased microbial activity and anaerobic biodegradation processes (Nielsen and Christensen, 1994; EPRI, 1996; King et al., 1999; Campbell et al., 1996; Landmeyer et al., 1998; Ong et al., 2001).

Biodegradation of low-ring PAHs under anoxic and anaerobic conditions has been observed in laboratory-scale incubations of contaminated harbor, estuarine, and aquifer sediments. Milhelcic and Luthy (1988a) observed naphthalene and acenaphthalene mineralization in soil-water laboratory incubations under nitrate-reducing conditions after a lag phase of approximately 10 days and 15-20

days, respectively. In a subsequent study, these researchers determined that the lag phase was a result of the time it took for a small population of organisms to attain sufficient densities to exhibit detectable PAH degradation (Milhelcic and Luthy, 1988b). McNally et al. (1998) observed degradation of anthracene, phenanthrene, and pyrene to non-detectable levels within four days under strict nitrate-reducing conditions by three pseudomonad strains isolated from contrasting environments. More recently, Rockne et al. (2000) demonstrated mineralization of naphthalene under nitrate-reducing conditions by three pure culture isolates from contaminated Eagle Harbor (Puget Sound) sediments. These works support growing evidence that the fate of PAH compounds in contaminated systems may be strongly influenced by nitrate-reduction. All PAH-degrading, nitrate-reducing bacteria that have been identified belong to the β- and γ-Proteobacteria, as shown in Table 2.6.

Although large microbial growth yields were predicted for PAH degradation coupled to metal-reduction, reports of PAH-degradation under metal-reducing conditions are rare. Nielsen and Christensen (1994) measured the degradation of select PAH compounds in a landfill leachate plume of varying aqueous geochemical environments using field measurements and laboratory incubations with site sediments. These researchers reported that the degradation of PAH compounds were limited to aerobic and iron (III)-reducing conditions. Andersen and Lovley (1999) observed naphthalene mineralization under iron (III)-reducing conditions in sediments from a petroleum-contaminated aquifer in Bemidji, Minnesota, but not in sediments from the Fe(III)-reducing zone of other petroleum-contaminated aquifers studied. The rate of naphthalene mineralization correlated positively to the presence of iron (III) in aquifer sediments and to benzene, toluene, and acetate mineralization under iron (III)-reducing conditions. These researchers noted that uncontaminated sediments at the Bemidji site adapted to anaerobic benzene degradation merely by the addition of benzene, whereas sediments of the other petroleum contaminated aquifers did not. This indicated that Bemidji sediments naturally contained Fe(III) reducers capable of degradation of unsubstituted aromatic hydrocarbons. In a later study, Rooney-Varga et al. (1999) observed significant enrichment in bacteria of the *Geobacter* cluster, specifically of the family *Geobacteraceae*, in Fe(III)-reducing regions of the aquifer. These researchers noted in microcosms established with contaminated site sediments the enrichment of Geobacter spp., a genus within the δ-Proteobacteria associated with bacteria capable of coupling of the complete oxidation of organic compounds to the reduction of iron and other metals (Lovley et al., 1993).

Both naphthalene and phenanthrene have been shown to mineralize under sulfate-reducing conditions without a detectible lag period in heavily contaminated sediments taken from San Diego

Bay, San Diego, California (Coates et al., 1996; Coates et al., 1997). Sulfate reduction was necessary for PAH oxidation in these sediments whereas sediments from less contaminated regions of the harbor were not able to mineralize naphthalene or phenanthrene. Bedessem et al. (1997) observed extensive naphthalene mineralization (66% in 13 days) under sulfate-reducing conditions in laboratory microcosms established from sediments of two coal tar-impacted aquifers. These researchers identified naphthenol as a potential metabolic intermediate based on GC/MS analyses of stabilized naphthalene-degrading consortia. Zhang and Young (1997) showed that sediments collected from Arthur Kill in the New York/New Jersey Harbor also displayed mineralization of naphthalene and phenanthrene under sulfidogenic conditions, but with an initial lag period of 120 to 150 days. Subsequent studies with the same isolates revealed no apparent lag and rapid mineralization. HPLC and GC/MS analysis of the byproducts of degradation following incubation with [^{13}C]bicarbonate indicated that the reaction was initiated by a carboxylation step to yield 2-naphthoic acid or phenanthrene carboxylic acid, respectfully. These results were supported by the work of Meckenstock et al. (2000), who identified carboxylation as the initial step in the mineralization of naphthalene in sulfate-reducing isolates from contaminated aquifer soils in Stuttgart, Germany.

Galushko et al. (1999) isolated several sulfate-reducing bacteria from highly contaminated marine sediments in Germany that grew on naphthalene as the only organic carbon source. These researchers characterized one strain (strain NaphS2) phylogenetically and realized a close affiliation to all known monoaromatic hydrocarbon-degrading sulfate-reducing bacteria of the δ-Proteobacteria. Hayes and Lovley (2002) evaluated 16S rDNA sequences of bacteria associated with naphthalene mineralization under sulfate-reducing conditions enriched from contaminated San Diego Bay sediments and identified several organisms of the δ-Proteobacteria, closely related strain NaphS2. Analysis of 16S rDNA sequences in San Diego Bay sediments showed that 6-8% of the sequences from contaminated sites were closely related to the 16S rDNA sequence of NaphS2, whereas no sequences of the NaphS2 phylotype were recovered from nearby uncontaminated sediments. PAH-degrading sediments originating from Island End River (Boston, MA), Tampa Bay (Florida) and Liepaja Harbor (Latvia) were also observed to contain 16S rDNA sequences belonging to the NaphS2 phylotype based on amplification with a PCR primer designed on the phylotypic sequence of NaphS2-like bacteria, suggesting these bacteria may play an important role in naphthalene degradation under sulfate-reducing conditions in contaminated harbor sediments.

2.8.3 Bioavailability of PAHs

Bioavailability of the strongly hydrophobic PAH compounds is of concern where conversion of environmental PAH pollution to innocuous byproducts is the remedial goal. Soils that have been contaminated with PAHs for a long time (aged soils) typically hold less bioavailable compounds than soils that are recently contaminated (Hatzinger and Alexander, 1995; Carmichael et al., 1997; Erickson et al., 1993). However, in some instances, PAH compounds sorbed to soil or sediment surfaces may be more bioavailable as they may be brought into closer proximity to microorganisms that are similarly sorbed on the surfaces (Laor et al., 1999; Poeton et al., 1999). Some soil organisms have been shown to be capable of producing biosurfactants that may enhance mass transfer rates from the sorbed or NAPL phases, resulting in different bioavailability as compared to microorganisms that rely strictly on physical-chemical mass transfer from these phases (Stucki and Alexander, 1987; Deschênes et al., 1996; Guerin and Boyd, 1992; Aitken et al., 1998; Burd and Ward, 1996; Daghler et al., 1997; Voparil and Mayer, 2000; Mata-Sandoval et al., 2000). The overall influence these biosurfactant producing organisms have on the rate and extent of biodegradation in the subsurface remains to be determined (Bouchez et al., 1995; Volkering et al, 1992; Volkering et al., 1993; Wick et al., 2001; Aitken et al., 1998; Guerin and Boyd, 1992). At the present time, there are only a few empirical approaches to estimate the bioavailability or the amount of PAH that is available for biodegradation in a given soil or sediment (Joo, 2004).

2.8.4 Outstanding issues

Several gaps remain in the understanding of biodegradation of PAH compounds in contaminated systems. For natural attenuation to become a viable remedial option, a better understanding of the capacity of indigenous microbial consortia to transform PAHs into innocuous byproducts must be realized. Current knowledge of the biodiversity of PAH contaminated soils and sediments is largely derived from deterministic approaches, relying on the cultivability of microorganisms capable of degrading PAH compounds. These culture-dependent techniques may allow the study of only a small fraction of the biodiversity present in natural systems (Amann et al., 1995; Atlas and Bartha, 1992). For instance, recent evidence has suggested that PAH-degrading isolates are sensitive to simple selective pressures applied during cultivation such as inclusion or lack of solid surfaces or nonaqueous phase liquids (NAPLs) in the cultivation procedures (Bastiaens et al., 2000; Friedrich et al., 2000; Colores et al., 2000; Grosser et al., 2000). Current information regarding the genotypic and phylotypic diversity of PAH-degrading organisms may be biased by these

limitations of cultivability, and the natural metabolic activity of PAH-contaminated systems may be underestimated (Ahn et al., 1999; Lloyd-Jones et al., 1999; Widada et al., 2002). Future efforts to expand the breadth of our understanding of the genotypic and phylotypic bases for PAH-degradation should hinge around techniques that do not rely on cultivation.

2.9 Documenting Intrinsic Degradation Potential: Classical Approaches

Classical approaches to documenting natural attenuation at contaminated sites include evidencing long-term reduction of contaminant concentrations at appropriate monitoring locations with statistical techniques, plume-scale modeling based on measured site hydrological, soil physical-chemical, and aqueous geochemical properties, and screening site soils and sediments in laboratory-scale bioassays for biodegradation of pollutants of interest (EPRI, 1996; King et al., 1999; Davis et al., 1999). Although these approaches have been successful for documenting monoaromatic and aliphatic hydrocarbon biodegradation at fuel release sites, their use at PAH contaminated sites, where environmentally relevant concentrations may approach detection limits and significant variability in measured concentrations are common, may result in much longer-term monitoring efforts to deal with uncertainty in the data.

Plume-scale modeling of complex mixed contaminant plumes typically associated with PAH contaminated sites may lead to gross misinterpretation of site-level data when models are not applied with careful evaluation of the underlying assumptions. Environmental PAH contamination often involves complex waste mixtures, diverse and dynamic microbial consortia, and a broad and heterogeneous spatial distribution of geochemical environments often exhibiting localized micro-anaerobic conditions that become more predominant where the macro-scale influx of dissolved oxygen decreases. The consumption of any particular pollutant(s) emanating from a chemically complex mixed source may elicit a particular geochemical response(s). Monitoring only select "representative" groundwater pollutants emanating from a complex coal-tar source region (usually only 5-20% of the pollutants) may lead to the false impression that an observed reduction in terminal electron accepting compounds (TEAs) are directly and completely attributable to reduction in specific pollutants (U.S. EPA, 1999). Models of natural attenuation based on approaches that rely on mass balances between "biodegraded" pollutants and reduction in terminal electron acceptors exhibited in situ such as the instantaneous reaction approach should be carefully evaluated when applied to specific hydrocarbon compounds, especially in the complex waste mixtures emanating from environmental PAH contamination.

Although laboratory-scale incubations with contaminated site media may provide linkage between biodegradation of PAH compounds and the use of TEAs, these studies typically result in altered (enriched) microbial community structures that may not accurately reflect in-situ conditions (Amann et al., 1995). Furthermore, temporal heterogeneity in the aqueous geochemistry and microbial community structure at many PAH-contaminated sites may complicate data interpretation for modeling and monitoring efforts leading to additional difficulty when investigating natural attenuation as a potential remedial mechanism (Langworthy et al, 1998). Therefore a gap exists between interpreting microcosm study results as related to field-scale processes, hindering modeling effectiveness. Displaying MNA at PAH-contaminated sites will require much more effort (increased number of sampling events over a longer monitoring time frame, increased density of the monitoring well network both in numbers of wells and shorter distances between wells, and provision of conclusive tertiary lines of evidence) than at classical fuel-release sites to attain regulatory approval.

2.10   Documenting Intrinsic Degradation Potential: Emerging Molecular Approaches

The advent of emerging molecular techniques have made possible the identification and enumeration of complex microbial ecologies without cultivation. These technologies may be particularly useful in site characterizations and monitoring programs for documenting intrinsic microbial activity on PAH compounds, and hold promise for displaying sustained remediation potential as well as reducing monitoring events and time frames. Molecular techniques may be integrated into MNA approaches by monitoring for the presence and activity of organisms and catabolic genes related to the degradation of PAH pollutants at contaminated sites as evidenced in laboratory incubations with site soils or sediments, providing linkage between the two scales (Fleming et al., 1993; Zhou et al., 1997; Stapleton et al., 2000; Mesarch et al., 2000; Wilson et al., 1999; Laurie and Lloyd-Jones, 2000). The information gained may lead to better decision making regarding the use of MNA as a remedial mechanism, provide a much more accurate assessment of sustained intrinsic bioremediation potential, and aid in evaluating modeling assumptions. Typical emerging molecular techniques include fluorescence in situ hybridization (FISH), phospholipids ester-linked fatty acid (PLFA) profiles, terminal restriction fragment length polymorphisms (T-RFLP), gene-probing, and ribosomal RNA gene clone libraries (Kuske et al., 1997; Barns et al., 1999; Dunbar et al., 2000; Ritchie et al. 2000; Liesack and Stackebrandt, 1992; Weiss et al., 1996; Hugenholtz et al., 1998a, Hugenholtz et al., 1998b; Dojka et al., 2000; Dunbar et al., 1999). The

following describes how emerging molecular techniques are providing new and powerful information valuable to studies of intrinsic remediation potential.

2.10.1 Perturbation in Intrinsic Microbial Community Structure

Applied to contaminated sites, molecular microbiological techniques may be useful for identifying perturbations in contaminated aquifer community structures as compared to nearby pristine aquifer community structures, leading to identification of specific microbial taxa active in the degradation of contaminants of interest. (Dojka et al., 1998; Smit et al., 1997; MacNaughton et al., 1999; Rooney-Varga et al., 1999; Shi et al., 1999). Alternatively, these techniques may be applied to enrichment cultures with contaminated soils or sediments to infer degrading species. The presence of microorganisms associated with enrichment in PAH-degrading enrichment cultures in situ may imply intrinsic remediation potential. The primary goal of these studies is to show a phylotypic response to anthropogenic contamination and to link that response to the degradation of pollutants of interest.

These types of techniques have been applied to many monoaromatic and chlorinated hydrocarbon contaminated sites. Zarda et al. (1998) determined that increased numbers of soil bacteria, predominantly of the δ-Proteobacteria subdivision (of which many are sulfate reducers), and increased whole-cell hybridization rate (compared to DAPI counts) were associated with increased contaminant concentrations in a mono-aromatic hydrocarbon-contaminated aquifer. Since whole-cell hybridization rates are linked to cellular rRNA content, these results suggested that the mono-aromatic compounds were being used as growth substrates under sulfate-reducing conditions. Röling et al. (2001) observed changes in the denaturing gradient gel electrophoresis (DGGE) profiles of a landfill leachate plume that corresponded to changes in the redox environment. These researchers concluded that Geobacter spp. and iron reducing conditions deserved more attention in future natural attenuation studies. Pickup et al. (2001) determined that high phenol concentrations in a tar-acid polluted aquifer corresponded to a significant decline in bacterial populations. Although there was a high level of microbial diversity between sampling locations as determined by thermal gradient gel electrophoresis (TGGE), these researchers observed no significant trends between community structure and sampling levels, boreholes, or phenol concentration. Fang and Barcelona (1998) observed considerable microbial diversity throughout a jet fuel contaminated aquifer by analyzing phospholipids ester-linked fatty acids (PLFA) of aquifer materials. Hydrocarbon-contaminated anaerobic environments contained higher biomass and diversity than non-contaminated aerobic regions, suggesting anaerobic biodegradation of the jet fuel hydrocarbons. Richardson et al.

(2002) demonstrated that the combined the use of clone libraries, T-RFLP, FISH, and quantitative PCR can overcome individual limitations of each technique, providing a powerful tool for characterizing complex microbial communities as well as tracking and monitoring specific microbial species in environmental systems. Using a combination of these tools, they identified *Dehalococcoides* sp. as an important element of enrichment communities that dechlorinate TCE completely to ethane.

Application of these methods to PAH-contaminated soils and sediments is limited. One noteworthy publication is that of Eriksson et al. (2003) who studied the degradation of 11 two- to five-ring PAHs at low temperatures under aerobic and nitrate-reducing conditions in enrichment cultures from four northern and arctic soils exposed to diesel fuel, polychlorinated biphenyl, coal-tar, or creosote-PAH. These researchers noted that PAH degradation was severely limited by low temperatures in aerobic incubations whereas degradation under nitrate-reducing conditions was not substantially affected by a change in temperature from 20°C to 7°C. Using ribosomal intergenic spacer analysis, they identified microbes of the genera *Acidovorax*, *Bordetella*, *Pseudomonas*, *Sphingomonas*, and *Variovorax* in both their aerobic and nitrate-reducing enrichment cultures regardless of soil or sediment source.

2.10.2 Probing for Catabolic Genetic Elements

Gene-probing may also provide useful information regarding the potential for intrinsic PAH biodegradation in contaminated environmental systems. The use of gene probing requires identification of specific genetic sequences coding for production of catabolic enzymes related to the degradation of pollutants of interest. Several gene probes related to PAH degradation have been identified, some of which are summarized in Table 2.7.

The identification of gene probes related to PAH degradation has led to their application in PAH-contaminated systems. Langworthy et al. (1998) studied the genotypic and phenotypic responses of a riverine microbial community to PAH contamination in sediments from six locations along the Little Scioto River near Marion, Ohio. PLFA profiles were used to characterize the microbial community structure and nucleic acid analysis with autoradiographic techniques was used to quantify the frequency of the degradative genes (*alkB* (*alkane hydroxylase*), *nahA* (*naphthalene dioxygenase*), *nahH* (*2,3-catechol dioxygenase*), and *todC1/C2* (*toluene dioxygenase*)). These researchers observed mineralization of [UL-^{14}C] naphthalene, [UL-^{14}C]anthracene, [UL-^{14}C]fluorene, and [9-^{14}C]phenanthrene in laboratory incubations with heavily exposed (>100 µg·g^{-1} dry sediment)

and minimally exposed (<2 μg·g⁻¹ dry sediment) sediments (Langworthy et al., 2002). [7-
¹⁴C]benzo[a]pyrene mineralization was detected only in heavily exposed sediments. PAH
mineralization in exposed sediments was more extensive and initiated with shorter lag phases in all
cases. In situ, the total microbial biomass was highest in sediments of intermediate exposure, while
the most contaminated sediments held similar microbial biomass as uncontaminated sediments. The
community structure of uncontaminated sediments was dominated by gram positive bacteria,
anaerobic gram negative bacteria, and *Bacillus*-type organisms. Chronic exposure to PAHs resulted
in enrichment of aerobic gram negative bacteria and heterotrophic eukaryotes, suggesting
development of a food web whereby aerobic gram negative bacteria grew on PAH compounds and
served as a food source for predatory microeukaryotes. Seasonal variations were determined to be
just as influential on microbial community structure as exposure history, indicating that these types of
environmental stresses should be taken into consideration when attempting to identify alteration in the
microbial community structure due to anthropogenic contamination when evaluating intrinsic
bioremediation. All degradative gene sequences were identified in most sediments regardless of
exposure history, but *nahA* and *alkB* gene sequences occurred with significantly greater frequency in
contaminated sediments than in ambient sediments. These results clearly showed a response in the
microbial community structure to increased exposure to PAH pollutants and strongly supported
intrinsic bioremediation activity.

Ringleberg et al. (2001) combined gene probing and PLFA analysis to investigate genotypic
changes in the microbial community structure during successive biodegradation of specific PAH
compounds in bioslurry reactors to arrive at relationships that may be useful for evaluating in situ
microbial community structures for PAH-degrading potential. It was observed that biodegradation of
3-ring PAH moieties correlated to the growth of gram positive bacteria (i.e. *Rhodococcus* spp.) and
increases in naphthalene dioxygenase, biphenyl dioxygenase, and catechol 2,3-dioxygenase gene
copy numbers. Biodegradation of four ring PAH moieties was observed to correlate to the growth of
gram negative bacteria such as *Alcaligenes* and *Pseudomonas* spp., but not to an increase in the copy
number of any genetic elements of interest (toluene dioxygenase, toluene-4-monoxygenase, alkane
hydroxylase, biphenyl dioxygenase, catechol 2,3-dioxygenase, naphthalene dioxygenase, or 2-
nitrotoluene dioxygenase). These researchers speculated that such relationships may be useful for
probing in situ microbial communities at contaminated sites reducing reliance on costly and time
consuming laboratory treatability studies.

Although gene probing may eventually become a powerful tool for characterizing natural
microbial communities for PAH-degrading activity, the current extent of available genetic markers

may not be adequate for completely describing microbial metabolic capabilities (Widada et al., 2002). For instance, Berardesco et al. (1998) isolated 432 phenanthrene-degrading bacteria from intertidal sediments in the Boston Harbor including several *Pseudomonas* spp., *Vibrio* spp., *Burkholderia* spp., *Sphingomonas* spp., *Flavobacter*-like bacteria, and *Mycobacterium* spp. Less than 2.5% of the isolates hybridized to the nahAaAb (naphthalene dioxygenase) gene probe and 11.7% to the pY3-E16 gene probe encoding the upper pathway for catabolism of naphthalene, phenanthrene, and fluorene (Yang et al., 1994). These researchers concluded that the predominant genes that encode phenanthrene degradation in the diverse phenanthrene-degrading bacteria of the Boston Harbor sediments were not well characterized. This is supported by the work of Laurie and Lloyd-Jones (1999), who identified *phnAc* (*phenanthrene dioxygenase*) as a divergent gene cluster from classical *nah*-like genes for PAH degradation. In a later study these researchers noted that 53% of 79 naphthalene- and/or phenanthrene-degrading isolates from contaminated New Zealand soils failed to hybridize to *nahAc* (*naphthalene dioxygenase*), *phnAc* (*phenanthrene dioxygenase*), or GST (*glutathione S-transferase*) (Lloyd-Jones et al., 1999). Only a small fraction of phenanthrene-degrading bacteria hybridized to *nahAc*, and *phnAc* failed to hybridize to any naphthalene- or phenanthrene-degrading bacteria. These researchers hypothesized that the probing errors of this work were either due to the use of specific probes that have low sequence homology to similar catabolic genes of the unrepresented bacteria, or alternatively to uncharacterized genes for PAH catabolism.

2.10.3 Combined Molecular Microbiological and Isotopic Techniques

Several researchers are expanding the utility of molecular microbiological approaches by combining them with isotopic techniques to determine structure-function relationships in contaminated soils and sediments. Hansen et al. (1999) used a coupled PLFA and isotope tracer analysis to track ^{13}C enrichment in the phospholipids fatty acids of organisms incubated in soils with ^{13}C-toluene. These researchers were able to show 85% homology between ^{13}C-enriched PLFAs and those of a toluene degrading gram positive bacterium (strain YT2) isolated from the same soil. Pelz et al. (2001a) used similar ^{13}C-PLFA techniques to identify the in situ activity of *Azoarcus* spp. on toluene degradation under denitrifying conditions in petroleum hydrocarbon contaminated sediments from Studen, Switzerland. In a later study, these researchers identified *Desulfobacter* spp. active in growth on ^{13}C toluene based on ^{13}C-PLFA profiles of aquifer microcosms of the same site following incubation under sulfate-reducing conditions. An enrichment of organisms of the family *Desulfobacteriaceae* in the in situ community structure of the same contaminated sediments

exhibiting sulfate-reducing activity based on FISH supported their results. Johnsen et al. (2002) linked *Sphingomonas* spp. and other *β-Proteobacteria* to the degradation of phenanthrene in soils of a former asphalt production plant and a shipyard in Denmark by analyzing ^{13}C-labeled cell lipids following incubation with [^{13}C]phenanthrene. These researchers were also able to identify actinomycetes active in the degradation of phenanthrene in uncontaminated road-side soils, but did not recover 18:2ω6,9 PLFA from any soils tested suggesting that fungi did not assimilate the [^{13}C]phenanthrene. ^{13}C-PLFA techniques have also been used to identify styrene-degrading microorganisms in biofilters treating waste gases and phospholipids compositional changes of toluene-degrading bacteria in response to exposure to toluene (Alexandrina et al., 2001; Fang et al., 2000).

Radajewski and associates (2000) developed stable isotope probing (SIP) techniques to assess the diversity and population dynamics of methane oxidizing bacteria in the environment. After incubating environmental samples with ^{13}C-methanol, the community DNA was extracted and the ^{13}C-DNA fractionated from the ^{12}C-DNA by ultracentrifugation in cesium chloride/ethidium bromide density gradients. The ^{13}C-DNA fractions were used as templates for PCR with primers specific for bacterial, archaeal, and eukaryal small-subunit rRNA genes as well as mxaF. The amplified products were cloned, sequenced, and analyzed phylogenetically, revealing that the methylotrophs in their soils were confined to the *α-Proteobacteria* and *Acetobacterium* divisions, and were most closely related to genera that are rarely associated with methanol utilization. Padmanabhan et al. (2003) used ^{13}C-naphthalene and the SIP technique on uncontaminated soils from the Agricultural Research Station in Ithaca, New York and identified naphthalene-degrading *Acinetobacter* spp., *Variovorax* spp., and *Pseudomonas* spp.

In a select number of studies, researchers have been able to visually and quantitatively link the functional activity of microorganisms to their phylogenetic identity by incubating environmental samples with radioisotopic substrates and combining fluorescence in situ hybridizations with microautoradiography (known by several acronyms including MAR-FISH, MICRO-FISH, FISH-MAR, FISH-MARG, and STARFISH, but referred to as MICRO-FISH herein). By combining these techniques, these researchers can simultaneously visualize the incorporation of radioisotope into cellular mass and identify phylogenetic identity of organisms growing on the radioisotopic substrate. MICRO-FISH is a natural extension of microautoradiograghy-epifluorescence microscopy (MAR-EM), which incorporated the use of acridine orange direct counts or fluorescent antibodies for determining the substrate uptake and microbial growth in natural waters (Fliermans and Schmidt, 1975; Fuhrman and Azam, 1982; Meyer-Reil, 1978; Tabor and Neihof, 1982; Tabor and Neihof,

1984). More recently, it has been used in a similar fashion to visualize uptake patterns of simple organic and inorganic substrates into activated sludge, oceanic waters, and more recently, sewer biofilms (Nielsen et al., 1999; Lee et al., 1999; Ouverney and Fuhrman, 1999; Cottrell and Kirchman, 2000; Ito et al., 2002). Application of MICRO-FISH to identify organisms active in the uptake of xenobiotic compounds is limited to Yang et al. (2003), who used a coculture of *Pseudomonas putida* B2 and *Sphingomonas stygia* to demonstrate successful identification of microorganisms degrading o-nitrophenol.

Although combined isotopic and molecular approaches hold promise for enhancing site characterizations and monitored natural attenuation efforts, each technique has its limitations. For instance, stable carbon isotope-PLFA analyses may be limited in environments where several uncultivated organisms exist, potentially resulting in composite profiles unlike that of any single organism. The SIP technique has the distinct advantage of an ability to directly sequence the small subunit ^{13}C-rDNA of hydrocarbon-degrading bacteria to be assigned to a specific taxonomic clade. However, growth on sparingly soluble substrates may be limited by bioavailability. This may result in poor growth rates and low cell production inhibiting DNA-based stable isotope probing, which requires cell turn-over for new DNA to be constructed. Other methods such as RNA SIP and MICRO-FISH that do not require growth, but only maintenance of cell parts with isotopic carbon may be more appropriate to the study of structure-function relationships in HOC-contaminated systems. MICRO-FISH techniques may be hampered in cases where there exists limited information regarding the microbial community structure a-priori. All of the combined molecular microbiological and isotopic approaches rely on anabolism of the isotopic compound, and will fail to yield results where cometabolic or strict catabolic transformations take place. Labeling position on the isotopic compound may be of importance where dead-end metabolites are formed or where complete degradation requires several different species of microorganisms (e.g. initial attack by eukaryotic organisms followed by complete mineralization by commensal bacteria).

Aside from their limitations, molecular microbiological approaches hold promise for documenting intrinsic PAH biodegradation activity and sustainability in a more efficient and cost-effective manner than traditional approaches, potentially leading to greater acceptance of MNA at PAH contaminated sites. Technologies based on the emerging molecular microbiological techniques presented above that hold promise for impacting monitoring programs at the practical level are DNA microchip array technologies, the Biolog® system, quantitative PCR, and automated fluorescence in situ hybridization and flow cytometric systems, due to their current or pending future mechanization and potential for rapid and low cost turn-over of detailed microbial information.

2.11 Natural Attenuation of PAH-Contaminated Sites: Case Studies

Limited studies are available in the literature on the natural attenuation of sites contaminated with PAH compounds. The following is a summary of the results from these publications in which critical site parameters and degradation rates were reported. These results are tabulated in Table 2.8 along with results from other studies that have limited data. Where available, tertiary lines of evidence such as data from laboratory incubations with site sediments and/or results from molecular microbiological studies have been incorporated into the summaries. Regulatory acceptance of MNA at PAH contaminated sites may rely heavily on these tertiary lines of evidence, as much uncertainty may exist in monitoring data.

2.11.1 Case Study 1. EPRI Site No. 24, South Glenn Falls, Saratoga County, New York

This study was conducted to demonstrate and document the effectiveness of the removal of MGP tar source material and natural attenuation of the contaminant plume as a remediation alternative for MGP sites (EPRI, 1996). The 4.5-acre site is approximately 0.8 km northwest of the Hudson River and west of South Glenn Falls, New York. In the 1960's, several 200-liters drums of gas main sealant along with 15,000 to 60,000 liters of coal tar were pumped into a shallow, unlined trench at the site. The MGP waste has contaminated approximately 5,500 cubic meters of soil, forming a dissolved phase plume stretching approximately 430 m down-gradient. The geology of the site consists of a shallow (0.5 m) top soil layer underlain by 4.6 m of coarse to medium grained sands. Silt and clay to very fine-grained sands become predominant between 4.6 – 6 m below ground surface (bgs). Soil borings revealed a confining clay to silty clay layer between 6 to 7.3 m bgs. The sands were well sorted and stratified, characteristic of a glacial outwash deposit (EPRI, 1996). Hydraulic conductivities, measured by several slug tests and pumping tests, were found to range from 0.09 m/d to 8.16 m/d in the various silts and sediments. The average groundwater velocity through the site was estimated to be 0.096 m/d with an average horizontal hydraulic gradient of 0.0086 m/m. The average bulk density and porosity of the site soils were determined to be 1997 kg/m^3 and 0.35, respectively.

Remediation activities were initiated in 1987, which included source soil removal, groundwater contaminant, geochemistry, and microorganism sampling, laboratory batch biodegradation studies, and plume-scale modeling efforts with the numerical code MYGRT™. The focus of the monitoring program was the natural attenuation of the dissolved-phase plume following

source removal. Transects of the contaminant plume down the centerline and across the plume in several locations showed clearly that dissolved oxygen concentrations were depleted in regions of high PAH contamination suggesting that active bioremediation of the contaminant plume was occurring. Laboratory studies of site soils showed increased numbers of PAH-degrading organisms in the contaminated cores and elevated protozoa counts down-gradient of the source, supporting the premise that active bioattenuation was occurring in the contaminant plume (EPRI, 1996).

Investigations of the site soils within the dissolved-phase contaminant plume yielded organic carbon contents of the site soils between 0.5 % and 2.1 %, but in general less than 1%. Based on these results, the retardation coefficients for naphthalene, acenaphthylene, phenanthrene, and toluene were estimated to be 4.0, 2.7, 10, and 1.7, respectively. Using these coefficients with the MYGRT™ transport code and field sampling data, estimates of the first-order decay rate coefficients for naphthalene, acenaphthylene, phenanthrene, and toluene were found to be $2.7 \times 10^{-4} \, d^{-1}$, $2.7 \times 10^{-4} \, d^{-1}$, $2.7 \times 10^{-5} \, d^{-1}$, and $6.8 \times 10^{-4} \, d^{-1}$, respectively. Over the course of three years of monitoring the dissolved-phase plume after source removal, extensive dissipation in the naphthalene, acenaphthylene, and toluene plume sizes and concentrations were observed. No detectable phenanthrene was observed in any groundwater sample from any well three years after source removal. Modeling and monitoring results suggest that no naphthalene will be present at any location in the groundwater above the 10 μg/L detection limit by the year 2030.

2.11.2 Case Study 2. Former Manufacturing Gas Plant (FMGP) site, Charleston, South Carolina, U.S.A.

This study was conducted to assess whether contamination from a FMGP site that operated from 1855 to 1957 in downtown Charleston, South Carolina would impact the adjacent Cooper River. The path of the plume from the FMGP site to the Cooper River transverses an 8-acre National Park Service property (Campbell et al., 1996). According to Landmeyer et al. (1998), the geology of the property consists of two Quaternary lithostratigraphic marine units, the Wando Formation and Holocene deposits, overlain by fill. The fill is composed of sand, silt, wood, sawdust, concrete, bricks, cinders and various other scrap materials. The depth of the fill varies from 3 to 6.1 m deep, and is considered to be an unconfined (fill) aquifer. The Wando Formation consists of soft organic clay overlain by gray sand with a lower depth of about 23 m below ground level while the upper depth varied between 10.6 and 16.8 m below ground level (Campbell et al., 1996). It is considered to be the lower confined aquifer at the site. The Holocene deposits provide a confining layer between

the upper unconfined fill aquifer and lower confined sand aquifer. These deposits are composed of clayey to silty sand and soft, organic-rich clay with a thickness that varies from 1.5 m to as much as 12.2 m (Landmeyer et al., 1998). The hydraulic conductivities were from 0.03 to 3 m/d for the upper unconfined fill aquifer and 4.9 m/d for the lower confined sand aquifer. The depth to water at the site is approximately 0.5 m below ground level.

An intrinsic bioremediation study was initiated in 1993 which included sampling of groundwater contaminants and geochemical parameters, laboratory analysis of adsorption coefficients and biodegradation rates with aquifer materials, and modeling efforts of the plumes with the numerical code SUTRA (Campbell et al., 1996). The focus of the study was on the unconfined fill aquifer. During two sampling events of redox parameters in 1994 and again in 1997, dissolved oxygen was not present in any of the wells. High dissolved ferrous iron concentrations were observed in some wells. However, the presence of hydrogen at concentrations between 0.95 nM and 4.34 nM in these wells suggested that the ferrous iron was produced in earlier times of iron reducing conditions and that the aquifer was experiencing sulfate-reducing conditions (Landmeyer et al., 1998). This was evidenced by the concentrations of hydrogen sulfide and dissolved sulfate of up to 5.11 mg/L and 633 mg/L, respectively. The presence of methane up to 13.4 mg/L indicated that methanogenic bacteria were present within the contaminant plume as well. Campbell et al. (1996) determined through laboratory analyses that the first-order biodegradation rates of toluene using aquifer sediments were 0.84 d^{-1} and 0.0020 d^{-1} for aerobic and anaerobic environments, respectively while the laboratory adsorption coefficient was determined to be 0.94 L/kg. In the case of naphthalene, the first-order laboratory microbial degradation rates were 0.88 d^{-1} and 4.6 x 10^{-5} d^{-1} for aerobic and anaerobic environments, respectively. The naphthalene linear sorption coefficient for the sediments was estimated in the laboratory to be equal to or greater than 137 L/kg. Using site modeling techniques and field sampling data, these researchers reported best estimates for toluene first-order degradation rate constant and linear sorption coefficient to be 9 x 10^{-5} d^{-1} and 0.62 L/kg, respectively using hydraulic conductivities between 0.12 to 1.2 m/day. Using the same hydraulic conductivities the best-fit model estimates for the first-order degradation rate constant and linear sorption coefficient for naphthalene were 9.0 x 10^{-5} d^{-1} and 0.62 L/kg, respectively. These results showed that field degradation rates for these compounds were more closely related to anaerobic lab degradation rates. The model simulations using the modeled best-estimates indicated that toluene will not impact the Cooper River within 150 years but naphthalene will impact the Cooper River within this time period at a concentration of less than 5 mg/L.

2.11.3   Case Study 3. Creosote Source Emplacement, CFB Borden, Ontario, Canada

The natural attenuation study at the CFB Borden site was initiated on August 8, 1991. Coal tar creosote compounds were placed below the water table in two 1.5 m long by 5 m wide by 1.5 m deep excavations of an unused sand pit at CFB Borden, Ontario, Canada (Fowler et al., 1994; King and Barker, 1999). The source material consisted of 74 kg of creosote mixed with approximately 5,800 kg of sand and several kilograms of sodium chloride with a resulting residual creosote content of approximately 7% of the source pore volume. The geology of the site consisted of an unconsolidated aquifer of medium to fine sand of glacio-lacustrine origin with a hydraulic conductivity of approximately 6 m/d to 8.4 m/d, longitudinal dispersivity between 0.08 m and 0.036 m, and transverse dispersivity of 0.03 m to 0.039 m. The sand aquifer grades into silts and clays at a depth of approximately 9 m and the water table fluctuates between the ground surface and a depth of 1.5 m. The groundwater velocities were estimated to range between 0.081 m/d to 0.0947 m/d. The quality of the background groundwater was considered to be hard, with oxygen contents ranging up to 8.5 mg/L and averaging 2.47 mg/L, nitrate concentrations ranging from 0.6 mg/L to 6 mg/L, and sulfate concentrations were between 10 mg/L and 30 mg/L. The groundwater contained low dissolved organic carbon (<0.7 mg/L) and the temperature and pH varied between 6-15 °C and 7.1 to 7.9, respectively. The aquifer material had organic carbon contents ranging from 0.01% to 0.09% with an average of 0.02%. The porosity, bulk density, and solids density of the aquifer material taken as the volume-weighted arithmetic means of 36 samples were estimated to be 0.33, 1.81 g/cm^3, and 2.71 g/cm^3, respectively.

Groundwater samples were obtained from various multilevel samplers over the course of four years. Retardation coefficients were estimated from field data (based on chloride migration) for phenol (1.05), m-xylene (2.5 at 5.9 m from the source and 3.7 at 24.05 m from the source), naphthalene (2.6 at 5.9 m from the source and 3.5 at 24.05 m from the source), and dibenzofuran (3.12 at 5.9 m from the source) (King and Barker, 1999; King et al., 1999). Laboratory batch sorption experiments yielded linear distribution coefficients (L/kg) of 0.22 for naphthalene, 1.80 for phenanthrene, 0.67 for dibenzofuran, 0.83 for carbazole, and 0.24 for 1-methylnaphthalene, resulting in estimates of the linear retardation coefficients based solely on sorption of 2.2, 10.87, 4.67, 5.55, and 2.31, respectively. Batch sorption experiments for phenol and m-xylene yielded linear distribution coefficients equal to zero. Therefore, estimates of the linear distribution coefficients were made based on the octanol-water partition coefficients and equaled 0.01 for phenol and 0.11 for m-xylene, resulting in retardation coefficients of 1.05 and 1.6, respectively (King et al., 1999).

Redox parameters were monitored at 1,008 and 1,357 days after source emplacement both inside and outside the creosote plume. Average dissolved oxygen concentrations dropped from 2.47 mg/L outside the plume to 0.13 mg/L inside the plume. Nitrate and ammonia concentrations were greatly variable, however, the average values decreased from 2.35 mg/L to 1.51 mg/L and 0.62 mg/L to 0.21 mg/L, respectively, from outside to inside the contaminant plume. In addition, anaerobic degradation of the compounds was suggested by increases in reduced iron (0 mg/L to 0.2 mg/L), reduced manganese (<0.05 mg/L to 0.13 mg/L), and methane (0.001 mg/L to 0.036 mg/L) and a decrease in sulfate (14.1 mg/L to 11.6 mg/L) from outside to inside the contaminant plume. Phospholipids fatty acids analysis of aquifer cores indicated a higher concentration of microorganisms inside the contaminant plume than outside the plume.

Phenol was observed to deplete quickly from the source material and migrate as a discrete slug after 439 days, at which time the peak concentration was only 7% of the 55 day concentration compared to 44% for chloride, suggesting significant transformation given its low sorptivity. In contrast, dibenzofuran, naphthalene, phenanthrene, carbazole, 1-methylnaphthalene, and m-xylene were not completely released from the source. m-Xylene was observed to increase in extent from zero to 626 days followed by recession back to the source at 1,008 days and 1,357 days due to transformation. The dibenzofuran plume was observed to reach steady state by 1,008 days as the mass flux into the plume was balanced by mass transformation within the plume. Phenanthrene was observed to rapidly expand into the aquifer from 626 to 1,008 days and then receded and decreased in mass at 1,357 days. Like dibenzofuran, carbazole was observed to reach steady state between 1,008 and 1,357 days, but was attributed to a decrease in source loading. The naphthalene and 1-methylnaphthalene plumes steadily increased in extent and mass over the time course of the sampling while the source fluxes decreased. All compounds were observed to be transformed in the contaminant plume, with half-lives of 78 d, 1,215 d, 11 - 49 d, 173 d, 99 d, 41d, and 110 d for m-xylene, naphthalene, phenanthrene, 1-methylnaphthalene, phenol, dibenzofuran, and carbazole, respectively; the estimated first order decay coefficients were 8.9×10^{-3} d^{-1}, 5.7×10^{-4} d^{-1}, $0.014 - 0.063$ d^{-1}, 4.0×10^{-3} d^{-1}, 7×10^{-3} d^{-1}, 0.017×10^{-3} d^{-1}, and 6.3×10^{-3} d^{-1}, respectively. However, the phenanthrene half-life may be subjected to significant error due to the assumption of linearity between sampling events and large changes in phenanthrene concentration. Based upon the modeling results, it was expected that the naphthalene plume would continue to advance for at least two more years before reaching steady-state.

2.11.4 Case Study 4. Pulse Injection, Columbus Air Force Base, Macrodispersion Experiment Site
(MADE), Columbus, Mississippi

This natural attenuation study was initiated on June 26, 1990. The objective of this study was to measure degradation due to natural attenuation of a pulse injection of tritiated water, benzene, p-xylene, naphthalene, and o-dichlorobenzene in the saturated region of an unconfined aquifer at the macrodispersion experiment (MADE) site of Columbus Air Force Base, Columbus, Mississippi. At approximately 40 m down-gradient of the injection source, lower hydraulic conductivity regions prevail (0.86 m/d). From 40 m to approximately 200 m down-gradient of the injection source, the upper 3 m of the aquifer has an average hydraulic conductivity of 86 m/d while the hydraulic conductivity of the soil underlying this region remains low. Three hundred and twenty eight sampling wells were on the site, most of which contained multilevel samplers (Boggs et al., 1992).

A mass balance based on spatial moment analysis and compared with tritium migration was used to estimate biodegradation rates. A pulse of 9,600 L of dilute tracer and the organic compounds was released over 47.5 hours through 0.6 m screened intervals, 4 m below the phreatic surface, in five injection wells spaced at 1 m intervals forming a line normal to the direction of the hydraulic gradient. Concentrations in the injection fluid were 55.6 μCi/L tritium, 51.5 mg/L p-xylene containing 2.77 μCi/L ^{14}C radiolabeled p-xylene, 68.1 mg/L benzene, 7.23 mg/L naphthalene, and 32.8 mg/L o-dichlorobenzene. Aqueous samples were taken from multilevel samplers at 27, 132, 224, 328, and 440 days after injection, and dissolved oxygen concentrations were monitored 8 days prior to and 48, 111, 161, 264, and 330 days after injection.

Linear distribution coefficients estimated from batch studies on the aquifer material for naphthalene, o-dichlorobenzene, p-xylene, and benzene were 0.085 L/kg, 0.065 L/kg, 0.048 L/kg, and 0.059 L/kg, respectively. However, because of the strong influence of degradation, the effects of sorption on organic solute distributions were considered minimal and therefore ignored in assessing degradation rates. The temporal average dissolved oxygen concentration in the contaminant plume was determined to be 3.8 mg/L with a minimum individual value of 2.6 mg/L, suggesting aerobic conditions. Degradation in the Columbus aquifer material was observed to be approximately first order with an initial lag period attributed to microbial adaptation, cell growth and substrate limitation. The maximum first-order degradation plus dilution rates were taken directly from plots of contaminant concentration versus time. The degradation rates were then corrected to yield degradation rates for the four compounds by subtracting the first-order rate of migration of tritium out of the region of interest from these maximum values. The resulting approximate first order

degradation rate constants obtained from this method were 0.0066 d^{-1}, 0.0141 d^{-1}, 0.0063 d^{-1}, and

0.0059 d^{-1} for benzene, p-xylene, naphthalene, and o-dichlorobenzene, respectively.

In later studies, changes in the subsurface catabolic gene frequencies (*alkB*, *nahA*, *nahH*, *todC1C2*, and *xylA*) before emplacement and during natural attenuation of a model jet fuel mixture of similar composition to the previous injection mixture (containing: benzene, 7.6 mg·kg^{-1}; toluene, 1083 mg·kg^{-1}; ethylbenzene, 1163 mg·kg^{-1}; p-xylene, 1134 mg·kg^{-1}; naphthalene, 1282 mg·kg^{-1}; decane, 11713 mg·kg^{-1}; and potassium bromide, 45 mg·kg^{-1} as a conservative tracer) were characterized (Stapleton and Sayler, 1998; Stapleton et al., 2000). Prior to emplacement of the source material, the presence of all target gene sequences was observed in nearly all of the 60 samples analyzed. The average percent of the microbial community containing specific catabolic genetic elements were 10.8 (±11.2), 7.6 (±8.5), 11.1 (±12.0), 7.3 (±5.2), and 2.5 (±1.8) for *alkB*, *nahA*, *nahH*, *todC1C2*, and *xylA*, respectively. The average total (uncontaminated) biomass was estimated using hybridization to the 16S rDNA Universal oligonucleotide to be 7.7 x 10^8 ± 4.7 x 10^8 cells per gram sediment. Mineralization of benzene (20-60%), toluene (60-90%), naphthalene (60-90%), and phenanthrene (60-90%) after 14 days was observed in laboratory incubation with uncontaminated site sediments following lag phases of 1-5 days.

248 days following emplacement of the source material, the mineralization potentials of the site sediments in the plume increased over background values (e.g. naphthalene: averages of 21 and 40% and maximums of 42 and 60% in two samples at 24 hours incubation and less than 5% in background samples; toluene: averages of 5-10% and maximums of 10 and 32% in 24 hours and less than 5% in background samples). The largest impact on total microbial biomass in the aquifer occurred near the source trench, which initially exhibited a growth response at 164 days followed by a significant drop at 278 days following source emplacement. The presence of all catabolic genetic elements showed significant response to the hydrocarbon exposure suggesting the development of pollutant-degrading microbial community within the contaminant plume. At 40 days after source emplacement, the percent of the microbial community containing specific catabolic genetic elements in the source trench were 11%, 5%, 9%, 13%, and 1% for *alkB*, *nahA*, *nahH*, *todC1C2*, and *xylA*, respectively. The percent of the microbial community containing these genetic elements increased substantially at later times following source emplacement, peaking at 52% (462 days), 29% (164 days), 66% (278 days), 68% (164 days), and 83% (278 days) for *alkB*, *nahA*, *nahH*, *todC1C2*, and *xylA*, respectively. Sediments in the contaminant plume region responded similarly, but to a lesser extent. These results supported extensive potential of the intrinsic microbial community of this aquifer to respond to the anthropogenic contaminants observed in laboratory incubations with site

sediments, and highlighted the potential for molecular microbiological techniques to support monitoring efforts for MNA at PAH contaminated sites.

2.11.5   Case Study 5. Unlined Municipal and Industrial Landfill, Vejen, Denmark

The objective of this study was to identify specific redox environments controlling the fate of specific xenobiotic organic contaminants in a contaminant plume resulting from leachate leaking from an unlined municipal and industrial landfill in Vejen, Denmark. The landfill operated between 1962 and 1981. The leachate has been characterized and determined to contain BTEX, herbicides, phenols, substituted benzenes, and naphthalene (Lyngkilde and Christensen, 1992). The site geology consists of a shallow, unconfined, sandy glacioalluvial aquifer, confined at the bottom by a clay deposit at a depth of 20 m close to the landfill and rising to a depth of 10 m at a distance of 400 m to 500 m down-gradient of the landfill. Small clay lenses can be found within the aquifer with a single substantial clay lens stretching out into the aquifer from below the landfill. The pore water velocity in the landfill was estimated to be 0.41 m/d to 0.55 m/d.

Monitoring of the site was conducted at 41 well nests of two monitoring wells, each with a 10 cm sampling screen set at different depths, all within 130 m of the landfill and set upon the plume centerline. Prior to initiation of the study, redox sensitive parameters were monitored and it was estimated that the groundwater within the contaminant plume was primarily anaerobic. A methanogenic region stretching to less than 50 m from the landfill was followed by sulfidogenic, ferro-/manganogenic, and nitrate-reducing redox zones. Aerobic conditions were again observed at about 300 m down-gradient of the landfill.

Using chloride as a conservative tracer, the site was monitored for 285 days to observe the leachate plume characteristics. It was observed that the contaminant plume was stationary, and therefore the rate of source influx was balanced by degradation, dilution and dispersion. Changes in the chloride concentration were used to estimate dispersive losses and thus allowed for the estimation of degradative losses by subtracting dispersive losses from the overall change in concentration with distance for a specific compound. Utilizing this method, it was observed that the compounds studied completely degraded under anaerobic (ferrogenic) conditions. First-order degradation rate constants estimated from half lives taken from the plots of corrected compound disappearance versus distance for BTEX and naphthalene were 0.009 d^{-1} to 0.013 d^{-1} and 0.011d^{-1} to 0.015 d^{-1}, respectively (Lyngkilde and Christensen, 1992). Further studies of indigenous microcosms in aerobic, denitrifying, ferrogenic, and methanogenic conditions showed that naphthalene could only be

degraded under aerobic or ferrogenic conditions (Nielsen and Christensen, 1994; Albrechtsen and Christensen, 1994).

2.11.6 Case Study 6. Former Manufacturing Gas Plant (FMGP) site, Dubuque, Iowa, U.S.A.

The Dubuque Key City FMGP site is located on the south side of downtown Dubuque, Iowa, approximately 0.8 km west of the Mississippi River. The site originally operated as a coking facility (prior to 1862 until 1907), and was converted to and operated as a manufactured gas and peaking facility from 1907 to 1939. After plant closure, the site and the property directly to the west of the site housed petroleum service stations that operated between 1950 and 1993. Historic manufactured gas plant operations, waste disposal practice and leaking storage tanks in the manufactured gas plant facility resulted in contamination of the site with coal tar and MGP residuals. Leaking gasoline tanks at the petroleum service stations further complicated the contamination at the site and possibly increased the mobility and extent of migration of higher molecular weight polycyclic aromatic hydrocarbons (PAHs) that may be solublized by the gasoline. Natural attenuation as a remedial technology was investigated at this site (Ong et al., 2001).

The geology of the site may be divided into four units: a mixed fill, cohesive and granular alluvium, a granular alluvial aquifer and bedrock. The mixed fill is from 0.6 to 4.8 m thick and consists of sand, silt, clay, gravel and debris in varying proportions. The fill is underlain by a 1.5 to 5.8 m thick unit of interbedded cohesive and granular alluvium. The cohesive and granular alluvium is in turn underlain by an alluvial aquifer that ranges from 1.5 m to about 24.4 m thick. The alluvial aquifer is primarily composed of fine to medium grained sand and is underlain by sedimentary bedrock. The depth to groundwater at the site varies between 2.7 m to greater than 5.8 m bgs. The estimated hydraulic conductivities of the aquifer based upon slug tests in monitoring wells ranged from 1.5 m/d to 623 m/d. Hydraulic gradients on the site range from 0.004 to 0.006 m/m, with slight downward vertical gradients. Groundwater flows primarily from west-northwest to east-southeast through the site and towards the Mississippi River with a seepage velocity of between 56 m/yr and 84 m/yr.

Depleted dissolved oxygen, manganese, sulfate, and nitrate, and increased sulfide, nitrite, total and ferrous iron, and ammonia were measured in various monitoring wells located within the contaminant plume. These results indicate that various microbial processes are occurring within the plume. Utilizing a section of wells bisecting the plume and extending from the source region, reduction of several PAH and BTEX compounds with distance was observed. Assuming a steady-

state plume and first-order decay, the overall attenuation rate coefficients for several PAH and BTEX compounds were estimated. The overall attenuation rates were 0.0063 d^{-1}, 0.0081 d^{-1}, 0.0029 d^{-1}, 0.0028 d^{-1}, and 0.0043 d^{-1} for benzene, naphthalene, acenaphthylene, anthracene, and phenanthrene, respectively.

2.12   Summary and Outstanding Issues

There are not many studies on natural attenuation of PAH-contaminated sites. In the studies above, the first-order decay rates of naphthalene, acenaphthylene and phenanthrene based on modeling of field data were estimated to be 0.00057 to 0.0063 d^{-1}, 0.00027 d^{-1}, and 0.000027 to 0.063 d^{-1}, respectively. These studies tended to focus on the degradation of low molecular weight PAH compounds. The environmental fate of higher molecular weight PAHs (more than three rings) were not documented and remain unknown. Laboratory studies have indicated that higher molecular weight PAH compounds may be used as carbon and energy sources or biodegraded via cometabolism that is stimulated by the addition of low molecular weight PAH compounds or their metabolites. Organisms that can directly degrade higher molecular weight PAH compounds typically have the ability to use lower molecular weight PAH compounds. However, because of the complex nature of the pollution at many of the PAH-contaminated sites, it is unclear how the presence of low molecular weight PAHs will impact the biodegradation of the high molecular weight PAHs and vice versa.

The above studies have focused on merely showing a depletion of the PAH compounds at the field-scale, albeit from changes in source loading, sorption, degradation, or dispersion (dilution), and the use of simple models and laboratory studies to estimate the fate of PAHs in the environment. Modeling attenuation of these compounds typically involves several assumptions that may include steady-state plumes or rapid degradation rates (allowing the neglect of sorption), linear and reversible sorption models, and assumed source dissolution rates that remain constant. Aside from obvious limitations associated with characterizing source term and hydraulic modeling, modeling limitations imposed by these assumptions may preclude their usefulness as recent evidence has suggested that PAH sorption and desorption are highly non-linear and hysteric processes, and the strength of sorption can vary greatly with different geosorbents.

There is evidence from the measurement of geochemical parameters in the above studies that alternate electron acceptors (other than dissolved oxygen) are being consumed in PAH-contaminated plumes at various sites. At the field-scale, geochemical environments tend to intertwine and lose clear definition. Laboratory studies of PAH degradation with soils under different electron acceptor

conditions display a diversity of conditions under which PAH compounds may biodegrade including aerobic, nitrate reducing, ferrogenic, and sulfidogenic conditions. However, these studies are performed in strictly isolated geochemical environments, not allowing for the study of the relative importance of each electron acceptor in a complex mixed geochemical environment such as those commonly observed at the field-scale. Degradation of PAH compounds at a contaminated site may well take place in micro-aerophilic regions interbedded in anaerobic regions or sulfidogenic regions interbedded in ferrogenic regions, etc. It is reasonable to assume not all geochemical environments may be important at a particular site, and the relative importance of each may change from site to site. Furthermore, there is no direct evidence that the existence of a particular geochemical environment even correlates with the biodegradation of PAH rather than non-PAH compounds such as degradation byproducts or co-contaminating compounds. This makes delineation of important redox conditions for microbial degradation of PAH compounds at the site level difficult with current methods, complicating modeling and monitoring efforts as all geochemical environments must be considered. Elucidating the dominant electron acceptor conditions for the biodegradation of PAHs in PAH-contaminated plumes will assist in formulating strategies to stimulate and enhance the attenuation processes at these sites. Without an understanding of the biodegradation of PAHs in complex mixtures and the role of each electron acceptor, better models cannot be developed to predict the fate of PAH compounds during natural attenuation.

Some of the field conditions which were not addressed in the cited studies include the impact of residual contamination (in the form of nonaqueous phase liquids or coating of the soils with contaminants such as coal tar) on the solubilities and the final fate and transport of the PAHs. Furthermore, the impact of co-contaminating compounds such as volatile organic carbons and cyanide on the degradation, solubility, and transport of PAHs were not studied. Soils taken from several different environments have been shown to contain organisms capable of PAH degradation in different geochemical environments that are not consistent from site to site. Most studies of natural attenuation of PAH compounds, however, have continued to regard natural microbial communities as a homogenous "black box". Natural microbial communities are dynamic in composition and activity in time and space, and therefore the microbial "black box" of these complex sites should not be assumed homogenous and consistent.

Tertiary lines of evidence may be necessary to support efforts of monitored natural attenuation at PAH contaminated sites. The classical approach is incubation of site sediments under specific redox conditions to "screen" the sediments for biodegradation potential. In many cases these studies affect the soil or sediment microbial community structure from that of the in situ condition,

resulting in ambiguity regarding the applicability of laboratory results to modeling and monitoring efforts. Emerging molecular microbiological approaches may be well suited for bridging the gap between laboratory and field-scale studies, and in some cases may provide direct access to tertiary lines of evidence without cultivation saving time and effort. The examples presented above highlight the potential utility of emerging molecular microbiological techniques towards MNA efforts at PAH contaminated sites.

As the trend in natural attenuation policy shifts from merely displaying disappearance of contaminants at the field-scale to determining precisely the fate of the compounds (the definitive reasons for the depletion), the circumstantial evidences of attenuation processes will need to be supported by more direct evidence. Future studies will require a shift toward methods that better describe source releases and specifically track the fate and attenuation of PAH compounds from dilution, sorption, and biodegradation processes. These methods must have the capability of opening the microbial "black-box" at contaminated sites and allow the study of the specific microbiological fate of contaminants under hypoxic and changing heterogeneous conditions. Based on the few studies presented above, natural attenuation of low molecular weight PAHs appears to be promising for these sites. The exact fate of PAH compounds in general, especially the higher molecular weight PAHs, needs further investigation.

2.13   References

Ahn, Y., J. Sanseverino, and G. S. Sayler (1999) Analyses of polycyclic aromatic hydrocarbon-degrading bacteria isolated from contaminated soils, *Biodegradation*, 10(2), 149-157.

Aitken, M. D., W. T. Stringfellow, R. D. Nagel, C. Kazunga, and S. H. Chen (1998) Characteristics of phenanthrene-degrading bacteria isolated from soils contaminated with polycyclic aromatic hydrocarbons, *Can. J. Microbiol.*, 44(8), 743-752.

Albrechtsen, H. J. and T. H. Christensen (1994) Evidence for microbial iron reduction in a landfill leachate-polluted aquifer (Vejen, Denmark), *Appl. Environ. Microbiol.*, 60(11), 3920-3925.

Alexandrina, M., C. Klief, and A. Lipski (2001) Stable-isotope-based labeling of styrene-degrading microorganisms in biofilters, *Appl. Environ. Microbiol.*, 67(10), 4796-4804.

Amann R. I., B. J. Binder, R. J. Olson, S. W. Chisholm, R. Devereux, and D. A. Stahl (1990) Combination of 16S rRNA-targeted oligonucleotide probes with flow cytometry for analyzing mixed microbial populations, *Appl. Environ. Microbiol.*, 56(6), 1919-1925.

Amann, R. I., W. Ludwig, and K.-H. Schleifer (1995) Phylogenetic identification and in situ detection of individual microbial cells without cultivation, *Microbiol. Rev.*, **59**(1), 143-169.

Anderson, R. T. and D. R. Lovley (1999) Naphthalene and benzene degradation under Fe(III)-reducing conditions in petroleum-contaminated aquifers, *Bioremediation*, **3**(2), 121-135.

Arvin, E., and J. Flyvberg (1992) Groundwater pollution arising from the disposal of creosote waste, *J. Inst. Water Environ. Manag.*, **6**, 646-652.

Atlas, R. M., and R. Bartha (1992) Hydrocarbon biodegradation and oil spill bioremediation, In K. C. Marshall (Ed.) *Advances in Microbial Ecology, Vol. 12*, Plenum Press, New York, NY, 287-339.

Bakermans, C. (1999) Progress report – Diversity of expressed biodegradation genes in a contaminated field site, EPA Grant No. U915386, Cornell University.

Barbé, P., P. Lecomte, and R. Pazdej (1998). Characteristics of soils polluted by PAH, in *Contaminated Soil '98; Proceedings of the Sixth International FZK/TNO Conference on Contaminated Soil, 17-21 May 1998, Edinburgh, UK, Volume 2*, Thomas Telford Publishing, London, UK, 825-828.

Barns, S. M., S. L. Takala, and C. R. Kuske (1999) Wide distribution and diversity of members of the bacterial kingdom *Acidobacterium* in the environment, *Appl. Environ. Microbiol.*, **65**(4), 1731-1737.

Bastiens, L., D. Springael, P. Wattiau, H. Harms, R. DeWatcher, H. Verachtert, and L. Diels (2000) Isolation of adherent polycyclic aromatic hydrocarbon (PAH)-degrading bacteria using PAH-sorbing carriers, *Appl. Environ. Microbiol.*, **66**(5), 1834-1843.

Bayard, R. M., L. Barna, and R. Gourdon (1998). Influence of organic pollutants on sorption of naphthalene in contaminated soils, in *Contaminated Soil '98; Proceedings of the Sixth International FZK/TNO Conference on Contaminated Soil, 17-21 May 1998, Edinburgh, UK, Volume 2*, Thomas Telford Publishing, London, UK, 849-850.

Bayard, R. M., L. Barna, M. Borhane, and R. Gourdon (2000). Influence of the presence of PAHs and coal tar on naphthalene sorption in soils, *J. Contam. Hydrol.*, **46**(1-2), 61-80.

Bedessem, M. E., N. G. Swoboda-Colberg, and P. J. S. Colberg (1997) Naphthalene mineralization coupled to sulfate reduction in aquifer-derived enrichments, *FEMS Microbiol. Lett.*, **152**(2), 213-218.

Berardesco, G., S. Dyhrman, E. Gallagher, and M. P. Shiaris (1998) Spatial and temporal variation of phenanthrene-degrading bacteria in intertidal sediments, *Appl. Environ. Microbiol.*, **64**(7), 2560-2565.

Evaluation of bacterial strategies to promote bioavailability of hydrophobic pollutants for efficient bioremediation of contaminated soils (BIOVAB) (2000) EC Contract BIO4-CT97-2015, Vlaamse Instelling voor Technologisch Onderzoek (Vito), Mol, Belgium (coordinator), 53 pp.

Black & Veatch (1998) Interim remedial action report for soil and source material, prepared for IES Utilities Inc., Black & Veatch Waste Science, Inc., Kansas City, MO.

Bogan, B. W., L. M. Lahner, and J. R. Paterek (2001) Limited roles for salicylate and phthalate in bacterial PAH bioremediation, *Biorem. J.*, **5**(2), 93-100.

Boggs, J. M., S. C. Young, and L. M. Beard (1992) Field study of dispersion in a heterogeneous aquifer, 1. Overview and site description, *Water Resour. Res.*, **28**(12), 3281-3291.

Boldrin, B., A. Tiehm, and C. Fritzsche (1993) Degradation of phenanthrene, fluorene, fluoranthene, and pyrene by a *Mycobacterium* sp, *Appl. Environ. Microbiol.*, **59**(6), 1927-1930.

Boonchan, S., M. L. Britz, and G. A. Stanley (1998) Surfactant-enhanced biodegradation of high molecular weight polycyclic aromatic hydrocarbons by *Stenotrophomonas maltophilia*, *Biotechnol Bioeng.*, **59**(4), 482-94.

Bossert, I. D. and R. Bartha (1986) Structure-biodegradability relationships of polycyclic aromatic hydrocarbons in soil, *Bull. Environ. Contam. Toxicol.*, **37**(4), 490-495

Bouchez, M., D. Blanchet, and J. P. Vandecasteele (1995) Substrate availability in phenanthrene biodegradation: transfer mechanism and influence on metabolism, *Appl. Microbiol. Biotechnol.*, **43**(5), 952-960.

Bouchez, M., D. Blanchet, and J. P. Vandecasteele (1995) Degradation of polycyclic aromatic hydrocarbons by pure strains and by defined strain associations: inhibition phenomena and cometabolism, *Appl. Microbiol. Biotechnol.*, **43**(1), 156-164.

Bouchez, M., D. Blanchet, and J. P. Vandecasteele (1996) The microbiological fate of polycyclic aromatic hydrocarbons: carbon and oxygen balances for bacterial degradation of model compounds, *Appl. Microbiol. Biotechnol.*, **45**(4), 556-561.

Broholm, K., P. R. Jørgensen, A. B. Hansen, E. Arvin, and M. Hansen (1999) Transport of creosote compounds in a large, intact, macroporous clayey till column, *J. Contam. Hydrol.*, **39**(3-4), 309 – 329.

Brown, T. L., H. E. LeMay Jr., and B. E. Bursten (1994) *Chemistry: The Central Science*. Prentice Hall, Englewood Cliffs, N.J.

Brusseau, M. L., R. E. Jessup, and P. S. C. Rao (1991) Nonequilibrium sorption of organic chemicals: elucidation of rate-limiting processes, *Environ. Sci. Technol.*, **25**(1), 134-142.

Burd, G., and O. P. Ward (1996) Involvement of a surface-active high molecular weight factor in degradation of polycyclic aromatic hydrocarbons by *Pseudomonas marginalis*, *Can. J. Microbiol.*, **42**(8), 791-797.

Burton, M. B., M. M. Martinson, and K. D. Barr (1988) Biotech USA, in *5th Annual Industrial Water and Waste Conference*, San Francisco, CA, November, Elsevier, New York, NY.

Caldini, G., G. Cenci, R. Manenti, and G. Morozzi (1995) The ability of an environmental isolate of *Pseudomonas fluorescens* to utilize chrysene and other four-ring polynuclear aromatic hydrocarbons, *Appl. Microbiol. Biotechnol.*, **44**(1-2), 225-229.

Campbell, B. G., M. D. Petkewich, J. E. Landmeyer, and F. H. Chapelle (1996) *Geology, hydrogeology, and potential of intrinsic bioremediation at the National Park Service Dockside II Site and adjacent areas, Charleston, South Carolina, 1993–1994, Rep. No. 96-4170*, U.S. Geological Services, Columbia, S.C.

Carmichael, L. M., R. F. Christman, and F. K. Pfaender (1997) Desorption and mineralization kinetics of phenanthrene and chrysene in contaminated soils, *Environ. Sci. Technol.*, **31**(1), 126-132.

Chen, S. H., and M. D. Aitken (1999) Salicylate stimulates the degradation of high-molecular weight polycyclic aromatic hydrocarbons by *Pseudomonas saccharophila* P15, *Environ. Sci. Technol.*, **33**(3), 435-439.

Chiou, C. T., D. E. Kile, and D. W. Rutherford (2000) Sorption of selected organic compounds from water to a peat soil and its humic-acid and humin fractions: potential sources of the sorption nonlinearity, *Environ. Sci. Technol.*, **34**(7), 1254-1258.

Cho, J. S., J. T. Wilson, F. P. Beck, Jr. (2000) Measuring vertical profiles of hydraulic conductivity - with in-situ direct-push methods, *J. Environ. Eng.*, **126**(8), 775-776.

Cline, P. V., J. J. Delfino, and P. S. C. Rao (1991) Partitioning of aromatic constituents into water from gasoline and other complex solvent mixtures, *Environ. Sci. Technol.*, **25**(5), 914-920.

Coates, J. D., R. T. Anderson, and D. R. Lovley (1996a) Oxidation of polycyclic aromatic hydrocarbons under sulfate-reducing conditions, *Appl. Environ. Microbiol.*, **62**(3), 1099-1101.

Coates, J. D., R. T. Anderson, J. C. Woodward, E. J. P. Phillips, and D. R. Lovely (1996b) Anaerobic hydrocarbon degradation in petroleum-contaminated sediments under sulfate-reducing and artificially imposed iron-reducing conditions, *Environ. Sci. Technol.*, **30**(9), 2784-2789.

Coates, J. D., J. C. Woodward, J. Allen, P. Philp, and D. R. Lovley (1997) Anaerobic degradation of polycyclic aromatic hydrocarbons and alkanes in petroleum-contaminated marine harbor sediments, *Appl. Environ. Microbiol.*, **63**(9), 3589-3593.

Cole, J. R., B. Chai, T. L. Marsh, R. J. Farris, Q. Wang, S. A. Kulam, S. Chandra, D. M. McGarrell, T. M. Schmidt, G. M. Garrity, J. M. Tiedje, (2003) The Ribosomal Database Project (RDP-II): previewing a new autoaligner that allows regular updates and the new prokaryotic taxonomy, *Nucleic Acids Res.*, **31**(1), 442-443.

Colores, G. M., R. E. Macur, D. M. Ward, and W. P. Inskeep (2000) Molecular analysis of surfactant-driven microbial population shifts in hydrocarbon-contaminated soil, *Appl. Environ. Microbiol.*, **66**(7), 2959-2964.

Coover M. P., and R. C. C. Sims (1987) The effects of temperature on polycyclic aromatic hydrocarbon persistence in an unacclimated agricultural soil, *Hazard. Waste Hazard. Mater.*, **4**(2), 181 – 192.

Cottrell, M. T., and D. L. Kirchman (2000) Natural assemblages of marine proteobacteria and members of the *Cytophaga-Flavobacter* cluster consuming low- and high-molecular-weight dissolved organic matter, *Appl. Environ. Microbiol.*, **66**(4), 1692-1697.

Cutright, T. J., and S. Lee (1994) Remediation of PAH-contaminated soil using *Achromobacter* sp., *Energy Sources*, **16**(3), 279-287.

Cuypers, C., T. Grotenhuis, J. Joziasse, W. Rulkins (2000) Rapid persulfate oxidation predicts PAH bioavailability in soils and sediments, *Environ. Sci. Technol.*, **34**(10), 2057-2063.

Daane, L. L., I. Harjono, G. J. Zylstra, and M. M. Häggblom (2001) Isolation and characterization of polycyclic aromatic hydrocarbon-degrading bacteria associated with the rhizosphere of salt marsh plants, *Appl. Environ. Microbiol.*, **67**(6), 2683-2691.

Daims, H., A. Brühl, R. Amann, K. H. Schleifer, and M. Wagner (1999) The domain-specific probe EUB338 is insufficient for the detection of all bacteria: development and evaluation of a more comprehensive probe set, *Syst. Appl. Microbiol.*, **22**(3), 434-444.

Dagher, F., E. Déziel, P. Lirette, G. Paquette, J. G. Bisaillon, and R. Villemur (1997) Comparative study of five polycyclic aromatic hydrocarbon degrading bacterial strains isolated from contaminated soils, *Can. J. Microbiol.*, **43**(4), 368-377.

Davis J. I., and W. C. Evans (1964) Oxidative metabolism of naphthalene by soil pseudomonads. The ring fission mechanism, *Biochem. J.*, **91**(2), 251-261.

Davis, G. B., C. Barber, T. R. Power, J. Theirrin, B. M. Patterson, J. L. Rayner, and Q. Wu (1999) The variability and intrinsic remediation of a BTEX plume in anaerobic sulphate-rich groundwater, *J. Contam. Hydrol.*, **36**(3-4), 265-290.

Dean, J. H., M. J. Murray and E. C. Ward (1986) Toxic responses of the immune system, in *Casarett and Doull's Toxicology: The Basic Science of Poisons, Third Edition*, C.D. Klaassen, M.O. Amdur and J. Doull, Eds., Macmillian Publishing Co., New York, NY, 271-272.

Dean-Ross, D. and C. E. Cerniglia (1996) Degradation of pyrene by *Mycobacterium flavescens*, *Appl. Microbiol. Biotechnol.*, **46**(3), 307-312.

Dean-Raymond, D., and R. Bartha (1975) Biodegradation of some polynuclear aromatic petroleum components by marine bacteria, *Dev. Ind. Microbiol.*, **16**(1), 97-110.

Delorme, P., and M. Carlier (1998) Study of transfer mechanisms of the residues in the soils of former manufactured gas plant sites, in *Contaminated Soil '98; Proceedings of the Sixth International FZK/TNO Conference on Contaminated Soil, 17-21 May 1998, Edinburgh, UK, Volume 2*, Thomas Telford Publishing, London, UK, 831-832.

Deschénes, L., P. Lafrance, J. P. Villeneuve, and R. Samson (1996) Adding sodium dodecyl sulfate and *Pseudomonas aeruginosa* UG2 biosurfactants inhibits polycyclic aromatic hydrocarbon biodegradation in a weathered creosote-contaminated soil, *Appl. Microbiol. Biotechnol.*, **46**(5-6), 638-646.

Dojka, M. A., P. Hugenholtz, S. K. Haack, and N. R. Pace (1998) Microbial diversity in a hydrocarbon- and chlorinated-solvent-contaminated aquifer undergoing intrinsic bioremediation, *Appl. Environ. Microbiol.*, **64**(10), 3869-3877.

Dojka, M. A., J. K. Harris, and N. R. Pace (2000) Expanding the known diversity and experimental distribution of an uncultured phylogenetic division of bacteria, *Appl. Environ. Microbiol.*, **66**(4), 1617-1621.

Dunbar, J., S. Takala, S. M. Barns, J. A. Davis, and C. R. Kuske (1999) Levels of bacterial community diversity in four arid soils compared by cultivation and 16S rRNA gene cloning, *Appl. Environ. Microbiol.*, **65**(4), 1662-1669.

Dunbar, J., L. O. Ticknor, and C. R. Kuske (2000) Assessment of microbial diversity in four Southwestern United States soils by 16S rRNA terminal restriction fragment analysis, *Appl. Environ. Microbiol.*, **66**(7), 2943-2950.

Durate, J. C., S. D. David, A. Eusebio, and A. G. F. Menaia (1997) Biotechnology for waste management and site restoration-III: degradation of polycyclic aromatic hydrocarbons by microorganisms from contaminated soil, Kluwer Academic Publishers, 187-192.

Durant, N. D., L. P. Wilson, and E. J. Bouwer (1994) Screening for natural subsurface biotransformation of polycyclic aromatic hydrocarbons at a former manufactured gas plant, in *Bioremediation of Chlorinated and Polycyclic Aromatic Hydrocarbon Compounds*, R. E. Hinchee, A. Leeson, L. Semprini, S. K. Ong (Eds.), Lewis Publishers, Boca Raton, FL, 456-461.

Edison Electric Institute (1984) *Handbook on Manufactured Gas Plant Sites*, Utility Solid Waste Activities Superfund Committee, Edison Electric Institute, Washington D.C.

Electric Power Research Institute (EPRI) (1996) *Characterization and Monitoring Before and After Source Removal at a Former Manufactured Gas Plant (FMGP) Disposal Site, EPRI Rep. No. TR-105921*, Research Projects W02879-12; W02879-38, Palo Alto, Calif.

Ellis, L. B. M., B. K. Hou, W. Kang, and L. P. Wackett (2003) The University of Minnesota Biocatalysis/Biodegradation Database: post-genomic datamining, *Nucleic Acids Res.*, **31**(1), 262-265.

Erickson, D. C., R. C. Loehr, and E. F. Neuhauser (1993) PAH loss during bioremediation of manufactured gas plant site soils, *Water Res.*, **27**(5), 911-919.

Eriksson, M., E. Sodersten, Z. Yu, G. Dalhammar, and W. W. Mohn (2003) Degradation of polycyclic aromatic hydrocarbons at low temperature under aerobic and nitrate-reducing conditions in enrichment cultures from Northern soils, *Appl. Environ. Microbiol.*, **69**(1), 275-284.

Fang, J., M. J. Barcelona, and P. J. Alvarez (2000) Phospholipid compositional changes of five pseudomonad archetypes grown with and without toluene, *Appl. Microbiol. Biotechnol.*, **54**(3), 382-389.

Fang, J., M. J. Barcelona, R. V. Krishnamurthy, and E. A. Atekwana (2000) Stable carbon isotope biogeochemistry of an aquifer contaminated with fuel hydrocarbons, *Appl. Geochem.*, **15**(2), 157-169.

Field, J. A., F. Boelsma, H. Baten, and W. H. Rulkens (1995) Oxidation of anthracene in water/solvent mixtures by the white-rot fungus, *Bjerkandera* sp. strain BOS55, *Appl. Microbiol. Biotechnol.*, **44**(1-2), 234-240.

Fleming, J. T., J. S. Sanseverino, and G. S. Sayler (1993) Quantitative relationship between naphthalene catabolic gene frequency and expression in predicting PAH degradation in soils at town gas manufacturing sites, *Environ. Sci. Technol.*, **27**(6), 1068-1074.

Fliermans, C. B., and E. L. Schmidt (1975) Autoradiography and immunofluorescence combined for autecological study of single cell activity with nitrobacter as a model system, *Appl. Microbiol.*, **30**(4), 676-684.

Foght, J. M. and D. W. Westlake (1988) Degradation of polycyclic aromatic hydrocarbons and aromatic heterocycles by a *Pseudomonas* species, *Can. J. Microbiol.*, **34**(10), 1135-1141.

Fowler, M. G., P. W. Brooks, M. Northcott, and M. W. G. King (1994) Preliminary results from a field experiment investigating the fate of some creosote compounds in a natural aquifer, *Adv. Org. Geochem.*, **22**(3-5), 641-649.

Fredrickson, J. K., D. L. Balkwill, G. R. Drake, M. F. Romine, D. B. Ringelberg, and D. C. White (1995) Aromatic-degrading *Sphingomonas* isolates from the deep subsurface, *Appl Environ. Microbiol.*, **61**(5), 1917-1922.

Friedrich, M., R. J. Grosser, E. A. Kern, W. P. Inskeep, and D. M. Ward (2000) Effect of model sorptive phases on phenanthrene biodegradation: molecular analysis of enrichments and isolates suggests selection based on bioavailability, *Appl. Environ. Microbiol.*, **66**(7), 2703-2710.

Fuhrman, J. A. and F. Azam (1982) Thymidine incorporation as a measure of heterotrophic bacterioplankton production in marine surface waters: evaluation and field results, *Marine Biol.*, **66**(1), 109-120.

Galushko, A., D. Minz, B. Schrink, and F. Widdel (1999) Anaerobic degradation of naphthalene by a pure culture of a novel type of marine sulphate-reducing bacterium, *Environ. Microbiol.*, **1**(5), 415-420.

Gauthier, M. J., B. Lafay, R. Christen, L. Fernandez, M. Acquaviva, P. Bonin, and J. C. Betrand (1992) *Marinobacter hydrocarbonoclasticus* gen. nov., sp. nov., a new, extremely halotolerant, hydrocarbon-degrading marine bacterium, *Int. J. System. Bacteriol.*, **42**(4), 568-576.

Geiselbrecht, A. D., R. P. Herwig, J. W. Deming, and J. T. Staley (1996) Enumeration and phylogenetic analysis of polycyclic aromatic hydrocarbon-degrading marine bacteria from Puget Sound sediments, *Appl. Environ. Microbiol.*, **62**(9), 3344-3349.

Geiselbrecht, A. D., B. P. Hedlund, M. A. Tichi, and J. T. Staley (1998) Isolation of marine polycyclic aromatic hydrocarbon (PAH)-degrading *Cycloclasticus* strains from the Gulf of Mexico and comparison of their PAH degradation ability with that of Puget Sound *Cycloclasticus* strains, *Appl. Environ. Microbiol.*, **64**(12), 4703-4710.

Ghosh, U., J. S. Gillette, R. G. Luthy, and R. N. Zare (2000) Microscale location, characterization, and association of polycyclic aromatic hydrocarbons on harbor sediment particles, *Environ. Sci. Technol.*, **34**(9), 1729-1736.

Ghoshal, D., I. You, and I. C. Gunsalus (1987) Nucleotide sequence and expression of gene *nahH* of plasmid NAH7 and homology with gene *xylE* of TOL pWWO, *Gene*, **55**(1), 19-28.

Ghoshal, S., A. Ramaswami, and R. Luthy (1996) Biodegradation of naphthalene from coal tar and heptamethylnonane in mixed batch systems, *Environ. Sci. Technol.*, **30**(4), 1282-1291.

Goyal, A. K. and G. J. Zylstra (1996) Molecular cloning of novel genes for polycyclic aromatic hydrocarbon degradation from *Comamonas testosteroni* GZ39, *Appl. Environ. Microbiol.*, **62**(1), 230-236.

Grimberg, S. J., W. T. Stringfellow and M. D. Aitken (1996) Quantifying the biodegradation of phenanthrene by *Pseudomonas stutzeri* P16 in the presence of a nonionic surfactant, *Appl. Environ. Microbiol.*, **62**(7), 2387-2392.

Grosser, R. J., D. Warshawsky, and J. R. Vestal (1991) Indigenous and enhanced mineralization of pyrene, benzo(a)pyrene, and carbazole in soils, *Appl. Environ. Microbiol.*, **57**(12), 3462-3469.

Grosser, R. J., M. Friedrich, D. M. Ward, and W. P. Inskeep (2000) Effect of model sorptive phases on phenanthrene biodegradation: different enrichment conditions influence bioavailability and selection of phenanthrene-degrading isolates, *Appl. Environ. Microbiol.*, **66**(7), 2695-2702.

Guerin, W. F., and S. A. Boyd (1992) Differential bioavailability of soil-sorbed naphthalene to two bacterial species, *Appl. Environ. Microbiol.*, **58**(4), 1142-1152.

Gustafsson, V., F. Haghseta, C. Chan, J. MacFarlane, and P. M. Gschwend (1997) Quantification of the dilute sedimentary soot phase: implications for PAH speciation and bioavailability, *Environ. Sci. Technol.*, **31**(1), 203-209.

Hanson, J. R., J. L. Macalady, D. Harris, and K. M. Scow (1999) Linking toluene degradation with specific microbial populations in soil, *Appl. Environ. Microbiol.*, **65**(12), 5403-5408.

Hatheway, A. W. (1997) Manufactured gas plants: yesterday's pride, today's liability, *Civil Eng.*, November, 38-41.

Hatzinger, P. B. and M. Alexander (1995) Effect of aging of chemicals in soil on their biodegradability and extractability, *Environ. Sci. Technol.*, **29**(2), 537-545.

Hawthorne, S. B. and C. B. Grabanski (2000) Correlating selective supercritical fluid extraction with bioremediation behavior of PAHs in a field treatment plot, *Environ. Sci. Technol.*, **34**(19), 4103-4110.

Hayes, L. A. and D. R. Lovley (2002) Specific 16S rDNA sequences associated with naphthalene degradation under sulfate-reducing conditions in harbor sediments, *Microb. Ecol.*, **43**(1), 134-145.

Hedlund, B. P., A. D. Geiselbrecht, T. J. Blair, and J. T. Sraley (1999) Polycyclic aromatic hydrocarbon degradation by a new marine bacterium, *Neptunomonas naphthovorans* gen. nov., sp. nov., *Appl. Environ. Microbiol.*, **65**(1), 251 – 259.

Heitkamp, M. A. and C. E. Cerniglia (1987) Effects of chemical structure and exposure on the microbial degradation of polycyclic aromatic hydrocarbons in freshwater and estuarine ecosystems, *Environ. Toxicol. Chem.*, **6**(3), 535-546.

Heitkamp, M. A., J. P. Freeman, D. W. Miller, and C. E. Cerniglia (1988) Pyrene degradation by a *Mycobacterium* sp.: identification of ring oxidation and ring fission products, *Appl. Environ. Microbiol.*, **54**(10), 2556-2565.

Heitkamp, M. A., and C. E. Cerniglia (1988) Mineralization of polycyclic aromatic hydrocarbons by a bacterium isolated from sediment below an oil field, *Appl Environ Microbiol.*, **54**(6), 1612-1614.

Heitkamp, M. A., and C. E. Cerniglia (1989) Polycyclic aromatic hydrocarbon degradation by a *Mycobacterium* sp. in microcosms containing sediment and water from a pristine ecosystem, *Appl. Environ. Microbiol.*, **55**(8), 1968-1973.

Howard, P. H., R. S. Boethling, W. F. Jarvis, W. M. Meylan, and E. M. Michalenko (1991) *Handbook of Environmental Degradation Rates*, Lewis Publishers, Chelsea, MI.

Huang, W., and W. J. Weber Jr. (1997) A distributed reactivity model for sorption by soils and sediments. 10. Relationships between desorption, hysteresis, and the chemical characteristics of organic domains, *Environ. Sci. Technol.*, **31**(9), 2562-2569.

Hugenholtz, P., C. Pitulle, K. L. Hershberger, and N. R. Pace (1998a) Novel division level bacterial diversity in a Yellowstone hot spring, *J. Bacteriol.*, **180**(2), 366-376.

Hugenholtz, P., B. M. Goebel, and N. R. Pace (1998b) Impact of culture-independent studies on the emerging phylogenetic view of bacterial diversity, *J. Bacteriol.*, **180**(18), 4765-4774.

Ito, T., J. L. Nielsen, S. Okabe, Y. Watanabe, and P. H. Nielsen (2002) Phylogenetic identification and substrate uptake patterns of sulfate-reducing bacteria inhabiting an oxic-anoxic sewer

biofilm determined by combining microautoradiography and fluorescent in situ hybridization, *Appl. Environ. Microbiol.*, **68**(1), 356-364.

Johnsen, A. R., A. Winding, U. Karlson, and P. Roslev (2002) Linking of microorganisms to phenanthrene metabolism in soil by analysis of 13C-labeled cell lipids, *Appl. Environ. Microbiol.*, **68**(12), 6106-6113.

Jonker, M. T. O., and Smedes, F. (2000) Preferential sorption of planar contaminants in sediments from Lake Ketelmeer, The Netherlands, *Environ. Sci. Technol.*, **34**(9), 1620-1626.

Joo, I. (2004) Assessment of bioavailability of polycyclic aromatic hydrocarbon (PAH) in coal-tar contaminated soils, Master's Thesis, Iowa State University, Ames, Iowa.

Kasai, Y., H. Kishira, and S. Harayama (2002) Bacteria belonging to the genus *Cycloclasticus* play a primary role in the degradation of aromatic hydrocarbons released in a marine environment, *Appl. Environ. Microbiol.*, **68**(11), 5625-5633.

Kanaly, R., R. Bartha, S. Fogel, and M. Findlay (1997) Biodegradation of benzo[a]pyrene added in crude oil to uncontaminated soil, *Appl. Environ. Microbiol.*, **63**(11), 4511-4515

Kanaly, R. A., and S. Harayama (2000) Biodegradation of high-molecular-weight polycyclic aromatic hydrocarbons by bacteria, *J. Bacteriol.*, **182**(8), 2059-2067.

Karapanagioti, H. K., S. Kleineidam, D. A. Sabatini, P. Grathwohl, and B. Ligouis (2000) Impacts of heterogeneous organic matter on phenanthrene sorption: equilibrium and kinetic studies with aquifer material, *Environ. Sci. Technol.*, **34**(3), 406-414.

Kasterner M., Streibich S., and Beyer M. (1999). "Formation of bound residue during microbial degradation of [C-14] anthracene in soil." *Appl. Environ. Microbiol.*, 65, 1834-1842.

Kastner, M., M. Jammali-Breuer, and B. Mahro (1994) Enumeration and characterization of the soil microflora from hydrocarbon-contaminated soil sites able to mineralize polycyclic aromatic hydrocarbons (PAH), *Appl. Microbiol. Biotechnol.*, 41, 267-273.

Kazunga, C. and M. D. Aitken (2000) Products from the incomplete metabolism of pyrene by polycyclic aromatic hydrocarbon-degrading bacteria, *Appl. Environ. Microbiol.*, **66**(5), 1917-1922.

Kazunga, C., M. D. Aitken, A. Gold, and R. Sangaiah (2001) Fluoranthene-2,3- and -1,5-diones are novel products from the bacterial transformation of fluoranthene, *Environ. Sci. Technol.*, **35**(5), 917-922.

Keck, J., R. C. Sims, M. Coover, K. Park, and B. Symons (1989) Evidence for cooxidation of polynuclear aromatic hydrocarbons in soil, *Water Res.*, **23**(12), 1467-1476.

Kincannon D. F., and Y. S. Lin (1985) Microbial degradation of hazardous wastes by land treatment, *Proceedings of the Purdue Industrial Waste Conference*, Purdue University, IN, 40, 607-19.

King, M. W. G., and J. F. Barker (1999a) Migration and natural fate of a coal tar creosote plume 1. Overview and plume development, *J. Contam. Hydrol.*, 39(3-4), 249-279.

King, M. W. G., J. F. Barker, J. F. Devlin, and B. J. Butler (1999b) Migration and natural fate of a coal tar creosote plume 2. Mass balance and biodegradation indicators, *J. Contam. Hydrol.*, 39(3-4), 281-307.

Kjartanson, B. H., S. K. Ong, G. A. Stenback, and S. W. Rogers (2000) Des Moines Two Rivers FMGP Site, Department of Civil and Construction Engineering, Iowa State University, Ames, IA.

Kjartanson, B. H., S.K. Ong, G.A. Stenback, and S.W. Rogers (2001) Dubuque Key City FMGP Site, Department of Civil and Construction Engineering, Iowa State University, Ames, IA.

Kleespies, M., R. M. Kroppenstedt, F. A. Rainey, L. E. Webb, and E. Stackebrandt (1996) *Mycobacterium holderi* sp. nov., a new member of the fast-growing mycobacteria capable of degrading polycyclic aromatic hydrocarbons, *Int. J. Syst. Bacteriol.*, 46(3), 683-687.

Knopp, D., M. Siefert, V. Väänänen, and R. Niessner (2000) Determination of polycyclic aromatic hydrocarbons in contaminated water and soil samples by immunological and chromatographic methods, *Environ. Sci. Technol.*, 34(10), 2035-2041.

Komatsu, T., T. Omori, and T. Kodama (1993) Microbial degradation of the polycyclic aromatic hydrocarbons acenaphthene and acenaphthylene by a pure bacterial culture, *Biosci. Biotechnol. Biochem.*, 57(5), 864-865.

Kotterman, M. J. J., H. J. Reiberg, A. Huge, and J. A. Field (1998) Polycyclic aromatic hydrocarbon oxidation by the white-rot fungus, *Bjerkandera sp.* Bos55 in the presence of nonionic surfactants, *Biotechnol. Bioeng.*, 57(2), 220-227.

Krauss, M., W. Wilcke, and W. Zech (2000) Availability of polycyclic aromatic hydrocarbons (PAHs) and polychlorinated biphenyls (PCBs) to earthworms in urban soils, *Environ. Sci. Technol.*, 34(20), 4335-4340.

Kuske, C. R., S. M. Barns, and J. D. Busch (1997) Diverse uncultivated bacterial groups from soils of the arid Southwestern United States that are present in many geographic regions, *Appl. Environ. Microbiol.*, 63(9), 3614-3621.

LaGrega, M. D., P. L. Buckingham, and J. C. Evans (1994) *Hazardous Waste Management*, McGraw Hill, Inc., New York, NY.

Landmeyer, J. E., F. H. Chapelle, M. D. Petkewich, and P. M. Bradley (1998) Assessment of natural attenuation of aromatic hydrocarbons in groundwater near a former manufactured-gas plant, South Carolina, USA, *Environ. Geol.*, 34(4), 79–292.

Langworthy, D. E, R. D. Stapleton, G. S. Sayler, and R. H. Findlay (1998) Genotypic and phenotypic responses of a riverine microbial community to polycyclic aromatic hydrocarbon contamination, *Appl. Environ. Microbiol.*, 64(9), 3422-3428.

Laor, Y., P. F. Strom, and W. J. Farmer (1999) Bioavailability of phenanthrene sorbed to mineral-associated humic acid, *Water Res.*, 33(7), 1719-1729.

Laurie, A. D. and G. Lloyd-Jones (2000) Quantification of phnAc and nahAc in contaminated New Zealand soils by competitive PCR, *Appl. Environ. Microbiol.*, 66(5), 1814-1817.

Larsen, B. R., (1997) Remediating MGP brownfields, *Pollut. Eng.*, 29(5), 66-69.

Lee, L. S., M. Hagwall, J. J. Delfino, and P. S. C. Rao (1992a) Partitioning of polycyclic aromatic hydrocarbons from diesel fuel into water, *Environ. Sci. Technol.*, 26(11), 2104-2110.

Lee, L. S., P. S. C. Rao, and I. Okuda (1992b) Equilibrium partitioning of polycyclic aromatic hydrocarbons from coal tar into water, *Environ. Sci. Technol.*, 26(11), 2110-2115.

Lee, N., P. H. Nielsen, K. H. Andreasen, S. Juretschko, J. L. Nielsen, K. H. Schleifer, and M. Wagner (1999) Combination of fluorescent in situ hybridization and microautoradiography – a new tool for structure-function analyses in microbial ecology, *Appl. Environ. Microbiol.*, 65(3), 1289-1297.

Lee, P. H., S. K. Ong, J. Golchin, and G. L. Nelson (1999) Extraction method for analysis of PAHs in coal-tar-contaminated soils, *Pract. Period. Hazard., Toxic, Radioact. Waste Manag.*, 3(4), 155-162.

Lee, P. H., S. K. Ong, J. Golchin, and G. L. Nelson (2001) Use of solvents to enhance PAH biodegradation of coal-tar contaminated soils, *Water Res.*, 35(16), 3941-3949.

Leuking, A. D., W. Huang, S. Soderstrom-Scwartz, M. Kim, and W. J. Weber Jr. (2000) Relationship of soil organic matter characteristics to organic contaminant sequestration and bioavailability, *J. Environ. Qual.*, 29(2), 317-323.

Liesack, W. and E. Stackebrandt (1992) Occurrence of novel groups of the domain *Bacteria* as revealed by analysis of genetic material isolated from an Australian terrestrial environment, *J. Bacteriol.*, 174(15), 5072-5078.

Llobet-Brossa, E., R. Roselló-Mora, and R. Amann (1998) Microbial community composition of Wadden Sea sediments as revealed by fluorescence in situ hybridization, *Appl. Environ. Microbiol.*, 64(7), 2691-2696.

Lloyd-Jones, G., A. D. Laurie, D. W. F. Hunter, and R. Fraser (1999) Analysis of catabolic genes for naphthalene and phenanthrene degradation in contaminated New Zealand soils, *FEMS Microbiol. Ecol.*, **29**(1), 69-79.

Lovley, D. R., S. J. Giovannoni, D. C. White, J. E. Champine, E. J. Phillips, Y. A. Gorby, and S. Goodwin (1993) *Geobacter metallireducens* gen. nov. sp. nov., a microorganism capable of coupling the complete oxidation of organic compounds to the reduction of iron and other metals, *Arch. Microbiol.*, **159** (4), 336-344.

Loy, A., M. Horn, and M. Wagner (2003) probeBase - an online resource for rRNA-targeted oligonucleotide probes, *Nucleic Acids Res.*, **31**(1), 514-516.

Luthy, R. G., G. R. Aiken, M. L. Brusseau, S. D. Cunningham, P. M. Gschwend, J. J. Pignatello, M. Reinhard, S. J. Traina, W. J. Weber Jr., and J. C. Westall (1997) Sequestration of Hydrophobic Organic Contaminants by Geosorbents, *Environ. Sci. Technol.*, **31**(12), 3341-3347.

Lyngkilde, J., and T. H. Christensen (1992) Fate of organic contaminants in the redox zones of a landfill leachate plume (Vejen, Denmark), *J. Contam. Hydrol.*, **10**(4), 291-307.

MacDonald, J. A. (2000) Evaluating natural attenuation for groundwater cleanup, *Environ. Sci. Technol.*, **34**(15): 346A-353A.

MacFarlane, I. D., G. D. McCleary, H. L. Hoffman, and C. M. Logan (1994) Considering microbial conditions at a former manufactured gas plant, in *Bioremediation of Chlorinated and Polycyclic Aromatic Hydrocarbon Compounds*, R. E. Hinchee, A. Leeson, L. Semprini, S. K. Ong (Eds.), Lewis Publishers, Boca Raton, FL, pp. 462-468.

MacIntyre, W. G., M. Boggs, C. P. Antworth, and T. B. Stauffer (1993) Degradation kinetics of aromatic organic solutes introduced into a heterogeneous aquifer, *Water Resour. Res.*, **29**(12), 4045-4051.

MacLeod, C. J. A., and K. T. Semple (2000) Influence of contact time on extractability and degradation of pyrene in soils, *Environ. Sci. Technol.*, **34**(23) 4952-4957.

MacNaughton, S. J., J. R. Stephen, A. D. Venosa, G. A. Davis, Y. J. Chang, and D. C. White (1999) Microbial population changes during bioremediation of an experimental oil spill, *Appl. Environ. Microbiol.*, **65**(8), 3566-3574.

Mahaffey, W. R., D. T. Gibson, and C. E. Cerniglia (1988) Bacterial oxidation of chemical carcinogens: formation of polycyclic aromatic acids from benz[a]anthracene, *Appl. Environ. Microbiol.*, **54**(10), 2415-2423.

Manz W., R. Amann, W. Ludwig, M. Wagner, and K. H. Schleifer (1992) Phylogenetic oligodeoxynucleotide probes for the major subclasses of *Proteobacteria*: problems and solutions, *Syst. Appl. Microbiol.*, **15**(4), 593-600.

Manz W., R. Amann, W. Ludwig, M. Vancanneyt, and K. H. Schleifer (1996) Application of a suite of 16S rRNA-specific oligonucleotide probes designed to investigate bacteria of the phylum *cytophaga-flavobacter-bacteroides* in the natural environment, *Microbiol.*, **142**(5), 1097-1106.

Manz, W., M. Eisenbrecher, T. R. Neu, and U. Szewzyk (1998) Abundance and spatial organization of gram-negative sulfate reducing bacteria in activated sludge investigated by in situ probing with specific 16S rRNA targeted oligonucleotides, *FEMS Microbiol. Ecol.*, **25**(1), 43-61.

Mata-Sandoval, J. C., J. Karns, and A. Torrents (2000) Effect of ramnolipids produced by *Pseudomonas aeruginosa* UG2 on the solubilization of pesticides, *Environ. Sci. Technol.*, **34**(23), 4923-4930.

McFarland, M. J., and R. C. Sims (1991) Thermodynamic framework for evaluating PAH degradation in the subsurface, *Ground Water*, **29**(6), 885-895.

McGinnis, G. D., H. Borazjani, L. K. McFarland, D. F. Pope, and D. A. Strobel (1988) *Characterization and laboratory testing soil treatability studies for creosote and pentachlorophenol sludges and contaminated soil*, USEPA Report No. 600/2-88/055. Robert S. Kerr Environmental Laboratory, Ada, OK.

McNally, D. L., J. R. Mihelcic, and D. R. Lueking (1998) Biodegradation of three- and four-ring polycyclic aromatic hydrocarbons under aerobic and denitrifying conditions, *Environ. Sci. Technol.*, **32**(17), 2633-2639.

Meckenstock, R. U., E. Annweiler, W. Michaelis, H. H. Richnow, and B. Schink (2000) Anaerobic naphthalene degradation by a sulfate-reducing enrichment culture, *Appl. Environ. Microbiol.*, **66**(7), 2743-2747.

Meier, H., R. Amann, W. Ludwig, and K. H. Schleifer (1999) Specific oligonucleotide probes for in situ detection of a major group of gram-positive bacteria with low DNA G+C content, *Syst. Appl. Microbiol.*, **22**(2), 186-196.

Melcher, R. J., S. E. Apitz, and B. B. Hemmingsen (2002) Impact of irradiation and polycyclic aromatic hydrocarbon spiking on microbial populations in marine sediment for future aging and biodegradability studies, *Appl. Environ. Microbiol.*, **68**(6), 2858-2868.

Mesarch, M. B., C. H. Nakatsu, and L. Nies (2000) Development of catechol 2,3-dioxygenase-specific primers for monitoring bioremediation by competitive quantitative PCR, *Appl. Environ. Microbiol.*, **66**(2), 678-683.

Meyer-Reil, L. A. (1978) Autoradiography and epifluorescence microscopy combined for the determination of number and spectrum of actively metabolizing bacteria in natural waters, *Appl. Environ. Microbiol.*, **36**(3), 506-512.

Michel G. A., I. V. Huis, and J. Weners (1995) Biological PAH degradation in dredge sludges, In *Bioremediation of Recalcitrant Organics*, Hinchee, R.E., Hoppel, R.E., and Anderson, D.B. (eds.), Battelle Press, Columbus, Ohio, 17-22.

Milhelcic, J. R., and R. G. Luthy (1988a) Degradation of polycyclic aromatic hydrocarbon compounds under various redox conditions in soil-water systems, *Appl. Environ. Microbiol.*, **54**(5), 1182-1187.

Mihelcic, J. R., and R. G. Luthy (1988b) Microbial degradation of acenaphthene and naphthalene under denitrification conditions in soil-water systems, *Appl. Environ. Microbiol.*, **54**(5), 1188-1198.

Mihelcic, J. R., and R. G. Luthy (1991) Sorption and microbial degradation of naphthalene in soil-water suspensions under denitrification conditions, *Environ. Sci. Technol.*, **25**(1), 169-177.

Mueller, J. G., P. J. Chapman, and P. H. Pritchard (1989a) Action of a fluoranthene-utilizing bacterial community on polycyclic aromatic hydrocarbon components of creosote, *Appl. Environ. Microbiol.*, **55**(12), 3085-3090.

Mueller, J. G., P. J. Chapman, and P. H. Pritchard (1989b) Creosote-contaminated sites - their potential for bioremediation, *Environ. Sci. Technol.*, **23**(10), 1197-1201.

Mueller, J. G., P. J. Chapman, B. O. Blattmann, and P. H. Pritchard (1990) Isolation and characterization of a fluoranthene-utilizing strain of *Pseudomonas paucimobilis*, *Appl. Environ. Microbiol.*, **56**(4), 1079-1086.

Mueller, J. G., R. Devereux, D. L. Santavy, S. E. Lantz, S. G. Willis, and P. H. Pritchard (1997) Phylogenetic and physiological comparisons of PAH-degrading bacteria from geographically diverse soils, *Antonie Van Leeuwenhoek*, **71**(4), 329-343.

Nam, K., and M. Alexander (1998) Role of nanoporosity and hydrophobicity in sequestration and bioavailability: tests with model solids, *Environ. Sci. Technol.*, **32**(1), 71-74.

National Research Council (NRC) (2000) Natural attenuation for groundwater remediation, Committee on Intrinsic Remediation, Water Science and Technology Board, Board on

Radioactive Waste Management, Commission on Geosciences, Environment, and Resources, National Academy Press, Washington, D.C.

Neef, A. (1997) Anwendung der in situ einzelzell-identifizierung von bakterien zur populations analyse in komplexen mikrobiellen biozönosen, Doctoral thesis, Technische Universität München, Munich, Germany.

Neff, J. M. (1985) Polycyclic aromatic hydrocarbons, in *Fundamentals of Aquatic Toxicology*, G. M. Rand and S. R. Petrocelli (Eds.), Hemisphere Publishing Corporation, Washington, D.C.

Nielsen, P. H., and T. H. Christensen (1994) In situ measurement of degradation of specific organic compounds under aerobic, denitrifying, iron(III)-reducing, and methanogenic groundwater conditions, in *Bioremediation of Chlorinated and Polycyclic Aromatic Hydrocarbon Compounds*, R. E. Hinchee, A. Leeson, L. Semprini, S. K. Ong (Eds.), Lewis Publishers, Boca Raton, FL, 416-422.

Nielsen, P. H., K. Andreasen, N. Lee, and M. Wagner (1999) Use of microautoradiography and fluorescent in situ hybridization for characterization of microbial activity in activated sludge, *Water Sci. Technol.*, 39(1), 1-9.

Novotny, M., J. W. Strand, S. L. Smith, D. Wiesler, and F. J. Schwende (1981) Compositional studies of coal tar by capillary gas chromatography/mass spectrometry, *Fuel*, 60(2), 213 – 220.

Ong, S. K., B. H. Kjartanson, G. A. Stenback, J. Golchin, S. W. Rogers, and N. Miller (2001) Assessment of natural attenuation at a former manufactured gas plant site, *Proc., 6th Int. In Situ and On Site Bioremediation Conf.*, June 4-8, San Diego, CA.

Ouverney, C. C., and J. A. Furhman (1999) Combined microautoradiography - 16S rRNA probe technique for determination of radioisotope uptake by specific microbial cell types in situ, *Appl. Environ. Microbiol.*, 65(4), 1746-1752.

Padmanabhan, P., S. Padmanabhan, C. DeRito, A. Gray, D. Gannon, J. R. Snape, C. S. Tsai, W. Park, C. Jeon, and E. L. Madsen (2003) Respiration of 13C-labeled substrates added to soil in the field and subsequent 16S rRNA gene analysis of 13C-labeled soil DNA, *Appl. Environ. Microbiol.*, 69(3), 1614-1622.

Park K. S., R. C. Sims, and R. Dupont (1990) Transformation of PAHs in soil systems, *J. Environ. Eng.*, 116(3), 632-640.

Pelz, O., A. Chatzinotas, N. Andersen, S. M. Bernasconi, C. Hesse, W. R. Abraham, and J. Zeyer (2001) Use of isotopic and molecular techniques to link toluene degradation in denitrifying aquifer microcosms to specific microbial populations, *Arch. Microbiol.*, 175(4), 270-281.

Pelz, O., A. Chatzinotas, N. Andersen, S. M. Bernasconi, C. Hesse, W. R. Abraham, and J. Zeyer (2001) Tracing toluene-assimilating sulfate-reducing bacteria using 13C-incorporation in fatty acids and whole-cell hybridization, *FEMS Microbiol. Ecol.*, **38**(2-3), 123-131.

Peters, C., and R. Luthy (1993) Coal tar dissolution in water-miscible solvents: experimental evaluation, *Environ. Sci. Technol.*, **27**(13), 2831-2843.

Peters, C. A., P. A. Labieniec, and C. D. Knightes (1996) Multicomponent NAPL composition dynamics and risk, in *Proceedings of the ASCE Annual Convention: Non-aqueous Phase Liquids (NAPLs) in the Subsurface Environment: Assessment and Remediation*, L. N. Reddi (Ed.), Washington D.C., November 12-14, 681 – 692.

Poeton, T. S., H. D. Stensel, and S. E. Strand (1999) Biodegradation of polyaromatic hydrocarbons by marine bacteria: effect of solid phase on degradation kinetics, *Water Res.*, **33**(3), 868-880.

Pott, B., and T. Henrysson (1995) Ex situ bioremediation of polycyclic aromatic hydrocarbons in laboratory systems, In *Bioremediation of Recalcitrant Organics*, Hinchee, R.E., Hoppel, R.E., and Anderson, D.B. (eds.), Battelle Press, Columbus, Ohio, 39-44.

Priddle, M. W., and K. T. B. MacQuarrie (1994) Dissolution of creosote in groundwater: an experimental and modeling investigation, *J. Contam. Hydrol.*, **15**(1), 27-56.

Prince, R. C. and E. N. Drake (1999) Transformation and fate of polycyclic aromatic hydrocarbons in soil, in *Bioremediation of Contaminated Soils*, American Society of Agronomy, Crop Science Society of America, Soil Science Society of America, D. C. Adriano (Ed.), Madison, WI, 89-111.

Radajewski, S., P. Ineson, N. R. Parekh, and J. Colin Murrell (2000) Stable-isotope probing as a tool in microbial ecology, *Nature*, **403**(6770), 646-649.

Radding, S. B., T. Mill, C. W. Gould, D. H. Liu, H. L. Johnson, C. C. Bomberger, and C. V. Fojo (1976) *The Environmental Fate of Selected Polynuclear Aromatic Compounds*. U.S. Environmental Protection Agency, EPA-560/5-75-009, Cincinnati, OH.

Reid, B. J., J. D. Stokes, K. C. Jones, K. T. Semple (2000) Nonexhaustive cyclodextrin-based extraction technique for the evaluation of PAH bioavailability, *Environ. Sci. Technol.*, **34**(15), 3174-3179.

Richardson, R. E., V. K. Bhupathiraju, D. L. Song, T. A. Goulet, and L. Alvarez-Cohen (2002) Phylogenetic characterization of microbial communities that reductively dechlorinate TCE based upon a combination of molecular techniques, *Environ. Sci. Technol.*, **36**(12), 2652-2662.

Ritchie, N. J., M. E. Schutter, R. P. Dick, and D. D. Myrold (2000) Use of length heterogeneity PCR and fatty acid methyl ester profiles to characterize microbial communities in soil, *Appl. Environ. Microbiol.*, **66**(4), 1668-1675.

Rockne, K. J., J. C. Chee-Sanford, R. A. Sanford, B. P. Helund, J. T. Staley, and S. E. Strand (2000) Anaerobic naphthalene degradation by microbial pure cultures under nitrate-reducing conditions, *Appl. Environ. Microbiol.*, **66**(4), 1595-1601.

Roller, C., M. Wagner, R. Amann, W. Ludwig, and K. H. Schleifer (1994) In situ probing of Gram-positive bacteria with high DNA G+C content using 23S rRNA- targeted oligonucleotides, *Microbiol.*, **140**(10), 2849-2858. (Erratum in: *Microbiol.* (1995) **141**(5), 1267.)

Rölling, W. F. M., B. M. van Breukelen, M. Braster, B. Lin, and H. W. van Verseveld (2001) Relationships between microbial community structure and hydrochemistry in a landfill leachate-polluted aquifer, *Appl. Environ. Microbiol.*, **67**(10), 4619-4629.

Rooney-Varga, J. N., R. T. Anderson, J. L. Fraga, D. Ringelberg, and D. R. Lovley (1999) Microbial communities associated with anaerobic benzene degradation in a petroleum-contaminated aquifer, *Appl. Environ. Microbiol.*, **65**(7), 3056-3063.

Roslev, P., N. Iversen, and K. Henricksen (1998) Direct fingerprinting of metabolically active bacteria in environmental samples by substrate specific radiolabeling and lipid analysis, *J. Microbiol. Meth.*, **31**(3), 99-111.

Saito, A., T. Iwabuchi, and S. Harayama (2000) A novel phenanthrene dioxygenase from *Nocardiodes* sp. strain KP7: expression in *Escherichia coli*, *J. Bacteriol.*, **182**(8), 2134-2141.

Schwab A. P., M. K. Banks, and M. Arunachalam (1995) Biodegradation of polycyclic aromatic hydrocarbons in Rhizosphere soil, In *Bioremediation of Recalcitrant Organics*, Hinchee, R.E., Hoppel, R.E., and Anderson, D.B. (eds.), Battelle Press, Columbus, Ohio, 23 - 29.

Shi, Y., M. D. Zwolinski, M. E. Schreiber, J. M. Bahr, G. W. Sewell, and W. J. Hickey (1999) Molecular analysis of microbial community structures in pristine and contaminated aquifers: field and laboratory microcosm experiments, *Appl. Environ. Microbiol.*, **65**(5), 2143-2150.

Shairis, M. P. and J. J. Clooney (1983) Replica plating method for estimating phenanthrene-utilizing and phenanthrene-cometabolizing microorganisms, *Appl. Environ. Microbiol.*, **45**(2), 706-710.

Simon, M. J., T. D. Osslund, R. Saunders, B. D. Ensley, S. Suggs, A. Harcourt, W. Suen, D. L. Cruden, D. T. Gibson, and G. J. Zylstra (1993) Sequences of genes encoding naphthalene dioxygenase in *Pseudomonas putida* strains G7 and NCIB 9816-4, *Gene*, **127**(1), 31-37.

Simpkin T. J., and G. Giesbrecht (1994) Slurry bioremediation of polycyclic aromatic hydrocarbons in sediments from industrial complex, In *Bioremediation of Chlorinated and Polycyclic Aromatic Hydrocarbon Compounds,* Hinchee, R.E., Leeson, A., Semprini, L., and Ong, S.K. (eds.), Lewis Publishers, Boca Raton, FL., 484-488.

Sims, R. C., and M. R. Overcash (1983) Fate of polynuclear aromatic compounds (PNAs) in soil-plant systems, *Residue Rev.,* **88**(1), 1-68.

Smit, E., P. Leeflang, and K. Wernars (1997) Detection of shifts in microbial community structure and diversity in soil caused by copper contamination using amplified ribosomal DNA restriction analysis, *FEMS Microbiol. Lett.,* **23**(2-3), 249-261.

Stahl, D. A., and R. Amann. (1991) Development and application of nucleic acid probes, in *Nucleic acid techniques in bacterial systematics,* E. Stackebrandt and M. Goodfellow (ed.), John Wiley & Sons Ltd., Chichester, England, 205-248.

Stapelton, R. D., G. S. Sayler, J. M. Boggs, E. L. Libelo, T. Stauffer, and W. G. Macintyre (2000) Changes in subsurface catabolic gene frequencies during natural attenuation of petroleum hydrocarbons, *Environ. Sci. Technol.,* **34**(10), 1991-1999.

Stapleton, R. D., S. Ripp, L. Jimenez, S. Cheol-Koh, J. T. Fleming, I. R. Gregory, and G. S. Sayler (1998) Nucleic acid analytical approaches in bioremediation: site assessment and characterization, *J. Microbiol. Methods,* **32**(2), 165-178.

Stapelton, R. D., and G. S. Sayler (1998) Assessment of the microbiological potential for the natural attenuation of petroleum hydrocarbons in a shallow aquifer system, *Microb. Ecol.,* **36**(3), 349-361.

Stringfellow, W. T., and M. D. Aitken (1995) Competitive metabolism of naphthalene, methylnaphthalene, and fluorene by phenanthrene degrading pseudomonads, *Appl. Environ. Microbiol.,* **61**(1), 357 – 362.

Stringfellow, W. T., and L. Alvarez-Cohen (1999) Evaluating the relationship between the sorption of PAHs to bacterial biomass and biodegradation, *Water Res.,* **33**(11), 2535-2544.

Stucki, G., and M. Alexander (1987) Role of dissolution rate and solubility in biodegradation of aromatic compounds, *Appl. Environ. Microbiol.,* **53**(2), 292-297.

Sutherland, J. B., J. P. Freeman, A. L. Selby, P. P. Fu, D. W. Miller, and C. E. Cerniglia (1990) Stereoselective formation of a K-region dihydrodiol from phenanthrene by *Streptomyces flavovirens, Arch. Microbiol.,* **154**(3), 260-266.

Sutherland, J. B., F. Rafi, A. A. Khan, and C. E. Cerniglia (1995) Mechanisms of polycyclic aromatic hydrocarbon degradation, in microbial transformation and degradation of toxic organic chemicals, L. Y. Young and C. E. Cerniglia (Eds.), Wiley-Liss, New York, NY, 269-306.

Tabor, P. S., and R. A. Neihof (1982) Improved microautoradiographic method to determine individual microorganisms active in substrate uptake in natural waters, *Appl. Environ. Microbiol.*, **44**(4), 945-953.

Tabor, P. S., and R. A. Neihof (1984) Direct determination of activities for microorganisms of Chesapeake Bay populations, *Appl. Environ. Microbiol.*, **48**(5), 1012-1019.

Tagger, S., N. Truffaunt, and J. Le Petit (1990) Preliminary study on relationships among strains forming a bacterial community selected on naphthalene from a marine sediment, *Can. J. Microbiol.*, **36**(10), 676-681.

Tanner, M. A., B. M. Goebel, M. A. Dojka, and N. R. Pace (1998) Specific ribosomal DNA sequences from diverse environmental settings correlate with experimental contaminants, *Appl. Environ. Microbiol.*, **64**(8), 3110-3113.

Theron, J. and T. E. Cleote (2000) Molecular techniques for determining microbial diversity and community structure in natural environments, *Crit. Rev. Microbiol.*, **26**(1), 37-57.

Thierrin, J., G. B. Davis, C. Barber, B. M. Patterson, F. Pribac, T. R. Power, and M. Lambert (1993) Natural degradation rates of BTEX compounds and naphthalene in a sulfate reducing groundwater environment, *Hydrol. Sci. J.*, **38**(4), 309-322.

Thierrin, J., G. B. Davis, and C. Barber (1995) A groundwater tracer test with deuterated compounds for monitoring in situ biodegradation and retardation of aromatic compounds, *Ground Water*, **33**(3), 469-475.

Trenz, S. P., K. H. Engesser, P. Fischer, and H. J. Knackmuss (1994) Degradation of fluorene by *Brevibacterium* sp. strain DPO 1361: a novel C-C bond cleavage mechanism via 1,10-dihydro-1,10-dihydroxyfluoren-9-one, *J. Bacteriol.*, **176**(3), 789-95.

Unge, A., R. Tombolini, L. Mølbak, and J. K. Jansson (1999) Simultaneous monitoring of cell number and metabolic activity of specific bacterial populations with a dual gfp-luxAB marker system, *Appl. Envir. Microbiol.*, **65**(2), 813-821.

U.S. EPA (1988) Test methods for evaluating solid waste physical/chemical methods, Method # 3540, Office of Solid Waste and Emergency Response, US Environmental Protection Agency, Washington, DC.

U.S. EPA (1999) Use of Monitored Natural Attenuation at Superfund, RCRA Corrective Action, and Underground Storage Tank Sites, Office of Solid Waste and Emergency Response Policy

Directive 9200.4-17P, EPA, Office of Solid Waste and Emergency Response, U.S. Government Printing Office, Washington, D.C., April 21, 41 pp.

U.S. EPA (2000) Superfund Sites, http://www.epa.gov/superfund/sites/index.htm, US Environmental Protection Agency, Washington, D.C., (accessed 5th of May, 2000).

Uz, I., Y. P. Duan, and A. Ogram (1998) Characterization of the PAH degrading bacterium, *Rhodococcus opacus* M213, *FEMS Microbiol. Lett.*, **185**(2), 231-238.

Vila, J., Z. López, J. Sabaté, C. Minguillón, A. M. Solanas, and M. Grifoll (2001) Identification of a novel metabolite in the degradation of pyrene by *Mycobacterium* sp. strain AP1: actions of the isolate on two- and three-ring polycyclic aromatic hydrocarbons, *Appl. Environ. Microbiol.*, **67**(12), 5497-5505.

Volkering, F., A. M. Bruere, and J. G. van Andel (1993) Effect of micro-organisms on the bioavailability and biodegradation of crystalline naphthalene, *Appl. Microbiol. Biotechnol.*, **40**(4), 535-540.

Volkering, F., A. M. Bruere, A. Sterkenburg, and J. G. van Andel (1992) Microbial degradation of polycyclic aromatic hydrocarbons: effect of substrate availability on bacterial growth kinetics, *Appl. Microbiol. Biotechnol.*, **36**(4), 548-552.

Voparil, I. M., and L. M. Mayer (2000) Dissolution of sedimentary polycyclic aromatic hydrocarbons into the lugworm's (*Arenicola marina*) digestive fluids, *Environ. Sci. Technol.*, **34**(7), 1221-1228.

Wallner, G., R. Amann, and W. Beisker (1993) Optimizing fluorescent in situ hybridization with rRNA-targeted oligonucleotide probes for flow cytometric identification of microorganisms, *Cytometry*, **14**(2), 136-143.

Walter, U., M. Beyer, J. Klein, and H. J. Rehm (1991) Degradation of pyrene by *Rhodococcus* sp. UW1, *Appl. Microbiol. Biotechnol.*, **34**(6), 671-676.

Wang, Y. and P. C. Lau (1996) Sequence and expression of an isocitrate dehydrogenase-encoding gene from a polycyclic aromatic hydrocarbon oxidizer, *Sphingomonas yanoikuyae* B1, *Gene*, **168**(1), 15-21.

Wang, R. F., W. W. Cao, and C. E. Cerniglia (1995) Phylogenetic analysis of polycyclic aromatic hydrocarbon degrading *mycobacteria* by 16S rRNA sequencing, *FEMS Microbiol. Lett.*, **130**(1), 75-80.

Weber, W. J. Jr., W. Huang, and H. Yu (1998) Hysteresis in the desorption of hydrophobic organic contaminants by soils and sediments, *J. Contam. Hydrol.*, **31**(1-2), 149-165.

Weiss, P., B. Schweitzer, R. Amann, and M. Simon (1996) Identification in situ and dynamics of bacteria on limnetic organic aggregates (lake snow), *Appl. Environ. Microbiol.*, **62**(6), 1998-2005.

Weissenfels, W. D., M. Beyer, and J. Klein (1990) Degradation of phenanthrene, fluorene, and fluoranthene by pure bacterial cultures, *Appl. Microbiol. Biotechnol.*, **32**(4), 479-484.

Weissenfels, W. D., M. Beyer, J. Klein, and H. J. Rehm (1991) Microbial metabolism of fluoranthene: isolation and identification of ring fission products, *Appl. Microbiol. Biotechnol.*, **34**(4), 528-535.

Wiedemeier, T. H., H. S. Rifai, C. Newel, J. T. Wilson (1999) Natural attenuation of fuels and chlorinated solvents in the subsurface, John Wiley and Sons, New York, NY.

Wick, L. Y., T. Colangelo, and H. Harms (2001) Kinetics of mass transfer-limited bacterial growth on solid PAHs, *Environ. Sci. Technol.*, **35**(2), 354-361.

Widada, J., H. Nojiri, K. Kasuga, T. Yoshida, H. Habe, and T. Omori (2002) Molecular detection and diversity of polycyclic aromatic hydrocarbon-degrading bacteria isolated from geographically diverse sites, *Appl. Microbiol. Biotechnol.*, **58**(2), 202-209.

Wilson, M. S., C. Bakermans, and E. L. Madsen (1999) In situ, real-time catabolic gene expression: extraction and characterization of naphthalene dioxygenase mRNA transcripts from groundwater, *Appl. Environ. Microbiol.*, **65**(1), 80-87.

Wolter, M. A., F. Zadrazil, R. Martens, and M. Bahadir (1997) Degradation of 8 highly condensed polycyclic aromatic hydrocarbons by *Pleurotus sp. Florida* in solid wheat-straw substrate, *Appl. Microbiol. and Biotechnol.*, **48**(3), 398-404.

World Health Organization. (1998) *Selected non-heterocyclic polycyclic aromatic hydrocarbons. Environmental Health Criteria* No. 202. World Health Organization, Geneva, Switzerland.

Xia, G., and W. P. Ball (2000) Polyani-based models for the competitive sorption of low-polarity organic contaminants on a natural sorbent, *Environ. Sci. Technol.*, **34**(7), 1246-1253.

Yang, Y., A. Zarda, and J. Zeyera (2003) Combination of microautoradiography and fluorescence in situ hybridization for identification of microorganisms degrading xenobiotic contaminants, *Environ. Toxicol. Chem.*, **22**(12), 2840–2844.

Ye, D. Y., M. A. Siddiqi, A. E. Maccubbin, S. Kumar, and H. C. Sikka (1996) Degradation of polynuclear aromatic hydrocarbons by *Sphingomonas paucimobilis*, *Environ. Sci. Technol.*, **30**(1), 136-142.

You, I. S., D. Ghoshal, and I. C. Gunsalus (1988) Nucleotide sequence of plasmid NAH7 gene nahR and DNA binding of the nahR product, *J. Bacteriol.*, **170**(12), 5409-5415.

You, I. S., D. Ghoshal, and I. C. Gunsalus (1991) Nucleotide sequence analysis of the *Pseudomonas putida* PpG7 salicylate hydroxylase gene (nahG) and its 3/-flanking region, *Biochem.*, **30**(6), 1635-1641.

Young, T. M. and W. J. Weber Jr. (1995) A distributed reactivity model for sorption by soils and sediments. 3. Effects of diagenetic processes on sorption energetics, *Environ. Sci. Technol.*, **29**(1), 92-97.

Zarda, B., D. Hahn, A. Chatzinotas, W. Schönhuber, A. Neef, R. Amann, and J. Zeyer (1997) Analysis of bacterial community structure in bulk soil by in situ hybridization, *Arch. Microbiol.*, **168**(3), 185-192.

Zhang, X. and L. Y. Young (1997) Carboxylation as an initial reaction in the anaerobic metabolism of naphthalene and phenanthrene by sulfidogenic consortia, *Appl. Environ. Microbiol.*, **63**(12), 4759-4764.

Zhou, J., A. V. Palumbo, and J. M. Tiedje (1997) Sensitive detection of a novel class of toluene-degrading denitrifiers, *Azoarcus tolulyticus*, with small-subunit rRNA primers and probes, *Appl. Environ. Microbiol.*, **63**(6), 2384-2390.
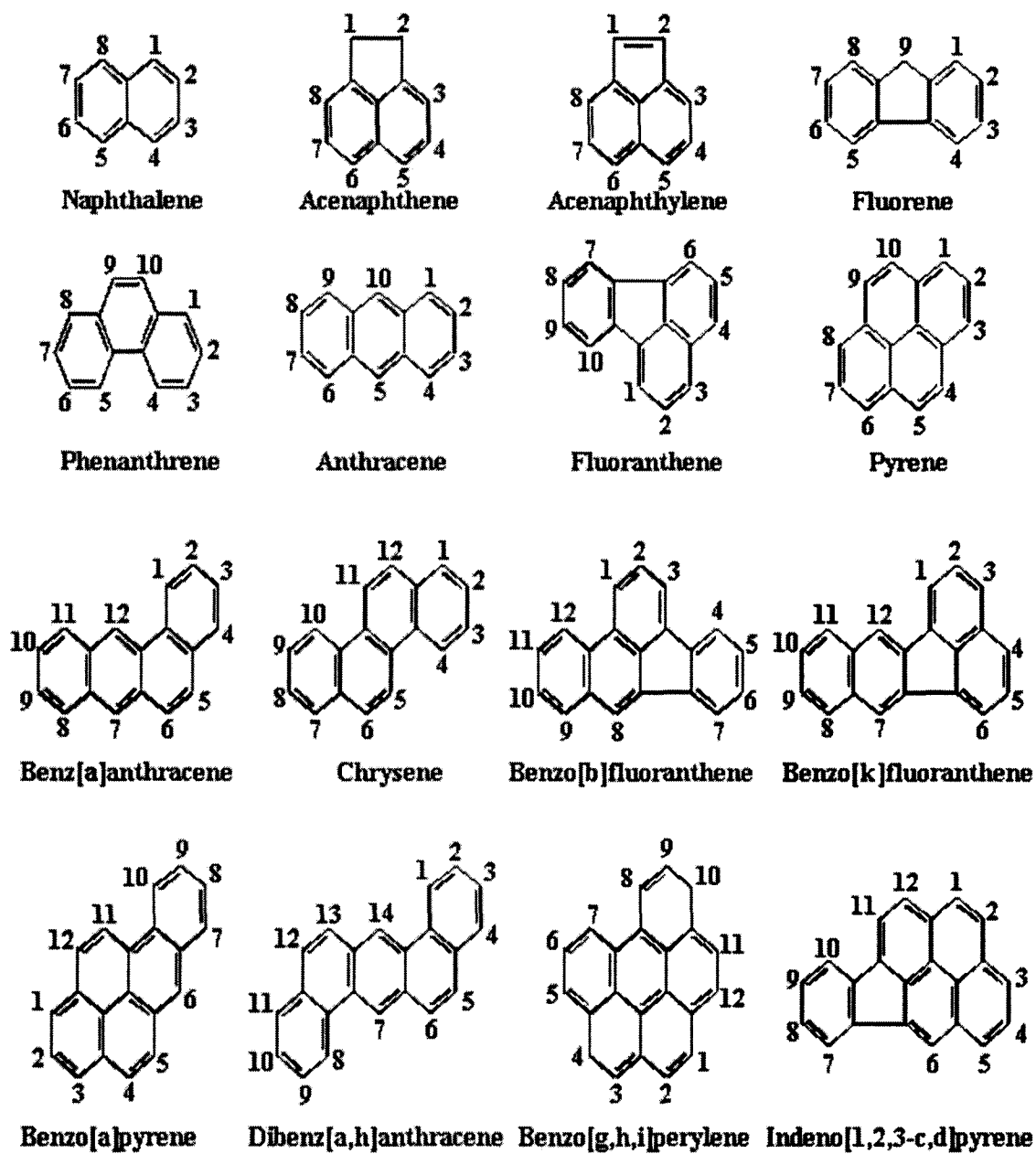
Figure 2.1   Structure of the 16 U.S. EPA priority pollutant PAH compounds

Table 2.1   Physical-chemical properties of polycyclic aromatic hydrocarbons (LaGrega et al., 1994; WHO, 1998)

PAH Compound Formula CAS RN	Aqueous Solubility ($\mu g \cdot L^{-1}$)[†]	Mol. Wt. ($g \cdot mol^{-1}$)	Melting Temp. (°C)	Vapor pressure (Pa)	Henry's Law Constant ($KPa \cdot m^3 \cdot mol^{-1}$)	Partitioning Coefficients		Freundlich Parameters[†]		
						log K_{ow}	log K_{oc}[†]	pH	K[‡]	1/n
Naphthalene $C_{10}H_8$ 91-20-3	31690	128.18	81.0	1.0E1	4.89E-2	3.37	3.11	NA	NA	NA
Acenaphthene $C_{12}H_{10}$ 83-32-9	3420	154.21	95.0	2.9E-1	1.48E-2	4.00	3.65	5.3	190	0.36
Acenaphthylene $C_{12}H_{10}$ 208-96-8	3930	152.20	93.0	8.9E-1	1.14E-3	3.70	3.40	5.3	115	0.37
Anthracene $C_{14}H_{10}$ 120-12-7	45	178.24	216.4	8.0E-4	7.30E-2	4.45	4.15	5.3	376	0.70
Fluorene $C_{13}H_{10}$ 86-73-7	1690	166.22	116.0	8.0E-2	1.01E-2	4.18	3.86	5.3	330	0.28
Phenanthrene $C_{14}H_{10}$ 85-01-8	1000	178.24	100.5	1.6E2	3.98E-3	4.46	4.15	5.3	215	0.44
Fluoranthene $C_{16}H_{10}$ 206-44-0	206	202.26	108.8	1.2E-3	6.5E-4 *	4.90	4.58	5.3	664	0.61
Pyrene $C_{16}H_{10}$ 129-00-0	130	202.26	150.4	6.0E4	1.1E-3	4.88	4.58	NR	389	0.39
Chrysene[¥] $C_{18}H_{12}$ 218-01-9	1.8	228.30	253.8	8.4E-5 *	NA	5.61	5.30	NR	716	0.46
Benz(a)anthracene[¥] $C_{18}H_{12}$ 56-55-3	5.7	228.30	160.7	2.8E-5	NA	5.60	6.14	NA	NA	NA
Benzo(b)fluoranthene[¥] $C_{20}H_{12}$ 205-99-2	14	252.32	168.3	6.7E-5 *	5.1E-5	6.06	5.74	NA	NA	NA
Benzo(k)fluoranthene[¥] $C_{20}H_{12}$ 207-08-9	4.3	252.32	215.7	1.3E-8 *	4.4E-5 *	6.06	5.74	7.1	181	0.57
Benzo(a)pyrene[¥] $C_{20}H_{12}$ 50-32-8	3.8	252.32	178.1	7.3E-7	3.4E-5 *	6.06	6.74	7.1	34	0.44
Dibenz(a,h)anthracene[¥] $C_{22}H_{14}$ 53-70-3	0.5	278.36	266.6	1.3E-8 *	7.0E-6	6.80	6.52	7.1	69	0.75
Indeno(1,2,3-cd)pyrene[¥] $C_{22}H_{12}$ 193-39-5	0.53	276.34	163.6	1.3E8 *	2.9E-5 *	6.50	6.20	NA	NA	NA
Benzo(g,h,i)perylene[¥] $C_{22}H_{12}$ 191-24-2	0.26	276.34	278.3	1.4E-8	2.7E-5 *	6.51	6.20	7	11	0.37

[†] From LaGrega et al., 1994; [¥] Probable Human Carcinogens; * at 20° C, others at 25° C, [‡] K reported in ($mg \cdot kg^{-1}$)
NA=Data not available. NR=Not reported

Table 2.2   Toxicological data for oral exposure to select PAH compounds

Compound U.S. EPA MCL ($\mu g \cdot L^{-1}$)	Noncarcinogenic Risk Factors ($mg \cdot kg^{-1} \cdot d^{-1}$)			Carcinogenic Risk Factors		Target Organ(s) and Non-Carcinogenic Critical Effect(s)
	NOAEL	LOAEL	RfD	Cancer Group[1]	Slope Factor ($d \cdot mg^{-1} \cdot kg^{-1}$)	
Naphthalene 100[†]	50	NA	0.02	C	NA	**Blood:** Hemolytic anemia; **Gastrointestinal tract:** Nausea, abdominal pain, diarrhea; **Nervous system:** lethargy, vertigo, convulsions, coma, cerebral edema, hemolysis; **Liver:** Jaundice, increased serum enzyme activity; **Kidneys:** Increased creatinine and blood urea nitrogen levels, proteinuria and hemoglobinuria, anuria, tubular necrosis, hemolysis; **Eyes:** Restricted visual fields, optic atrophy, and cataracts; **Reproduction:** Hemolytic anemia in infants exposed during pregnancy.
Acenaphthene 2000[§]	175	350	0.06	-	-	**Liver:** increased liver weights, hepatocellular hypertrophy, and increased cholesterol levels; **Reproductive System:** decreased ovary weights, inactivity of the ovaries and uterus, and fewer and smaller corpora lutea.
Anthracene 10000[§]	1000	NA	0.3	D	-	**Hematopoietic System:** decreased hemoglobin levels, reticulocytosis, and leucopenia; **Gastrointestinal tract:** melanosis of the colon and rectum
Fluoranthene NA	125	250	0.04	D	-	**Kidney:** nephropathy; **Liver:** increased liver weights and increased liver enzyme levels resulting in microscopic lesions.
Pyrene NA	75	125	0.03	D	-	**Kidney:** nephropathy and decreased kidney weights; **Liver:** increased liver weights **Blood:** slight hematologic effects
Benzo(a)pyrene 0.2	NA	NA	NA	B	7.3	**Blood:** red blood cell damage, leading to anemia; **Immune System:** suppressed immune system; **Reproductive system:** developmental and reproductive effects, Increased fetal mortality
2-Methylnaphthalene NA	NA	NA	0.004	-	-	**Respiratory System:** Pulmonary alveolar proteinosis

NA = Data not available at this time; NOAEL = No Observed Adverse Effects Level; LOAEL = Lowest Observed Adverse Effects Level; MCL = EPA maximum contaminant level from safe drinking water standards

[†] HAL = EPA health-advisory level, lifetime; [§] DWEL = EPA Drinking Water Equivalent Level

1. Cancer Group: B=Probable human carcinogen, C=Possible human carcinogen, D=Not classifiable as to human carcinogenicity

Table 2.3 Composition of several PAH mixtures and predicted effective solubilities of the PAH compounds.

Compound	Pure Solid Aqueous Solubility[†] (µg/L)	Fugacity Ratio[‡] (f^L/f^S)	Coal Tar Peters and Luthy (1993) 210 g/mol		Coal Tar Ghoshal et al. (1996) 226 g/mol		Coal Tar Creosote Mueller et al. (1989) 158 g/mol	
Source:			Mass Fraction (% by wt.)	Estimated Solubility[§] (µg/L)	Mass Fraction (% by wt.)	Estimated Solubility[§] (µg/L)	Mass Fraction (% by wt.)	Estimated Solubility[§] (µg/L)
Naphthalene	31690	3.57	2.16	4010	10	2000	11.05	15400
Acenaphthene	3420	5.0	1.52	410	1.3	370	3.4	690
Acenaphthylene	3930	4.55	0.68	150	0.37	86	NA	--
Anthracene	45	100	0.59	31	2	114	11.05	440
Fluorene	1690	7.69	1.4	230	NA	--	6.8	840
Phenanthrene	1000	5.56	2.12	140	0.16	11.3	11.05	550
Fluoranthene	206	7.14	0.3	4.6	0.55	9	3.4	39
Pyrene	130	20.0	0.5	14	NA	--	1.7	35
Chrysene	1.8	200	0.27	0.9	0.36	1.3	1.7	4.2
Benz(a)anthracene	5.7	25.0	0.31	0.4	NA	--	NA	--
Benzo(b)fluoranthene	14	26.6	NA	--	0.4	1.3	NA	--
Benzo(k)fluoranthene	4.3	76.9	NA	--	0.16	0.47	NA	--
Benzo(a)pyrene	3.8	33.3	1.8	1.9	0.36	0.41	0.85	0.67
Dibenz(a,h)anthracene	0.5	250	NA	--	0.04	NA	NA	--
Indeno(1,2,3-cd)pyrene	0.53	*NA*	NA	--	NA	--	NA	--
Benzo(g,h,i)perylene	0.26	333	NA	--	NA	--	NA	--

[†]   At 25°C

[‡]   Adapted from Peters et al., 1996

[§]   Based on Raoult's Law

NA   Data not available

68

Table 2.4   Half-lives and first-order decay rates of the 16 U.S. Priority PAH Pollutants in soils and sediments under aerobic conditions in laboratory and field studies.

Compound	Half-life (days)	First order decay rate, k (d^{-1})	Condition	Reference
Naphthalene	0.277	2.5	Soil slurry	Simpkin and Griesbrecht (1994)
Acenaphthene	134	0.0052	Soil[L]	Park et al. (1990)
Acenaphthylene	42 – 60	0.012 – 0.017	Soil[L]	Kincannon and Lin (1985)
Anthracene	55	0.0125	Soil[F]	Kasterner et al. (1999)
Fluorene	7 – 8	0.087 – 0.099	Soil slurry	Durate et al. (1997)
Phenanthrene	36	0.019	Sediment	Michel et al. (1995)
Fluoranthene	7 – 8	0.087 – 0.099	Soil slurry	Durate et al. (1997)
Pyrene	4.5	0.155	Soil[F]	Schwab et al. (1995)
Chrysene	33	0.021	Sediment	Michel et al. (1995)
Benzo(a)anthracene	75 – 80	0.0087 – 0.0092	Soil[F]	Pott and Henrysson (1995)
Benzo(b)fluoranthene	39	0.018	Sediment	Michel et al. (1995)
Benzo(k)fluoranthene	46	0.015	Sediment	Michel et al. (1995)
Benzo(a)pyrene	25	0.028	Soil[F]	Kanaly et al. (1997)
Dibenz(a,h)anthracene	420	0.0017	Soil[L]	Park et al. (1990)
Indeno(1,2,3-cd)pyrene	232	0.003	Soil[L]	Park et al. (1990)
Benzo(g,h,i)perylene	590 – 650	0.0011 – 0.0012	Soil[L]	Coover and Sims (1987)

[F] indicates field study

[L] indicates laboratory study

Table 2.5   Representative PAHs metabolized by different microorganisms

Compound	Rings	Predominant Sites of Initial Enzymatic Attack[1]	Microorganism(s)	Cmts[2]	References
Naphthalene	2	(1,2)	*Rhodococcus* sp.	S	Bouchez et al. (1996)
			Pseudomonas sp.	S	Aitken et al. (1998);Ryu et al. (1989)
			Acinetobacter calcoaceticus	S	Heitkamp et al. (1998)
			Mycobacterium sp.	S	Treccani et al. (1954)
			Nocardia sp.	S	Treccani et al. (1954)
			P. acidovorans	S	Jeffrey et al. (1975)
			P. fluorescens	S	Jeffrey et al. (1975)
			P. putida	S	Cerniglia et al. (1980)
			Oscillatoria sp.	S	Cerniglia and Gibson (1977)
Acenaphthene	3	(1,2), (6,7)	*Pseudomonas* sp.	S	Komatsu et al. (1993)
			Neptunomonas naphthovorans	C	Hedlund et al. (1999)
Acenaphthylene	3	(1,2)	*Pseudomonas* sp.	S	Komatsu et al. (1993)
Anthracene	3	(1,2), (6,7)	*Rhodococcus* sp.	S	Bouchez et al. (1996)
			Pseudomonas sp.	S	Bouchez et al. (1996)
			Bjerkandera sp.	S	Field et al. (1995)
Fluorene	3	(1,2), (1,1a), (3,4), 9	*Pseudomonas* sp.	S	Foght and Westlake (1988)
			Rhodococcus sp.	S	Bouchez et al. (1996)
			Pseudomonas saccharophila	C	Stringfellow and Aitken (1995)
			Mycobacterium sp.	C	Boldrin et al. (1993)
Phenanthrene	3	(1,2), (3,4), (9,10)	*Rhodococcus* sp.	S	Bouchez et al. (1996)
			Pseudomonas sp.	S	Bouchez et al. (1996)
			Mycobacterium flavescens	S	Dean-Ross and Cerniglia (1996)
			Mycobacterium sp.	S	Heitkamp et al. (1988)
			Flavobacterium sp.	S	Stucki and Alexander (1987)
			Beijerinckia sp.	S	Stucki and Alexander (1987)
			Pseudomonas putida	S	Jerina et al. (1976)
			Streptomyces flavovirens	S	Sutherland et al. (1990)
			Agmenellum quadruplicatum	S	Narro et al. (1992)
			Cunninghamella elegans	C	Cerniglia and Yang (1984)
			Phenerochaete chysosporium	C	Sutherland et al. (1991)
			Syncephalastrum racemosum	C	Sutherland et al. (1993)

[1] Sources: Kanaly and Harayama, 2000; Sutherland et al., 1995; Ellis et al., 2003

[2] Cmts = comments - indicates whether the microorganism utilized the PAH compound as sole carbon source (S) or via cometabolism (C).

70

Table 2.5   **Representative PAHs metabolized by different microorganisms (cont.)**

Compound	Rings	Predominant Sites of Initial Enzymatic Attack[1]	Microorganism(s)	Cmts[2]	References
Fluoranthene	4	(1,2), (2,3), (7,8)	*Rhodococcus* sp.	S	Bouchez et al. (1996)
			Pseudomonas sp.	S	Bouchez et al. (1996)
			Mycobacterium flavescens	S	Dean-Ross and Cerniglia (1996)
			Mycobacterium sp.	S	Boldrin et al. (1993)
			Pseudomonas paucimobilis	S	Mueller et al. (1990)
Pyrene	4	(1,2), (4,5)	*Rhodococcus* sp.	S	Walter et al. (1991)
			Pseudomonas sp.	S	Bouchez et al. (1996)
			Mycobacterium flavescens	S	Dean-Ross and Cerniglia (1996)
			Xanthamonas sp.	S	Grosser et al. (1991)
			Mycobacterium sp.	C, S	Ye et al. (1996); Heitkamp et al. (1988)
			Bacillus sp.	S	Kazunga and Aitken (2000)
			Alcaligenes denitrificans	C	Weisenfels et al. (1990)
			Cunninghamella elegans	C	Cerniglia et al. (1986)
			Penicillium sp.	C	Sack and Gunther (1993)
Chrysene	4	(1,2)	*Sphingomonas paucimobilis*	C	Ye et al. (1996)
			Pseudomonas fluorescens	S	Caldini et al. (1995)
			Achromobacter sp.	S	Cutright and Lee (1994)
Benzo(a)-anthracene	4	(3,4), (5,6), (8,9), (10,11)	*Sphingomonas paucimobilis*	C	Ye et al. (1996)
			Pseudomonas fluorescens	C	Caldini et al. (1995)
			Pleurotus sp. *Florida*	C	Wolter et al. (1997)
Benzo(b)-fluoranthene	5		*Sphingomonas paucimobilis*	C	Ye et al. (1996)
Benzo(k)-fluoranthene	5		*Achromobacter* sp.	C	Cutright and Lee (1994)
Benzo(a)pyrene	5	(4,5), (7,8), (9,10)	*Pseudomonas saccharophila* P15	C	Chen and Aitken (1999)
			Bjerkandera sp. BOS55	C	Kotterman et al. (1998)
			Sphingomonas paucimobilis	C	Ye et al. (1996)
			Xanthamonas sp.	C	Grosser et al. (1991)
			Mycobacterium sp.	C	Heitkamp and Cerniglia (1989)
Dibenz(a,h)anthracene	5		*Sphingomonas paucimobilis*	C	Ye et al. (1996)
			Achromobacter sp.	C	Cutright and Lee (1994)

[1] Sources: Kanaly and Harayama, 2000; Sutherland et al., 1995; Ellis et al., 2003

[2] Cmts = comments - indicates whether the microorganism utilized the PAH compound as sole carbon source (S) or via cometabolism (C).

Table 2.6   Phylotypic relatedness of bacteria associated with PAH mineralization as reported in literature.

Phylum/Class	Genus/Species	Geographical source	Reference(s)
Aerobic			
α-Proteobacteria	*Sphingomonas*	New Jersey; Texas; Illinois; Germany; Florida; Boston Harbor; Sweden; France; South Carolina	Bogan et al., 2001; Frederickson et al., 1995; Wang et al., 1996; Kazunga et al., 2001; Bastiens et al., 1998; Daane et al., 2001
β-Proteobacteria	*Alcaligenes*; *Burkholderia*; *Bordetella*; *Acidovorax*; *Variovorax*; *Pseudomonas* sp. V-O7-10; *Comamonas*; *Copiotrophic ultramicrobacteria*	Boston Harbor; New Zealand; Canada; Sweden; Norway; New York; New Jersey; France; Florida; Japan	Eriksson et al., 2003; Laurie and Lloyd-Jones, 1999; Johnsen et al, 2002; Berardesco et al., 1998; Padmanabhan et al., 2003; Mueller et al, 1997; Bogan et al., 2001; Daane et al., 2001; Goyal and Zylstra, 1996
γ-Proteobacteria	*Cycloclasticus*; *Pseudomonas*; *Moraxella*; *Marinobacter*; *Vibrio*; *Halomonas*; *Pseudoalteromonas*; *Marinomonas*; *Acinetobacter*; *Stenotrophomonas*	Puget Sound; Gulf of Mexico; Boston Harbor; Canada; Sweden; New York; Florida; Germany; New Jersey; France; Japan	Geiselbrecht et al., 1996; Geiselbrecht et al., 1998; Daane et al, 2001; Kasai et al., 2002; Boonchan et al., 1998; Bogan et al., 2001; Mueller et al, 1997; Padmanabhan et al., 2003; Eriksson et al., 2003; Berardesco et al., 1998; Gauthier et al., 1992; Melcher et al., 2002; Tagger et al., 1990
Actinobacteria	*Mycobacterium*; *Rhodococcus*; *Arthrobacter*; *Streptomyces*; *Nocardiodes*; *Gordonia*; *Nocardia*; *Terrabacter*; *Tsukamurella*	Boston Harbor; Texas; Germany; Japan; Spain; New Jersey	Kastner et al., 1994; Grosser et al., 1991; Wang et al., 1995; Uz et al., 1998; Daane et al., 2001; Trenz et al., 1994; Sutherland et al., 1990; Saito et al., 2000; Johnsen et al, 2002; Berardesco et al., 1998; Kleespies et al., 1996; Heitkamp and Cerniglia, 1988; Vila et al., 2001
Firmicutes	*Bacillus cereus* P21; *Paenibacillus*	New Jersey; Delaware	Kazunga et al., 2001; Daane et al., 2001
Bacteriodetes	*Flavobacterium*	Boston Harbor	Berardesco et al., 1998; Shiaris and Clooney, 1983
Nitrate-Reducing			
β-Proteobacteria	*Variovorax*; *Bordetella*; *Alcaligenes*	Canada	Eriksson et al., 2003
γ-Proteobacteria	*Pseudomonas*; *Vibrio*	Canada; Puget Sound	Rockne et al., 2000; Eriksson et al., 2003
Sulfate-Reducing			
δ-Proteobacteria	Delta Proteobacterium NaphS2	San Diego Bay	Hayes and Lovley, 2002; Galushko et al., 1999

72

Table 2.7   Catabolic DNA Gene Probes used for studies of PAH biodegradation

Probe	Size	Related Enzyme	Origin	Reference
nahA	~1 kb	naphthalene dioxygenase	*Pseudomonas putida* G7	Simon et al., 1993
nahH	~1 kb	2,3-catechol dioxygenase	*Pseudomonas putida* G7	Ghoshal et al., 1987
nahG	~1 kb	Salicylate hydroxylase	*Pseudomonas putida* G7	You et al., 1991
nahR	~1.1 kb	NAH7 regulatory protein	*Pseudomonas putida* G7	You et al., 1988
nahAaAb	~2.4 kb	Naphthalene dioxygenase	*Pseudomonas putida* NCIB 9816	Berardesco et al., 1998
ntdAc	~0.3 kb	Naphthalene dioxygenase	*Pseudomonas* sp. Strain JS42	Ringleberg et al., 2001
bphC	~0.6 kb	Biphenyl dioxygenase	*Sphingomonas yanoikuyae* B1	Daane et al., 2001
pahA	~1 kb	PAH dioxygenase	*Pseudomonas putida* OUS82	Lloyd-Jones et al., 1999
pY3-E16	~16 kb	PAH dioxygenase	*Pseudomonas putida* NCIB 9816	Berardesco et al., 1998
phdA	~0.13 kb	phenanthrene dioxygenase	*Nocardiodes* sp. strain K7	Saito et al., 2000
phnAc	~1.4 kb	phenanthrene dioxygenase	*Burkholderia* sp. RP007	Laurie and Lloyd-Jones, 1999
GST	~0.5 kb	Glutathione S-transferase	*Sphingomonas* spp.	Lloyd-Jones and Lau, 1997

Table 2.8   Summary of Various Case Studies

Contamination Site Location	Site Geology Depth to Water (DTW) Average Pore Velocity, v_x Hydraulic Cond., K_h		Method Used for Rate Estimation	Compounds	Approx. Contam. Conc.	Electron Acceptor Cond.	Lin. Distn. Coeff. K_d (L/kg)	1st- Ord. Decay rate k (d^{-1})	Ref.
MGP Tar Burial Site South Glenn Falls, New York	**Graded sand over a confining clay layer** DTW = 2.7 m, v_x = 0.096 m/d, K_h = 0.09 m/d – 8.16 m/d		Whole field modeling	Naphthalene Acenaphthylene Phenanthrene Toluene	7 mg/kg NR NR NR	Mixed Mixed Mixed Mixed	0.81 0.46 2.43 0.19	0.00027 0.00027 0.000027 0.00068	EPRI (1996)
MGP Waste Baltimore Gas and Electric Spring Gardens Facility, Baltimore, Maryland	**Shallow Unconfined Aquifer with fill material underlain by sand and gravel inter-bedded with silt and clay lenses** DTW = 1.6 - 5 m v_x = NR K_h = NR	Gravel	Laboratory batch studies on core samples	Naphthalene Phenanthrene	1000 µg/L 1000 µg/L	Aerobic Aerobic	NR NR	0.0014 – 0.0069 0.0050 – 0.0053	Durant et al. (1994); MacFarlane et al. (1994)
		Sand	Laboratory batch studies on core samples	Naphthalene Phenanthrene	1000 µg/L 1000 µg/L	Aerobic Aerobic	NR NR	0.039 – 0.0084 0.0015 – 0.0092	
		Clayey Silt	Laboratory batch studies on core samples	Naphthalene Phenanthrene	1000 µg/L 1000 µg/L	Aerobic Aerobic	NR NR	0.0046 0.0053	
		Silty Clay	Laboratory batch studies on core samples	Naphthalene	1000 µg/L	Aerobic	NR	0.010	
MGP Waste FMGP, Charleston, South Carolina	**Soft organic clay overlain by sand and artificial fill** DTW = 0.46 m, v_x = NR $K_{h,fill}$ = 0.0305 - 3.05 m/d $K_{h,sand}$ = 4.88 m/d		Laboratory batch studies on core samples	Naphthalene Naphthalene Toluene Toluene	NR NR NR NR	Aerobic Anaerobic Aerobic Anaerobic	1.37 1.37 0.94 0.94	0.88 0.000046 0.84 0.0020	Campbell et al. (1996); Landmeyer et al. (1998)
			Whole field modeling	Naphthalene Toluene	NR NR	Anaerobic Anaerobic	0.62 0.62	0.00009 0.00009	

NR - not reported

Table 2.8   Summary of Various Case Studies (cont.)

Contamination Site Location	Site Geology Depth to Water (DTW) Average Pore Velocity, v_x Hydraulic Cond., K_h	Method Used for Rate Estimation	Compounds	Approx. Contam. Conc.	Electron Acceptor Cond.	Lin. Distn. Coeff. K_d (L/kg)	1st- Ord. Decay rate k (d^{-1})	Ref.
Emplaced Creosote Source Material CFB Borden, Ontario, Canada	**Unconsolidated sand aquifer underlain by silts and clays** DTW = 1.5 m, v_x = 0.066 - 0.0947 m/d K_h = 6.05 – 8.24 m/d	Whole field modeling	Naphthalene	1200 mg/kg	Mixed	0.22	0.00057	King et al. (1999)
			Phenanthrene	1500 mg/kg	Mixed	1.8	0.014 – 0.063	
			Carbazole	40 mg/kg	Mixed	0.83	0.0063	
			1-methylnaphthale ne	240 mg/kg	Mixed	0.24	0.0040	
Gasoline leakage Former Gas Station, Perth, Australia	**Thick clay aquitard overlain by 7 – 12 m fine dune sand** DTW = 1 to 1.8 m v_x = 0.27 – 0.47 m/d K_h = 8.6 to 29 m/d	In-situ tracer test	Naphthalene, tracer test		Sulfate Reducing	NR	0.018 – 0.026	Davis et al. (1999); Thierrin et al. (1993); Thierrin et al. (1995)
		Whole plume modeling on steady state plume	Naphthalene, whole plume	33 mg/kg 1100 µg/L	Sulfate Reducing	NR	0.0039 – 0.0050	
		Partial plume modeling on steady state Plume	Naphthalene, Partial plume	33 mg/kg 1100 µg/L	Sulfate Reducing	NR	0.00095 – 0.0027	
		In-situ tracer test	Toluene, tracer test		Sulfate Reducing	NR	0.0050 – 0.012	
		Whole plume modeling on steady state plume	Toluene, whole plume	670 mg/kg 75 mg/L	Sulfate Reducing	NR	0.0048 – 0.0073	
		Partial plume modeling on steady state Plume	Toluene, partial plume	670 mg/kg 75 mg/L	Sulfate Reducing	NR	0.0027 – 0.0063	

Table 2.8   Summary of Various Case Studies (cont.)

Contamination Site Location	Site Geology Depth to Water (DTW) Average Pore Velocity, v_x Hydraulic Cond., K_h	Method Used for Rate Estimation	Compounds	Approx. Contam. Conc.	Electron Acceptor Cond.	Lin. Distn. Coeff. K_d (L/kg)	1st- Ord. Decay rate k (d^{-1})	Ref.
Pulsed injection of aqueous compounds MADE Site Columbus AFB Mississippi	**Fluvial Sedimentation** DTW = NR v_x = NR K_h = 0.086 - 864 m/d	Whole field modeling	Naphthalene	7.23 mg/L	Aerobic	0.085	0.0063	MacIntyre et al. (1993)
			O-dichlorobenzene	32.8 mg/L	Aerobic	0.065	0.0059	
			p-Xylene	51.5 mg/L	Aerobic	0.048	0.0141	
			Benzene	68.1 mg/L	Aerobic	0.059	0.0066	
Landfill Leachate Vejen Landfill, Vejen, Denmark	**Clay deposit overlain by sandy alluvial aquifer** DTW = NR v_x = 150 – 200 m/yr K_h = NR	Whole field modeling of steady-state plume	Naphthalene	NR	Iron(III) Reducing	NR	0.013 – 0.015	Lyngkilde and Christensen (1992)
			BTEX	NR	Iron(III) Reducing	NR	0.009 – 0.011	
MGP Site Dubuque, Iowa	**Shallow unconfined aquifer with fine to medium grained sand** DTW = 2.7 - 5.8 m v_x = 0.15 - 0.23 m/d K_h = 1.50 - 623 m/d	Centerline transect of plume	Benzene	1 mg/L	Anaerobic	NR	0.0063*	Ong et al., 2001 Kjartanson et al., 2001
			Naphthalene	1 mg/L	Anaerobic	NR	0.0081*	
			Acenaphthene	0.15 mg/L	Anaerobic	NR	0.0033*	
			Phenanthrene	0.1 mg/L	Anaerobic	NR	0.0043*	
			Acenaphthylene	0.1 mg/L	Anaerobic	NR	0.0029*	

* - overall attenuation rate

3. Evidence of Intrinsic Bioremediation of a Coal-Tar Impacted Aquifer based on Coupled Reactive Transport and Biogeochemical Mass Balance Approaches

Shane W. Rogers, Say Kee Ong, Greg A. Stenback, Johanshir Golchin, and Bruce H. Kjartanson

3.1 Abstract

Coal-tar contamination resulting from former manufactured gas plant (FMGP) operations during the early 1900s has resulted in a contaminant plume in the shallow aquifer underlying a small area south of a small town in Northwestern Iowa. Site characterizations and groundwater monitoring were conducted to better define the microbial and geochemical response to the contamination. The monitoring results indicated a 450% increase in viable microorganisms based on standard heterotrophic plate counts coupled to hydrogeochemical evidence of aerobic and anaerobic respiration, supporting intrinsic bioremediation. Mass balances between contaminants and loss of terminal electron acceptors inside the source region and plume yielded a potential for destruction of 4.5 kg/yr contamination, primarily through aerobic respiration (16%), nitrate-reduction (74%), and sulfate-reduction (7.6%). A superposition of 2-D reactive transport analytical solutions was used to estimate the best-fit first-order degradation rate coefficients for benzene ($0.0084 \ d^{-1}$), ethylbenzene ($0.0076 \ d^{-1}$), xylenes ($0.0057 \ d^{-1}$), naphthalene ($0.0058 \ d^{-1}$), 1-methylnaphthalene ($0.0042 \ d^{-1}$), acenaphthene ($0.0011 \ d^{-1}$), acenaphthylene ($0.00069 \ d^{-1}$), and fluorene ($0.0058 \ d^{-1}$). Using these degradation rate coefficients, the overall contaminant mass transformation rate based on analytical modeling was estimated to be $3.6 \ kg \cdot yr^{-1}$, comparing favorably to estimates based on the geochemical mass balance approach. The results of this study illustrate how coupling a superposition of analytical solutions and lumped-hydrocarbon biogeochemical mass balance approaches can be used to estimate contaminant degradation rates in a hydrogeologically and chemically complex contaminated system, effectively providing evidence of intrinsic bioremediation.

3.2 Introduction

Monitored natural attenuation (MNA) is accepted as a cost-effective remedial alternative at many sites contaminated with aliphatic, monoaromatic, and low-ring polycyclic aromatic

hydrocarbon (PAH) pollutants in light petroleum fuels such as gasoline. The success of natural attenuation technology at these sites has prompted interest in MNA at former coal-gasification sites (for a review, see Chapter 2). All 16 U.S. EPA priority PAH pollutants have been shown to be biodegradable under aerobic conditions. Biodegradation of several 2- and 3-ring PAHs such as naphthalene, 2-methylnaphthalene, and phenanthrene under nitrate-reducing, iron-reducing, and sulfate-reducing conditions have been shown in laboratory microcosms from contaminated aquifer, harbor, and estuarine sediments (Zhang and Young, 1997; Coates et al., 1996; Galushko et al., 1999; Hayes and Lovley, 2002; Anderson and Lovley, 1999; McNally et al., 1999; Rockne et al., 2000; Eriksson et al., 2003). Combined with the fact that many coal-tar impacted sites exhibit depletion of terminal electron accepting compounds including oxygen, nitrate, and sulfate, and production of coupled reduced species such as soluble iron, manganese, nitrite, sulfide, and methane relative to nearby pristine groundwater, MNA as a remedial mechanism at PAH-contaminated sites warrants attention (EPRI, 1996; King et al., 1999a,b; Campbell et al., 1996; Landmeyer et al., 1998; Lyngkilde and Christensen, 1992). However, a recent report by the National Research Council (2000) on MNA ranked the current understanding of the fate and transport of PAH compounds at contaminated sites as "moderate" and thus the likelihood of successful application of natural attenuation technology as "low".

Practical factors and fundamental issues may limit the successful application of natural attenuation technologies at coal-tar impacted sites, especially in the estimation of intrinsic attenuation rates. Manufactured gas facilities were almost always located near railways and rivers, and were industrial centers for many communities. It is not uncommon for service stations and other industrial operations to be located on or near former coal-gasification sites. Therefore, many coal-tar contaminated sites have plumes that commingle with gasoline contamination, adding complications and complexity to natural attenuation efforts (Kjartanson et al., 2001; Ong et al., 2001). For instance, biodegradation of BTEX compounds in gasoline may elicit hydrogeochemical responses (e.g., consumption of terminal electron accepting compounds and nutrients), which may lead to misinterpretation of the measured geochemical data relative to coal-tar PAH contamination. Further, gasoline may act as a solvent for many PAH compounds, altering sorption properties, and in general affecting contaminant mobility (Weber et al., 2002). Close proximity to rivers often complicates groundwater modeling efforts at coal-tar impacted sites due to fluctuations of the groundwater surface in response to changes in the river stage.

Modeling contaminant fate and transport in coal-tar-impacted systems may also be complicated by factors directly related to the physical-chemical properties of PAHs. Source term

development can be particularly challenging, not only in estimating the mass of coal-tar DNAPL residuals within the source region, but also in modeling dissolution kinetics. For instance, several researchers have determined that Raoult's Law under the local equilibrium assumption may be valid for modeling coal-tar source regions (Eberhardt and Grathwohl, 2002; King et al., 1999b). However, Peters et al. (2000) showed that NAPL solidification dynamics during the weathering process may significantly impact the solubility of select PAHs to the extent that ideal solubility theory may not hold true in all cases. Variation in PAH solubility in the source region caused by phase change is difficult to incorporate accurately into fate and transport models, and may lead to larger estimates of biodegradation rates than actually realized in situ. This may be further complicated where commingled contaminants such as gasoline may solubilize and transport PAH components, only to deposit these PAHs as solids further down-gradient of the source region following weathering of the more biodegradable gasoline components.

PAH sorption behavior may also have significant impact on biodegradation rates estimated by fate and transport models. PAHs typically exhibit substantial sorption hysteresis and differential affinity (several orders of magnitude) to specific organic materials and such as soot, natural organic matter, coal-tar residuals, and biomass (Huang and Weber, 1997; Stringfellow and Alvarez-Cohen, 1999; Bayard et al., 1998; Pignatello, 2000). Using a single organic carbon to model sorption may provide a poor match to actual site conditions. Linear and reversible sorption is often assumed for simplification in modeling the fate and transport of PAHs in coal-tar impacted systems. Where this assumption is made, it can be reasoned that biodegradation rate coefficients will be overestimated, as the additional (non-reversible) sink of PAH compounds to the solid phase would be captured by the biodegradation rate in these simplified models. Although the impact on monoaromatic hydrocarbons may be relatively low, the large organic carbon partitioning coefficients of PAH compounds may also skew model estimates of the biodegradation rate where the solid and aqueous phase degradation rate coefficients are modeled in a lumped approach, as is commonly done in modeling the fate and transport of hydrocarbons in contaminated systems.

Another approach to approximating the assimilative capacity of natural systems is the application of stoichiometric balances between the disappearance of terminal electron acceptors (TEAs) relative to background conditions and the potential mass of selected pollutants mineralized (Suthersan, 1999; Wilson et al., 1985). Some researchers have suggested incorporating the loss of TEAs in the advection-dispersion reactive transport equation to model the degradation of selected contaminants using an instantaneous reaction approach (Newell et al., 1995; Davis et al., 1994). These approaches may be further supported by the growth of microbes within the contaminated

region. However, a potential weakness of these methods is that it is difficult to partition the use of terminal electron accepting compounds or attribute microbiological growth towards the degradation of any particular pollutant, especially in cases where complex contaminant mixtures of hundreds of compounds exist such as in commingled plumes of fuels and coal-tars. The instantaneous reaction assumption may be poor for PAH contamination, of which reported half lives and retardation coefficients are large. Further, commingled plumes often lead to spatial variability in geochemical response that may not be effectively captured with analytical modeling using an instantaneous reaction approach. Although PAH degradation is commonly observed in laboratory settings, there remains uncertainty about the specific activity of PAH-degrading organisms in-situ necessary to verify intrinsic bioremediation of PAH pollutants (Johnsen et al., 2002; Langworthy et al, 1998; Padmanabhan et al., 2003). These factors complicate monitoring and decision-making at coal-tar impacted sites to the extent that it is difficult to interpret results from simple modeling exercises to quickly estimate intrinsic remediation potential with short-term or limited data sets that may sometimes be effective for fuel release sites. In most cases, displaying intrinsic remediation potential at coal-tar impacted sites requires increased monitoring efforts to deal with the added uncertainty about interpreting the data.

In this study, the intrinsic bioremediation potential of a geologically complex coal-tar contaminated aquifer with a commingling BTEX plume is explored with a simplified lumped-hydrocarbon geochemical mass balance approach and with analytical modeling of select pollutants using a superposition of solutions to account for multiple contaminant sources and a unique groundwater flow regime. The specific objectives of this study are to (1) show how coupled analytical fate and transport solutions and lumped-hydrocarbon geochemical mass balance approaches can be used to better support intrinsic biodegradation of coal-tar impacted systems and (2) identify the variability in estimated mass degradation rates that can be expected by using different approaches to estimating biodegradation potential. The overall goal is to demonstrate the type(s) of natural attenuation processes active at the site, and to estimate the rate at which contaminants may be degrading in-situ (second line of evidence as required by the U.S. EPA (1999)).

3.3 FMGP Study Site

Figure 3.1 is a plan view of the FMGP site, showing the original layout of the buildings, gas holder and storage tanks, coal-tar cisterns, oil tanks, and coal storage areas. The facility used the carbureted water gas process upon opening in 1905 until closure in 1936. Site investigations have

shown free-phase coal-tar source material located under the former gas-holder tanks as well as shallow source material exposed at the ground surface in select areas of the site shown in Figure 3.1a. Contaminated soils and source materials were excavated to depths not greater than the water table elevation in 1997 (approximate maximum excavation depth of 2.4 m). The excavations were backfilled with clean sand to within 0.8 m of the ground surface, then capped with a 0.6 m layer of clay and topped with gravel (Black and Veatch, 1998). Subsequent soil investigations near the former gas holder and coal tar cisterns have revealed additional coal-tar DNAPL smeared between approximately 3 m below ground surface to the confining glacial till, upon which a thin layer of coal-tar may be pooling (Kjartanson et al., 2002).

The geology underlying the FMGP site was defined using monitoring well boring data, percussion probing direct-push technology (DPT) soil cores, and DPT electrical conductivity probing at the locations shown in Figure 3.1a. The groundwater potentiometric surface was defined using measured groundwater elevations in monitoring wells shown in Figure 3.1b. The shallow aquifer system comprises the four primary geologic units shown in Figure 3.2, including a highly transmissive coarse alluvium ($K \geq 0.01$ cm·s^{-1}) confined in depth by glacial till and overlain by a fine-grained silty alluvial layer and loess. At approximately 50 m down-gradient of the contaminant source area (underlying the FMGP site), the coarse alluvium thins significantly into a narrow band of fine alluvium, which extends for approximately 70 m along the hydraulic gradient, and after which the coarse alluvium layer thickens as the river is approached. This region of fine-grained alluvium has a low hydraulic conductivity (1.6×10^{-4} cm·s$^{-1} \leq K \leq 8.6 \times 10^{-6}$ cm·s^{-1}) and causes a sharp decline in the potentiometric surface between the FMGP site and the river. Monitoring wells slightly up-gradient of the thinned region of the alluvial layer and screened in the coarse alluvium display occasional flowing artesian conditions, suggesting that the groundwater in the fine-grained alluvial layer under the thick loess is at least semi-confined.

Groundwater sampling was conducted in August 2001, April 2002, and November 2002 to characterize the aqueous geochemistry and extent of groundwater contamination. In August 2001, groundwater was sampled from 18 monitoring wells and at 38 additional locations using DPT. In April 2002, the monitoring network was expanded and groundwater was sampled from 30 monitoring wells and at 12 additional DPT locations. In November of 2002, the groundwater monitoring well network was expanded to include sampling at 13 additional wells (43 total). Figure 3.1 shows all soil and groundwater sampling locations.

Groundwater was sampled by pumping from the boreholes at a flow rate not exceeding 400 mL/min (to minimize drawdown) and monitoring the purge water using a flow-through cell, in which

the dissolved oxygen, pH, oxidation-reduction potential, electrical conductivity, and temperature were monitored at five minute intervals. Upon stabilization of the geochemical parameters, as suggested by Golchin et al. (1999), groundwater samples were collected and stored on ice for on and off-site analysis. On-site geochemical analyses were performed within two hours of sampling using titrimetric and spectrophotometric methods. Off-site analyses were performed in commercial laboratories using standard (U.S. EPA) methods. Blind duplicates and negative controls were sent to the laboratories for quality control.

Figure 3.3 shows isoconcentration plots ($\mu g \cdot L^{-1}$) for the maximum concentrations of select contaminants measured in the groundwater at the FMGP site. Compounds of 4 or more rings were detected only within the coal tar source region of the former manufactured gas plant facility shown in Figure 3.1. Elevated concentrations of monoaromatic compounds and naphthalene, 1-methylnaphthalene, acenaphthylene, and acenaphthene were observed approximately 80 m down-gradient of the primary source region in several monitoring locations screened both in the fine-grained alluvium and the overlying loess. This possible secondary source seems to be absent the heavier molecular weight compounds characteristic of coal-tars. In the early 1990s, an underground fuel storage tank was excavated upon closure of a non-related facility near the possible secondary source region shown in the contaminant contours.

3.4 Models

3.4.1 Stoichiometric Mass Balance

Disappearance of TEAs or production of coupled reduced species in contaminated aquifers may indicate biodegradation of hydrocarbon contaminants. The use of stoichiometric relationships describing hydrocarbon mineralization under different TEA conditions may be useful in estimating hydrocarbon degradation in these contaminated systems. Based on the stoichiometry of the reaction, a utilization factor (UF) for each redox process equal to the molar mass of TEA consumed or oxidation-reduction reaction product produced per mole of contaminant degraded can be defined. The rate of contaminant mass destruction is thus related to the UF and the groundwater flow rate through the contaminated region.

The stoichiometric terminal electron acceptor and reduced species mass balance model boundaries are shown in Figure 3.4. Streamlines 1 and 2 were chosen to approximately encompass the contaminated region. Flux boundary 1 was defined immediately up-gradient of the source region. Flux boundary 2 was chosen to correspond approximately to the end of the coal tar source region and

to match the source region defined in the 2-D reactive transport model presented below. Flux boundary 3 was defined at the plume extent (1 $\mu g \cdot L^{-1}$). Based on the hydraulic gradient (0.076 $m \cdot m^{-1}$) and average hydraulic conductivity in the alluvial units (1.26 x 10^{-4} $cm \cdot s^{-1}$) within the plume region, an average Darcy velocity of 0.0082 $m \cdot d^{-1}$ was estimated. Assuming groundwater flow was restricted to the alluvial units, a flow rate of 1.76 $m^3 \cdot d^{-1}$ was estimated by multiplying the Darcy velocity by the average cross-sectional area in the plume region between streamlines 1 and 2 (214 m^2). The cross-sectional area was estimated by dividing the volume of the aquifer in the plume region (15,900 m^3 - determined by numerical integration between top of the till surface and bottom of the loess unit) by the average flow length through the region (74 m). As a verification, the change in head between monitoring wells 4 and 16 (see Figure 3.1) was estimated to be 0.76 cm based on the average cross sectional area of the source region between streamlines 1 and 2 (314 m^2), the average hydraulic conductivity of the coarse alluvium in the source region (0.049 $cm \cdot s^{-1}$), and the groundwater flow rate estimated above (1.76 $m^3 \cdot d^{-1}$). This was within the observed range of 0.30 to 1.5 cm.

Recharge of TEAs or reduced species to the source region would occur across flux boundary 1. Recharge of these compounds to the plume region would occur across flux boundary 2. For simplification in modeling, it was assumed mass transfer of TEAs and reduced species across streamlines 1 and 2 were negligible. In the actual scenario, mass transfer of TEAs across these boundaries due to dispersion and molecular diffusion may result in some destruction of contaminant mass.

Assuming steady-state conditions, the rate of consumption of TEAs, and thus the rate of degradation of contaminant mass ($C_\gamma H_\beta$) in the source region, is balanced by the rate of groundwater recharge of TEAs across flux boundary 1 (Q), and can be written:

$$\frac{dM_s}{dt} \approx \frac{\Delta C_\gamma H_\beta}{\Delta t} = \frac{\Delta TEA}{UF \cdot \Delta t} = \frac{\left(\overline{C}_{FB1,TEA} - \overline{C}_{S,TEA}\right)}{UF} \cdot Q \tag{1}$$

where $\dfrac{dM}{dt}$ is the rate contaminant mass degradation attributable to reduction of terminal electron acceptor or production of reduced species of interest, ΔTEA is the mass of TEA consumed, $\overline{C}_{FB1,TEA}$ is the molar TEA concentration on flux boundary 1, $\overline{C}_{S,TEA}$ is the average molar source region TEA concentration, and Q is the rate of groundwater flow between streamlines 1 and 2. Similarly, for the plume region, the rate of hydrocarbon consumption can be written:

$$\frac{dM_p}{dt} \approx \frac{\Delta C_\gamma H_\beta}{\Delta t} = \frac{\Delta TEA}{UF \cdot \Delta t} = \frac{\left(\overline{C}_{FB2,TEA} - \overline{C}_{P,TEA}\right)}{UF} \cdot Q \tag{2}$$

where $\overline{C}_{FB2,TEA}$ is the average concentration of TEA on flux boundary 2 and $\overline{C}_{P,TEA}$ is the average concentration of TEA in the plume. The same concept can be applied to the production of reduced species of oxidation-reduction reactions in the source ($\overline{C}_{S,RS}$) and plume ($\overline{C}_{P,RS}$) regions such that:

$$\frac{dM_s}{dt} \approx \frac{\Delta C_\gamma H_\beta}{\Delta t} = \frac{\Delta RS}{UF \cdot \Delta t} = \frac{\left(\overline{C}_{S,RS} - \overline{C}_{FB1,RS}\right)}{UF} \cdot Q \tag{3}$$

$$\frac{dM_p}{dt} \approx \frac{\Delta C_\gamma H_\beta}{\Delta t} = \frac{\Delta RS}{UF \cdot \Delta t} = \frac{\left(\overline{C}_{P,RS} - \overline{C}_{FB2,RS}\right)}{UF} \cdot Q \tag{4}$$

where ΔRS is the mass of reduced species produced.

Without more detailed information regarding the potential of individual components of the coal-tar contaminants to degrade under specific redox conditions within the aquifer (e.g. attributing mass TEA use towards degradation of specific contaminants), a lumped equivalent hydrocarbon approach was used. It has been shown that differences in the biodegradability of PAH compounds are related to their solubility, whereby less soluble compounds tend to be more recalcitrant in natural systems (Park et al, 1990; Heitkamp and Cerniglia, 1987; McGinnis et al., 1988). Therefore, a mass-weighted average hydrocarbon based on the aqueous concentrations of individual contaminants over a contaminated region may provide a reasonable estimated equivalent hydrocarbon compound for mass balance between TEAs or reduced species and hydrocarbon mass degraded.

Following this approach, the molar fraction of each of the 16 U.S. EPA Priority PAH pollutants, BTEX compounds, 1-methylnaphthalene, and 2-methylnaphthalene were averaged over all groundwater monitoring locations within either (1) the contaminant source region, or (2) the contaminant plume region down-gradient of the source area, as shown in Figure 3.4. It was assumed that the monitoring wells were well distributed such that a weighting factor to decluster the data was not necessary. The average molar fraction of each compound was multiplied by the total number of carbon atoms and hydrogen atoms in the compound, respectively. The resulting equivalent carbon atoms and hydrogen atoms for each contaminant were summed over all contaminants to arrive at the

total number of carbon atoms (γ) and hydrogen atoms (β) in the equivalent hydrocarbon, $C_\gamma H_\beta$. Based on this approach, the equivalent hydrocarbon compounds for the source and plume regions were determined to be $C_{10.0}H_{9.13}$, and $C_{9.32}H_{8.59}$, respectively.

The two regions used for this estimate represent differences in the mobility of strongly hydrophobic compounds such as pyrene and benzo(a)pyrene that tend to be isolated to the source region relative to compounds such as naphthalene and BTEX which extend further into the plume. These differences result in a higher molecular weight equivalent hydrocarbon in the source region than estimated for the plume, and allow for a better comparison of the geochemical mass balance model to the results of 2-D reactive transport analytical modeling of the plume region in a later section.

The balanced equations for complete hydrocarbon mineralization under the six primary terminal electron accepting conditions for an equivalent hydrocarbon compound, $C_\gamma H_\beta$ are given in Table 3.1. Nitrate reduction was represented as three possible reactions to account for nitrite and ammonium as end products as measured in situ. The stoichiometric equation for sulfate reduction also accounts for sulfide production, allowing a comparison of model prediction based on these two species.

3.4.2   2-D Analytical Model

Superposition of 2-D reactive transport analytical solutions (Domenico and Schwartz,1990) may be used to estimate biodegradation rate coefficients of groundwater contaminants via a least-squares fitting of monitoring well data (Stenback et al., 2004). For a constant contaminant source region of width Y, in a homogenous, isotropic medium with groundwater seepage velocity of v_x, the down-gradient concentration of a contaminant at any location (x,y) and time (t) can be expressed as:

$$C(x,y,t) = \left(\frac{C_o}{4}\right)\exp\left\{\left(\frac{x}{2\alpha_x}\right)\left[1-\sqrt{1+\frac{4\lambda\alpha_x}{v_x}}\right]\right\}\text{erfc}\left(\frac{x-v_c t\sqrt{1+4\lambda\alpha_x/v_x}}{2\sqrt{\alpha_x v_c t}}\right) \bullet$$
$$\left\{\text{erf}\left(\frac{y+Y/2}{2\sqrt{\alpha_y x}}\right)-\text{erf}\left(\frac{y-Y/2}{2\sqrt{\alpha_y x}}\right)\right\} \tag{5}$$

where C_0 is source concentration, x is distance in the direction of groundwater flow, y is the transverse distance from the plume centerline, t is zero at the time of source emplacement, v_c is the

retarded contaminant velocity, α_x is the longitudinal dispersivity, α_y is the transverse dispersivity, and λ is the overall aqueous plus solid phase first-order degradation rate coefficient (Stenback et al, 2004).

The retarded contaminant velocity, v_c, for a given compound can be determined by dividing the seepage velocity by the retardation factor, R, such that:

$$v_c = \frac{v_x}{R} = \frac{v_x}{\left(1 + \dfrac{B_d K_{oc} f_{oc}}{\phi}\right)} \tag{6}$$

where B_d is the soil bulk density, f_{oc} is the fraction of organic carbon in the soil, ϕ is the soil porosity, and K_{oc} is the organic carbon partitioning coefficient of the contaminant. For stable contaminant plumes, a steady-state approximation can be applied by allowing t in equation 5 to approach infinity.

The rate of mass consumption at any time (t) can be estimated by multiplying λ by the total dissolved mass within the contaminated aquifer ($\overline{M_T}$). Since the concentrations of contaminants vary in space, this must be performed by integrating over the volume of contaminated aquifer water such that:

$$\frac{dM}{dt} = -\lambda\left(\overline{M_T}\right) = -\lambda\phi \int_x \int_y z(x,y)C(x,y,t)\,dy\,dx \tag{7}$$

where $z(x,y)$ is the depth of the aquifer, assumed to equal the difference between the till surface and the bottom of the loess unit at any position (x,y). This was defined to be consistent with the geochemical mass balance model and derivation of average groundwater velocity. Equation 7 can be solved by numerical integration (grid size times concentration) over a grid covering the area of contamination at time (t), based on the best-fit kriged geological surfaces determined from soil sampling (see Figures 3.1 and 3.2), such that:

$$\frac{dM}{dt} \approx -\lambda\phi A_{elem} \cdot \sum_1^k \left[z \cdot C(x,y,t)\right] \tag{8}$$

where A_{elem} is the grid size (9.94 m^2) and k is the number of elements within the contaminated region.

Figure 3.5 shows the placement of the contaminant sources and locations of groundwater monitoring wells used in the model fitting procedure relative to the approximate extent of PAH and BTEX groundwater contamination (1 $\mu g \cdot L^{-1}$). The source locations, sizes, and orientations were selected relative to groundwater flow and the extent of the estimated source region. Twenty groundwater monitoring locations down-gradient of the source area were used in estimating first-order degradation rate constants of several contaminants. Concentrations measured in nested monitoring wells (those with several screened intervals of varying elevation) were averaged for modeling purposes. Based on soil characterizations as described by Biyani (2002), the fraction of organic carbon, porosity, and bulk density of the aquifer system were estimated to be 0.0039, 0.32, and 1.8 kg/L, respectively. As suggested by Wiedemeier et al. (1999), the approximate plume extents were used to define the longitudinal and transverse dispersivities (10m and 2m, respectively). These values were held constant for modeling purposes. A transient solution was used whereby the time for source Y_1 and Y_2 emplacement was set to 75 years to coincide with the MGP operations. A third source region, source Y_3, was assumed in the model to account for a possible secondary contaminant source observed in groundwater measurements where a fuel storage tank was removed approximately 15 years prior to this investigation. Only those compounds observed to be elevated in this region were modeled with a third source. The model was fitted to the site data by varying the overall degradation rate coefficient, λ, and the three source concentrations, Y_1, Y_2, and Y_3, within a range of concentrations observed within the source region. Linear, reversible, and homogenous sorption was assumed for simplicity, although PAH compounds may exhibit non-linear and irreversible isotherm behavior that may vary with time, location, and competition among contaminants for sorption sites (see Allen-King et al., 2002),. Irreversible sorption of contaminants or sorption hysteresis in the actual aquifer would manifest in a larger overall degradation rate coefficient estimated by the analytical solution than the actual aquifer degradation rate coefficient.

3.5 Results and Discussion

3.5.1 Geochemical response to contamination

Figures 3.6-3.9 are isoconcentration plots and centerline transects of common TEAs and reduced species observed in contaminant plumes. Shown are average concentrations measured at sampling locations along the jagged transect A-A' over the three sampling events (August 2001, April 2002, and November 2002) and the values of the kriged surface along the straight transect A-A'

reported in the isoconcentration plots. Transect A-A' begins approximately 30 meters up-gradient of the coal-tar source region to include background groundwater values. Table 3.2 shows the concentrations of TEAs and key water quality parameters measured in groundwater sampled from select uncontaminated background and contaminated monitoring wells (average values) and DPT locations (one-time measurements).

As can be seen in Figure 3.6, the dissolved oxygen depletes rapidly within the contaminant source region and remains generally below 1 mg/L within the contaminant plume (see Table 3.2). The ORPs measured in the groundwater reflect well the measured dissolved oxygen, except at a location approximately 100 m along transect A-A'. Up to and at this location, the ORP is in a condition of rebound as dissolved contaminants from the FMGP source region are declining. The ORP drops again over the next 15 m into the region of the possible secondary source. The inconsistency between the ORP and dissolved oxygen may be due to a relatively slow recharge of dissolved oxygen from the groundwater-soil gas interface. Although little evidence of contamination close to the river exists, the ORP and dissolved oxygen remain low through the remainder of the transect. This is likely due to the depths at which the groundwater was sampled (approximately 12 m) and subsequently low oxygen penetration into the aquifer.

Figure 3.7 supports the occurrence of nitrate reduction within the contaminated source region. A large reduction in nitrate is coupled to a significant elevation in nitrite and ammonium, which attenuate once the nitrate is consumed. Based on background groundwater measurements which consistently result in nitrate concentrations of 13-16 mg/L at three monitoring well locations (e.g., MW4 in Table 3.2) as well as several one-time direct-push groundwater sampling locations), nitrate may play a key role in microbial degradation of the coal-tar constituents at this site. Delineation between nitrate consumed as a terminal electron acceptor and nitrate consumed for microbial growth could not be established but would have the net effect of reducing nitrate-reduction.

Figure 3.8 shows total dissolved iron and manganese. The oxidized forms of these metals are relatively insoluble, therefore changes in total dissolved metals are strongly influenced by the reduced forms. Based on the increased soluble metals concentrations, there may have been significant metal reduction near the coal-tar source. It is unclear why the less energetically favorable iron (III) reduction occurred prior to the more favorable manganese (IV) reduction in this aquifer. However, it may be related to local differences in availability of oxidized iron or manganese. Differences in local soil mineralogy may also explanation secondary peaks in soluble metals observed in groundwater sampled from wells past the contaminant plume.

Groundwater concentrations of sulfide that were significantly higher than background, coupled with hydrogen sulfide odors from groundwater samples collected in this region indicate sulfate reduction. Figure 3.9 shows the measured sulfate and sulfide concentrations along transect A-A'. Sulfide production was coupled to a drop in measured groundwater concentrations of sulfate in the possible secondary source region (see GMW 13 in Table 3.2). The lighter hydrocarbons observed in this region (BTEX, naphthalene. etc.) have been shown to degrade under sulfate-reducing conditions by several researchers (e.g., Coates et al., 1996; Galushko et al., 1999; Hayes and Lovley, 2002). Standard heterotrophic plate counts confirm biological growth in this region of the plume (see Table 3.2, MW13).

Extensive spatial heterogeneity can be seen in the hydrogeochemical response to the coal-tar and BTEX contamination. Spatial and temporal heterogeneity was also observed in standard heterotrophic plate counts across the contaminated aquifer. This level of heterogeneity is very difficult to resolve in analytical fate and transport models, and would violate instantaneous reaction assumptions. Numerical approaches to estimating degradation rates based on mass balance approaches may be more realistic to these types of scenarios. Standard heterotrophic plate counts per milliliter and 95% confidence intervals within the source, plume, and background regions (average of all monitoring locations in these regions) were 2008 ±235 (n=21), 1905 ±373 (n=23), and 429 ±174 (n=28), respectively, suggesting microbial growth within the contaminant source region and plume, and support intrinsic remediation potential. Methane production was not detected within this aquifer system (Black and Veatch, 1998).

3.5.2 Stoichiometric Terminal Electron Acceptor Mass Balance

Table 3.3 shows the results of the stoichiometric mass balance approach. Nitrate reduction was computed both under the assumption of complete denitrification and with the end products nitrite and ammonium. Mass consumption under sulfate reducing conditions was determined using both sulfate loss and hydrogen sulfide production for comparison. Based on the results presented in Table 3.3 and a groundwater flow of 1.76 m^3/d through the source region and contaminant plume, microbially-mediated reactions may be responsible for the destruction of 4.5 kg of contaminant mass per year.

3.5.2.1   Source region

97.8% of the transformed contaminant mass in the source region based on consumption of terminal electron accepting compounds was attributable to reduction of oxygen and nitrate (17.7% and 80.1%, respectively). Although regions of metal reduction (iron and manganese) are apparent based on groundwater measurements, metal reduction was attributable to only a small fraction of potential contaminant mineralization (2.2%, total). Sulfate concentrations increased in the source region relative to the background groundwater on flux boundary 1. This may be related to a single low sulfate concentration measurement in the one time groundwater sample GPW17 (see Figure 3.9). Geochemical evidence of sulfate reduction in the form of hydrogen sulfide production was not observed in this region.

3.5.2.2   Plume region

Rapid consumption of oxygen and nitrate in the source region resulted in low concentrations at flux boundary 2. Higher average concentrations of these TEAs in the plume region than on flux boundary 2 were observed, possibly due to rebounding near the plume fringes. Consequently, net mass degradation attributable to nitrate-reduction or aerobic oxidation in the plume region could not be established based on equations 1 and 2. Similarly, the relatively high concentration of soluble metals on flux boundary 2 compared to the average concentration of metals in the plume region resulted in no calculated mass degradation due to metal reduction. This indicates one weakness of this approach, in that it does not account for flux of TEAs across the model boundaries (infiltration/diffusion across the air-water interface or diffusion/dispersion across streamlines 1 or 2). Given that dissolved oxygen and nitrate are present at low concentrations within the plume, aerobic respiration and nitrate reduction likely occur to some degree. Iron and manganese reduction may be reasonable, as secondary peaks in ferrous iron and manganese (II) occur in the post plume region (see Figure 3.8). By measuring complete redox couples (i.e. sulfate and sulfide or nitrate and nitrite), some of the model limitations with regards to TEA flux across the model boundaries may be negated. For instance, a secondary peak in ammonium within the plume region resulted in elevated ammonium concentrations relative to flux boundary 2 (see Figure 3.7 and Table 3.3) allowing for estimation of nitrate reduction to ammonium in the plume region. However, some redox couples can only be monitored with aqueous measurements in the oxidized or reduced states.

The presence of hydrogen sulfide in the plume region shown in Figure 3.9 and Table 3.3 was associated with redox potentials as low as -247 mV (measured at GMW 20, HS⁻ = 0.65 mg/L) indicating that sulfate-reduction may be the primary redox process in the contaminant plume region.

Table 3.3 shows reasonable agreement between degradation of contaminants based on changes in sulfate and hydrogen sulfide. However, the distribution of these species in the contaminant plume region should be spatially correlated and inversely related. The spatial heterogeneity in sulfate concentrations without coupled changes in hydrogen sulfide (e.g. GPW 17) make correlation between these species poor (see Figure 3.9). Large concentrations of sulfate coupled with natural variability in the measurements and the precision of the analytical techniques may mask the use of sulfate as a TEA. For instance, the calculated difference in sulfate concentration between flux boundary 2 and the plume region is 3 $mg \cdot L^{-1}$, less than 2.2% of the concentration on flux boundary 2 (137 $mg \cdot L^{-1}$). Use of more sensitive redox species such as hydrogen sulfide may be more appropriate for mass balance approaches.

3.5.3 2-D Analytical Modeling

Table 3.4 shows the best-fit degradation rate coefficients (λ) and source concentrations ($C_{o,1}$, $C_{o,2}$, and $C_{o,3}$) of the superimposed analytical solutions for several BTEX and PAH compounds as determined using the Solver package in Microsoft® Excel. Also shown in Table 3.4 are the sum of squares of the errors (SSE) between measured and modeled concentrations over all twenty sampling locations and the correlation coefficient describing the goodness of fit of the model to the actual data (r^2). In general, a high r^2 value indicated the overall goodness of fit of the modeled concentrations to the measured concentrations, whereas the SSE was particularly sensitive to the goodness of fit of individual monitoring locations. An SSE of 1000 would indicate that the total difference between the measured and modeled concentrations at all 20 monitoring locations was less than 32 $\mu g \cdot L^{-1}$. Care should be exercised in interpreting the goodness of fit, as it may be strongly influenced by large concentrations in a select few monitoring locations. Model fitted concentrations agreed well to measured site data for most compounds (SSE<1000 and r^2 > 0.99).

The best-fit degradation rate coefficients of the superimposed analytical solutions varied between 1.3 x 10^{-5} d^{-1} (phenanthrene, R_f = 308) to 8.4 x 10^{-3} d^{-1} (benzene, R_f = 2.6), and agreed favorably to those presented by others (see Chapter 2). In the case of phenanthrene, the degradation rate is low enough to assume that the extent of the plume can be explained without degradation. For naphthalene, an average measured concentration of 144 $\mu g \cdot L^{-1}$ at GMW 17 (see Figures 3.1b and 3.3d) could not be explained by the model (best-fit concentration = 16 $\mu g \cdot L^{-1}$). In fitting this monitoring well, the model over-predicts the concentration of two nearby monitoring wells by 42 $\mu g \cdot L^{-1}$ and 60 $\mu g \cdot L^{-1}$, respectively, by forcing a large concentration at source Y_1, explaining the large

SSE of 21800. GMW 17 is located directly adjacent to several above ground fuel storage tanks and a refueling location for gasoline trucks. Elevated concentrations of several BTEX compounds have also been observed in this monitoring well (see Figure 3.3).

Also presented in Table 3.4 are the mass transformation rates within the contaminant plume as determined by numerical integration (see eq. 8). The mass transformation rates for both the source region and plume region were determined for direct comparison to the lumped-hydrocarbon geochemical mass balance model. However, since λ was determined in the plume region, which is low in dissolved oxygen and nitrate, its application to contaminant mass transformation in the source region where considerable aerobic respiration and nitrate reduction are occurring may be questionable. It is expected that the rate of mass transformation in the source region would be larger than the plume region, as was evidenced in the lumped-hydrocarbon geochemical mass balance model approach. Based on these two approaches, the magnitude of mass transformation in the source region ranged between 46-90% of the total mass transformation. These results highlight the need for more reliable alternatives to estimating degradation rates through reactive transport modeling for determining mass transformation in source regions. The total mass transformation rates (sum of all modeled compounds in the source and plume regions) presented in Table 3.4, however, compared well (same order of magnitude) to the transformation rates determined through the geochemical mass balance (see Table 3.3).

Differences in the results of the two mass transformation estimates in the plume region may be due to errors inherent to either modeling approach. For instance, transformation and loss of $HS^-_{(aq)}$ to $H_2S_{(g)}$ from the groundwater would lower the stoichiometric estimate of mass degradation rate in the mass balance model. The lack of the ability to quantify mass degradation due to consumption of TEAs as they are recharged into the contaminant plume through the streamline boundaries or air-water interface may further lower the mass transformation estimate. Mass loss to irreversible sorption or phase change of PAH contaminants in the aquifer would result in overall degradation rate coefficients (λ) that are large compared to actual biodegradation rate coefficients. This would result in artificially inflated mass transformation rates based on equation 8. By summing the mass transformation rate of only a relative few select pollutants, however, it could be expected that this method may provide a conservative estimate of overall mass transformation rate. In this study, the lumped-hydrocarbon geochemical mass balance model provided a more conservative estimate of overall contaminant mass transformation rate compared to analytical modeling approaches. This suggests that the effects of processes such as contaminant phase change and sorption hysteresis may influence degradation rates fitted by models of the fate and transport of PAHs under the assumptions

used in this exercise. However, the results were within the same order of magnitude, and show the utility of using a combination of simple lumped-hydrocarbon geochemical mass balance approaches and superposition techniques with the 2-D reactive transport analytical solution in systems of complex geology and possible multiple sources.

3.6 Conclusions

The FMGP site of this study is located approximately 200 m up-gradient a nearby river. Based on groundwater monitoring, contamination emanating from the site and a potential secondary contaminant source identified approximately 80m down-gradient of the coal-tar source region have not impacted the river. Assuming source concentrations and degradation rate coefficients were to remain infinitely the same (steady-state assumption), reactive transport modeling would suggest that some compounds may eventually reach the river. However, infinite source assumptions may lead to over-prediction of contaminant plume extents. Further investigation into source term development (including total mass and potential for phase change) and a more detailed study of attenuation potential are required to yield a more reliable prediction of contaminant plume front migration.

Geochemical and biological evidence at the FMGP site suggest microbially-mediated reactions active within the contaminated region. Evidence includes reduction of available TEAs (dissolved oxygen, nitrate, and sulfate) and production of coupled reduced species (nitrite, ammonium, ferrous iron, manganese (II), and hydrogen sulfide) within the contaminated aquifer relative to the background groundwater. This was coupled with associated microbial growth as evidenced by standard heterotrophic plate counts in the contaminant source and plume region relative to background heterotrophic plate counts.

Mass balances based on loss in terminal electron accepting compounds or production of reduced species produced estimates of the potential biodegradation of 4.1 kg/yr contaminant mass in the source region and 0.46 kg/yr contaminant mass in the resulting plume. The results of the mass balance exercise indicated that oxygen and nitrate availability may limit intrinsic bioremediation in this system. A superposition of three 2-D Domenico and Schwartz (1990) analytical solutions were used to estimate degradation rate coefficients of specific compounds measured within the contaminant plume. Using numerical integration techniques and these coefficients, the overall contaminant mass transformation rates were determined to be 1.7 $kg\cdot yr^{-1}$ in the source region and 2.0 $kg\cdot yr^{-1}$ in the contaminant plume. These values compared well (within an order of magnitude) to the geochemical modeling presented above. The differences may be related to several errors including

analytical error in measuring hydrogeochemical parameters in situ, spatial heterogeneity of TEAs and reduced species in the aquifer system, numerical error introduced within the modeling techniques, or overestimation of degradation rate coefficients due to relaxing the analytical model relative to contaminant phase change and sorption hysteresis.

Further studies on the intrinsic biodegradation potential of site soils under different terminal electron accepting conditions using lab-scale bioassays may be necessary to verify whether the measured reduction of TEAs within the contaminant source region and plume relative to the clean background aquifer are due to degradation of the specific compounds of interest, or are artifacts of other components of the fuel mixture. The site microbial community structure and function related to the degradation of specific compounds have not been identified, but would provide much more reliable evidence of intrinsic bioremediation potential. However, this work is significant in that it shows that it is possible to couple a superposition of reactive transport analytical solutions with a terminal electron acceptor mass balance approach to estimate contaminant depletion in a hydrogeologically (variable groundwater flow direction) and chemically complex (commingled plumes) contaminated system, providing estimates of contaminant mass reduction rates and evidence valuable towards evaluating the intrinsic remediation potential of coal-tar impacted aquifers.

3.7 References

Allen-King, R. M., P. Grathwohl, and W. P. Ball (2002) New modeling paradigms for the sorption of hydrophobic organic chemicals to heterogeneous carbonaceous matter in soils, sediments, and rocks, *Adv. in Water Res.*, 25(8-12), 985-1016.

Anderson, R. T. and D. R. Lovley (1999) Naphthalene and benzene degradation under Fe(III)-reducing conditions in petroleum-contaminated aquifers, *Bioremediation*, 3(2), 121-135.

Bayard, R. M., L. Barna, and R. Gourdon (1998) Influence of organic pollutants on sorption of naphthalene in contaminated soils, *Contaminated Soil '98: Proc. 6th Inter. FZK/TNO Conf. on Contaminated Soil*, Thomas Telford, London, 2, 849-850.

Biyani, R. (2002) Modeling groundwater flow and transport of contaminants at the Cherokee Former Manufactured Gas Plant site, Iowa, M.S. Thesis, Iowa State University, Ames, IA.

Black & Veatch (1998) Interim remedial action report for soil and source material, Prepared for IES Utilities Inc., Black & Veatch Waste Science, Inc.

Campbell, B. G., M. D. Petkewich, J. E. Landmeyer, and F. H. Chapelle (1996) *Geology, hydrogeology, and potential of intrinsic bioremediation at the National Park Service*

Dockside II Site and adjacent areas, Charleston, South Carolina, 1993–1994, Rep. No. 96-4170, U.S. Geological Services, Columbia, S.C.

Coates, J. D., R. T. Anderson, and D. R. Lovley (1996) Oxidation of polycyclic aromatic hydrocarbons under sulfate-reducing conditions, *Appl. Environ. Microbiol.*, **62**(3), 1099-1101.

Davis, J. W., N. J. Kliker, and C. L. Carpenter (1994) Natural biological attenuation of benzene in ground water beneath a manufacturing facility, *Ground Water*, **32**(2), 215-226.

Domenico, P. A., and F. W. Schwartz (1990) Physical and chemical hydrogeology, Second Edition, John Wiley & Sons, Inc., New York, New York.

Eberhardt, C., and P. Grathwohl (2002) Time scales of organic contaminant dissolution from complex source zones: coal tar pools vs. blobs, *J. Contam. Hydrol.*, **59**(1-2), 45-66.

Electric Power Research Institute (EPRI) (1996) Characterization and monitoring before and after source removal at a former manufactured gas plant (FMGP) disposal site, EPRI Rep. No. TR-105921, Palo Alto, Calif.

Eriksson, M., E. Sodersten, Z. Yu, G. Dalhammar, and W. W. Mohn (2003) Degradation of polycyclic aromatic hydrocarbons at low temperature under aerobic and nitrate-reducing conditions in enrichment cultures from northern soils, *Appl. Environ. Microbiol.*, **69**(1), 275-284.

Galushko, A., D. Minz, B. Schrink, and F. Widdel (1999) Anaerobic degradation of naphthalene by a pure culture of a novel type of marine sulphate-reducing bacterium, *Environ. Microbiol.*, **1**(5), 415-420.

Golchin, J., G. A. Stenback, B. H. Kjartanson, S. K. Ong, and M. E. Holland (1999) Development of a groundwater monitoring protocol for monitored enhanced natural attenuation, Proceedings of the *Twelfth International Symposium on Environmental Biotechnologies and Site Remediation Technologies & Utility Industry Environmental Issues, Challenges, and Solutions*, IGT, December 6-10, 1999, Orlando, Florida.

Hayes, L. A. and D. R. Lovley (2002) Specific 16S rDNA sequences associated with naphthalene degradation under sulfate-reducing conditions in harbor sediments, *Microb. Ecol.*, **43**(1), 134-145.

Heitkamp, M. A. and C. E. Cerniglia (1987) Effects of chemical structure and exposure on the microbial degradation of polycyclic aromatic hydrocarbons in freshwater and estuarine ecosystems, *Environ. Toxicol. Chem.*, **6**(3), 535-546.

Huang, W., and W. J. Weber, Jr. (1997) A distributed reactivity model for sorption by soils and sediments. X: Relationships between desorption, hysteresis, and the chemical characteristics of organic domains, *Environ. Sci. Technol.*, **31**(9), 2562-2569.

Johnsen, A. R., A. Winding, U. Karlson, and P. Roslev (2002) Linking of microorganisms to phenanthrene metabolism in soil by analysis of 13C-labeled cell lipids, *Appl. Environ. Microbiol.*, **68**(12), 6106-6113.

King, M. W. G., and J. F. Barker (1999a) Migration and natural fate of a coal tar creosote plume 1. overview and plume development, *J. Contam. Hydrol.*, **39**(3-4), 249-279.

King, M. W. G., J. F. Barker, J. F. Devlin, and B. J. Butler (1999b) Migration and natural fate of a coal tar creosote plume 2. Mass balance and biodegradation indicators, *J. Contam. Hydrol.*, **39**(3-4), 281-307.

Kjartanson, B. H., S. K. Ong, G. A. Stenback, and S. W. Rogers (2001) Dubuque Key City FMGP site, Dept of Civil and Construction Engineering, Iowa State University, Ames, Iowa.

Kjartanson, B. H, G. A. Stenback, S. K. Ong, S. W. Rogers, and R. Biyani (2002) Optimized ground water monitoring for MENA and site closure, Interim Report, Work Performed for Year 1 at the Cherokee FMGP Site, Prepared by ISU for Alliant Energy, May 2002.

Landmeyer, J. E., F. H. Chapelle, M. D. Petkewich, and P. M. Bradley (1998) Assessment of natural attenuation of aromatic hydrocarbons in groundwater near a former manufactured-gas plant, South Carolina, USA, *Environ. Geol.*, **34**(4), 79–292.

Langworthy, D. E., R. D. Stapleton, G. S. Sayler, and R. H. Findlay (1998) Genotypic and phenotypic responses of a riverine microbial community to polycyclic aromatic hydrocarbon contamination, *Appl. Environ. Microbiol.*, **64**(9), 3422-3428.

Lyngkilde, J., and T. H. Christensen (1992) Fate of organic contaminants in the redox zones of a landfill leachate plume (Vejen, Denmark), *J. Contam. Hydrol.*, **10**(4), 291-307.

McGinnis, G. D., H. Borazjani, L. K. McFarland, D. F. Pope, and D. A. Strobel (1988) *Characterization and laboratory testing soil treatability studies for creosote and pentachlorophenol sludges and contaminated soil*, USEPA Report No. 600/2-88/055. Robert S. Kerr Environmental Laboratory, Ada, OK.

McNally, D. L., J. R. Mihelcic, and D. R. Lueking (1999) Biodegradation of mixtures of polycyclic aromatic hydrocarbons under aerobic and nitrate-reducing conditions, *Chemosphere*, **38**(6), 1313-1321.

National Research Council (NRC) (2000) Natural attenuation for groundwater remediation, Committee on Intrinsic Remediation, Water Science and Technology Board, Board on

Radioactive Waste Management, Commission on Geosciences, Environment, and Resources, National Academy Press, Washington, D.C.

Newell, C. J., J. W. Winters, H. S. Rifai, R. N. Miller, J. Gonzales, T. H. Wiedemeier (1995) Modeling intrinsic remediation with multiple electron acceptors: results from seven sites, National Ground Water Association, Proceedings of the Petroleum Hydrocarbons and Organic Chemicals in Ground Water Conference, Houston, Texas, November 1995, 33-48.

Ong, S. K., B. H. Kjartanson, G. A. Stenback, J. Golchin, S. W. Rogers, and N. Miller (2001) Assessment of natural attenuation at a former manufactured gas plant site, *Proceedings of the 6th international In-Situ and On-Site Bioremediation Conference*, San Diego, CA.

Padmanabhan, P., S. Padmanabhan, C. DeRito, A. Gray, D. Gannon, J. R. Snape, C. S. Tsai, W. Park, C. Jeon, and E. L. Madsen (2003) Respiration of 13C-labeled substrates added to soil in the field and subsequent 16S rRNA gene analysis of 13C-labeled soil DNA, *Appl. Environ. Microbiol.*, **69**(3), 1614-1622.

Park, K. S., R. C. Sims, and R. Dupont (1990) Transformation of PAHs in soil systems, *J. Environ. Eng.*, **116**(3), 632-640.

Peters, C. A., K. H. Wammer, and C. D. Knightes (2000) Multicomponent NAPL solidification thermodynamics, *Transport Porous Med.*, **38**(1-2), 57-77.

Pignatello, J.J.(2000) The measurement and interpretation of sorption and desorption rates for organic compounds in soil media., In Advances in Agronomy, Sparks, D. L. (ed.), 69, 1-73, Academic Press, San Diego, California.

Rockne, K. J., J. C. Chee-Sanford, R. A. Sanford, B. P. Helund, J. T. Staley, and S. E. Strand (2000) Anaerobic naphthalene degradation by microbial pure cultures under nitrate-reducing conditions, *Appl. Environ. Microbiol.*, **66**(4), 1595-1601.

Stenback, G. A., S. K. Ong, S. W. Rogers, B. H. Kjartanson (2004) Impact of transverse and longitudinal dispersion on first-order degradation rate estimation, *J. Contam. Hydrol.*, in press.

Stringfellow, W. T., and L. Alvarez-Cohen (1999) Evaluating the relationship between the sorption of PAHs to bacterial biomass and biodegradation, *Water Res.*, **33**(11), 2535-2544.

Suthersan, S. S. (1999) In-situ bioremediation, in Remediation Engineering: Design Concepts, S.S. Suthersan (Ed.), CRC Press, Boca Ratan.

U.S. EPA (1999) Use of Monitored Natural Attenuation at Superfund, RCRA Corrective Action, and Underground Storage Tank Sites, Office of Solid Waste and Emergency Response Policy

Directive 9200.4-17P, EPA, Office of Solid Waste and Emergency Response, U.S. Government Printing Office, Washington, D.C., April 21, 41 pp.

Weber, W. J. Jr., S. H. Kim, and M. D. Johnson (2002) Distributed reactivity model for sorption by soils and sediments. 15. High-concentration co-contaminant effects on phenanthrene sorption and desorption, *Environ. Sci. Technol.*, **36**(16), 3625-3634.

Wiedemeier, T. H., H. S. Rifai, J. T. Wilson, and C. Newell, (1999) Natural attenuation of fuels and chlorinated solvents in the subsurface, John Wiley & Sons, New York, New York.

Wilson, J. T., J. F. McNabb, J. W. Cochran, T. H. Wang, M. B. Tomson, and P. B. Bedient (1985) Influence of microbial adaptation on the fate of organic pollutants in groundwater, *Environ. Toxicol. Chem.*, **4**(5), 721-726.

Zhang, X. and L. Y. Young (1997) Carboxylation as an initial reaction in the anaerobic metabolism of naphthalene and phenanthrene by sulfidogenic consortia, *Appl. Environ. Microbiol.*, **63**(12), 4759-4764.

Table 3.1   Balanced stoichiometric equations for complete mineralization of an equivalent hydrocarbon compound $C_\gamma H_\beta$

TEA Condition and Stoichiometric Relationship

Aerobic Oxidation

$$C_\gamma H_\beta + (\gamma + 0.25\beta)O_2 \rightarrow \gamma CO_2 + 0.5\beta H_2O$$

Nitrate Reduction

to ammonium: $C_\gamma H_\beta + (0.5\gamma + 0.125\beta)NO_3^- + (\gamma + 0.25\beta)H^+ + (0.5\gamma - 0.375\beta)H_2O \rightarrow \gamma CO_2 + (0.5\gamma + 0.125\beta)NH_4^+$

to nitrite: $C_\gamma H_\beta + (2\gamma + 0.5\beta)NO_3^- \rightarrow \gamma CO_2 + (2\gamma + 0.5\beta)NO_2^- + (0.5\beta)H_2O$

denitrification: $C_\gamma H_\beta + (0.8\gamma + 0.2\beta)NO_3^- + (0.8\gamma + 0.2\beta)H^+ \rightarrow \gamma CO_2 + (0.4\gamma + 0.1\beta)N_2 + (0.4\gamma + 0.6\beta)H_2O$

Mn(IV) reduction

$$C_\gamma H_\beta + (2\gamma + 0.5\beta)Mn^{4+} + 2\gamma H_2O \rightarrow \gamma CO_2 + (4\gamma + \beta)H^+ + (2\gamma + 0.5\beta)Mn^{2+}$$

Fe(III) reduction

$$C_\gamma H_\beta + (4\gamma + \beta)Fe^{3+} + 2\gamma H_2O \rightarrow \gamma CO_2 + (4\gamma + \beta)H^+ + (4\gamma + \beta)Fe^{2+}$$

Sulfate Reduction

$$C_\gamma H_\beta + (0.5\gamma + 0.125\beta)SO_4^{2-} + (0.75\gamma + 0.1875\beta)H^+ \rightarrow \gamma CO_2 + (0.25\gamma + 0.0625\beta)H_2S + (0.25\gamma + 0.0625\beta)HS^- + 0.5\beta H_2O$$

Methanogenesis

$$C_\gamma H_\beta + (\gamma - 0.25\beta)H_2O \rightarrow (0.5\gamma - 0.125\beta)CO_2 + (0.5\gamma + 0.125\beta)CH_4$$

Table 3.2   **Measured groundwater characteristics**

Analyte (Units)	Monitoring Well: Location: Screen Length(s): Screen Midpoint: Screen Midpoint:	MW 4 up-gradient 3.05 m 354.84 m msl	MW 11 down-gradient 1.52 m 345.34 m msl	MW 5 source 3.05 m 357.14 m msl 352.35 m msl	GMW 15 plume 1.22 m 354.1 m msl 352.3 m msl	GMW 13 2nd source 1.22 m 353.0 m msl 350.2 m msl
Inorganics/Nutrients (mgL^{-1})						
Calcium		147	208	219 175	170 150	204 72
Magnesium		40.4	56	40.3 44.3	46 40	56 19
Sodium		59	59.7	26.4 77	48 100	302 231
Potassium		4.2	3.7	4.7 3.4	4.2 2.6	3.2 5.4
Ferrous Iron		0.01	0.88	0.07 1.18	0.31 2.28	0.81 0.37
Total Iron		0.01	1.8	0.02 1.37	0.35 2.29	1.30 0.34
Total Manganese		ND	1.32	1.48 1.78	1.25 1.60	0.35 0.23
Chloride		124	136	32.3 126	83.2 141	280 100
Sulfate		135	165	208 158	175 138	110 140
Sulfide		0.004	0.001	0.009 0.003	0.005 0.003	0.001 1.00
Nitrate+Nitrite (as N)		15.3	0.4	3.5 6.0	0.31 0.20	0.41 1.02
Nitrite (as N)		0.007	0.02	0.021 0.58	0.005 0.005	0.006 0.026
Ammonium (as N)		ND	0.06	0.01 0.01	0.05 0.03	0.40 0.36
Total Phosphorus		ND	0.12	ND[a] ND	ND ND	0.19 0.26
Ortho-Phosphate		ND	ND	ND ND	-[b] -	0 0.3
Total Hardness (as $CaCO_3$)		586	822	703 551	627 526	850 273
Alkalinity (as $CaCO_3$)		298	484	434 400	405 428	802 287
Water Quality Parameters						
Dissolved Oxygen (mgL^{-1})		6.1	1.2	0.3 ƒ[c]	0.25 0.26	0.49 0.7
Temperature (°C)		11.7	11.1	11.7 ƒ	10.1 10.9	12.8 14.4
pH		7.07	6.85	7.1 ƒ	6.96 7.16	7.02 -
Electrical Conductivity (μScm^{-1})		1100	1320	1160 ƒ	1298 1421	2250 1870
Redox Potential (mV)		66	-6	3 ƒ	-17 -87	-16 -
Turbidity (NTU)		5.3	2.5	4.12 ƒ	13.7 14.2	4.8 -
Bacterial						
Plate Count ($CFUmL^{-1}$)		172	69	7 5510	ND 2	440 18000

a. ND = not detected, **b.** " – " = data not available, **c.** ƒ = Coal tar in the purge water, readings not collected

Table 3.3 Estimated biodegradation of contaminants in the source area and plume based on consumption of terminal electron acceptors or production of reduced species.

Redox Process	Source Region $(C_{10.04}H_{9.13})$				Plume Region $(C_{9.32}H_{8.59})$				Total
	$\overline{C}_{FB1}$	$\overline{C}_s$	UF	$\dfrac{dM_s}{dt}$	$\overline{C}_{FB2}$	$\overline{C}_p$	UF	$\dfrac{dM_p}{dt}$	$\dfrac{dM_T}{dt}$
	$(mg{\cdot}L^{-1})$	$(mg{\cdot}L^{-1})$		$(gm{\cdot}d^{-1})$	$(mg{\cdot}L^{-1})$	$(mg{\cdot}L^{-1})$		$(gm{\cdot}d^{-1})$	$(gm{\cdot}d^{-1})$
Aerobic oxidation (ΔO_2):	5.32	1.91	12.3	1.97	1.29	1.53	11.5	NA[a]	1.97
Nitrate reduction									
to ammonium (ΔNH_4^+):	0.046	0.126	6.16	0.213	0.090	0.209	5.73	0.313	0.526
to nitrite (ΔNO_2^-):	0.001	0.197	24.6	0.130	0.029	0.012	22.9	NA	0.130
denitrification (ΔNO_3^- - ΔNH_4^+ - ΔNO_2^-):	10.7	5.53	9.86	8.55	0.605	0.884	9.17	NA	8.55
Assuming only denitrification (ΔNO_3^-):	10.7	5.25	9.86	9.01	0.605	0.765	9.17	NA	9.01
Manganese reduction (ΔMn^{2+}):	0.239	0.990	24.6	0.126	1.78	0.782	22.9	NA	0.126
Iron reduction (ΔFe^{2+}):	0.718	2.08	49.3	0.113	2.36	1.45	45.9	NA	0.113
Sulfate reduction									
based on sulfate (ΔSO_4^{2-}):	118	140	6.16	NA	137	134	5.73	1.15	1.15
based on sulfide (ΔHS^-)	0.007	0.004	3.08	NA	0.001	0.422	2.87	0.941	0.941
Total Mass Transformation Rate:				**11.1**				**1.25**	**12.4**

a.   NA = Not applicable, difference in concentration of terminal electron acceptor is positive or reduced species is negative relative to influx concentration.

Table 3.4   **2-D non-steady- and steady-state first-order degradation coefficients estimated by analytical modeling**

Compound	$C_{o,1}$	$C_{o,2}$	$C_{o,3}$	R_f	λ [a]	SSE	r^2	Mass Transformation Rate		
								Total	Source Region [a]	Plume Region
	$(\mu g \cdot L^{-1})$	$(\mu g \cdot L^{-1})$	$(\mu g \cdot L^{-1})$		(d^{-1})			$(gm \cdot d^{-1})$	$(gm \cdot d^{-1})$	$(gm \cdot d^{-1})$
Benzene	2200	870	3000	2.6	0.0084	33	1.000	2.6	0.92	1.7
Ethylbenzene	1700	0	600	12	0.0076	170	0.999	0.71	0.39	0.32
Xylenes	1000	540	280	6.2	0.0057	5.5	1.000	1.3	0.53	0.76
Naphthalene	6900	0	130	29	0.0058	21800	0.994	3.0	1.6	1.4
Acenaphthylene	450	850	170	56	0.00069	76	0.999	0.24	0.11	0.13
Acenaphthene	110	490	130	98	0.0011	280	0.952	0.79	0.028	0.052
Fluorene	120	160		158	0.0058	1.7	0.998	0.29	0.18	0.11
Phenanthrene	320	320		308	<0.0001	34	0.988	NA [b]	NA	NA
1-Methylnaphthalene	990	880	270	56	0.0042	770	0.995	1.7	0.79	0.92
Total Mass Transformation Rate								**9.89**	**4.56**	**5.33**

a.   Source and plume regions as defined in Figure 3.4.
b.   NA = not applicable, mass transformation rate <0.001 $gm \cdot d^{-1}$
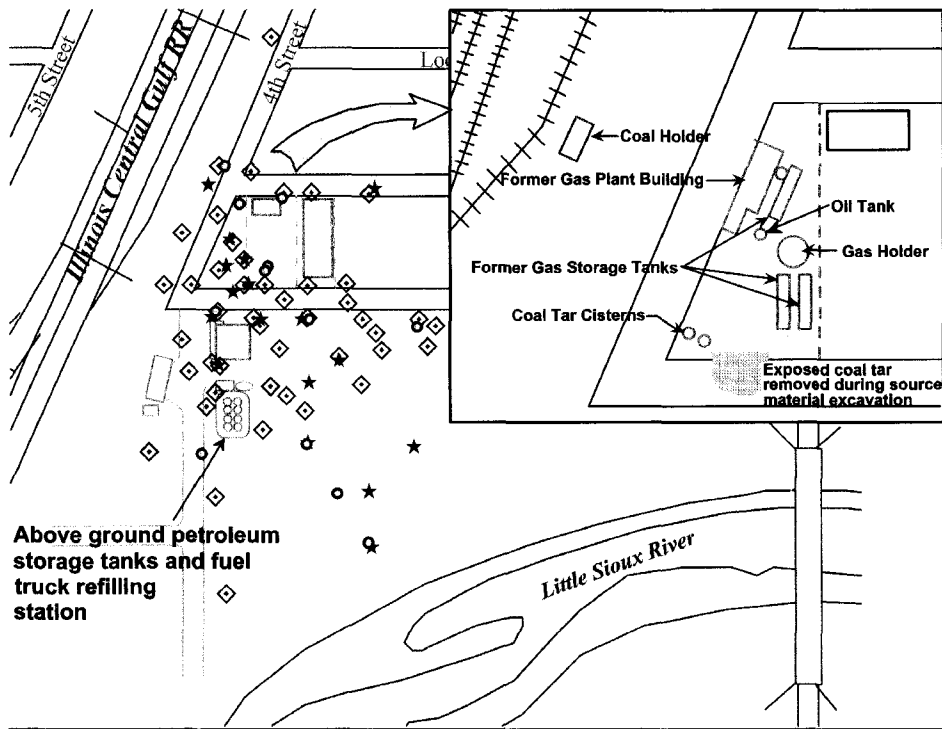
a.
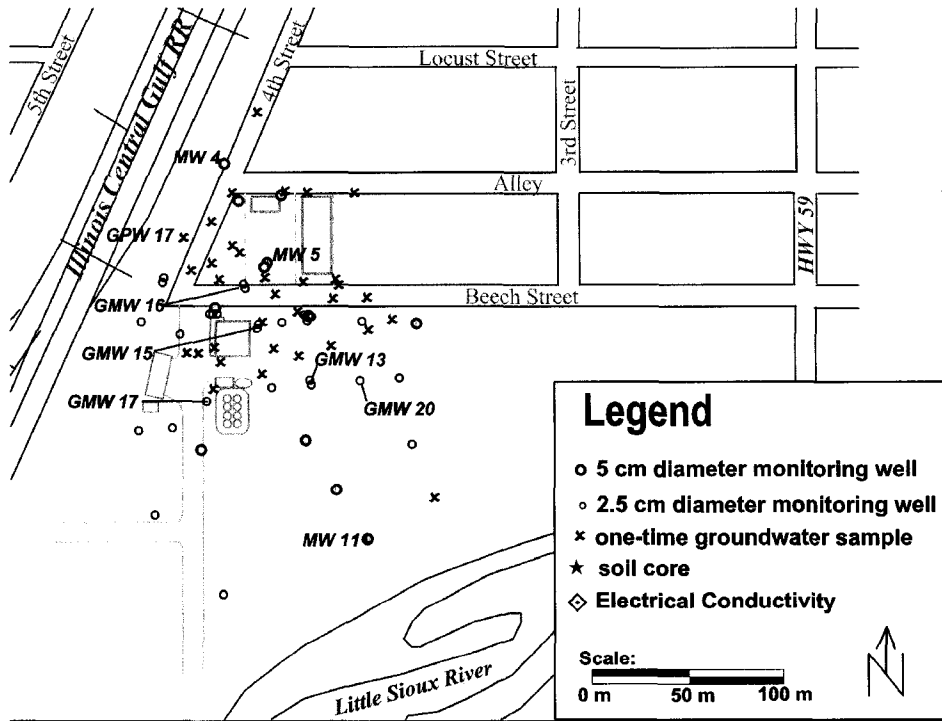
b.

Figure 3.1 FMGP site plan view. a. Soil sampling and electrical conductivity direct-push locations. Insert shows the original site structures and area of exposed coal tar prior to source soil removal. b. Groundwater sampling locations. Select monitoring locations relevant to Table 3.2 are indicated.

Geologic Unit	Hydraulic Conductivity (cm/s)	Organic Carbon Content (f_{oc})
Loess	$1.6 \times 10^{-5} - 8.4 \times 10^{-6}$	0.026 - 0.039
Fine-Grained Silty-Alluvium	$2.4 \times 10^{-5} - 1.6 \times 10^{-4}$	0.007
Coarse Alluvium	$7.9 \times 10^{-2} - 1.0 \times 10^{-2}$	0.0015 - 0.026
Glacial Till	not measured	not measured

Approximate region of thinning in coarse alluvium and intrusion of low hydraulic conductivity loess and fine-grained silty alluvium ➤
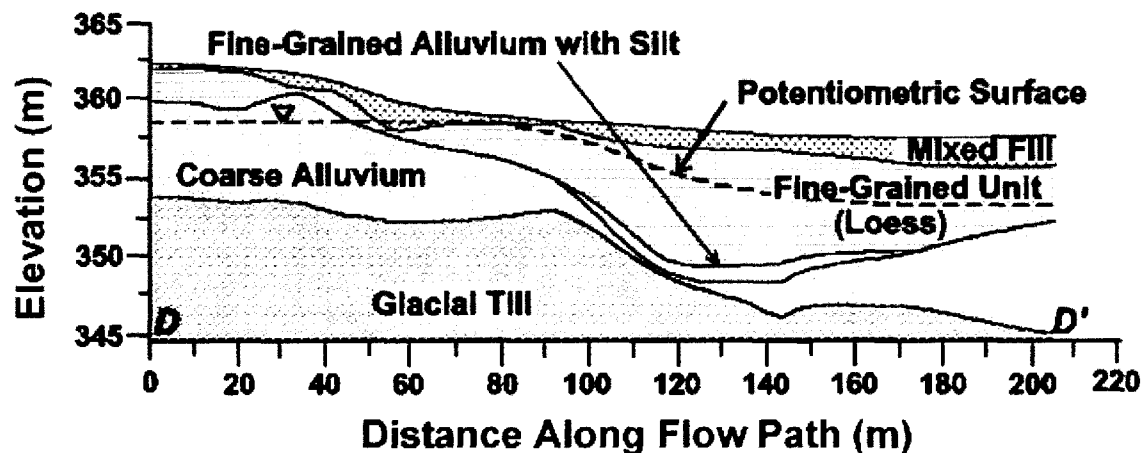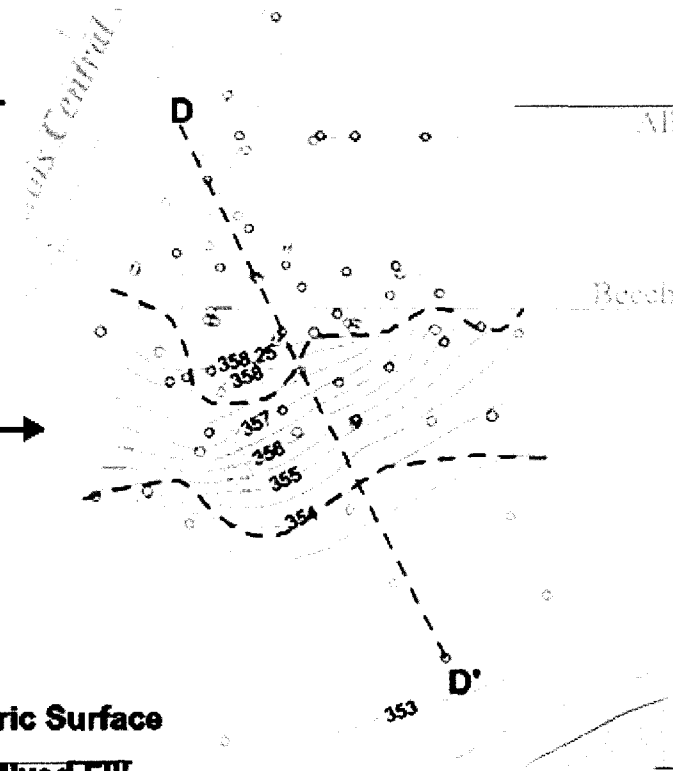
Figure 3.2   Groundwater potentiometric surface contours (meters above mean sea level) in plan view, and geological profile along cross-section D-D'. Circles indicate the groundwater monitoring locations. The approximate region of intrusion of low-hydraulic conductivity soils into the coarse alluvium is indicated.
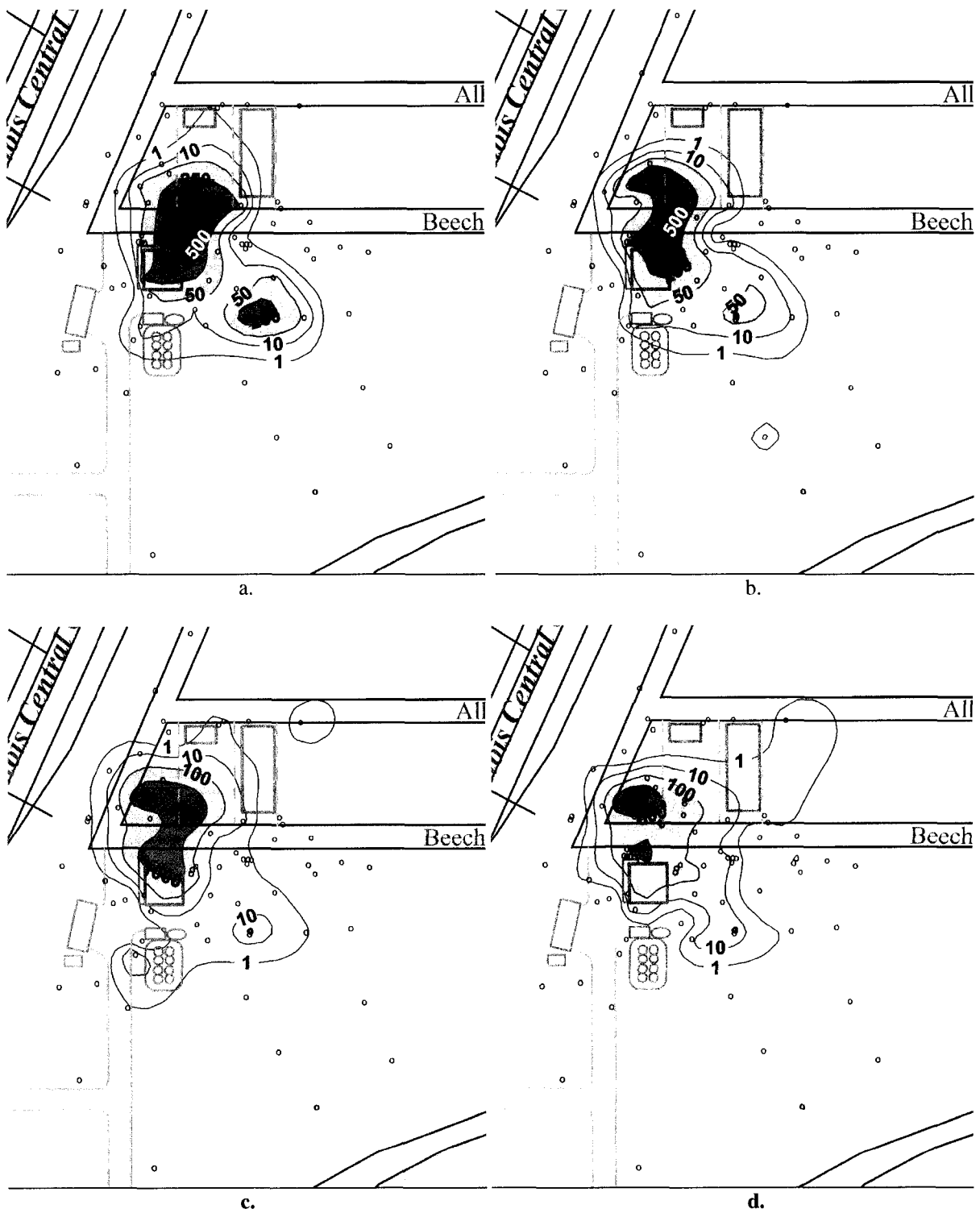
Figure 3.3 Groundwater contaminant concentration contours (µg·L⁻¹) for *(a)* Benzene, *(b)* Xylenes (total), *(c)* Naphthalene, and *(d)* Acenaphthylene. Small circles indicate groundwater sampling locations.
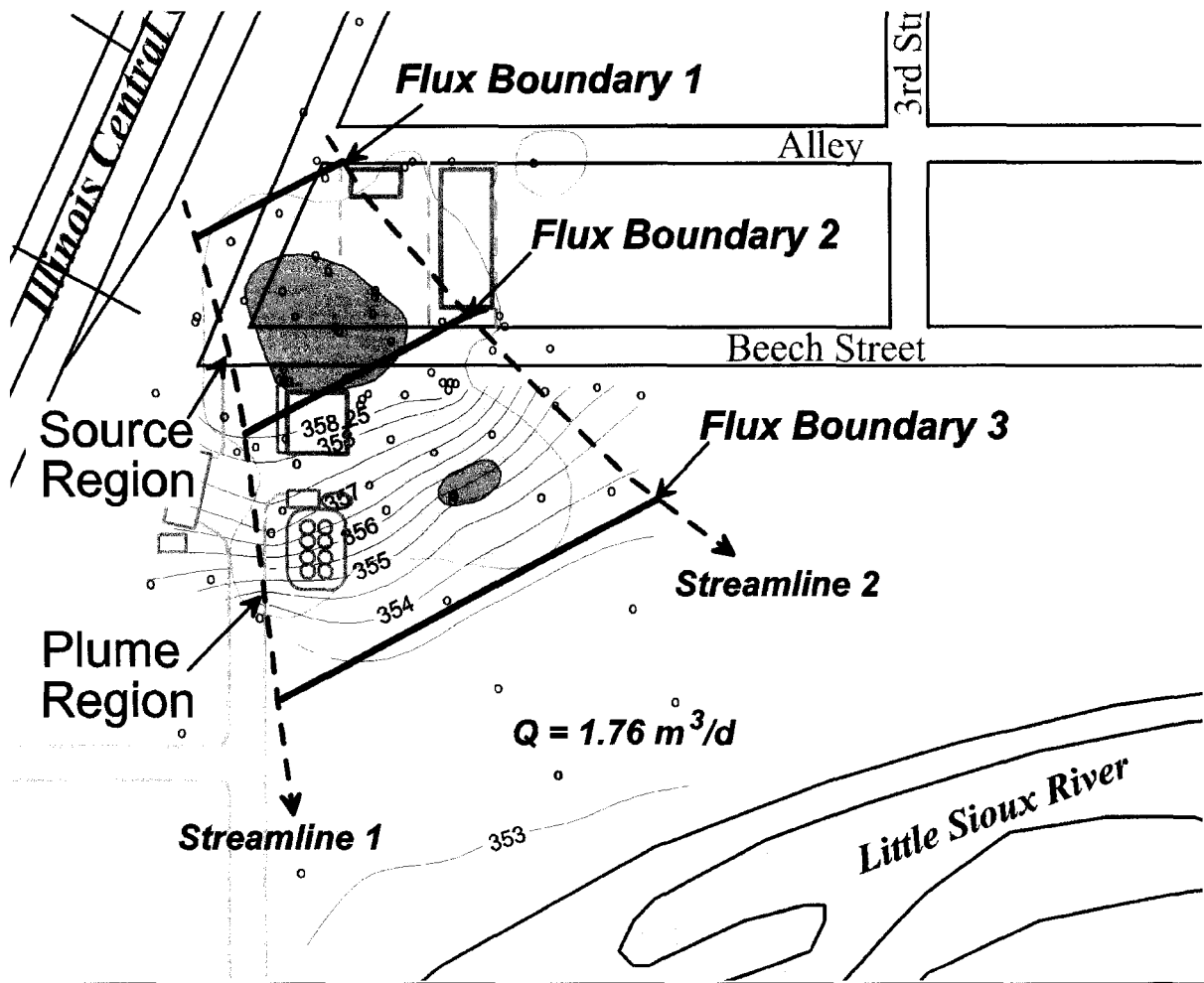
Figure 3.4 Stoichiometric terminal electron acceptor and reduced species mass balance model boundaries. The estimated extent of the contaminant source region (dark gray) and dissolved-phase contaminant plume (light gray, 1 µg·L^{-1}) are shown relative to the model source and plume regions.
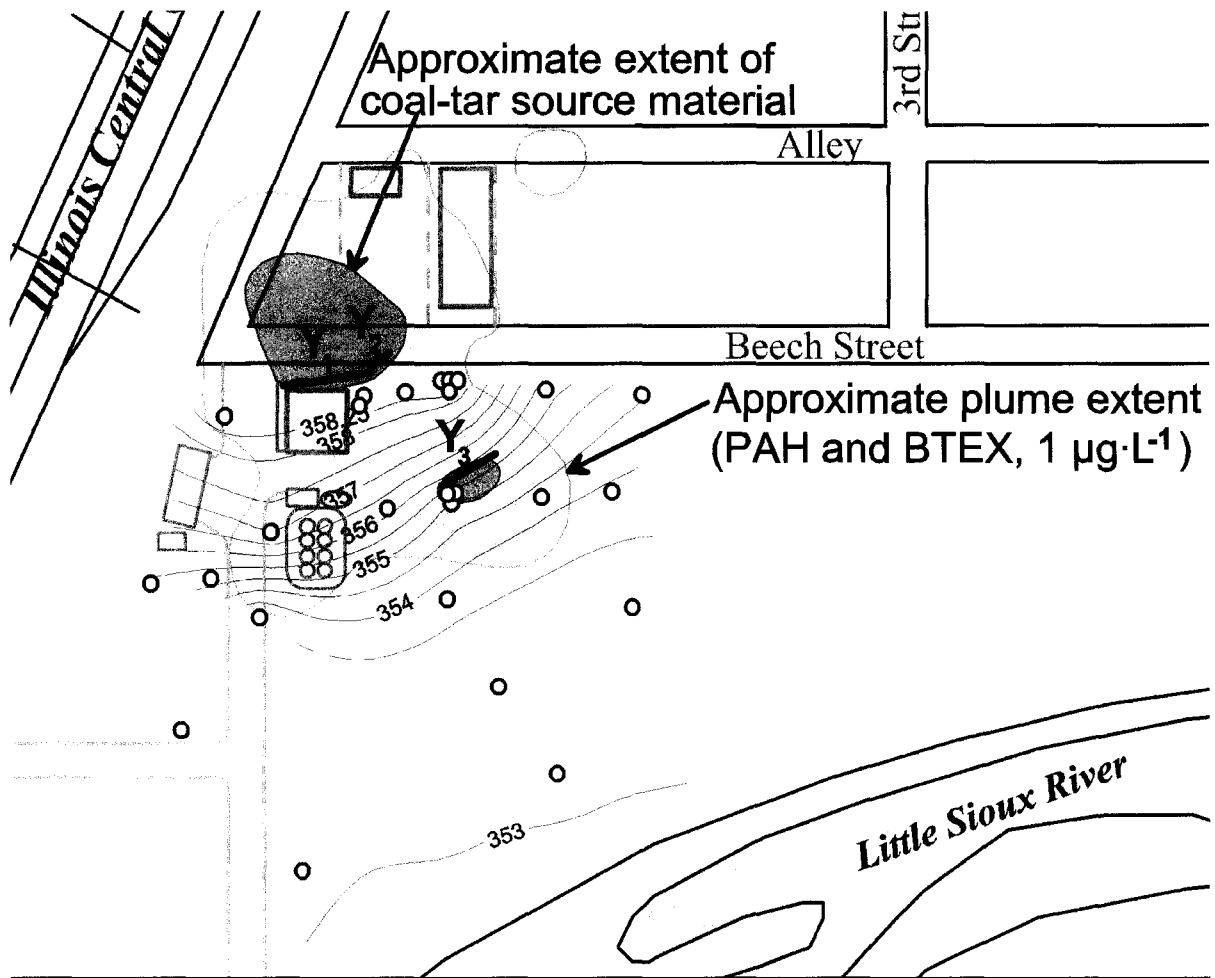
Figure 3.5 2-D reactive transport analytical solution source placement and monitoring well locations. Y_1, Y_2, and Y_3, indicate model source locations. Groundwater monitoring locations are also indicated (o).
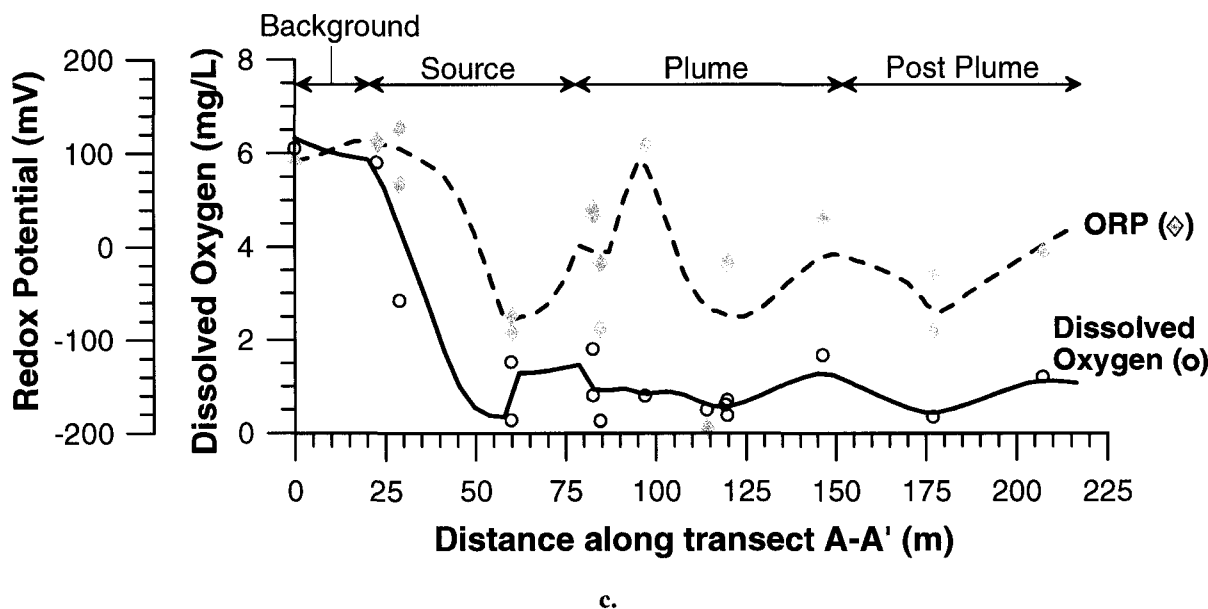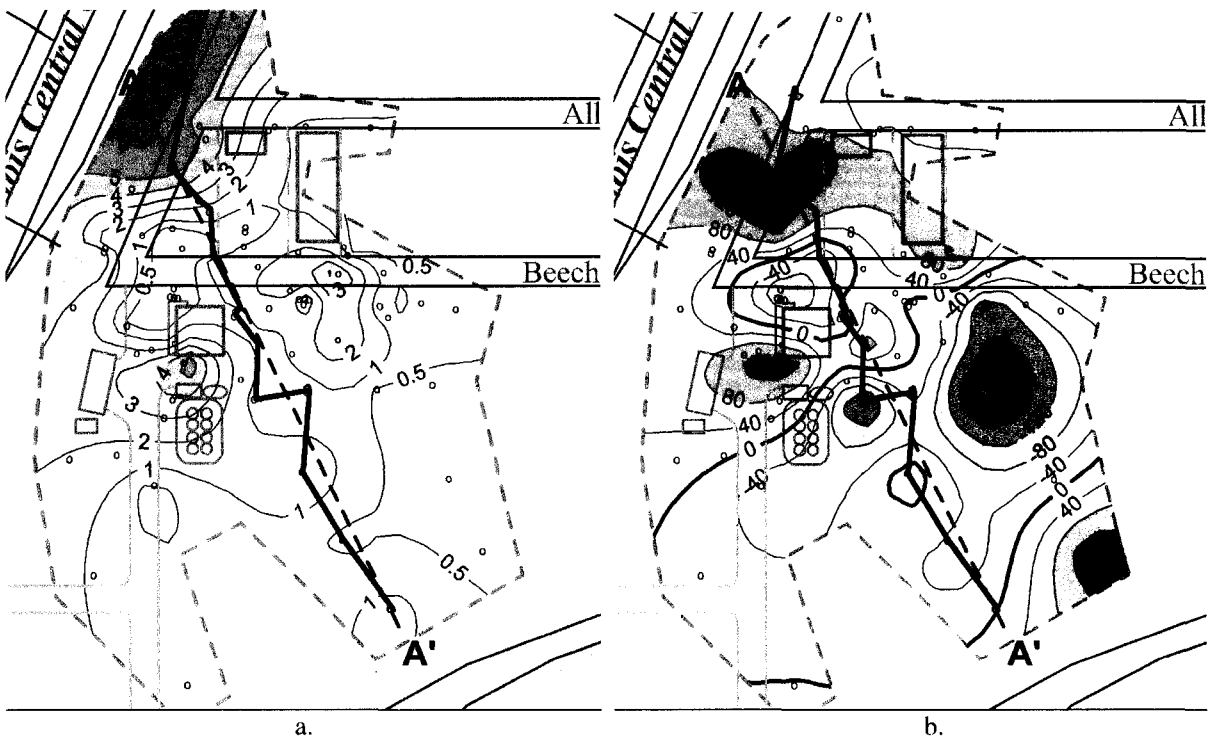
Figure 3.6   Isoconcentration contours for (a) dissolved oxygen and (b) redox potential, ORP. (c) Dissolved oxygen and oxidation reduction potential along transect A-A'. Data points represent measured groundwater values at locations indicated on the jagged transect. Smoothed lines represent the best-fit kriged surface along transect A-A' using the Surfer® Software package (Golden Software).
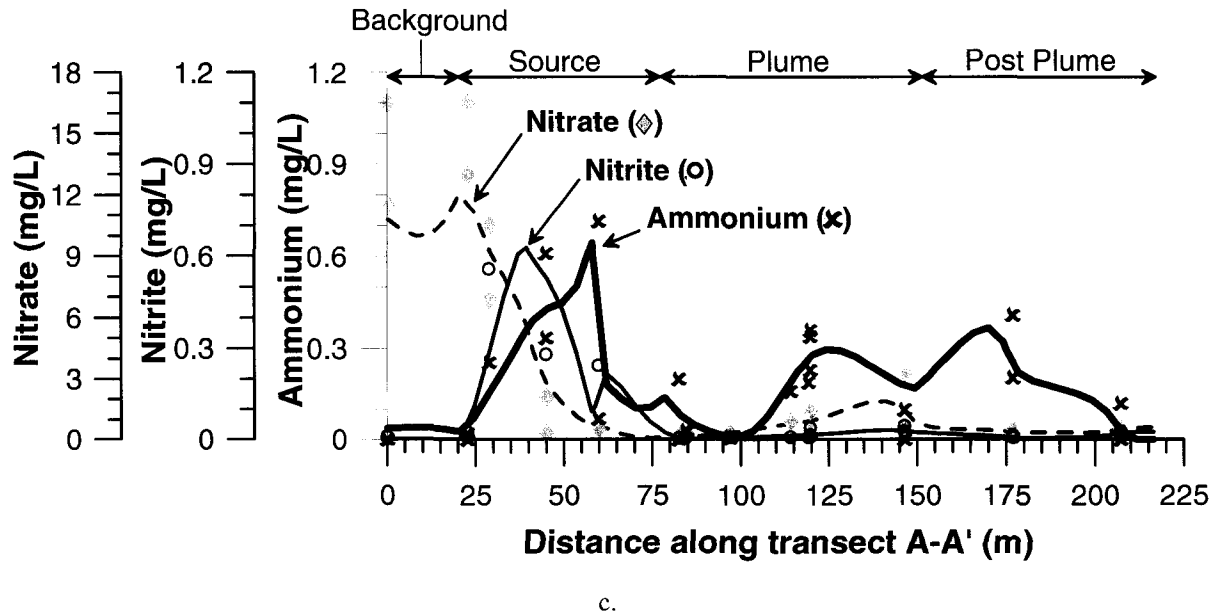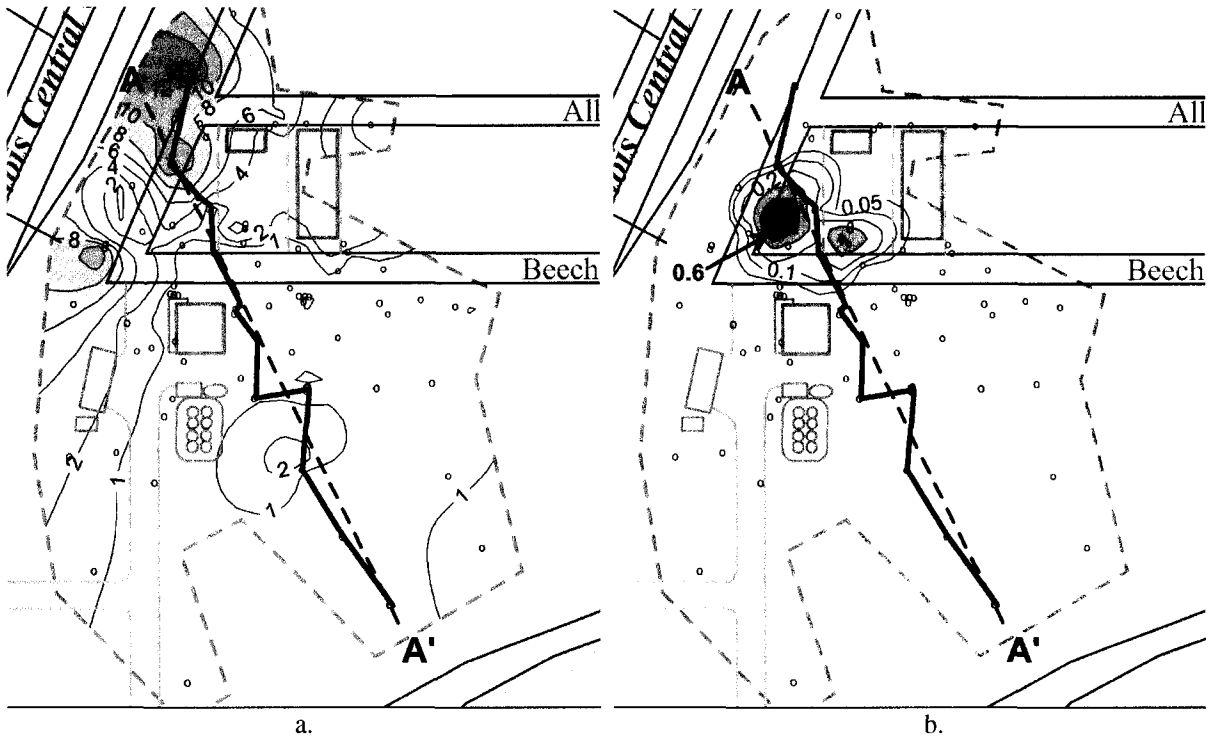
Figure 3.7   Groundwater contours for (a) nitrate and (b) nitrite. (c) Nitrate, nitrite, and
ammonium along transect A-A'. Data points represent measured groundwater
values at locations indicated on the jagged transect. Smoothed lines represent
the best-fit kriged surface along transect A-A' using the Surfer® Software
package (Golden Software).
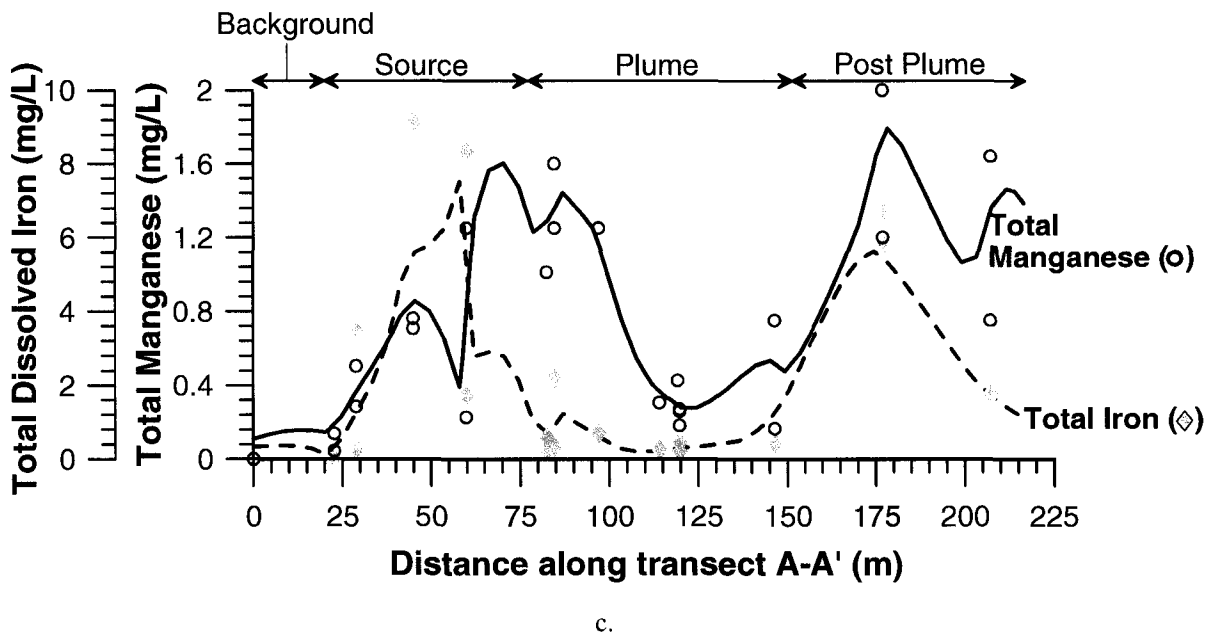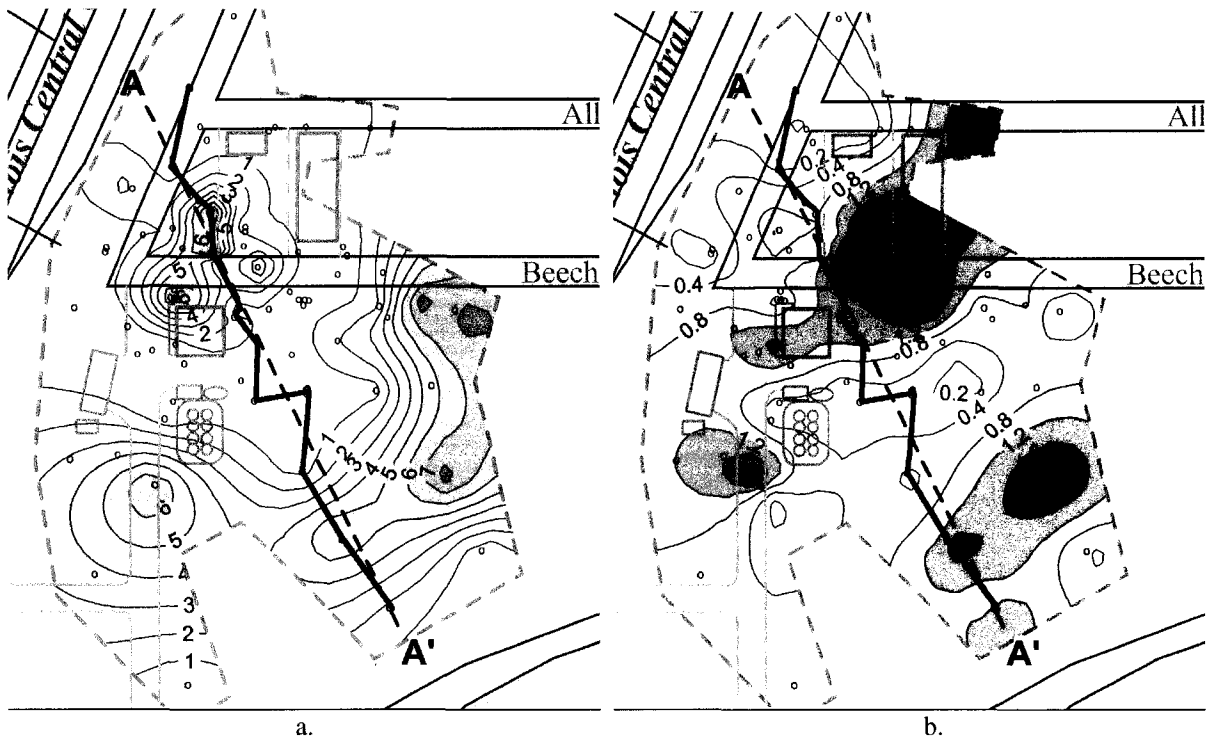
Figure 3.8   Groundwater contours for (a) total dissolved iron and (b) total dissolved manganese. (c) Total iron and total manganese along transect A-A'. Data points represent measured groundwater values at locations indicated on the jagged transect. Smoothed lines represent the best-fit kriged surface along transect A-A' using the Surfer® Software package (Golden Software).
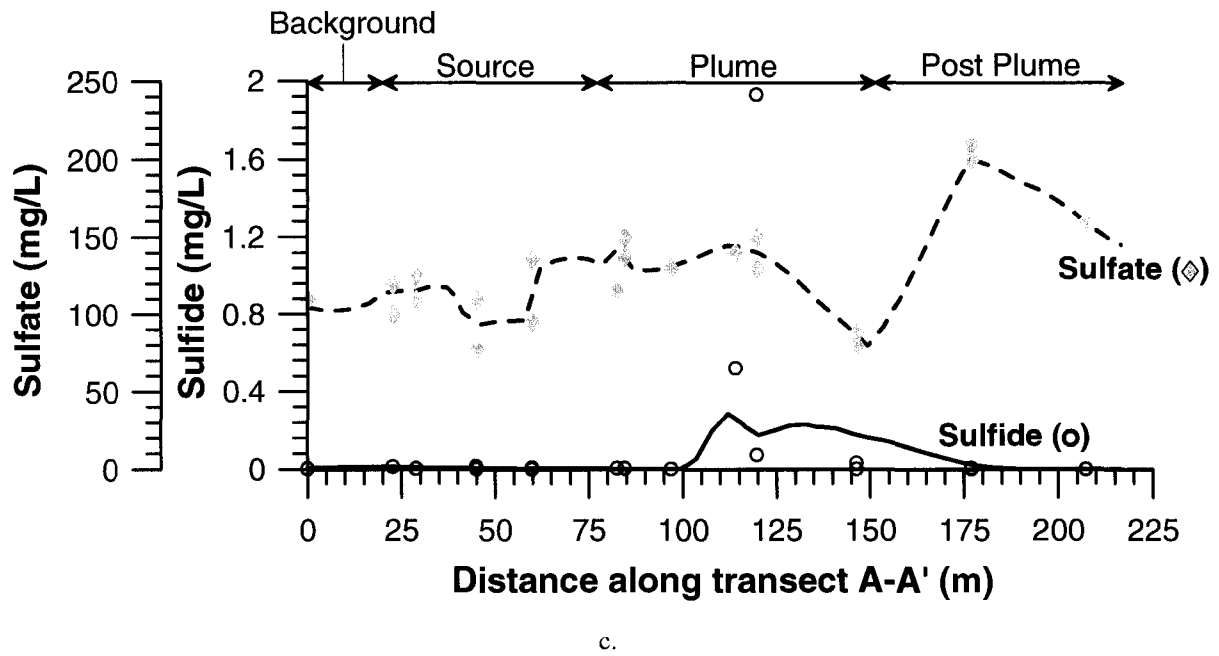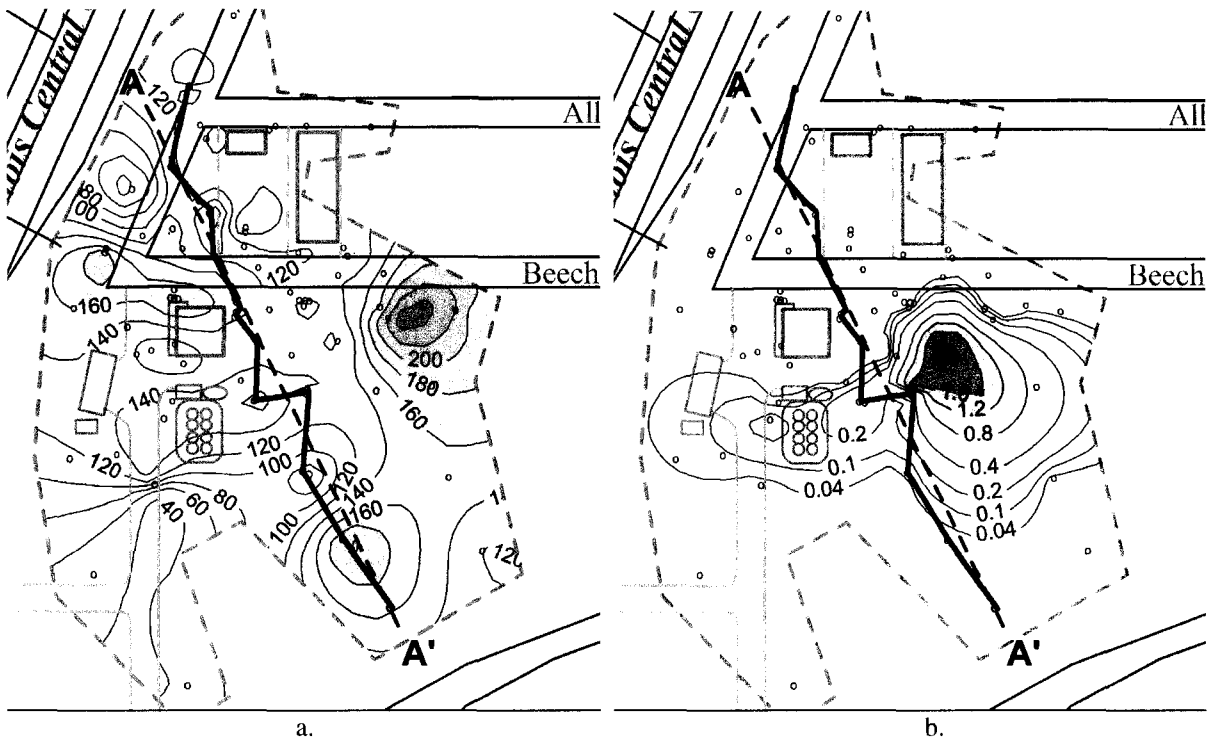
Figure 3.9   Groundwater contours for (a) sulfate and (b) sulfide. (c) Sulfate and sulfide
along transect A-A'. Data points represent measured groundwater values at
locations indicated on the jagged transect. Smoothed lines represent the best-fit
kriged surface along transect A-A' using the Surfer® Software package (Golden
Software).

4. Spatial Heterogeneity in Microbial Community Structure, Geochemistry, and Mineralization of PAH Compounds in a Coal-Tar Impacted Aquifer: Implications for Investigating Intrinsic Bioremediation

Shane W. Rogers, Say Kee Ong, and Thomas B. Moorman

4.1 Abstract

The microbial community structure and mineralization of select PAH compounds in aquifer sediments originating from a coal-tar distillate plume of varying geochemical composition were investigated spatially using total direct microbial counting and whole-cell hybridizations, incubations with site sediments under select redox conditions exhibited in situ, and whole-cell hybridizations coupled with microautoradiography (MICRO-FISH). Total DAPI counts in the coal-tar source region reached 1.45×10^7 organisms per gram sediments, three orders of magnitude greater than DAPI-stained cell counts in the non-affected sediments, suggesting active growth on the coal-tar constituents in situ. Mineralization of [UL-^{14}C]naphthalene in incubations under anaerobic nitrate-amended conditions averaged $1.49 \pm 0.18\%$ over the course of 43 days with no apparent lag in sediments associated with in situ nitrate-reduction. Similarly, mineralization of naphthalene under anaerobic sulfate-amended conditions was observed with no apparent lag ($1.5 \pm 0.07\%$, 23 days) in sediments associated with groundwater hydrogen sulfide concentrations as high as $2.5 \ mg \cdot L^{-1}$ and oxidation reduction potentials as low as -247 mV. Sulfate-reducing bacteria comprised as much as 37% of the in situ microbial community structure in these sediments. Mineralization of naphthalene ($2.24 \pm 0.32\%$, 22 days) and [9-^{14}C]phenanthrene ($2.05 \pm 0.41\%$, 22 days) under iron-reducing conditions was observed with no apparent lag, but did not correlate well to in situ aqueous geochemical indicators of iron-reduction. Based on whole cell hybridizations on site sediments, *Actinobacteria* dominated the aerobic (>1 mg/L dissolved oxygen) in situ microbial community structures, followed by *γ-Proteobacteria*, *Bacteriodetes*, and *β-Proteobacteria*. Under aerobic conditions, up to 61% mineralization of naphthalene and 42% mineralization of phenanthrene was observed. Enrichment of *β-* and *γ-Proteobacteria* in the microbial community structures of site sediments following aerobic incubations indicated that they were active in PAH degradation.

MICRO-FISH confirmed these results but also indicated that *Actinobacteria* were active in the uptake of [9-^{14}C]phenanthrene, even though their populations declined in aerobic incubations. These results supported in situ observations of the microbial community structure, but suggested that inference of the activity of specific bacterial phylotypes in the uptake of PAH pollutants based on perturbation in laboratory incubations versus in situ microbial community structures alone may not be robust, and may lead to erroneous conclusions about the activity of PAH-degrading bacteria in situ. MICRO-FISH also supported the works of others in that most bacteria capable of aerobic mineralization of PAH compounds reported in literature cluster within specific phylotypes including the *Actinobacteria*, *α-*, *β-*, and *γ-Proteobacteria*. The results of this study strongly support active natural attenuation of PAH compounds within this contaminated aquifer and suggest that direct evidence of intrinsic degradation of PAH pollutants is necessary to effectively demonstrate natural attenuation at complex PAH contaminated sites.

4.2 Introduction

Polycyclic aromatic hydrocarbon (PAH) contamination is a common environmental challenge found at creosote works, coal gasification sites, coking industries, and petroleum refineries. Remedial efforts at PAH-contaminated sites are typically costly as PAHs tend to be associated with dense nonaqueous phase liquids that persist as residual contamination, coating soils surfaces and pooling on impermeable layers deep in aquifer systems making free product recovery difficult, and providing a long-term source of groundwater contamination. All 16 U.S. EPA Priority PAH compounds are susceptible to aerobic biodegradation in laboratory studies, and many PAH-contaminated sites exhibit changes in geochemical environments commonly associated with increased microbial activity and intrinsic bioremediation (EPRI, 1996; King et al., 1999; Campbell et al., 1996; Landmeyer et al., 1998; Ong et al., 2001). Recent research showing biodegradation of low-ring PAHs in anaerobic incubations of contaminated harbor, estuarine, and aquifer sediments supports monitored natural attenuation as a remedial approach at PAH-contaminated sites (Bedessem et al., 1997; Coates et al., 1997; Zhang and Young, 1997; McNally et al., 1998; Andersen and Lovley, 1999; Galushko et al., 1999; Meckenstock et al., 2000; Rockne et al., 2000: Hayes and Lovley, 2002). For natural attenuation to become a viable remedial option, a better understanding of the capacity of indigenous microbial consortia to transform PAHs into innocuous byproducts must be realized.

Our current knowledge of the biodiversity of PAH contaminated soils and sediments is largely derived from the isolation and cultivation of microorganisms capable of degrading PAH

compounds. These culture-dependent techniques may allow the study of only a small fraction of the biodiversity present in natural systems (Amann et al., 1995; Atlas and Bartha, 1992). Therefore, current information regarding the genotypic and phylotypic diversity of PAH-degrading organisms may be biased by limitations of cultivability, and the natural metabolic activity of PAH-contaminated systems may be underestimated (Ahn et al., 1999; Lloyd-Jones et al., 1999; Widada et al., 2002). Furthermore, extensive spatial and temporal heterogeneity in the aqueous geochemistry and microbial community structure at many PAH-contaminated sites may complicate modeling and monitoring efforts when investigating natural attenuation as a potential remedial mechanism (Langworthy et al, 1998).

The U.S. EPA recommends a three-tiered approach to evaluate natural attenuation as a remedial mechanism for contaminated sites. This approach primarily relies on historical data displaying a clear and meaningful trend of decreasing contaminant mass, which is supported by *indirect* measures of intrinsic remediation, such as changes in the geochemical environment potentially related to biodegradation of pollutants, coupled with modeling approaches to estimate the rate at which the pollutants will be reduced to required levels (U.S. EPA, 1999). Although plume-scale modeling may lead to reasonable estimates of the overall rate of hydrocarbon degradation, the potential for specific hydrocarbon degradation within complex mixed contaminant plumes typically associated with PAH pollution cannot be accurately assessed from plume-scale data. For instance, the consumption of any particular pollutant within a chemically complex mixed source may elicit a particular geochemical response(s). Further, potential analytical errors associated with groundwater sampling coupled with the heterogeneous nature of most aquifers may lead to misinterpretation of site-data that result in incorrect deductions regarding the transformation of pollutants to innocuous byproducts based on modeling studies. For this reason, the U.S. EPA suggests tertiary lines of evidence based on field or microcosm studies that *directly* demonstrate microbial activity in the aquifer material and its ability to transform the contaminants of concern (U.S.EPA, 1999). However, laboratory-scale assays with contaminated site media typically result in an altered (enriched) microbial community structure that may not accurately reflect in-situ conditions. Therefore a gap exists between interpreting results from microcosm studies and field-scale processes. Studies that have employed molecular microbial approaches such as those performed by Langworthy et al (1998), Padmanabhan et al. (2003), and Eriksson et al. (2003), linking laboratory microcosm data to the field-scale, are needed to better assess intrinsic bioremediation potential at PAH-contaminated sites.

One approach to linking laboratory microcosm and field-scale data is to identify phylotypically or genotypically relevant microorganisms based on laboratory microcosms with site

soils or sediments, then probe for the presence of those organisms in-situ. Johnsen et al. (2002) noted that PAH mineralization in soil was dominated by bacteria in a limited number of taxonomic groups including nocardioforms, sphingomonads, *Burkholderia*, pseudomonads, and *Mycobacterium*. A more extensive review of several studies reveals a high degree of relatedness between PAH-degrading bacteria isolated from soils and sediments globally (see Table 4.1). PAH-degrading bacteria tend to cluster within specific phylotypes, even though the genes that encode for enzymes related to PAH degradation in many cases are plasmid-borne and transposable. This suggests that other phenotypic characteristics such as cell hydrophobicity or the ability to produce biosurfactants may be equally important to displaying the PAH-degrading phenotype as the availability of specific genetic elements the environment. However, it may also be that specific phenotypic characteristics lead to cultivability, thus culture techniques do not fully capture the suite of organisms capable of degrading PAH compounds in the environment. The phylotypic relatedness displayed by PAH-degrading bacteria suggests that specific molecular probe sets may be useful for tracking the presence of PAH-degrading bacteria in complex systems. As can be seen from Table 4.1, aerobic PAH degrading bacteria cluster phylotypically within the *α-Proteobacteria, β-Proteobacteria, γ-Proteobacteria*, and *Actinobacteria*. However, some *Firmicutes* and *Flavobacterium* species have been reported to aerobically degrade PAHs. The select few denitrifying bacteria that degrade PAH compounds cluster within the *β-* and *γ-Proteobacteria*. The only taxonomically identified sulfate-reducing bacteria having the PAH-degrading phenotype is a *δ-Proteobacteria*, and clusters closely with all known sulfate-reducing monoaromatic-hydrocarbon degrading bacteria (Galushko et al., 1999). Metal-reducing or methanogenic PAH-degrading bacteria have yet to be identified.

The intent of this study is to apply coupled molecular microbiological approaches towards the investigation of the intrinsic remediation potential of a coal-tar impacted aquifer in northwestern Iowa. Previous site-level characterizations of the groundwater contamination, aqueous geochemistry, and plume-scale modeling evidence the biodegradation of coal-tar constituents under both aerobic and anaerobic (nitrate-reducing, metal-reducing, and sulfate-reducing) conditions. However significant spatial heterogeneity in the aqueous geochemistry and hydraulic properties of the aquifer have been observed, complicating data interpretation. Coupled with the complex nature of the coal-tar pollution as well as potential secondary sources of contamination, the specific reduction in U.S. EPA regulated "priority" PAH pollutants in-situ remains ambiguous. To confirm the hypothesis that priority PAH pollutants are supporting the growth of the indigenous microbial consortia, direct evidence of the degradation of PAH compounds is required. If the indigenous microbial consortia were growing significantly on PAH compounds, enrichment in phylotypically-relevant bacteria

(microbial phylotypes associated with the PAH-degrading phenotype) relative to the nearby uncontaminated aquifer microbial community structure would be expected. Coupled with laboratory microcosms showing mineralization of specific priority PAH pollutants, this information may provide strong direct evidence for intrinsic remediation.

The objectives of this study are to (1) determine whether the in-situ microbial community structure is related to (a) known PAH-degrading microbial phylotypes and (b) reflects the aqueous geochemistry observed in groundwater measurements; (2) identify whether the aqueous geochemical environments exhibited in-situ are related to the degradation of U.S. EPA priority PAH compounds based on laboratory incubations with contaminated site sediments; (3) determine whether the relative enrichment of specific microbial phylotypes observed in situ as described in objective 1 correlate to the enrichment of specific microbial phylotypes observed in laboratory incubations of objective 2, further supporting in-situ microbial growth on priority PAH pollutants; and (4) using contaminated site sediments containing coal-tar free product, identify whether the observed enrichment in specific microbial phylotype(s) are related to growth on a specific model PAH, phenanthrene. The application of these objectives towards the goal of displaying intrinsic remediation potential and implications for future investigations of natural attenuation at PAH-contaminated sites are discussed.

4.3 Cherokee FMGP Study Site

The subsurface hydrology, contaminant plume extents, and hydrogeochemistry of the former manufactured gas plant (FMGP) study site located in Cherokee, Iowa are described in detail in Chapter 3. Briefly, coal-tar and BTEX contamination resulting from FMGP operations and possible gasoline spillage pervades the aquifer underlying the FMGP site (see Figure 4.1). The shallow semi-confined aquifer system is comprised of four primary geologic units that underlay a top layer of mixed fill including (1) loess, (2) fine-grained silty alluvium, (3) highly transmissive coarse alluvium, and (4) glacial till. Because of the thinning of the alluvium layer and the presence of fine-grained silty alluvium, there is a region of sharp hydraulic gradient between the site and nearby Little Sioux River. The difference in potentiometric surface between the site and river greatly reduces the influence of river stage on groundwater elevations in the contaminated region of the aquifer.

Changes in terminal electron accepting compounds in the contaminated aquifer relative to background (uncontaminated) locations along the plume centerline indicate increased microbial activity in the contaminated sediments. Background concentrations of dissolved oxygen and nitrate-N, as high as 6.1 mg/L and 16.5 mg/L, respectively, rapidly deplete within the contaminant source

region, over which there is a measured reduction in groundwater oxidation-reduction potential (see Chapter 3). Depletion of nitrate is coupled to significant increases in nitrite and dissolved ammonia further supporting nitrate reduction. Increased concentrations of ferrous iron and manganese (II) have also been observed in the contaminant source region and plume relative to nearby uncontaminated groundwater. Groundwater sulfate concentrations generally measure greater than 200mg/L, and may support sulfate reduction in the contaminant plume as evidenced by a decrease in sulfate concentrations and production of hydrogen sulfide linked to groundwater oxidation-reduction potentials of -247 mV or less. Methane was not detected at any location within the aquifer (Black and Veatch, 1998). Standard plate counts per mL ($\pm$95% confidence interval) on groundwater samples from the monitoring wells within the source, plume, and background regions were 2008 $\pm$235 (n=21), 1905 $\pm$373 (n=23), and 429 $\pm$174 (n=28), respectively, suggesting microbial growth within the source region and contaminant plume.

4.4 Materials and Methods

4.4.1 Sediment core sampling for intrinsic microbial community structure

Continuous sediment cores were extracted using Geoprobe direct push technology at eight locations corresponding to the background aquifer, source zone, and several locations in the contaminant plume exhibiting specific groundwater geochemical environments of interest as shown in Figure 4.1. Four-foot sections from the continuous cores were immediately cut in half, and the center of the top one inch of sediments from the cut section were discarded. Approximately 5 to 10 grams of sediments in the center of the core were removed with a sterile spoon, placed in a 50 mL screw-cap sterile tube containing 30 mL 4% paraformaldehyde/phosphate buffered saline (0.13 M NaCl, 7mM Na_2HPO_4, and 3mM NaH_2PO_4, pH 7.2), vortexed for 3 minutes, and stored on ice until taken to the laboratory (maximum holding time was 2 days). The remaining core sections were capped, sealed with electrical tape, and maintained on ice. At the laboratory, the cores were placed in the refrigerator at 4°C until further analysis. A total of 15 sediment samples were preserved for microbial community structure analysis using fluorescence in-situ hybridization (FISH) from the locations indicated in Figure 4.1.

4.4.2 Extraction of microorganisms from sediments

Paraformaldehyde-fixed samples were washed in phosphate buffered saline (PBS, pH 7.2), and brought to 20 mL in PBS. Extraction of microorganisms from the preserved sediments was performed using a slightly modified method of Unge et al. (1999). Briefly, 0.4 g of acid-washed polyvinylpolypirollidone (PVPP) was added to each 50 mL tube containing 20 mL preserved sediment-PBS solution and vortexed for 3 minutes. Bulk sediment and bound humic material were allowed to settle for 20 minutes and the supernatant was poured into a sterile 50 mL tube. Cells were extracted two more times with 10 mL PBS and the supernatants were combined. The pooled supernatants were vortexed for one minute and centrifuged at 100 x g for 6 minutes, then poured into sterile 50 mL screw-cap tubes and washed in 50% ethanol-PBS, pH 7.2. Sediment-cell slurries were stored in 15 mL of the ethanol-PBS solution at -20°C for six months prior to fluorescence in-situ hybridization to improve the detection of microbes, particularly of the alpha subdivision of the Proteobacteria (Zarda et al., 1997). Preliminary studies showed that recovery of cells from the sediments using these methods was effective. More than 80% of *Escherichia coli* added to sediments could be recovered (n=3) based on counts with a probe specific for *E. coli*.

4.4.3 Metabolism of ^{14}C-radiolabeled substrates

The potential for intrinsic biodegradation of PAH compounds was measured in laboratory incubations of sediments from cores GPS 22, GPS 23, GPS 25, GPS 26, and GPS 27 (see Figure 4.1). Incubations were performed under aerobic and anaerobic (nitrate-amended, iron-amended, and sulfate-amended) conditions with ^{14}C-PAH compounds based on associated in-situ groundwater geochemistry and historical exposure of the sediments to the PAHs as listed in Table 4.2. Thirty grams homogenized sediment (passing a #4 sieve) from individual cores were added to a 100 mL amber serum bottle. For aerobic incubations, 30 mL sterile basal salts medium (2 mM KH_2PO_4, 2 mM K_2HPO_4, 9.9 mM NH_4Cl, 0.5 mM $MgCl_2 \cdot 6H_2O$, 0.5 mM $CaCl_2 \cdot 2H_2O$, and 0.1 mM $FeCl_2 \cdot 4H_2O$, pH 7.1), which was sparged with air for 30 minutes, was added to the serum bottle. A 3 mL culture tube containing 2 mL of 2 M sodium hydroxide solution was carefully placed into each serum bottle to serve as a $^{14}CO_2$ trap. Bottles were sealed with butyl rubber stoppers.

Anaerobic incubations were prepared similar to the aerobic assays, except that the nitrate-amended medium contained 200 mM KNO_3 and the sulfate-amended medium contained 200 mM Na_2SO_4. Poorly crystalline iron (III) oxide (200 mg) was added to the serum bottles for the iron-amended assays. All anaerobic media were sparged with helium for 30 minutes prior to use. After

sealing with butyl rubber stoppers, the headspace was immediately removed via a needle attached to a vacuum line (1 minute at -82 kPa) while agitating mildly to remove entrapped air, and exchanged with helium (1 minute at 97 kPa). This process was repeated two more times, resulting in a positive pressure helium headspace of 97 kPa. Three hundred seventy five microliters of oxygen-free and sterile nitrilotriacetic acid (328 mM) was injected into the ferrogenic assays through the septa to act as a chelator of the iron (III) oxide, followed by 375 μL oxygen-free and sterile 106.6 mM $FeCl_2$ solution to act as a reductant. Oxygen-free and sterile $Na_2S \cdot 9H_2O$ solution (375 μL) was injected into the sulfidogenic assays through the butyl rubber septa to act as a reductant. Either 321,000 dpm of [UL-^{14}C]naphthalene (specific activity, 20 mCi·mmol^{-1}; Sigma, St. Louis, Mo.), 400,000 dpm of [9-^{14}C]phenanthrene (specific activity, 15 mCi·mmol^{-1}; Sigma), 625,000 dpm of [4,5,9,10-^{14}C]pyrene (specific activity, 40 mCi·mmol^{-1}; Sigma), or 385,000 dpm of [7-^{14}C]benzo(a)pyrene (specific activity, 30 mCi·mmol^{-1}; Sigma) was injected directly into the sediment-slurry through the septa, and the bottles carefully swirled by hand.

The mineralization assays were conducted in triplicate plus one abiotic degradation control. Select assays (aerobic: GPS 22, naphthalene and phenanthrene, and GPS 23 phenanthrene; nitrate-reducing: GPS 22) were re-ran in triplicate to confirm reproducibility. The base medium for the abiotic controls was supplemented with 20 g/L sodium azide. All bottles were incubated at 20°C. $^{14}CO_2$ evolution in the aerobic bioassays was monitored by exchanging the 2 N NaOH solution via syringe through the septa. The NaOH was added to 13 mL of Ultima Gold XR Liquid Scintillation Cocktail (Packard Instrument Company, Perkin Elmer, Downers Grove, IL), and the amount of $^{14}CO_2$ evolved was determined by liquid scintillation counting. Prior to sampling the anaerobic assays, the headspace pressure was relieved by penetrating the septa with a needle attached to a 0.5 mm inside diameter tube submerged in water at the outlet to prevent air entry. The 2 N NaOH trap solutions were exchanged in a manner similar to the aerobic assays, then the remaining headspace of the anaerobic assays was purged by vacuum and exchanged with helium 3 times as described above to maintain anaerobic conditions. A positive helium pressure was maintained throughout the experiments. Headspace air in the aerobic bottles was exchanged following each sampling interval by first vacuuming the headspace from the serum bottles (1 minute at -82 kPa), then simultaneously vacuuming the headspace from the bottles and allowing atmospheric air to recharge via needles pushed through the septa (3 minutes of purge time, 3 minutes equilibration time).

4.4.4   Oligonucleotide Probes

Oligonucleotide probes specific to *Archaea*, and several members of the Domain *Bacteria* were selected based on their common detection in soils and sediments, relevance to the PAH-degrading phenotype, and to represent specific functions such as sulfate reduction (see Table 4.3). The oligonucleotide probes were synthesized with either Cy 3 (Cy 3; Amersham, Zurich, Switzerland), TAM, or FITC reactive dye covalently bound to the 5'-end (Invitrogen Corp., Huntsville, AL). The dye-oligonucleotide conjugates (1:1) were lyophilized and stored dry in sterile microfuge tubes at -20 °C in the dark. Prior to use, the dry probes were reconstituted in TE buffer (10 mM Tris-HCl, 1 mM EDTA, pH 8.0), covered with aluminum foil, and stored at -20 °C. The specificity of the group specific probes within their target group have been reported as 88.3%, 91.8%, 76.6%, 92.6%, 90.8%, 52.1%, 41.9% (of all *Cytophagales*), 33.1% (of all *Cytophagales*), and 82.5% for the Domain *Archaea* (ARCH915), Domain *Bacteria* (EUB338-I, II, III), α-*Proteobacteria* (ALF968), β-*Proteobacteria* (BET42a), γ-*Proteobacteria* (GAM42a), *Firmicutes* (LGC354a,b,c), "Bacteriodes", "Flavobacteria", and "Sphingobacteria" of the *Bacteriodetes* (CF319a), "Bacteriodes" of the *Bacteriodetes* (BAC303), and *Actinobacteria* (HGC69a), respectively, given up to 0.4 weighted mismatches per probe (Loy et al., 2003). The probe SRB385 is known to not capture all sulfate reducing bacteria, but may be sufficient for the purposes of this study (Manz et al., 1998).

4.4.5   Total cell counts

DAPI (Sigma, St. Louis, MO) was used to stain cells non-specifically. Total direct DAPI cell counts were determined by transferring 0.7 mL of the cell suspension onto 0.8 mL Nycodenz (Nycomed) (density = 1.3 g/mL) in sterile 1.5 mL microcentrifuge tubes and centrifuged at 10,000 x g for 15 minutes to pellet the remaining sediments. After centrifugation, the top 0.5 mL were discarded, and the next 0.5 mL (containing the banded microbial fraction) were transferred to sterile 1.5 mL microcentrifuge tubes. The microbial fraction was supplemented with 20 µL of DAPI solution (100 ng µL^{-1}) and incubated for 7 minutes in the dark. Following incubation, the entire solution was transferred to a 15 mL vacuum filtration tower containing a pre-wetted 25 mm diameter polycarbonate filter (0.22 µm pore size) and 5 mL of sterile PBS (pH 7.2). The filter was washed three times under vacuum with 3 mL of PBS. The filters were transferred onto slides with Citifluor mounting medium (Citifluor, Canterbury, UK), and examined under a Nikon Eclipse 400 microscope fitted with a digital imaging system, high pressure mercury lamp, and UV-2E/C filter. The cells were counted from duplicate slides at 600x magnification by randomly counting 20 fields on each slide

covering an area of 0.0169 mm² each from a total area of 201 mm² per filter using Image-Pro Plus software (v. 4.5.1, Media Cybernetics, Silver Spring, MD).

4.4.6   Whole-cell hybridization

Following total cell counts, whole-cell hybridizations were performed to assess the aquifer microbial community structure. Cell-sediment suspension (1 mL) was added to a sterile 1.5 mL microfuge tube, and pelleted such that the supernatant could be carefully discarded. The cells-sediment pellet was resuspended in 300 µL pre-warmed (46°C) hybridization buffer (0.9 M NaCl, 20 mM Tris-HCl (pH 7.2), 2.5 mM EDTA, and 0.01% sodium dodecyl sulfate (SDS) in the presence of 20-35% formamide (ARCH915, BAC303, HGC69a, and SRB385 = 20%; EUB338 (I-III), BET42a, and GAM42a = 30%; ALF968, CF319a, LGC354(a,b,c)=35%;NON338=20-35%)). Four ng·µL⁻¹ of the relevant probe(s) were added to the tubes which were incubated at 46°C for 90 min. Following hybridization, cells were pelleted, washed once in pre-warmed (48°C) buffer (20 mM Tris-HCl (pH 7.2), 2.5 mM EDTA, 0.01% SDS, and either 308, 102, or 80 mM NaCl depending on the formamide concentration during hybridization (20%, 30%, or 35%, respectively)) to remove any unbound probe, then held in 1 mL wash buffer at 48°C for 10 minutes, after which the cells and sediments were pelleted and resuspended in 700 µL cold (4°C) PBS, pH 7.4. The suspension was loaded onto 800 µL Nycodenz (Nycomed) (density = 1.3 g/mL), centrifuged at 10,000 x g for 15 minutes, and the banded bacterial fraction recovered and DAPI-stained as described before. The entire solution was transferred to filters and prepared for microscopy as described previously.

The probe-stained cells were counted relative to DAPI-stained cells under a G-2E/C filter for Cy3 and TAM-labeled cells, B-2E/C filter for FITC-labeled cells, and UV-2E/C filter to determine the total direct DAPI count. Between 1,000 and 5,400 DAPI-counter-stained cells per probe condition were examined and the counts corrected based on non-specific binding of the nonsense probe NON338.

4.4.7   MICRO-FISH

An aerobic incubation with GPS 22 sediments and [9-¹⁴C]phenanthrene was used to identify relationships between the microbial community structure and growth on phenanthrene. A 14 mL vial containing 2 grams of sediments, 2 mL of air-sparged basal salts medium, and 20 µCi (44,400,000 dpm) [9-¹⁴C]phenanthrene (specific activity, 15 mCi·mmol⁻¹; Sigma) was prepared as described above

(section 4.4.3). When $^{14}CO_2$ production reached late log phase (26 days), the shell vial containing NaOH was removed and 10 mL 4% paraformaldehyde was added to the 14 mL vial. The vial was vortexed for three minutes, placed in a 4°C refrigerator for 24 hours, and the microbes extracted from the sediments as described above (section 4.4.2).

One milliliter of the cell-sediment suspension was washed repeatedly in 50% ethanol until additional washes resulted in no further removal of ^{14}C, thus minimizing extraneous cell-bound [9-^{14}C]phenanthrene that could potentially interfere with the autoradiographic response. Based on liquid scintillation counting of the wash solution, three washes with 50% ethanol were required. The washed cells-sediment pellet was resuspended in 700 µL PBS, pH 7.4, loaded onto 800 µL Nycodenz (Nycomed) (density = 1.3 g/mL) in a 1.5 mL sterile microfuge tube, centrifuged at 10,000 x g for 15 minutes, and the banded bacterial fraction recovered as before. The banded bacterial fraction was transferred to a 15 mL vacuum filtration tower containing a pre-wetted 25 mm diameter polycarbonate filter (0.22 µm pore size) and 5 mL PBS (pH 7.4). The filter was washed three times under vacuum with 3 mL each of PBS, transferred cell-side down onto a 22 mm square cover glass (No. 2) treated with a 2% solution of 3-aminopropyltriethoxysilane (Sigma, St. Louis, MO), clamped between two glass slides using binder clips, and placed in a 42°C oven for 1 hour, after which the filter was peeled away leaving the cells adhered to the cover glass. The cells were dehydrated using 50%, 80%, and 96% ethanol, respectively, three minutes each, and the cover glasses placed cell-side up on microscope slides. The cells were then treated with 30 µL of hybridization buffer (as described above) containing 4 ng·µL^{-1} of the relevant probe(s) and 4 ng·µL^{-1} DAPI, covered with a Hybri-Slip (Sigma, St. Louis, MO), placed into 50 mL plastic tubes (humidity chambers) and hybridized at 46°C for 90 minutes. Following hybridization, the cover glasses were washed for 15 minutes at 48°C in the appropriate wash buffer (described above) then carefully dried under a stream of filtered air.

Microautoradiography was performed in the dark using a method similar to Cottrell and Kirchman (2000). Cover glasses were dipped in molten (43°C) Kodak NBT-2 autoradiographic emulsion diluted 2 parts emulsion and 1 part deionized water. After incubation at 4°C for 10 days, the slides were warmed to room temperature and the emulsion developed using Kodak Dektol developer, a deionized water stop bath, and Kodak fixer, as per manufacturer's instructions. The cover glasses were air dried, mounted on clean glass slides using Citifluor AF1 mounting medium (Citifluor Ltd., Canterbury, UK), and examined under a Nikon Eclipse 400 microscope using a G-2E/C filter for Cy3 and TAM-labeled cells, B-2E/C filter for FITC-labeled cells, and UV-2E/C filter to determine the total direct DAPI count. Silver grain formation corresponding to hybridized cells

was determined by switching between fluorescence and bright-field modes. Digital imaging analysis was performed using Image-Pro Plus (v. 4.5.1, Media Cybernetics, Inc., Silver Spring, MD).

4.5 Results

4.5.1 Total DAPI-direct counted microbes in aquifer sediments

Table 4.4 shows the total direct DAPI counts with depth at eight sampling locations corresponding to background sediments (GPS21), the coal-tar source region (GPS22), and several locations in the contaminant plume (GPS23-GPS28). Total microbial populations varied between 1.5 ± 1.1 x 10^4 cells·g sediment^{-1} in the background region to 1450 ± 90 x 10^4 cells·g sediment^{-1} in the region of the free-phase coal-tar source material, and in general decreased along the plume centerline moving out of the coal-tar source region (see Figure 4.1). At GPS26, which is located within a region of possible secondary source contamination, the DAPI-stained cell count per gram sediments increased again, presumably in response to increased hydrocarbon mass. At GPS28, located approximately at the plume boundary, the DAPI-stained cell count increased to levels near that of the source region. The reason for increased cell counts at this location remains unclear.

Microbial counts with depth were generally similar, except at GPS22 and GPS26. The difference in microbial numbers at these locations may be related to differences in sediments PAH concentrations and toxicity effects. Sediments at 5.5 m and 7.9 m, with 710-2010 mg/kg and 1890-6100 mg/kg PAH (as the sum of the 16 U.S. EPA priority PAH pollutants), respectively, had an order of magnitude lower DAPI count than at 6.7 m, where the PAH concentration was 250-305 mg/kg.

4.5.2 Microbial community structure of aquifer sediments

Presented in Table 4.4 are the percent of each probe-detected group of microbes relative to total DAPI counts and the 95% confidence interval based on counts of repetitive microscopic fields. Larger confidence bands about the mean probe-detected counts were observed where probe counts were low. Since a minimum of 1028 DAPI-counterstained cells were counted for each probe, a minimum detection limit of 0.1% of the total DAPI count was set. The loss of cells during the hybridization procedure relative to the DAPI-staining procedure presented above was generally less than 10%.

Neglecting the results for GPS24 (3.7 m bgs), the sum of FISH-stained *Bacteria* and *Archaea* resulted in the detection of between 38.2 - 74.9% of the DAPI-stained cells in the sediment samples.

This range agreed favorably to previously reported values for soils and sediments (Llobert-Brossa et al., 1998, Zarda et al., 1997). A similar percentage of DAPI-stained cells identified by FISH in the background sediments as compared to hydrocarbon contaminated sediments was observed, suggesting that the probe set used was fairly robust in describing the microbial community within this contaminated aquifer (see GPS 21, Table 4.4). For GPS24 (3.7 m bgs), only 17% of the DAPI-stained cells were detected with these probes. It is unclear as to why these cells did not hybridize well, but it may be related to specific factors in sample collection and/or preservation and storage of this particular sediment sample. The lack of a probe for Prokaryotes in this study almost certainly contributed to the difference between total DAPI-stained organisms and the sum of FISH-detected cells.

The spatial heterogeneity observed in the in situ microbial community structure reflected well the aqueous geochemistry and supported enrichment of known PAH-degrading phylotypes. *Actinobacteria* (high DNA G+C content gram positive bacteria) and *γ-Proteobacteria* dominated the microbial community structure within the contaminated aquifer underlying the Cherokee FMGP site (Figure 4.2 and Table 4.4). These bacteria comprised a more significant portion of the microbial community in sediments associated with aerobic regions of the aquifer (GPS 21, GPS 22, and GPS 23) as compared to more anaerobic sediments (GPS 25, GPS 26, and GPS 27).

There was significant enrichment of *β-Proteobacteria* (BET42a) (nearly 29% of all detected bacteria and 18% of the DAPI-stained cells) in sediments of the coal-tar source region (sediment core GPS 22, 6.7 m bgs) which were associated with aerobic and nitrate reducing aqueous geochemistry. The lowest acetone extractable sum of U.S EPA priority PAH pollutants of sediment core GPS 22 are at 6.7 m bgs (as described above). This suggests that these organisms lack special phenotypic characteristics that allow them to grow in more toxic environments located a few meters directly above and below the depth they were detected at. *β-Proteobacteria* were insignificant at all other locations throughout the site.

α-Proteobacteria (ALF968) were also relatively enriched in the coal-tar source region, but only in the highly contaminated sediments associated with the pooled source material of core GPS22 at 7.9 m bgs (6.6% of the EUB338 probe-conferred bacteria). *α-Proteobacteria* were also detected in the highly anaerobic sediment core GPS27 near the secondary source region (6.7% of the EUB338 probe-stained bacteria). CF319a-hybridized cells were in general were more enriched in deeper rather than shallow sediment samples. These cells comprised nearly 17% of the DAPI-stained cells in GPS28.

The probe SRB385 targets sulfate-reducing bacteria, predominately of the δ-Proteobacteria. SRB385 is also complimentary to several members of the Actinobacteria within the Streptosporangium, Thermomonospora, Frankia, and Blastococcus genera (Cole et al., 2003), but is not complimentary to bacteria of any known genera within the Actinobacteria associated with PAH degradation. Although potential for duplication between SRB385 and HGC69a exists, positive hybridizations for SRB385 did not correspond to the positive detection with HGC69a in the Cherokee FMGP site sediments. The probe SRB385 primarily hybridized to organisms in sediment core GPS26 (18-24% of EUB-detected bacteria), and especially in GPS27 sediments, where nearly 99% of the bacteria but only 37% of DAPI-stained cells were detected with the SRB385 probe. As can be seen in Figure 4.2, sediment core GPS 26 is associated with sulfide concentrations as high as 1.9 mg·L^{-1} indicative of sulfate-reducing microbial activity. GPS 27 sediments are associated with the most anaerobic groundwater exhibited in situ, with measured values of the oxidation-reduction potential of -247 mV and hydrogen sulfide concentrations of greater than 2.4 mg·L^{-1}. Bacteriodes and Firmicutes (LGC354a,b,c) remained fairly insignificant across all sampling locations.

4.5.3   Respiration of ^{14}C PAH compounds in aquifer-derived sediments

Laboratory-scale incubations with site sediments under relevant redox conditions show potential for microbial degradation of select PAH pollutants. Figure 4.3 shows the $^{14}CO_2$ evolution from aerobic incubation studies with contaminated site sediments from cores GPS 22, GPS 23, GPS 25, GPS 26, and GPS 27. Based on historical exposure of the sediments to PAH pollution (see Table 4.1), incubations with benzo(a) pyrene were only conducted in sediments from the coal-tar source region (GPS 22). Incubations with pyrene were performed in sediment cores GPS 22 and GPS 23, whereas incubations with phenanthrene were performed in all cores except GPS 27, located near the potential secondary contamination source.

Aerobic naphthalene mineralization was similar in all sediments with no observable lag (<12 hours) and respiration of approximately 50 to 60% of the added [UL-^{14}C]naphthalene within 23 days of incubation (Figure 4.3). Mineralization of [9-^{14}C]phenanthrene was not as extensive, and depended on exposure history. In the highly contaminated source sediments of GPS 22, a 3 day lag phase was followed by conversion of 28.8 ± 1.1% of the added ^{14}C to $^{14}CO_2$. In the less contaminated sediments of cores GPS 23 and GPS 25, a lag in phenanthrene mineralization was not observed, and $^{14}CO_2$ production reached 34.4 ± 5.2% and 41.7 ± 4.6%, respectively within 23 days. In sediments from GPS 26, where phenanthrene exposure history was minimal, there was a 6 day lag phase and

relatively slow mineralization of [9-^{14}C]phenanthrene reaching only 18.4 ± 5.8% in 23 days. Benzo(a)pyrene mineralized to a small extent (0.63 ± 0.57%, 23 days) under aerobic conditions after a lag phase of approximately 15 days in sediments from GPS 22. Pyrene mineralization was not observed in the sediments of GPS 22 or GPS 23. The lack of [14]CO_2 production in aerobic incubations with [4,5,9,10-^{14}C]pyrene does not preclude metabolite formation by the microbial community (Kazunga and Aitken, 2000). Non-mineral metabolites were not monitored for the purposes of this study. [14]CO_2 evolution was not observed in control incubations.

In sediments from GPS 22, where the in situ groundwater geochemistry reflects active nitrate-reduction as evidenced by decreasing nitrate and increasing nitrite concentrations (see Figure 4.2), naphthalene mineralization in nitrate-amended incubations was observed with no apparent lag (Figure 4.4). Phenanthrene mineralization in nitrate-amended incubations with these sediments, however, was negligible. In nitrate-amended incubations with sediments from GPS 23, where the in-situ nitrate concentrations are less than 1 mg·L^{-1} and nitrite concentrations were decreasing relative to nearby upgradient groundwater concentrations, both naphthalene and phenanthrene mineralization were less that 0.1%. Repeating the nitrate-amended incubations for naphthalene in GPS 22 sediments yielded the same mineralization potential (data plotted in Figure 4.4(a)). Serial transfers to fresh nitrate-amended, anaerobic incubations without sediments yielded 0.81 ± 0.06% mineralization in 14 days (data not shown in Figure 4.4).

Anaerobic iron-amended incubations with site sediments from GPS 23, where elevated dissolved iron concentrations were found, did not display [14]CO_2 production with either naphthalene or phenanthrene (Figure 4.4(c)). However, in sediments from GPS 25, where the aqueous geochemistry was not indicative of microbially-mediated ferrogenic reactions, both naphthalene and phenanthrene were mineralized (2.24 ± 0.32% and 2.05 ± 0.41%, respectively at 22 days). It is not clear why the aqueous geochemical measurements did not reflect the potential for degradation under iron-reducing conditions. However, the GPS 25 sediment core contained significant precipitated iron evidenced by the red color of the aquifer sands, which could be a potential iron(III) source. Red coloration of the aquifer sediments was not observed in any other direct-push core.

Figure 4.4(e) shows the potential for naphthalene mineralization under sulfate-reducing conditions in the sediments from GPS 27. Naphthalene mineralization proceeded with no apparent lag (<12 hours) and reached 1.50 ± 0.07% of the added [UL-^{14}C]naphthalene within 23 days incubation.

4.5.4 Microbial community structure of GPS 22 and GPS 23 sediments following aerobic incubation

Table 4.5 shows the in situ microbial community structure of the aquifer sediments GPS 22 (5.5 m bgs, 6.7 m bgs, and 7.9 m bgs) and GPS 23 (3.7 m bgs and 6.1 m bgs) as compared to the community structure of the homogenized core sediments following aerobic incubation. There was approximately an order of magnitude microbial growth in the GPS 23 sediments during the incubation relative to the in-situ population based on DAPI-staining. However, the percent of DAPI-stained organisms identified by FISH did not change significantly (59% - 64%). In contrast, total DAPI-stained counts in GPS 22 sediments approximately doubled and increased in probe-detected cells from 44 – 63% in situ to 84% following incubation. The enrichment of the presumed PAH-degrading phylotypes β- and γ-Proteobacteria in aerobic incubations with site sediments suggest that these organisms may be active in the uptake of PAH compounds in situ. The dominance of Actinobacteria in situ was not reflected in the microbial community structure of site sediments following aerobic incubations.

Growth of all bacteria except for the Bacteriodes and Prevotella genera, Actinobacteria, and δ-Proteobacteria was observed in the GPS 23 sediment incubations. Fifty percent of the probe-detected bacteria were γ-Proteobacteria, which compared to 22% - 44% observed in situ. β-Proteobacteria and Bacteriodetes (hybridizing to the CF319a probe) were enriched in the bioassay relative to the in-situ structure as well. The enrichment of β-Proteobacteria was particularly significant (0.17% to 1.63% in-situ, as compared to 8.1% in the aerobic bioassay). Similarly, the Firmicutes increased from 0.3% or less in-situ to 6.8% in the aerobic incubations. α-Proteobacteria remained at the same level relative to total bacteria, but grew in population by almost two orders of magnitude. In contrast, the Actinobacteria, which were a significant component of the in-situ microbial community structure remained stagnant in population per gram sediment, but became much less significant in the final community structure. Bacteriodes and Prevotella (hybridizing to the BAC303 probe), δ-Proteobacteria, and Archaea were insignificant in the microbial community following aerobic incubation.

Incubations with GPS 22 sediments, resulted in significant enrichment of β-Proteobacteria, which dominated the final microbial community structure (56% of all bacteria). γ-Proteobacteria, which comprised between 9.7 and 36% of the in situ community structure, remained stationary in population per gram sediment and percent of the final community structure (10%). Similar to the incubations with GPS 23 sediments, Actinobacteria, which dominated the in situ microbial

community, declined sharply in representation following aerobic incubations. However, *Firmicutes* and *Bacteriodetes* did not enrich in the GPS 22 incubations, even though both were more strongly represented in the in situ microbial community of GPS 22 than GPS 23. *α-Proteobacteria*, which were significant in the highly contaminated sediments at 7.9 m bgs, were not detected following aerobic incubation. Similarly, *δ-Proteobacteria* and *Bacteriodes / Prevotella* (BAC303), which were detected in the in-situ microbial community were not detected following incubation.

4.5.5   MICRO-FISH

Microautoradiography resulted in autoradiograms in which silver grain formation coincided well with the spatial location of cells detected by whole cell hybridizations as shown in their respective fluorescence images (see Figures 4.5-4.8). The strong association of fluorescently labeled cells and silver grain formation allowed for counts of PAH-degrading cells.

Table 4.5 shows cells active in phenanthrene uptake following incubation with [9-^{14}C]phenanthrene in the highly contaminated sediments from GPS 22. From Table 4.5, it can be seen that 40% of all DAPI-stained organisms and 27% of all EUB-stained bacteria were active in the uptake of phenanthrene (see Figure 4.5). 82% of bacteria active in phenanthrene uptake were identified as *β-Proteobacteria*, which coincided with their enrichment following aerobic incubation as compared to the in situ microbial community structure. 40% of all detected *β-Proteobacteria* were active in growth on phenanthrene. 26% of the probe-detected *γ-Proteobacteria*, which did not increase in aerobic incubations relative to the in situ microbial community structure, also grew on phenanthrene, comprising 9.8% of all detected active bacteria. The *Actinobacteria* were shown to be active in the uptake of phenanthrene, but to a lesser extent than the Proteobacteria. 2.0% of all probe-detected active bacteria were *Actinobacteria*. Although *Firmicutes* and *Bacteriodetes* were detected following aerobic incubations, no silver grain formation was observed to coincide with these probe-detected cells (see Figure 4.8). 44% of active DAPI-stained organisms were not detected with the probes EUB338(I,II,III) or ARCH915. However, only 5.6% of the phenanthrene-degrading bacteria were not identified by the probe set used in this study. These results suggest that the probes used in this study were robust in describing aerobic PAH degrading bacterial phylotypes.

4.6 Discussion

4.6.1 Support for intrinsic remediation of PAH compounds

From the results presented above, there is strong evidence for intrinsic remediation of PAH compounds under aerobic conditions in the coal-tar impacted aquifer underlying the Cherokee FMGP site. Mineralization of naphthalene and phenanthrene, and to a lesser extent benzo(a)pyrene, in aerobic incubations with site sediments of cores GPS 22, GPS 23, GPS 25, and GPS 26 was observed. Whole cell hybridizations indicated growth of *Actinobacteria*, *β-Proteobacteria*, *γ-Proteobacteria*, and *Bacteriodetes* within the contaminant source region and plume, increasing between two to three orders of magnitude as compared to uncontaminated aquifer sediments. The microbial community structure of GPS 22 and GPS 23 sediments following aerobic incubation indicated that β- and γ-*Proteobacteria* were active in PAH degradation. Microautoradiography confirmed these results and indicated that *Actinobacteria* were also active in the uptake of [9-^{14}C]phenanthrene under aerobic conditions, even though their population declined in aerobic incubations. Concentrations of 0.5 – 2 mg·L^{-1} dissolved oxygen down-gradient from the source region in the contaminated aquifer may support extensive aerobic oxidation of PAH pollutants in situ.

Anaerobic incubations with site sediments showed naphthalene mineralization under nitrate-reducing conditions, which corresponded to in situ aqueous geochemical measurements showing consumption of approximately 16 mg·L^{-1} nitrate and production of nitrite within the coal-tar source region. The increased population of *β-Proteobacteria* within the intrinsic microbial community structure in these sediments further supports the potential for intrinsic naphthalene mineralization under nitrate-reducing conditions (see Table 4.1). Similarly, naphthalene mineralization under sulfate-reducing conditions was associated with sediments of core GPS 27, from which groundwater geochemistry displayed decreasing sulfate concentrations, elevated sulfide concentrations, and an oxidation-reduction potential of -247 mV. This was supported in the in situ microbial community structure, which was dominated by sulfate-reducing bacteria.

Evidence of naphthalene and phenanthrene mineralization under iron-reducing conditions in laboratory-scale incubations with core GPS 25 sediments did not agree with in situ measurements of ferrous iron. Further, the intrinsic microbial community structure was not clearly identified in this core using the probe set chosen for this study. This lack of detection with whole-cell hybridizations may be related to the presence of iron-reducing bacteria. One common metal-reducing bacterium that may use monoaromatic compounds as a growth substrate, *Geobacter metallireducens*, does not hybridize to the probe set used in this study (Cole et al., 2003). Metal-reduction has been linked to

several species of bacteria across different phylogenies, and may also explain the ambiguity in the results. At present, no oligonucleotide probes have been proposed that target only metal-reducing bacteria. The development of molecular probes that better identify metal-reducing bacteria would be helpful for these types of investigations of intrinsic bioremediation potential under specific redox conditions.

4.6.2   Implications for future investigations of natural attenuation of PAH compounds

This study provides direct evidence of the ability of the intrinsic microbial community to degrade specific PAH pollutants. Extensive spatial heterogeneity in the potential for select PAH pollutants to undergo aerobic and anaerobic mineralization was observed. For example, aerobic phenanthrene mineralization in laboratory-scale incubations varied in lag phase, rate, and extent depending on the source sediments and contaminant exposure history. However, this spatial heterogeneity was not observed in naphthalene mineralization. Furthermore, in-situ groundwater measurements of the coupled redox species nitrate/nitrite and sulfate/sulfide reflected the potential for anaerobic biodegradation of naphthalene, but not phenanthrene, in site sediments. Finally, as previously noted by Rölling et al. (2001), groundwater measurements of ferrous iron and Mn(II) which are susceptible to precipitation-dissolution reactions and lack measurable redox couples do not provide reliable indication of active biological reactions. This was evidenced in the iron-reducing incubations with GPS 23 and GPS 25 sediments (see Figure 4.4). Therefore, it is especially important to validate the relevance of observed redox processes in the field with direct measures of specific PAH pollutant degradation such as laboratory-scale incubations with site sediments. Without direct measures of intrinsic degradation potential of specific PAH pollutants, errors in estimating natural attenuation rates based on site-level measurement of terminal electron acceptor consumption using mass balance modeling approaches such as instantaneous reaction could yield erroneous results.

Further complicating mass balance approaches, PAH-degrading organisms may grow on many different carbon sources, with PAHs contributing only a fraction of the assimilated carbon. In this study, microautoradiography showed that only 18, 26, and 40% of the bacteria within the *Actinobacteria, γ-Proteobacteria*, and *β-Proteobacteria*, respectively, grew in part on [9-^{14}C]phenanthrene. The growth of microorganisms not metabolizing the phenanthrene was at the expense of other (unidentified) carbon sources within the coal-tar contaminated sediments. This implies that these organisms also derived energy from compounds other than phenanthrene, thus resulting in some net depletion of dissolved oxygen not attributable to phenanthrene degradation.

This should be taken into account where mass-balance or instantaneous-reaction modeling approaches are used to estimate PAH mass destroyed and/or the time to achieve remediation goals. Appropriate tertiary lines of evidence capable of indicating uptake of PAH pollutants under specific redox conditions may be required to validate assumptions of terminal electron acceptor partitioning associated with degradation of PAH pollutants made in mass-balance or instantaneous-reaction modeling approaches.

Although direct evidence such as laboratory-scale incubations with site sediments and molecular microbiological data can support natural attenuation as a remedial mechanism at PAH contaminated sites, care must be taken in data analysis and interpretation. Changes in the in situ microbial community structures due to laboratory incubations may lead to misinterpretation and erroneous conclusions regarding the activity of specific organisms on PAH compounds. Although the *Actinobacteria* dominated the in-situ microbial community structure, their populations declined in aerobic incubations with site sediments, implying that these organisms were not involved in intrinsic degradation of the coal-tar constituents. However, *Actinobacteria* are known to be relatively slow-growing organisms that are fairly resistant to environmental stress (Bastiens et al., 2000). This may explain the enrichment of these organisms in-situ where environmental stress may be high, and decline relative to more opportunistic organisms such as the *β*- and *γ-Proteobacteria* in the aerobic incubations, where environmental stress is low. Considering these differences, the intrinsic microbial community structure would indicate that *Actinobacteria* are important in the degradation of coal-tar constituents, whereas bioassays would indicate the opposite. Based on microautoradiography, *β-Proteobacteria*, *γ-Proteobacteria*, and *Actinobacteria* were all active in growth on phenanthrene.

Finally, enrichment of specific bacterial phylotypes as part of the microbial community structure in situ, in laboratory-scale assays, or a combination of both may not necessarily indicate growth on specific contaminants of complex sources such as coal-tars. In this study, the growth of *Bacteriodetes* (hybridizing to the CF319a probe) in the aerobic bioassays as well as their presence as a part of the site microbial community structure as shown in Figure 4.3 indicated these bacteria may be important to the degradation of coal-tar constituents in these sediments. However, microautoradiography showed that *Bacteriodetes* were not involved in the uptake of phenanthrene in these aquifer sediments. Caution should be exercised when using enriched or altered 16S rRNA-based community profiles to infer specific microbial functions.

4.7 References

Ahn, Y., J. Sanseverino, and G. S. Sayler (1999) Analyses of polycyclic aromatic hydrocarbon-degrading bacteria isolated from contaminated soils, *Biodegradation*, 10(2), 149-157.

Amann R. I., B. J. Binder, R. J. Olson, S. W. Chisholm, R. Devereux, and D. A. Stahl (1990) Combination of 16S rRNA-targeted oligonucleotide probes with flow cytometry for analyzing mixed microbial populations, *Appl. Environ. Microbiol.*, 56(6), 1919-1925.

Amann, R. I., W. Ludwig, and K.-H. Schleifer (1995) Phylogenetic identification and in situ detection of individual microbial cells without cultivation, *Microbiol. Rev.*, 59(1), 143-169.

Anderson, R. T. and D. R. Lovley (1999) Naphthalene and benzene degradation under Fe(III)-reducing conditions in petroleum-contaminated aquifers, *Bioremediation*, 3(2), 121-135.

Atlas, R. M., and R. Bartha (1992) Hydrocarbon biodegradation and oil spill bioremediation, In K. C. Marshall (Ed.) *Advances in Microbial Ecology, Vol. 12*, Plenum Press, New York, NY, 287-339.

Bastiens, L., D. Springael, P. Wattiau, H. Harms, R. DeWatcher, H. Verachtert, and L. Diels (2000) Isolation of adherent polycyclic aromatic hydrocarbon (PAH)-degrading bacteria using PAH-sorbing carriers, *Appl. Environ. Microbiol.*, 66(5), 1834-1843.

Bedessem, M. E., N. G. Swoboda-Colberg, and P. J. S. Colberg (1997) Naphthalene mineralization coupled to sulfate reduction in aquifer-derived enrichments, *FEMS Microbiol. Lett.*, 152(2), 213-218.

Berardesco, G., S. Dyhrman, E. Gallagher, and M. P. Shiaris (1998) Spatial and temporal variation of phenanthrene-degrading bacteria in intertidal sediments, *Appl. Environ. Microbiol.*, 64(7), 2560-2565.

Black & Veatch (1998) Interim remedial action report for soil and source material, prepared for IES Utilities Inc., Black & Veatch Waste Science, Inc., Kansas City, MO.

Bogan, B. W., L. M. Lahner, and J. R. Paterek (2001) Limited roles for salicylate and phthalate in bacterial PAH bioremediation, *Biorem. J.*, 5(2), 93-100.

Boonchan, S., M. L. Britz, and G. A. Stanley (1998) Surfactant-enhanced biodegradation of high molecular weight polycyclic aromatic hydrocarbons by *Stenotrophomonas maltophilia*, *Biotechnol Bioeng.*, 59(4), 482-94.

Campbell, B. G., M. D. Petkewich, J. E. Landmeyer, and F. H. Chapelle (1996) *Geology, hydrogeology, and potential of intrinsic bioremediation at the National Park Service Dockside II Site and adjacent areas, Charleston, South Carolina, 1993–1994, Rep. No. 96-4170*, U.S. Geological Services, Columbia, S.C.

Coates, J. D., J. C. Woodward, J. Allen, P. Philp, and D. R. Lovley (1997) Anaerobic degradation of polycyclic aromatic hydrocarbons and alkanes in petroleum-contaminated marine harbor sediments, *Appl. Environ. Microbiol.*, **63**(9), 3589-3593.

Cole, J. R., B. Chai, T. L. Marsh, R. J. Farris, Q. Wang, S. A. Kulam, S. Chandra, D. M. McGarrell, T. M. Schmidt, G. M. Garrity, J. M. Tiedje, (2003) The Ribosomal Database Project (RDP-II): previewing a new autoaligner that allows regular updates and the new prokaryotic taxonomy, *Nucleic Acids Res.*, **31**(1), 442-443.

Cottrell, M. T., and D. L. Kirchman (2000) Natural assemblages of marine proteobacteria and members of the *Cytophaga-Flavobacter* cluster consuming low- and high-molecular-weight dissolved organic matter, *Appl. Environ. Microbiol.*, **66**(4), 1692-1697.

Daane, L. L., I. Harjono, G. J. Zylstra, and M. M. Häggblom (2001) Isolation and characterization of polycyclic aromatic hydrocarbon-degrading bacteria associated with the rhizosphere of salt marsh plants, *Appl. Environ. Microbiol.*, **67**(6), 2683-2691.

Daims, H., A. Brühl, R. Amann, K. H. Schleifer, and M. Wagner (1999) The domain-specific probe EUB338 is insufficient for the detection of all bacteria: development and evaluation of a more comprehensive probe set, *Syst. Appl. Microbiol.*, **22**(3), 434-444.

Electric Power Research Institute (EPRI) (1996) *Characterization and Monitoring Before and After Source Removal at a Former Manufactured Gas Plant (FMGP) Disposal Site*, EPRI Rep. No. TR-105921, Research Projects W02879-12; W02879-38, Palo Alto, Calif.

Eriksson, M., E. Sodersten, Z. Yu, G. Dalhammar, and W. W. Mohn (2003) Degradation of polycyclic aromatic hydrocarbons at low temperature under aerobic and nitrate-reducing conditions in enrichment cultures from Northern soils, *Appl. Environ. Microbiol.*, **69**(1), 275-284.

Fredrickson, J. K., D. L. Balkwill, G. R. Drake, M. F. Romine, D. B. Ringelberg, and D. C. White (1995) Aromatic-degrading *Sphingomonas* isolates from the deep subsurface, *Appl Environ. Microbiol.*, **61**(5), 1917-1922.

Galushko, A., D. Minz, B. Schrink, and F. Widdel (1999) Anaerobic degradation of naphthalene by a pure culture of a novel type of marine sulphate-reducing bacterium, *Environ. Microbiol.*, **1**(5), 415-420.

Gauthier, M. J., B. Lafay, R. Christen, L. Fernandez, M. Acquaviva, P. Bonin, and J. C. Betrand (1992) *Marinobacter hydrocarbonoclasticus* gen. nov., sp. nov., a new, extremely halotolerant, hydrocarbon-degrading marine bacterium, *Int. J. System. Bacteriol.*, **42**(4), 568-576.

Geiselbrecht, A. D., R. P. Herwig, J. W. Deming, and J. T. Staley (1996) Enumeration and phylogenetic analysis of polycyclic aromatic hydrocarbon-degrading marine bacteria from Puget Sound sediments, *Appl. Environ. Microbiol.*, **62**(9), 3344-3349.

Geiselbrecht, A. D., B. P. Hedlund, M. A. Tichi, and J. T. Staley (1998) Isolation of marine polycyclic aromatic hydrocarbon (PAH)-degrading *Cycloclasticus* strains from the Gulf of Mexico and comparison of their PAH degradation ability with that of Puget Sound *Cycloclasticus* strains, *Appl. Environ. Microbiol.*, **64**(12), 4703-4710.

Goyal, A. K. and G. J. Zylstra (1996) Molecular cloning of novel genes for polycyclic aromatic hydrocarbon degradation from *Comamonas testosteroni* GZ39, *Appl. Environ. Microbiol.*, **62**(1), 230-236.

Grosser, R. J., D. Warshawsky, and J. R. Vestal (1991) Indigenous and enhanced mineralization of pyrene, benzo(a)pyrene, and carbazole in soils, *Appl. Environ. Microbiol.*, **57**(12), 3462-3469.

Hayes, L. A. and D. R. Lovley (2002) Specific 16S rDNA sequences associated with naphthalene degradation under sulfate-reducing conditions in harbor sediments, *Microb. Ecol.*, **43**(1), 134-145.

Heitkamp, M. A., and C. E. Cerniglia (1988) Mineralization of polycyclic aromatic hydrocarbons by a bacterium isolated from sediment below an oil field, *Appl Environ Microbiol.*, **54**(6), 1612-1614.

Johnsen, A. R., A. Winding, U. Karlson, and P. Roslev (2002) Linking of microorganisms to phenanthrene metabolism in soil by analysis of 13C-labeled cell lipids, *Appl. Environ. Microbiol.*, **68**(12), 6106-6113.

Kasai, Y., H. Kishira, and S. Harayama (2002) Bacteria belonging to the genus *Cycloclasticus* play a primary role in the degradation of aromatic hydrocarbons released in a marine environment, *Appl. Environ. Microbiol.*, **68**(11), 5625-5633.

Kastner, M., M. Jammali-Breuer, and B. Mahro (1994) Enumeration and characterization of the soil microflora from hydrocarbon-contaminated soil sites able to mineralize polycyclic aromatic hydrocarbons (PAH), *Appl. Microbiol. Biotechnol.*, 41, 267-273.

Kazunga, C. and M. D. Aitken (2000) Products from the incomplete metabolism of pyrene by polycyclic aromatic hydrocarbon-degrading bacteria, *Appl. Environ. Microbiol.*, **66**(5), 1917-1922.

Kazunga, C., M. D. Aitken, A. Gold, and R. Sangaiah (2001) Fluoranthene-2,3- and -1,5-diones are novel products from the bacterial transformation of fluoranthene, *Environ. Sci. Technol.*, **35**(5), 917-922.

King, M. W. G., J. F. Barker, J. F. Devlin, and B. J. Butler (1999) Migration and natural fate of a coal tar creosote plume 2. Mass balance and biodegradation indicators, *J. Contam. Hydrol.*, **39**(3-4), 281-307.

Kleespies, M., R. M. Kroppenstedt, F. A. Rainey, L. E. Webb, and E. Stackebrandt (1996) *Mycobacterium holderi* sp. nov., a new member of the fast-growing mycobacteria capable of degrading polycyclic aromatic hydrocarbons, *Int. J. Syst. Bacteriol.*, **46**(3), 683-687.

Landmeyer, J. E., F. H. Chapelle, M. D. Petkewich, and P. M. Bradley (1998) Assessment of natural attenuation of aromatic hydrocarbons in groundwater near a former manufactured-gas plant, South Carolina, USA, *Environ. Geol.*, **34**(4), 79-292.

Langworthy, D. E, R. D. Stapleton, G. S. Sayler, and R. H. Findlay (1998) Genotypic and phenotypic responses of a riverine microbial community to polycyclic aromatic hydrocarbon contamination, *Appl. Environ. Microbiol.*, **64**(9), 3422-3428.

Llobet-Brossa, E., R. Roselló-Mora, and R. Amann (1998) Microbial community composition of Wadden Sea sediments as revealed by fluorescence in situ hybridization, *Appl. Environ. Microbiol.*, **64**(7), 2691-2696.

Lloyd-Jones, G., A. D. Laurie, D. W. F. Hunter, and R. Fraser (1999) Analysis of catabolic genes for naphthalene and phenanthrene degradation in contaminated New Zealand soils, *FEMS Microbiol. Ecol.*, **29**(1), 69-79.

Loy, A., M. Horn, and M. Wagner (2003) probeBase - an online resource for rRNA-targeted oligonucleotide probes, *Nucleic Acids Res.*, **31**(1), 514-516.

Manz W., R. Amann, W. Ludwig, M. Wagner, and K. H. Schleifer (1992) Phylogenetic oligodeoxynucleotide probes for the major subclasses of *Proteobacteria*: problems and solutions, *Syst. Appl. Microbiol.*, **15**(4), 593-600.

Manz W., R. Amann, W. Ludwig, M. Vancanneyt, and K. H. Schleifer (1996) Application of a suite of 16S rRNA-specific oligonucleotide probes designed to investigate bacteria of the phylum *cytophaga-flavobacter-bacteroides* in the natural environment, *Microbiol.*, **142**(5), 1097-1106.

Manz, W., M. Eisenbrecher, T. R. Neu, and U. Szewzyk (1998) Abundance and spatial organization of gram-negative sulfate reducing bacteria in activated sludge investigated by in situ probing with specific 16S rRNA targeted oligonucleotides, *FEMS Microbiol. Ecol.*, **25**(1), 43-61.

McNally, D. L., J. R. Mihelcic, and D. R. Lueking (1998) Biodegradation of three- and four-ring polycyclic aromatic hydrocarbons under aerobic and denitrifying conditions, *Environ. Sci. Technol.*, **32**(17), 2633-2639.

Meckenstock, R. U., E. Annweiler, W. Michaelis, H. H. Richnow, and B. Schink (2000) Anaerobic naphthalene degradation by a sulfate-reducing enrichment culture, *Appl. Environ. Microbiol.*, **66**(7), 2743-2747.

Meier, H., R. Amann, W. Ludwig, and K. H. Schleifer (1999) Specific oligonucleotide probes for in situ detection of a major group of gram-positive bacteria with low DNA G+C content, *Syst. Appl. Microbiol.*, **22**(2), 186-196.

Melcher, R. J., S. E. Apitz, and B. B. Hemmingsen (2002) Impact of irradiation and polycyclic aromatic hydrocarbon spiking on microbial populations in marine sediment for future aging and biodegradability studies, *Appl. Environ. Microbiol.*, **68**(6), 2858-2868.

Mueller, J. G., R. Devereux, D. L. Santavy, S. E. Lantz, S. G. Willis, and P. H. Pritchard (1997) Phylogenetic and physiological comparisons of PAH-degrading bacteria from geographically diverse soils, *Antonie Van Leeuwenhoek*, **71**(4), 329-343.

Neef, A. (1997) Anwendung der in situ einzelzell-identifizierung von bakterien zur populations analyse in komplexen mikrobiellen biozönosen, Doctoral thesis, Technische Universität München, Munich, Germany.

Ong, S. K., B. H. Kjartanson, G. A. Stenback, J. Golchin, S. W. Rogers, and N. Miller (2001) Assessment of natural attenuation at a former manufactured gas plant site, *Proc., 6th Int. In Situ and On Site Bioremediation Conf.*, June 4-8, San Diego, CA.

Padmanabhan, P., S. Padmanabhan, C. DeRito, A. Gray, D. Gannon, J. R. Snape, C. S. Tsai, W. Park, C. Jeon, and E. L. Madsen (2003) Respiration of 13C-labeled substrates added to soil in the field and subsequent 16S rRNA gene analysis of 13C-labeled soil DNA, *Appl. Environ. Microbiol.*, **69**(3), 1614-1622.

Rockne, K. J., J. C. Chee-Sanford, R. A. Sanford, B. P. Helund, J. T. Staley, and S. E. Strand (2000) Anaerobic naphthalene degradation by microbial pure cultures under nitrate-reducing conditions, *Appl. Environ. Microbiol.*, **66**(4), 1595-1601.

Roller, C., M. Wagner, R. Amann, W. Ludwig, and K. H. Schleifer (1994) In situ probing of Gram-positive bacteria with high DNA G+C content using 23S rRNA- targeted oligonucleotides, *Microbiol.*, **140**(10), 2849-2858. (Erratum in: *Microbiol.* (1995) **141**(5), 1267.)

Rölling, W. F. M., B. M. van Breukelen, M. Braster, B. Lin, and H. W. van Verseveld (2001) Relationships between microbial community structure and hydrochemistry in a landfill leachate-polluted aquifer, *Appl. Environ. Microbiol.*, **67**(10), 4619-4629.

Saito, A., T. Iwabuchi, and S. Harayama (2000) A novel phenanthrene dioxygenase from *Nocardiodes* sp. strain KP7: expression in *Escherichia coli*, *J. Bacteriol.*, **182**(8), 2134-2141.

Shairis, M. P. and J. J. Clooney (1983) Replica plating method for estimating phenanthrene-utilizing and phenanthrene-cometabolizing microorganisms, *Appl. Environ. Microbiol.*, **45**(2), 706-710.

Stahl, D. A., and R. Amann. (1991) Development and application of nucleic acid probes, in *Nucleic acid techniques in bacterial systematics*, E. Stackebrandt and M. Goodfellow (ed.), John Wiley & Sons Ltd., Chichester, England, 205-248.

Sutherland, J. B., J. P. Freeman, A. L. Selby, P. P. Fu, D. W. Miller, and C. E. Cerniglia (1990) Stereoselective formation of a K-region dihydrodiol from phenanthrene by *Streptomyces flavovirens*, *Arch. Microbiol.*, **154**(3), 260-266.

Tagger, S., N. Truffaunt, and J. Le Petit (1990) Preliminary study on relationships among strains forming a bacterial community selected on naphthalene from a marine sediment, *Can. J. Microbiol.*, **36**(10), 676-681.

Trenz, S. P., K. H. Engesser, P. Fischer, and H. J. Knackmuss (1994) Degradation of fluorene by *Brevibacterium* sp. strain DPO 1361: a novel C-C bond cleavage mechanism via 1,10-dihydro-1,10-dihydroxyfluoren-9-one, *J. Bacteriol.*, **176**(3), 789-95.

Unge, A., R. Tombolini, L. Mølbak, and J. K. Jansson (1999) Simultaneous monitoring of cell number and metabolic activity of specific bacterial populations with a dual gfp-luxAB marker system, *Appl. Envir. Microbiol.*, **65**(2), 813-821.

U.S. EPA (1999) Use of Monitored Natural Attenuation at Superfund, RCRA Corrective Action, and Underground Storage Tank Sites, Office of Solid Waste and Emergency Response Policy Directive 9200.4-17P, EPA, Office of Solid Waste and Emergency Response, U.S. Government Printing Office, Washington, D.C., April 21, 41 pp.

Uz, I., Y. P. Duan, and A. Ogram (1998) Characterization of the PAH degrading bacterium, *Rhodococcus opacus* M213, *FEMS Microbiol. Lett.*, **185**(2), 231-238.

Vila, J., Z. López, J. Sabaté, C. Minguillón, A. M. Solanas, and M. Grifoll (2001) Identification of a novel metabolite in the degradation of pyrene by *Mycobacterium* sp. strain AP1: actions of the isolate on two- and three-ring polycyclic aromatic hydrocarbons, *Appl. Environ. Microbiol.*, **67**(12), 5497-5505.

Wallner, G., R. Amann, and W. Beisker (1993) Optimizing fluorescent in situ hybridization with rRNA-targeted oligonucleotide probes for flow cytometric identification of microorganisms, *Cytometry*, **14**(2), 136-143.

Wang, Y. and P. C. Lau (1996) Sequence and expression of an isocitrate dehydrogenase-encoding gene from a polycyclic aromatic hydrocarbon oxidizer, *Sphingomonas yanoikuyae* B1, *Gene*, **168**(1), 15-21.

Wang, R. F., W. W. Cao, and C. E. Cerniglia (1995) Phylogenetic analysis of polycyclic aromatic hydrocarbon degrading *mycobacteria* by 16S rRNA sequencing, *FEMS Microbiol. Lett.*, **130**(1), 75-80.

Widada, J., H. Nojiri, K. Kasuga, T. Yoshida, H. Habe, and T. Omori (2002) Molecular detection and diversity of polycyclic aromatic hydrocarbon-degrading bacteria isolated from geographically diverse sites, *Appl. Microbiol. Biotechnol.*, **58**(2), 202-209.

Zarda, B., D. Hahn, A. Chatzinotas, W. Schönhuber, A. Neef, R. Amann, and J. Zeyer (1997) Analysis of bacterial community structure in bulk soil by in situ hybridization, *Arch. Microbiol.*, **168**(3), 185-192.

Zhang, X. and L. Y. Young (1997) Carboxylation as an initial reaction in the anaerobic metabolism of naphthalene and phenanthrene by sulfidogenic consortia, *Appl. Environ. Microbiol.*, **63**(12), 4759-4764.

Table 4.1   Phylotypic relatedness of bacteria associated with PAH mineralization as reported in literature.

Phylum/Class	Genus/Species	Geographical source	Reference(s)
Aerobic			
α-Proteobacteria	*Sphingomonas*	New Jersey; Texas; Illinois; Germany; Florida; Boston Harbor; Sweden; France; South Carolina	Bogan et al., 2001; Frederickson et al., 1995; Wang et al., 1996; Kazunga et al., 2001; Bastiens et al., 1998; Daane et al., 2001
β-Proteobacteria	*Alcaligenes; Burkholderia; Bordetella; Acidovorax; Variovorax; Pseudomonas* sp. V-O7-10; *Comamonas; Copiotrophic ultramicrobacteria*	Boston Harbor; New Zealand; Canada; Sweden; Norway; New York; New Jersey; France; Florida; Japan	Eriksson et al., 2003; Laurie and Lloyd-Jones, 1999; Johnsen et al, 2002; Berardesco et al., 1998; Padmanabhan et al., 2003; Mueller et al, 1997; Bogan et al., 2001; Daane et al., 2001; Goyal and Zylstra, 1996
γ-Proteobacteria	*Cycloclasticus; Pseudomonas; Moraxella; Marinobacter; Vibrio; Halomonas; Pseudoalteromonas; Marinomonas; Acinetobacter; Stenotrophomonas*	Puget Sound; Gulf of Mexico; Boston Harbor; Canada; Sweden; New York; Florida; Germany; New Jersey; France; Japan	Geiselbrecht et al., 1996; Geiselbrecht et al., 1998; Daane et al, 2001; Kasai et al., 2002; Boonchan et al., 1998; Bogan et al., 2001; Mueller et al, 1997; Padmanabhan et al., 2003; Eriksson et al., 2003; Berardesco et al., 1998; Gauthier et al., 1992; Melcher et al., 2002; Tagger et al., 1990
Actinobacteria	*Mycobacterium; Rhodococcus; Arthrobacter; Streptomyces; Nocardiodes; Gordonia; Nocardia; Terrabacter; Tsukamurella*	Boston Harbor; Texas; Germany; Japan; Spain; New Jersey	Kastner et al., 1994; Grosser et al., 1991; Wang et al., 1995; Uz et al., 1998; Daane et al., 2001; Trenz et al., 1994; Sutherland et al., 1990; Saito et al., 2000; Johnsen et al, 2002; Berardesco et al., 1998; Kleespies et al., 1996; Heitkamp and Cerniglia, 1988; Vila et al., 2001
Firmicutes	*Bacillus cereus* P21; *Paenibacillus*	New Jersey; Delaware	Kazunga et al., 2001; Daane et al., 2001
Bacteriodetes	*Flavobacterium*	Boston Harbor	Berardesco et al., 1998; Shiaris and Clooney, 1983
Nitrate-Reducing			
β-Proteobacteria	*Variovorax; Bordetella; Alcaligenes*	Canada	Eriksson et al., 2003
γ-Proteobacteria	*Pseudomonas; Vibrio*	Canada; Puget Sound	Rockne et al., 2000; Eriksson et al., 2003
Sulfate-Reducing			
δ-Proteobacteria	Delta Proteobacterium NaphS2	San Diego Bay	Hayes and Lovley, 2002; Galushko et al., 1999

139

Table 4.2 Historical aromatic hydrocarbon exposure of Cherokee FMGP aquifer sediments used in bioassays.

Pollutant	Pure Aqueous Solubility (µg/L)	Measured groundwater pollutant concentrations mean (±standard deviation) (µg/L)				
		GPS 22[a]	GPS 23	GPS 25	GPS 26	GPS 27
Monoaromatics						
Benzene	1780000	80 (±40)	750 (±610)	530 (±400)	270 (±440)	92 (±22)
Ethylbenzene	152000	540 (±450)	770 (±280)	300 (±460)	65 (±92)	33 (±15)
Toluene	515000	200 (±150)	200 (±120)	33 (±40)	1.1 (±2.2)	0.9 (±0.8)
Xylenes	198000	550 (±360)	720 (±260)	270 (±260)	34 (±42)	29 (±24)
2-Ring PAH						
Naphthalene	31700	6880 (±11960)	3990 (±2770)	1380 (±2120)	9.8 (±21)	1.6 (±0.6)
1-Methylnaphthalene	28500	2000 (±3550)	470 (±100)	300 (±180)	17 (±32)	1.1 (±1.2)
2-Methylnaphthalene	25400	2520 (±5360)	210 (±220)	13 (±17)	ND	ND
3-Ring PAH						
Acenaphthene	3420	330 (±660)	62 (±26)	45 (±20)	7.3 (±12)	ND
Acenaphthylene	3930	1420 (±2470)	330 (±56)	200 (±120)	12 (±20)	0.3 (±0.5)
Fluorene	1690	1450 (±3050)	98 (±36)	22 (±21)	ND	0.1 (±02)
Phenanthrene	1000	2010 (±4330)	79 (±49)	44 (±20)	0.6 (±1.4)	ND
Anthracene	45	540 (±1170)	16 (±15)	4.2 (±4.0)	ND	ND
4-Ring PAH						
Fluoranthene	206	780 (±1740)	8.8 (±12)	0.5 (±1.0)	ND	ND
Pyrene	130	1110 (±2490)	2.8 (±4.8)	0.4 (±0.9)	ND	ND
Benzo[a]anthracene	5.7	290 (±640)	4.4 (±7.5)	ND	ND	ND
Chrysene	1.8	250 (±550)	2.3 (±3.8)	ND	ND	ND
5-Ring PAH						
Benzo[b]fluoranthene	14	98 (±220)	0.6 (±1.1)	ND	ND	ND
Benzo[k]fluoranthene	4.3	80 (±180)	ND	ND	ND	ND
Benzo[a]pyrene	3.8	270 (±600)	0.5 (±0.9)	ND	ND	ND
Dibenz[a,h]anthracene	0.50	22 (±49)	ND	ND	ND	ND
6-Ring PAH						
Benzo[g,h,i]perylene	0.26	180 (±400)	2.2 (±3.8)	ND	ND	ND
Indeno[1,2,3-c,d]pyrene	0.53	120 (±260)	1.4 (±2.5)	ND	ND	ND

a. = Free product observed in sediment core
ND = Not detected above 1 µg/L (BTEX) or 0.1 µg/L (PAH)

Table 4.3   Target organisms and oligonucleotide probes used in this study.

Target Organisms Specificity	Probe Name	Target	Target Site [a]	Oligonucleotide Sequence (5' – 3')	Fluor [b]	Ref.
Domain _Archaea_	ARCH915	16S rRNA	915-934	GTG-CTC-CCC-CGC-CAA-TTC-CT	FITC	c
Domain _Bacteria_	EUB338	16S rRNA	338-355	GCT-GCC-TCC-CGT-AGG-AGT	Cy3, FITC	d
	EUB338-II	16S rRNA	338-355	GCA-GCC-ACC-CGT-AGG-TGT	Cy3, FITC	e
	EUB338-III	16S rRNA	338-355	GCT-GCC-ACC-CGT-AGG-TGT	Cy3, FITC	e
Proteobacteria						
α-_Proteobacteria_	ALF968	16S rRNA	968-986	GGT-AAG-GTT-CTG-CGC-GTT	FITC	f
β-_Proteobacteria_	BET42a	23S rRNA	1027-1043	GCC-TTC-CCA-CTT-CGT-TT	FITC	g
γ-_Proteobacteria_	GAM42a	23S rRNA	1027-1043	GCC-TTC-CCA-CAT-GCT-TT	CY3	g
Sulfate Reducing Bacteria Some sulfate-reducing bacteria of the δ-_Proteobacteria_, other δ-_Proteobacteria_ and several gram positive bacteria	SRB385	16S rRNA	385-402	CGG-CGT-CGC-TGC-GTC-AGG	FAM	d
Gram Positive Bacteria						
Actinobacteria Gram Positive Bacteria with High DNA G+C Content	HGC69a	23S rRNA	1901-1918	TAT-AGT-TAC-CAC-CGC-CGT	Cy3	h
Firmicutes Gram Positive Bacteria with Low DNA G+C Content	LGC354a	16S rRNA	354-371	TGG-AAG-ATT-CCC-TAC-TGC	FITC	i
	LGC354b	16S rRNA	354-371	CGG-AAG-ATT-CCC-TAC-TGC	FITC	i
	LGC354c	16S rRNA	354-371	CCG-AAG-ATT-CCC-TAC-TGC	FITC	i
Bacteriodetes						
Bacteriodetes	CF319a	16S rRNA	319-336	TGG-TCC-GTG-TCT-CAG-TAC	Cy3	j
Bacteriodes and _Prevotella_ genera	BAC303	16S rRNA	303-319	CCA-ATG-TGG-GGG-ACC-TT	FITC	j
Nonsense control probe	NONEUB	16S rRNA	338-355	CGA-CGG-AGG-GCA-TCC-TCA	FITC	k

a. 16S or 23S rRNA position according to _Escherichia coli_ numbering, b.Fluor = fluorochrome. Fluorescent markers were linked to the 5' end., c. Stahl and Amann, 1991, d. Amann et al., 1990, e. Daims et al., 1999, f. Neef, 1997, g. Manz et al., 1992, h. Roller et al., 1994, i. Meier et al., 1999, j. Manz et al., 1996, k. Wallner et al., 1993

Table 4.4   Microbial community structure of the Cherokee FMGP site sediments.

Core	Sample Depth (m)	Total Direct DAPI[a] (x 10^4)	Bacteria[b]	Archaea	Proteobacteria				Gram Positives		CFB Cluster	
					α	β	γ	δ (SRB385)	High DNA G+C content	Low DNA G+C content	Bacteriodetes	Bacteriodes and Prevotella genera
GPS 21	6.1	1.5 ± 1.1	64.0	0.2	-[c]	0.6	15.4	-	20.2	0.2	1.8	0.2
			13.6	0.4		0.6	7.2		5.3	0.0	0.4	0.0
	7.3	5.6 ± 6.5	57.1	0.3	-	1.0	18.0	1.8	22.2	0.5	5.4	0.3
			7.9	0.4		0.7	4.8	1.0	5.0	0.3	1.2	0.3
GPS 22	5.5	347 ± 25	57.8	-	0.1	4.5	5.6	0.6	36.0	0.4	1.7	0.5
			8.2		0.2	0.6	1.9	1.3	3.5	0.6	0.7	0.5
	6.7	1450 ± 90	62.9	-	0.1	18.0	12.5	0.1	24.9	0.2	7.2	0.6
			3.7		0.2	4.7	4.8	0.1	5.0	0.3	1.7	0.2
	7.9	439 ± 58	44.4	5.3	2.9	0.7	15.9	-	29.2	0.1	7.2	-
			7.5	2.3	1.1	0.2	6.6		6.2	0.3	1.3	
GPS 23	3.7	139 ± 14	59.4	-	0.2	1.0	12.9	-	21.7	-	3.3	-
			5.6		0.4	1.1	4.3		3.5		1.1	
	6.1	653 ± 36	64.3	-	-	0.1	28.3	-	33.1	0.2	2.4	0.4
			6.4			0.2	7.4		5.3	0.4	1.1	0.4
GPS 24	3.7	120 ± 23	16.0	1.0	0.8	-	-	7.1	0.4	0.1	0.8	-
			3.8	1.2	0.7			1.4	0.5	0.2	1.1	
	6.1	72 ± 6.9	52.2	0.2	-	1.4	16.1	2.6	25.3	0.8	5.3	0.6
			9.8	0.3		1.5	3.2	1.0	3.2	0.7	1.8	0.7
GPS 25	3.7	36 ± 4.3	45.7	-	-	0.7	1.0	2.7	-	-	-	-
			8.3			0.6	0.9	1.7				
	6.1	6.3 ± 1.5	67.3	-	1.0	-	15.8	6.2	16.2	-	2.9	1.6
			6.4		0.9		7.3	1.3	3.1		1.7	1.6
GPS 26	6.1	216 ± 17	52.1	-	-	-	0.8	9.4	1.0	-	0.6	-
			7.3				0.5	3.8	0.5		0.6	
	7.9	7.1 ± 1.6	70.3	-	-	0.2	22.7	16.6	27.9	0.4	7.5	0.4
			4.9			0.4	5.1	3.5	10.3	0.5	0.9	0.4
GPS 27	9.1	71 ± 6.2	37.2	1.0	2.5	-	-	36.7	2.0	0.9	2.2	-
			8.8	1.3	1.3			2.6	1.7	1.8	2.1	
GPS 28	8.5	1160 ± 75	74.9	-	0.1	-	11.7	2.3	24.4	0.1	16.5	1.9
			9.0		0.1		3.1	0.8	3.4	0.2	2.1	0.4

a.   Reported as mean (x 10^4) ± 95% confidence interval (x 10^4), n=40
b.   Reported as percent of DAPI-stained organisms, mean ± 95% confidence interval (n≥5, minimum of 400 DAPI-counterstained cells)
c.   - = Not Detected (<0.1% of total DAPI Direct Count)

142

Table 4.5   Microbial community structure of GPS 22 and GPS 23 sediments and following aerobic incubations and MICRO-FISH with [9-^{14}C]phenanthrene. Active cells for GPS 22 indicate microbes associated with silver grain formation in MICRO-FISH.

Microbes	GPS 23			GPS 22				
	3.7 m bgs	6.1 m bgs	Post-Incubation	5.5 m bgs	6.7 m bgs	7.9 m bgs	Post-Incubation	Active Cells
Total Direct DAPI Count (Cells · gm sediment $^{-1}$)	139 ± 14	653 ± 36	3840 ± 386	347 ± 25	1450 ± 90	439 ± 58	2000 ± 147	809 ± 221
Bacteria (Cells · gm sediment $^{-1}$)	82 ± 7.8	420 ± 42	2410 ±329	201 ± 29	911 ± 53	195 ± 33	1670 ± 275	452 ± 8.2
Archaea (Cells · gm sediment $^{-1}$)	ND[b]	ND	ND	ND[b]	1.0 ± 2.0	23 ± 10	ND	ND
Proteobacteria								
α - *Proteobacteria*	0.3 ± 0.5 0.30%[c]	ND	7.9 ± 6.8 0.33%	0.4 ± 0.6 0.21%[c]	1.2 ± 2.4 0.13%	13 ± 4.6 6.59%	ND	ND
β - *Proteobacteria*	1.3 ± 1.5 1.63 %	0.7 ± 1.4 0.17%	194 ± 18 8.07%	16 ± 2 7.86%	261 ± 68 28.6%	2.9 ± 1.0 1.50%	935 ± 456 56.0%	373 ± 329 82.3% [d]
γ - *Proteobacteria*	18 ± 6.0 21.7%	185 ± 48 44.1%	1200 ± 421 50.00%	19 ± 6.6 9.68%	181 ± 70 19.9%	70 ± 29 35.7%	173 ± 60 10.3%	45 ± 28 9.84%
δ - *Proteobacteria*	ND	ND	ND	2.2 ± 4.5 1.12%	1.5 ± 1.9 0.17%	ND	ND	ND
Gram Positive Bacteria								
Actinobacteria	30 ± 4.9 36.5%	216 ± 35 51.5%	207 ± 80 8.59%	125 ± 12 62.4%	361 ± 73 39.6%	128 ± 27 65.8%	50 ± 24 3.01%	9.1 ± 5.5 2.01%
Firmicutes	ND	1.3 ± 2.6 0.30%	163 ± 74 6.76%	1.5 ± 2.0 0.76%	3.3 ± 4.0 0.36%	0.6 ± 1.1 0.29%	3.4 ± 5.1 0.20%	ND
CFB Cluster								
Bacteriodetes	4.5 ± 1.5 5.5%	16 ± 7.2 3.8%	198 ± 28 8.22%	5.7 ± 2.3 2.86%	104 ± 25 11.4%	32 ± 5.6 16.3%	9.9 ± 11 0.59%	ND
Bacteriodes and *Prevotella genera*	ND	2.4 ± 2.3 0.60%	ND	1.7 ± 1.9 0.87%	8.0 ± 3.2 0.88%	ND	ND	ND

a. Reported as **mean** ± 95% confidence interval *(x 10^4)*
b. ND = not detected
c. Percent of total *Bacteria*
d. Percent of active *Bacteria*

143
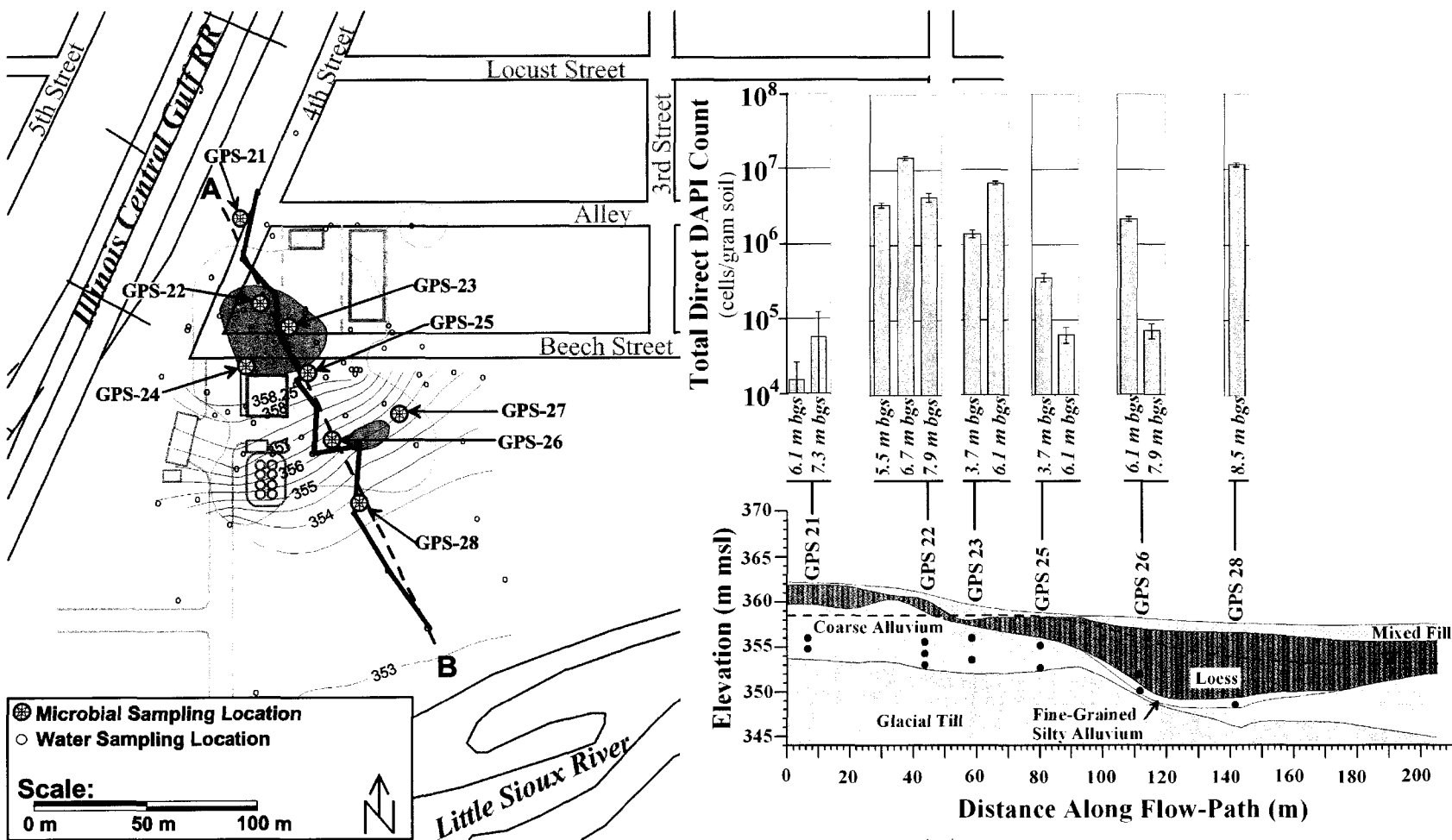
Figure 4.1   Cherokee FMGP site plan and profile. The dark gray contours show the estimated extent of PAH and BTEX source material (free product). The light gray contours indicate the approximate aerial extent of the PAH and BTEX contamination (2 μg/L). Contour lines indicate the water table elevation shown by the dashed line in the geological profile across transect A-B (inset). The red dots on the geological profile represent the microbial sampling depths at the locations indicated on the plan view of the site. Total direct DAPI microbial counts (per gram sediment) at each sampling location are shown (error bars indicate ±95% confidence interval, plotted on a $\log_{10}$ scale).
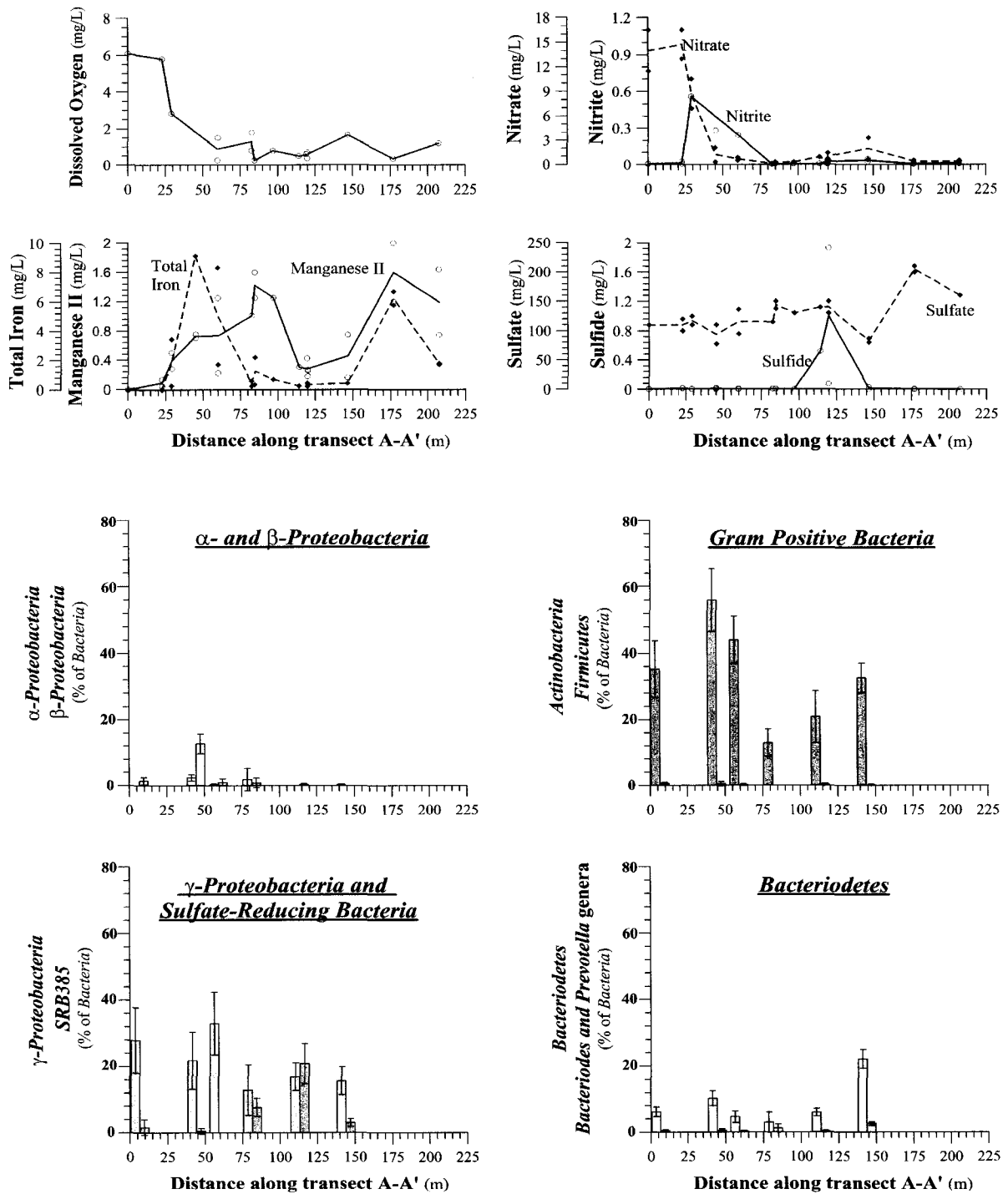
Figure 4.2 Average microbial community structure on transect A-B related to measured concentrations of common terminal electron acceptors and reduced species in situ. Shown are the mean percent (relative to *Bacteria*) of each phylogenetic group across all sample depths at each coordinate along transect A-B (GPSS 21, GPSS 22, GPSS23, GPSS 25, GPSS 26, and GPSS 28, respectively). The error bars indicate the 95% confidence interval.
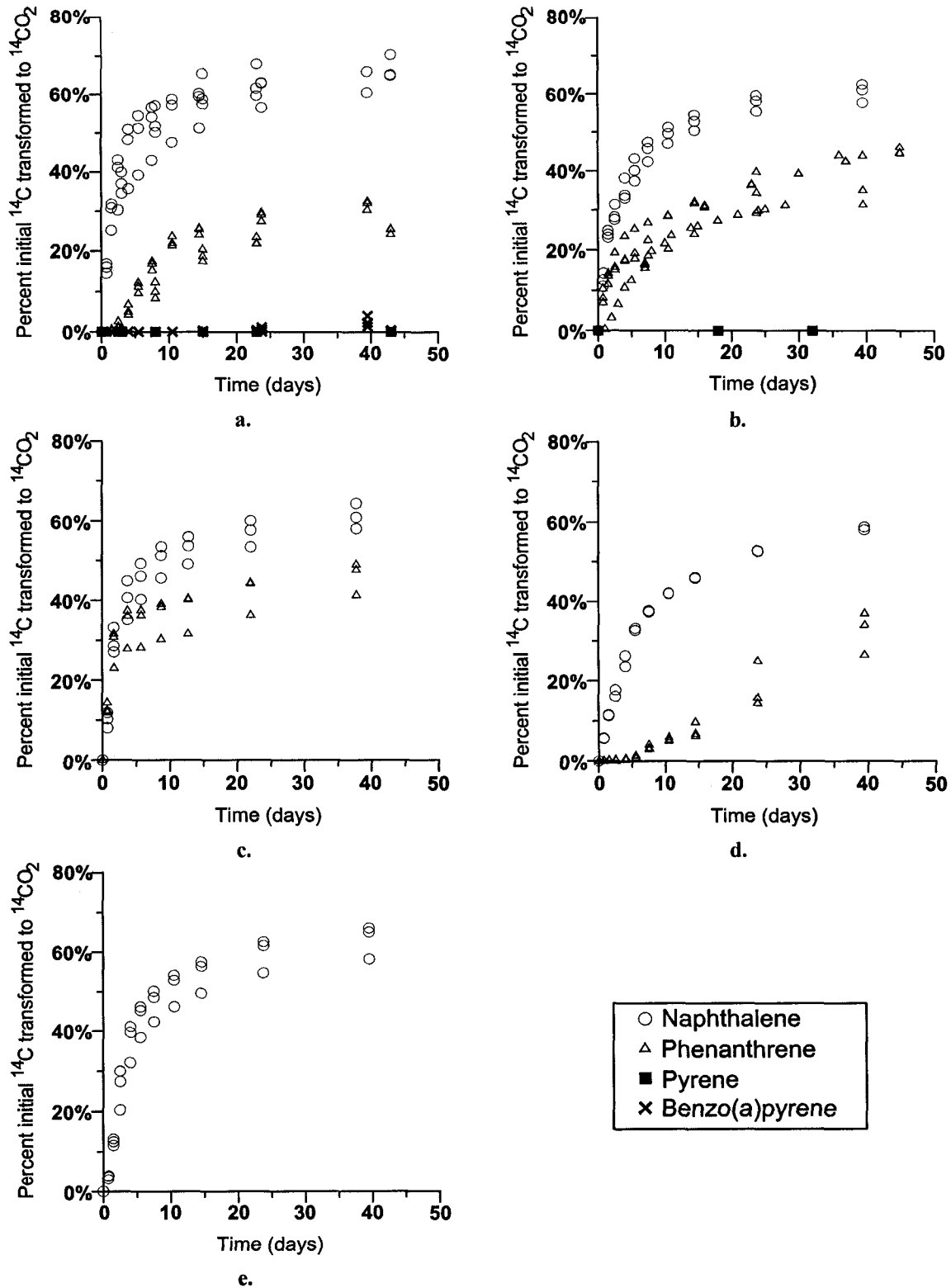
Figure 4.3 $^{14}CO_2$ evolution in aerobic incubations with Cherokee FMGP site sediments. (a) GPS 22, (b) GPS 23, (c) GPS 25, (d) GPS 26, (e) GPS 27
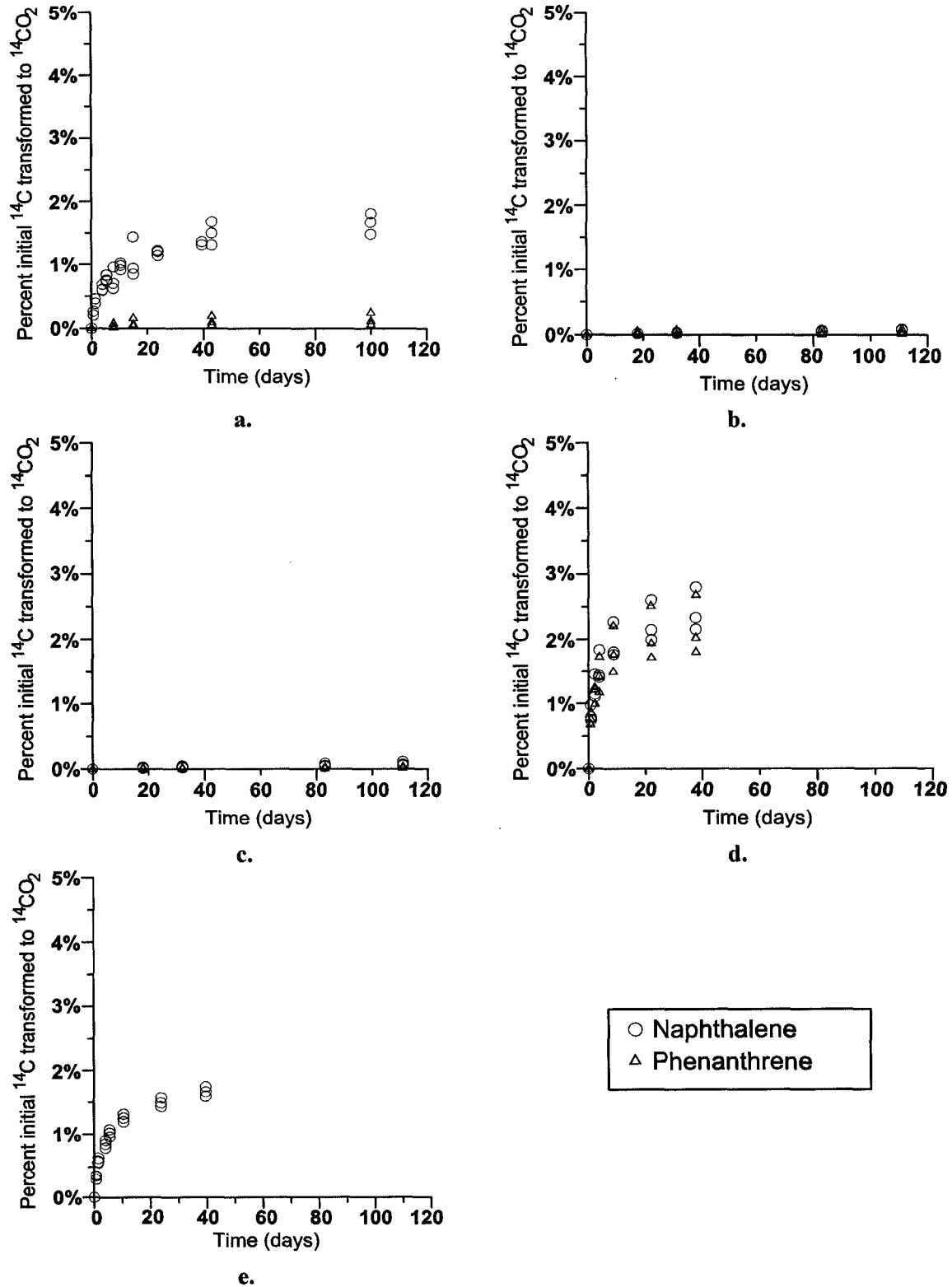
Figure 4.4   Anaerobic $^{14}CO_2$ evolution in site sediments. Nitrate-amended: (a) GPS 22 and (b) GPS 23; Iron-amended: (c)GPS 23 and (d) GPS 25; and Sulfate-amended: (e) GPS 27
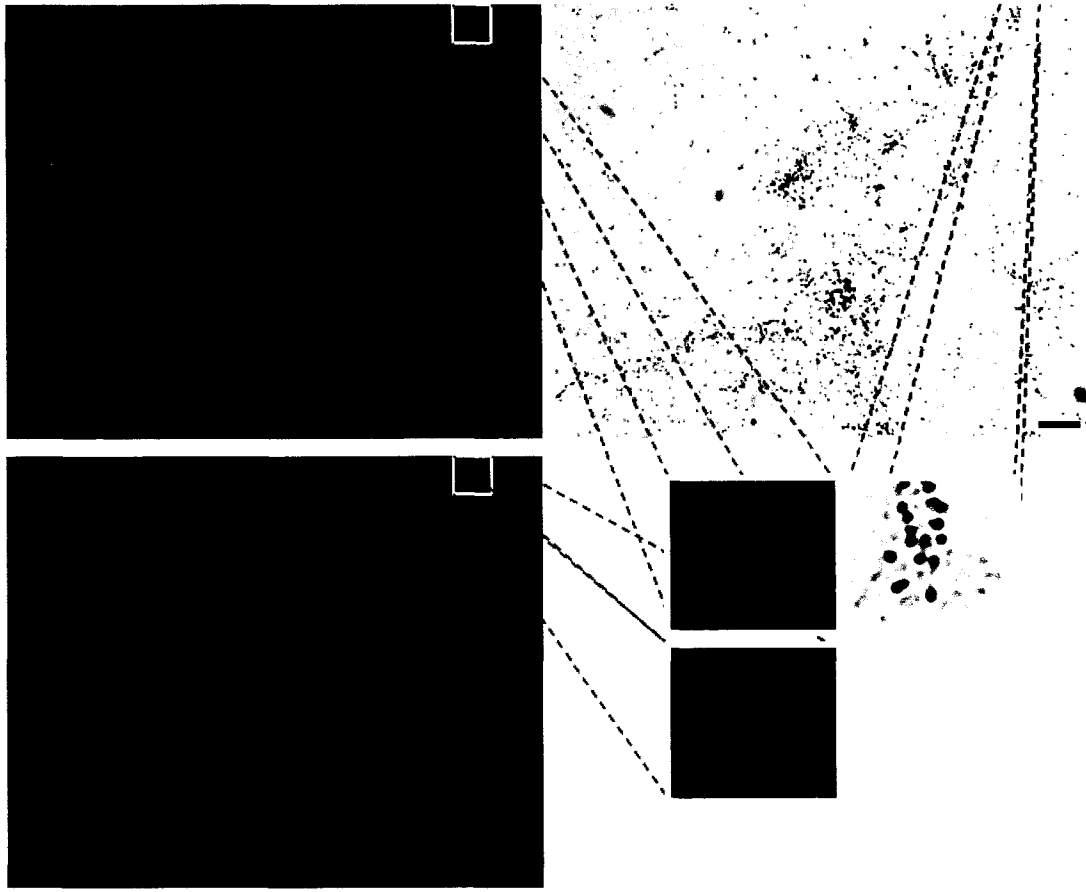
Figure 4.5   Fluorescence images and autoradiogram following MICRO-FISH assay with GPS 22 sediments: *Bacteria*. Blue cells represent DAPI-stained organisms. Cells hybridizing with the EUB338 probe set are shown in red. 27.1% of FISH-detected *Bacteria* were associated with silver grain formation indicating growth on [9-^{14}C] phenanthrene (inset). Archaea were not detected. Bar in autoradiogram represents 10 μm.
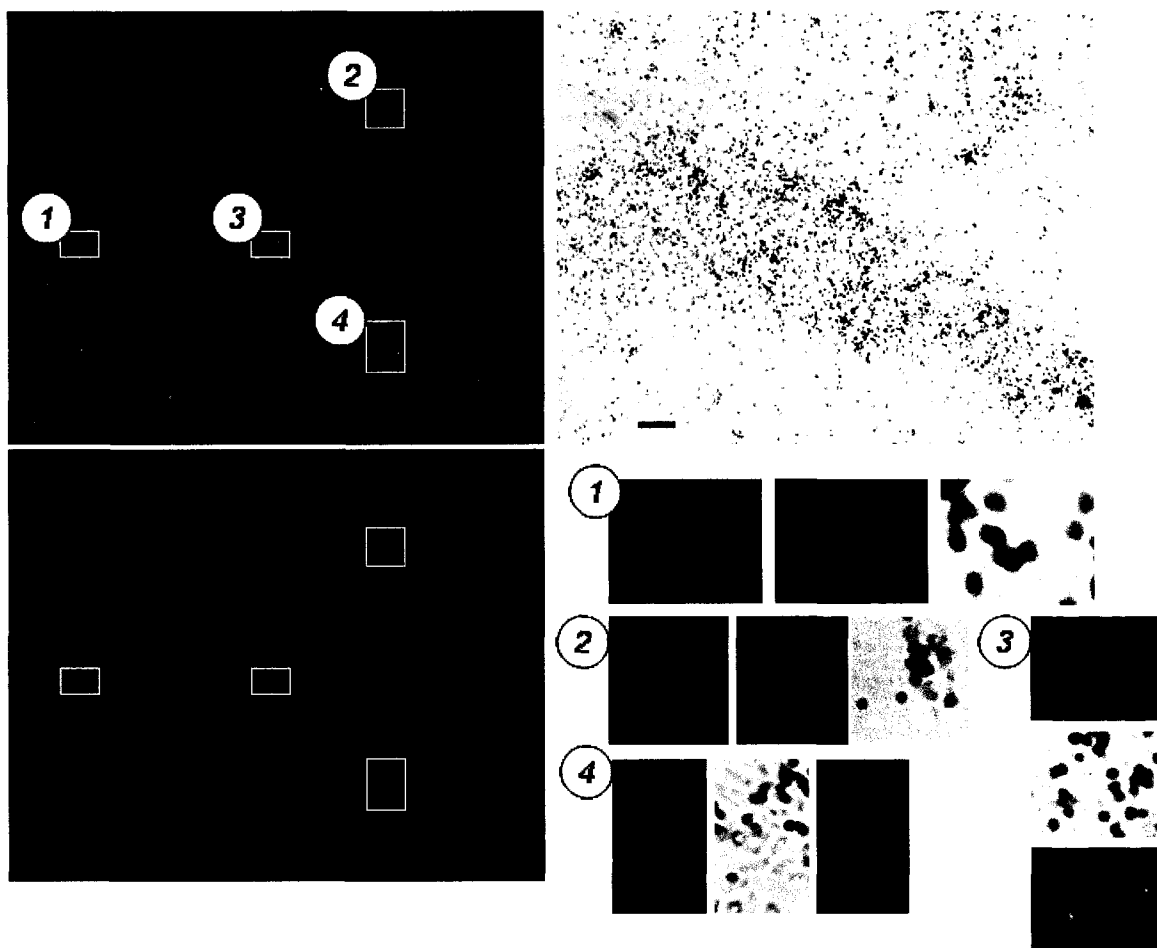
Figure 4.6   Fluorescence images and autoradiogram on following MICRO-FISH assay with
GPS 22 sediments: *β*- and *γ-Proteobacteria*. Blue cells represent DAPI-stained
organisms. *γ-Proteobacteria* (hybridizing with the GAM42a probe) are shown in
red. *β-Proteobacteria* (hybridizing with the BET42a probe) are shown in green.
39.9% of FISH-detected *β-Proteobacteria* (image sets 1, 3, and 4) and 25.7% of
FISH-detected *γ-Proteobacteria* (image sets 2 and 3) were associated with silver
grain formation indicating bacteria of these sub-divisions grew on [9-^{14}C]
phenanthrene. *α*- and *δ-Proteobacteria* were not detected. Bar in
autoradiogram represents 10 μm.
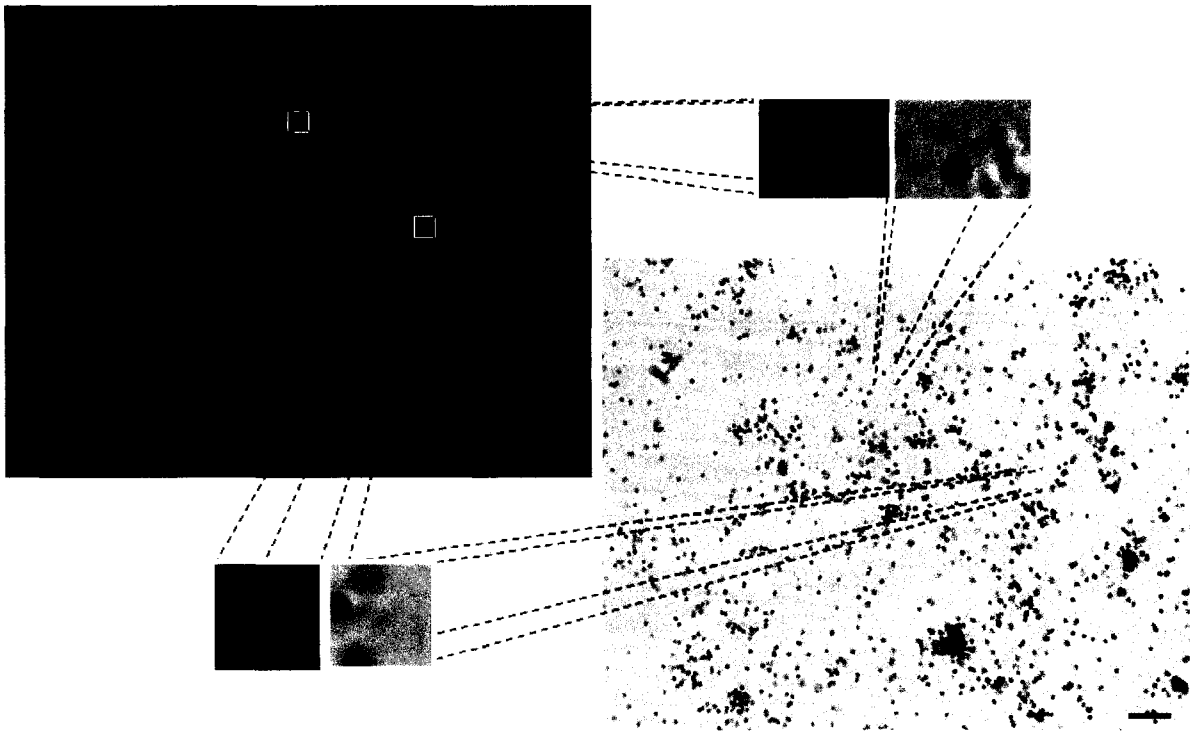
Figure 4.7   Fluorescence images and autoradiogram on following MICRO-FISH assay with
GPS 22 sediments: *Actinobacteria*. Blue cells represent DAPI-stained organisms.
Actinobacteria (hybridizing with the HGC69a probe) are shown in red. 18.1%
of all FISH-detected *Actinobacteria* were associated with silver grain formation
indicating growth on [9-^{14}C] phenanthrene. *Firmicutes* (hybridizing to the LGC
probe set) were not detected. Bar in autoradiogram represents 10 µm.
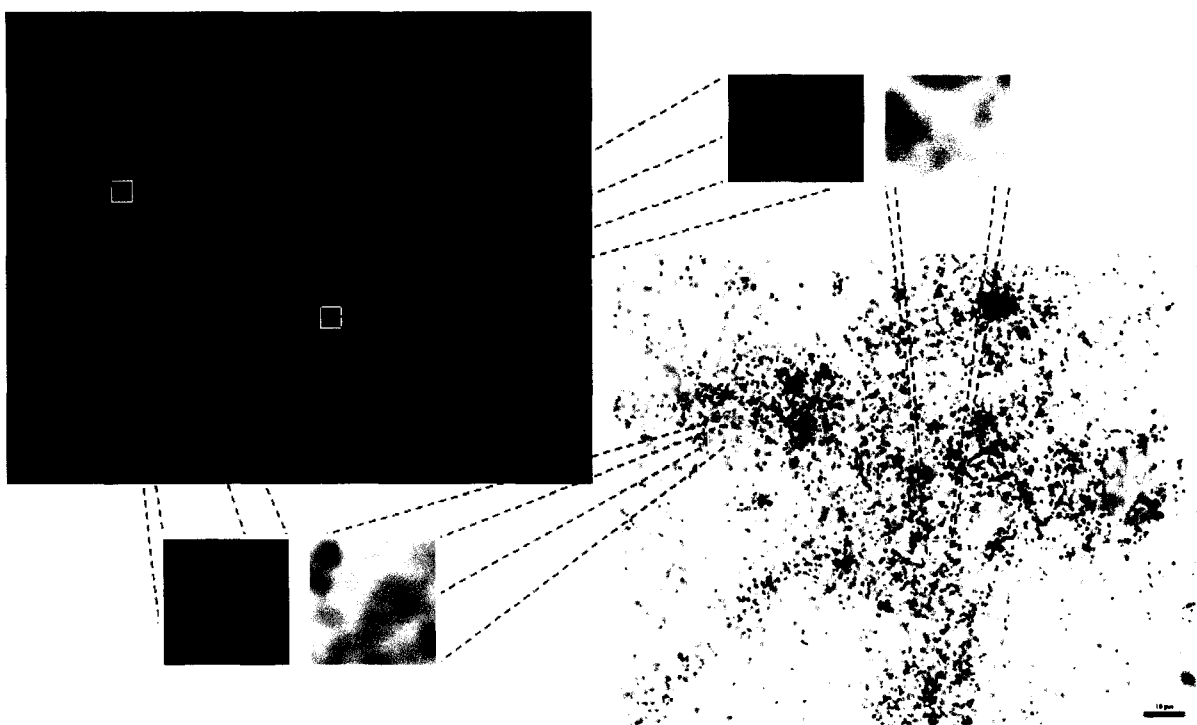
Figure 4.8   Fluorescence images and autoradiogram on following MICRO-FISH assay with GPS 22 sediments: *Bacteriodetes*. Blue cells represent DAPI-stained organisms. *Bacteriodetes* (hybridizing with the CF319a probe) are shown in red, and were not associated with silver grain formation indicating they did not grow on [9-^{14}C] phenanthrene. Bacteria belonging to the *Bacteriodes* and *Prevotella* genera (hybridizing to the BAC303 probe) were not detected. Bar in autoradiogram represents 10 μm.

5. WHOLE-CELL HYBRIDIZATIONS AND MICROAUTORADIOGRAPHY TO TRACK PHENANTHRENE UPTAKE IN COAL-TAR IMPACTED AQUIFER SEDIMENTS

Shane W. Rogers, Say Kee Ong, and Thomas B. Moorman

5.1 Abstract

In order to improve understanding of microbial biodiversity and PAH biodegradation in coal-tar impacted sediments, whole-cell hybridizations with rRNA-targeted oligonucleotide probes and microautoradiography were used to simultaneously determine the in situ identities and activities of individual microbial cells using phenanthrene as a growth substrate. We report adaptations to these molecular microbiological techniques that overcome problems caused by the presence of a solid phase, coal-tar source material, and sorption of a strongly hydrophobic radioisotopic substrate. Microbes were extracted from the contaminated sediments prior to application of whole-cell hybridization techniques due to intense background fluorescence caused by the presence of free-phase coal tars containing several aromatic hydrocarbons. Significant interference in the autoradiogram was observed when the procedure did not include several washes in 50% ethanol-PBS to remove bound [9-^{14}C]phenanthrene and/or radioisotopic metabolites from the cell surfaces prior to microautoradiography. Although phenanthrene mineralization exhibited a lag phase of 60 hours, positive autoradiographic responses could be obtained as early as 36 hours of incubation. Longer incubation resulted in significant deviation from the initial microbial community structure and activity of β-Proteobacteria not detected in shorter incubation periods (36 hours and 96 hours). Based on the lack of radioactivity associated with other bacterial taxa, the activity of β-Proteobacteria at 252 hours of incubation was attributed to growth on [9-^{14}C]phenanthrene and/or radioisotopic metabolites rather than endogenous respiration of decaying radioactive cell materials. This combination of incubation and extraction techniques with whole-cell hybridizations and microautoradiography expands the utility of similar cultivation-independent techniques, making possible the simultaneous exploration of microbial community structure and complex substrate uptake profiles in contaminated sediments.

5.2 Introduction

Advances in technologies for studying small sub-unit rRNA gene sequences have increased understanding of biodiversity in natural systems, especially for organisms that have resisted cultivation to date. Although knowledge of soil microbial diversity has expanded, little information exists linking the structure of microbial communities to specific metabolic functions of organisms within the community. In the case of hydrocarbon-contaminated site bioremediation, the structure-function relationship is of potential importance as regulatory acceptance of in situ bioremediation efforts hinge on the ability to definitively attribute decreasing hydrocarbon concentrations to microbial degradation, as opposed to abiotic processes that may lend to similar plume-scale behavior such as non-linear sorption, dispersion, and volatilization.

Combined whole-cell hybridization and microautoradiography is one technique that has been used to identify microbes active in the uptake of specific substrates in complex environmental samples. This technique was first applied by Lee et al. (1999), who visualized the uptake of several organic and inorganic substrates by specific cell types in activated sludge. This technique has also been applied to other aquatic environmental samples such as oceanic waters and sewer biofilms (Ouverney and Fuhrman, 1999; Cottrell and Kirchman, 2000; Ito et al., 2002). Although successful with simple substrates in aquatic systems, whole-cell hybridization and microautoradiography has yet to be applied to study the uptake of hydrophobic organic compounds by soil microorganisms in highly contaminated soils or sediments where the presence of the solid-phase, alternative carbon sources, and the hydrophobic nature of the substrate may greatly complicate the procedure. Successful application of this technique to contaminated soils and sediments may greatly advance understanding of biodiversity and ecosystem functioning in highly contaminated aquifer and estuarine systems, leading to more successful modeling and monitoring approaches.

The goal of this study was to develop effective procedures to combine whole-cell hybridizations and microautoradiography for phylogenetically identifying and enumerating organisms in coal-tar impacted sediments of a former manufactured gas facility active in the uptake of phenanthrene under aerobic conditions. The specific objectives of this work were to (1) identify and address potential interference on the autoradiographic response caused by sorption of strongly hydrophobic radioisotopic substrates onto cell interfaces (2) identify potential effects of incubation time on detection of "active" cells, perturbation of the microbial community structure, and potential carbon cycling that may lead to ambiguity in the resulting autoradiographic response. Phenanthrene was chosen as a model compound because of its strong hydrophobic nature and its predominance in the contaminated sediments.

5.3 Materials and Methods

5.3.1 Initial microbial community structure

The sediments used in this study were extracted from a coal-tar contaminated aquifer in northeastern Iowa in August 2001 and April 2002. The properties of the sediments used in this study are listed in Table 5.1. Prior to use, the sediments were homogenized by passing through a #4 sieve to remove the gravel fraction. 20 grams of the coal-tar impacted sediments were placed in 50 mL screw-cap sterile tubes containing 30 mL 4% paraformaldehyde/phosphate buffered saline (0.13 M NaCl, 7mM Na_2HPO_4, and 3mM NaH_2PO_4, pH 7.2), vortexed for 3 minutes, and placed in the refrigerator at 4°C for 24 hours. The paraformaldehyde-fixed samples were washed three times in phosphate buffered saline (PBS, pH 7.2), and brought to 20 mL in PBS. Extraction of microorganisms from the preserved sediments was performed using the method of Unge et al. (1999). Briefly, 0.4 g of acid-washed polyvinylpolypirollidone (PVPP) was added to the 50 mL tube containing 20 mL preserved sediment-PBS solution and vortexed for 3 minutes. Bulk sediment and bound humic material was allowed to settle for twenty minutes and the supernatant was poured into a sterile 50 mL tube. 10 mL of PBS was added to the original sediments and the tubes vortexed again for 3 minutes. After another settling period of twenty minutes, the supernatant was pooled with the original supernatant. This process was repeated one additional time, after which the pooled supernatants were vortexed for one minute and centrifuged at 100 x g for 6 minutes. Following centrifugation, the supernatants were poured into sterile 50 mL screw-cap tubes.

5.3.2 Aerobic Incubations

2 g coal-tar contaminated sediments and 2 mL sterile basal salts medium (2 mM KH_2PO_4, 2 mM K_2HPO_4, 9.9 mM NH_4Cl, 0.5 mM $MgCl_2•6H_2O$, 0.5 mM $CaCl_2•2H_2O$, and 0.1 mM $FeCl_2•4H_2O$, pH 7.1), which was sparged with air for 30 minutes, were added to 14 mL amber vials. 1.5 mL shell vials containing 1 mL of 2 N sodium hydroxide solution were carefully placed into the vials to serve as trap for $^{14}CO_2$ evolved. The vials were carefully sealed with a butyl rubber stopper using an aluminum crimp cap. 400,000 dpm of [9-^{14}C]phenanthrene (specific activity, 15 mCi/mmol; Sigma), was injected directly into three of the sediment-slurries through the butyl rubber septa, and the vials carefully swirled by hand. Three assays were amended with 10 μCi (22,200,000 dpm) [9-^{14}C]phenanthrene and no sodium hydroxide trap for MICRO-FISH. All assay bottles were incubated

at 20°C. $^{14}CO_2$ evolution was monitored in the aerobic assays by sampling the 1 N NaOH solution via syringe through the butyl rubber stoppers. The NaOH was added to 13 mL of Ultima Gold XR Liquid Scintillation Cocktail (Packard Instrument Company, Perkin Elmer, Downers Grove, IL), and the amount of $^{14}CO_2$ evolved was determined by liquid scintillation counting. The headspace on the assay vials was purged under vacuum and replaced with fresh air at each sampling interval to maintain aerobic conditions. At 36, 96, and 252 hours of incubation, respectively one MICRO-FISH assay was sacrificed by adding 10 mL 4% paraformaldehyde to the 14 mL vials. The vials were vortexed for three minutes, placed in a 4°C refrigerator for 24 hours, and the microbes extracted from the sediments as described above.

5.3.3   Oligonucleotide Probes and Stains

The DNA-intercalating dye 4',6-diamidino-2'-phenylindole (DAPI; Sigma, St. Louis, MO) was used to stain cells non-specifically. DAPI was stored dry at -20 °C, and prior to use was reconstituted at 100 ng μL-1 in sterile, nanopure water. The oligonucleotide probes used in this study are shown in Table 5.2. The oligonucleotide probes were synthesized with either Cy 3 (Cy 3; Amersham, Zurich, Switzerland), TAM, or FITC reactive dye covalently bound to the 5'-end (Invitrogen Corp., Huntsville, AL). The dye-oligonucleotide conjugates (1:1) were lyophilized and stored dry in sterile microfuge tubes at -20 °C in the dark. Prior to use, the dry probes were reconstituted in TE buffer (10 mM Tris-HCl, 1 mM EDTA, pH 8.0), covered with aluminum foil, and stored at -20 °C.

5.3.4   Total cell counts

Total direct DAPI counts were used to identify the proper dilutions for whole-cell hybridizations. 0.7 mL of cell suspension was transferred onto 0.8 mL Nycodenz (Nycomed) (density = 1.3 g/mL) in sterile 1.5 mL microcentrifuge tubes and centrifuged at 10,000 x g for 15 minutes to pellet the remaining sediments. After centrifugation, the top 0.5 mL were discarded, and the next 0.5 mL (containing the banded microbial fraction) were transferred to sterile 1.5 mL microcentrifuge tubes. The microbial fraction was supplemented with 20 μL of DAPI solution (100 ng μL^{-1}) and incubated for 7 minutes in the dark. Following incubation, the entire solution was transferred to a 15 mL vacuum filtration tower containing a pre-wetted 25 mm diameter polycarbonate filter (0.22 μm pore size) and 5 mL of sterile PBS (pH 7.2). The filter was washed three times under vacuum with 3

mL each of PBS. The filters were transferred onto slides, mounted with Citifluor mounting medium (Citifluor, Canterbury, UK), and examined under a Nikon Eclipse 400 microscope fitted with a digital imaging system, high pressure mercury lamp, and UV-2E/C filter. The cells were counted from duplicate slides at 600x magnification by randomly counting 20 fields on each slide covering an area of 0.0169 mm^2 each from a total area of 201 mm^2 per filter using Image-Pro Plus software (v. 4.5.1, Media Cybernetics, Silver Spring, MD).

5.3.5 MICRO-FISH

Density gradient centrifugation with Nycodenz was used to separate soil microorganisms from the remaining sediments prior to MICRO-FISH as described above. The banded microbial fractions were washed repeatedly in 50% ethanol-PBS until subsequent washes resulted in no additional removal of ^{14}C based on liquid scintillation counting. To visualize potential interference in the autoradiographic response caused by sorption of radioisotopic phenanthrene to cell surfaces, one set of MICRO-FISH was performed on cells not washed in ethanol from the 252 hour sample (hybridized with the EUB probe set). The washed pellets or unwashed banded bacterial fraction, respectively, were transferred to a 15 mL vacuum filtration tower containing a pre-wetted 25 mm diameter polycarbonate filter (0.22 μm pore size) and 5 mL PBS (pH 7.4). The filter was washed three times under vacuum with 3 mL each of PBS, transferred cell-side down onto a 22 mm square cover glass (No. 2) treated with a 4% solution of 3-aminopropyltriethoxysilane (Sigma, St. Louis, MO), clamped between two glass slides using binder clips, and placed in a 42°C oven for 1 hour, after which the filter was peeled away leaving the cells adhered to the cover glass. The cells were dehydrated using 50%, 80%, and 96% ethanol, respectively, three minutes each, and the cover glasses placed cell-size up on microscope slides. The cells were then brought into contact with a 30 μL drop of hybridization buffer (0.9 M NaCl, 20 mM Tris-HCl (pH 7.2), 2.5 mM EDTA, and 0.01% sodium dodecyl sulfate (SDS) in the presence of 20-35% formamide (ARCH915, BAC303, HGC69a, and SRB385 = 20%; EUB338 (I-III), BET42a, and GAM42a = 30%; ALF968, CF319a, LGC354(a,b,c)=35%;NON338=20-35%)) containing 4 ng·μL^{-1} of the relevant probe(s) and 4 ng·μL^{-1} DAPI and covered with a Hybri-Slip (Sigma, St. Louis, MO). The slides were placed into 50 mL plastic tubes with ChemWipes® wetted with 2 mL of hybridization solution (humidity chambers) and hybridized at 46°C for 90 minutes. Following hybridization, the cover glasses were washed for 15 minutes at 48°C in the appropriate wash buffer (20 mM Tris-HCl (pH 7.2), 2.5 mM EDTA, 0.01%

SDS, and either 308, 102, or 80 mM NaCl depending on the formamide concentration during hybridization (20%, 30%, or 35%, respectively)), then carefully dried under a stream of filtered air.

All autoradiographic procedures were performed in the dark using a method similar to Cottrell and Kirchman (2000). Briefly, the cover glasses were dipped in molten (43°C) Kodak NBT-2 autoradiographic emulsion diluted 2 parts emulsion and 1 part deionized water. After incubation at 4°C for 10 days, the slides were warmed to room temperature and developed using Kodak Dektol developer, a deionized water stop bath, and Kodak fixer, as per manufacturer's instructions. The cover glasses were air dried, mounted on clean glass slides using Citifluor AF1 mounting medium (Citifluor Ltd., Canterbury, UK), and examined under a Nikon Eclipse 400 microscope using a G-2E/C filter for Cy3 and TAM-labeled cells, B-2E/C filter for FITC- and FAM-labeled cells, and UV-2E/C filter to determine the total direct DAPI count. Silver grain formation associated with hybridized cells was determined by switching between fluorescence and bright-field modes. Digital imaging analysis was performed using Image-Pro Plus (v. 4.5.1, Media Cybernetics, Inc., Silver Spring, MD).

5.4 Results

5.4.1 Mineralization of [9-^{14}C]phenanthrene

Figure 5.1 shows $^{14}CO_2$ evolution during the aerobic incubations of the coal-tar impacted sediments. A 3 day lag phase was followed by conversion of 25.1 ± 0.9% of the added ^{14}C to $^{14}CO_2$ at 360 hours incubation. MICRO-FISH samples were sacrificed at 36 hours (lag-phase, 0.3% $^{14}CO_2$ evolution), 96 hours (early log phase, 5.3% $^{14}CO_2$ evolution), and 252 hours (late log-phase, 22.3% $^{14}CO_2$ evolution) of incubation.

5.4.2 MICRO-FISH: Sorption

An average of 2.51% of the added ^{14}C was removed from the cells during the first three washes in 50% ethanol prior to MICRO-FISH. Based on total direct DAPI counts and assuming homogenous distribution of the radioactivity to the cells, this resulted in a cellular radioactivity of approximately 0.016 dpm·cell^{-1} attributable to sorption of [9-^{14}C]phenanthrene and hydrophobic metabolites alone. Washed cells retained 0.33% of the initial ^{14}C added to the system, but microautoradiography-positive cells represented a much lower percent of the overall microbial

community structure based on MICRO-FISH results (see below). Microautoradiography-positive cells in the washed assays averaged 0.031 dpm·cell⁻¹.

Figure 5.2 shows the fluorescence image and autoradiogram superimposed and colored by image analysis for unwashed cells hybridized with the EUB338 probe set. As can be seen in Figure 5.2, there was significant interference in the autoradiographic response when the cells were not washed prior to MICRO-FISH. $51 \pm 1.5\%$ of un-washed DAPI-stained organisms were associated with silver grain cluster formation versus $11 \pm 3.2\%$ following a 50% ethanol-PBS wash series. Increased silver grain formation in the un-washed MICRO-FISH assay decreased the sensitivity of the technique as it became difficult to discriminate and attribute silver grain formation to specific cells when several cells were spatially located nearby silver grain clusters (increasing the number of false positives).

5.4.3   MICRO-FISH: Incubation time

When samples were washed prior to processing for MICRO-FISH, microautoradiography resulted in autoradiograms in which silver grain formation coincided well with the spatial location of cells detected by whole cell hybridizations as shown in their respective fluorescence images (see Figure 5.3). The strong association of fluorescently labeled cells and silver grain formation allowed for counts of "active cells", defined as those for which the probe-detected cell associates with silver grain cluster formation in the autoradiogram. Table 5.3 summarizes the MICRO-FISH results.

As can be seen in Figure 5.3 and Table 5.3, the fraction of active cells increased with incubation time. At 36 hours of incubation only 0.51% of DAPI-detected organisms were associated with silver grain formation, as compared to 2.25% and 11.4% at 96 hours and 252 hours, respectively. Identification of active cells decreased, however with increasing incubation times, potentially due to hybridization errors, growth of microbes not complementary to the probe set used, and/or loss of fluorescence signals where silver grain clusters became thick. At early incubation times (36 hours and 96 hours), Actinobacteria and γ-Proteobacteria correlated to silver grain cluster formation indicating that these organisms were active in phenanthrene uptake. At 252 hours incubation, the β-Proteobacteria were associated with nearly 10% of the positive autoradiograms. β-Proteobacteria, γ-Proteobacteria, and Actinobacteria all increased in population with incubation time, but remained stationary as a percent of the total microbial community structures. α-Proteobacteria, sulfate-reducing bacteria, Firmicutes, and Bacteriodetes all increased slightly in population with increasing incubation time, but decreased as a percent of the total microbial community structures. Bacteriodes

and *Prevotella* genera (BAC303) were relatively insignificant in all the microbial community structures.

5.5 Discussion

The results presented in Figure 5.3 and Table 5.3 show that MICRO-FISH can effectively identify the uptake of specific hydrophobic organic pollutants by microorganisms in highly contaminated soils or sediments. Interferences caused by the presence of the sediments and the sorption of the hydrophobic substrate to microbial cell walls are effectively accounted for in the procedure. In preliminary studies where separation of the microbes from the contaminated sediments was not performed, significant background fluorescence associated with aromatic hydrocarbon contamination and soil particles was observed, and made detection of probed cells difficult if at all possible (data not shown).

Although the sorption of ^{14}C to cell surfaces was only 2.1% of the total [9-^{14}C]phenanthrene added to the MICRO-FISH assays, sorption of radioisotopic phenanthrene and/or related metabolites to cell surfaces caused significant interference in the autoradiographic response. Stringfellow and Alvarez-Cohen (1999) measured phenanthrene biosorption on several species of bacteria and determined that biomass-water partitioning coefficients (K_p) ranged from 2.5 to 36 L·g biomass^{-1}, and were highest in Nocardioforms. Based on the organic carbon content of the sediments used in this study and an organic carbon-water partitioning coefficient for phenanthrene (log K_{oc}) of 4.15, the sediment-water partitioning coefficient would be approximately 20 to 370 L·g sediment^{-1}. These numbers are supported by the work of Shimizu et al. (2002), who measured sorption of phenanthrene to natural organic matter and synthesized liposome. These researchers determined that the equilibrium liposome-water partitioning coefficient was approximately 43% the equilibrium natural organic carbon-water partitioning coefficient. Based on the works above, significant sorption of [9-^{14}C]phenanthrene and related metabolites to microbial cell walls in this study was expected.

The effects of sorption of radioisotopes may also be exacerbated by incubation time and microbial growth. Nejidat et al. (2004) showed that cell hydrophobicity was strongest when cells were in stationary phase as compared to cells in early log-phase growth. Based on total DAPI-direct microbial counts, microbial growth may have reached stationary-phase by 252 hours of incubation, increasing the autoradiographic error (Total Direct DAPI counts were 1.29 x 10^7 at 252 hours and 2.00 x 10^7 at 576 hours (see Table 4.5, post-incubation)). Dehydrating the cells in an ethanol series

after transferring them to cover glasses may have removed some cell-bound ^{14}C, limiting false positives in the autoradiographic response.

One interesting aspect of the MICRO-FISH with un-washed cells was that only 51% of the cells correlated to silver-grain cluster formation. If homogenous sorption were to occur, it would be expected that all cells would yield positive autoradiograms. These results suggest potential heterogeneity in cell-surface hydrophobicity may have led to differences in cell radioactivity associated with sorption of [9-^{14}C]phenanthrene and related metabolites. In a recent study focusing on the isolation of PAH-degrading bacteria from contaminated soils and sediments, Bastiens et al. (2000) noted that PAH-degrading bacteria in contaminated soils exhibited significant differences in cell wall hydrophobicity which led to differences in PAH-degrading microbes isolated in liquid media versus cultivation on PAH-sorbing carriers. Their results would suggest that differences in phenanthrene sorption, and thus the autoradiographic response, should be expected.

In these sediments, significant ^{14}CO$_2$ evolution commenced following a 60 hour lag phase over which less than 1.5% of the [9-^{14}C]phenanthrene was respired. However, significant microbial growth over the first 36 hours of incubation was observed and was potentially at the expense of other carbon sources available in the coal-tar contaminant mixture. Although mineralization of phenanthrene was low over the first 36 hours, cells active in the uptake of [9-^{14}C]phenanthrene could be visualized with MICRO-FISH. However, the low number of detections associated with short incubation times becomes problematic when enumeration of active cells is desired. Where active cells represent less than one percent of the microbial community structure and microscopic field contain on average 100 microbes per field, several microscopic fields and/or slides are required to obtain a reasonable degree of statistical significance.

The choice of incubation time presents a trade-off between detection and relevance to in-situ conditions. Extending incubation times may allow for less difficulty in enumerating active cells. However, increased incubation times resulted in divergence of the microbial community structure from the in situ condition. Active cells increased significantly when incubations were extended into log-phase as indicated by ^{14}CO$_2$ evolution. At early log-phase (96 hours) the total microbial populations increased an order of magnitude, but the active cells detected in the MICRO-FISH procedure phylogenetically matched that identified in the lag phase at 36 hours incubation. By late log phase (252 hours) the total microbial populations increased nearly two orders of magnitude and the previously inactive β-Proteobacteria assimilated ^{14}C, potentially from degradation of [9-^{14}C]phenanthrene, a radioisotopic metabolite, or by endogenous decay of radioactive cell materials. None of the other microbial phylotypes produced silver grain clusters at 252 hours suggesting that the

onset of *β-Proteobacteria* activity was due to activation on phenanthrene and/or radioisotopic metabolites. This suggests increased $^{14}CO_2$ evolution in the early log-phase may have been due to growth of previously active bacteria whereas $^{14}CO_2$ evolution in late log-phase may be have been associated with both growth of [9-^{14}C]phenanthrene-degrading bacteria as well as activation of previously inactive bacteria on [9-^{14}C]phenanthrene and/or its radioisotopic metabolites.

5.6 Conclusions

In this study, whole-cell hybridizations and microautoradiography were effectively interfaced to identify phenanthrene-degrading organisms in complex coal-tar polluted sediments. MICRO-FISH was shown to be a sensitive molecular marker for identifying and quantifying the activity of phenanthrene-degrading organisms in a complex coal-tar contaminated sediments relative to the overall microbial community structure. The incubation time used for MICRO-FISH must be carefully balanced between obtaining a positive autoradiographic response and limiting divergence from the initial microbial community structure. The balance will depend largely on the objectives of the study at hand. The results of this study suggest that limited incubation times, even where a lag phase is exhibited in the laboratory-scale incubations, may be more appropriate for obtaining useful results for inference of the activity of specific microbial phylotypes in-situ. Longer incubation times may provide useful information regarding the presence and identification of potential pollutant degraders without cultivation, but may not accurately reflect the in-situ condition.

5.7 References

Amann R. I., B. J. Binder, R. J. Olson, S. W. Chisholm, R. Devereux, and D. A. Stahl (1990) Combination of 16S rRNA-targeted oligonucleotide probes with flow cytometry for analyzing mixed microbial populations, *Appl. Environ. Microbiol.*, 56(6), 1919-1925.

Bastiens, L., D. Springael, P. Wattiau, H. Harms, R. DeWatcher, H. Verachtert, and L. Diels (2000) Isolation of adherent polycyclic aromatic hydrocarbon (PAH)-degrading bacteria using PAH-sorbing carriers, *Appl. Environ. Microbiol.*, 66(5), 1834-1843.

Biyani, R. (2002) Modeling groundwater flow and transport of contaminants at the Cherokee Former Manufactured Gas Plant site, Iowa, M.S. Thesis, Iowa State University, Ames, IA.

Cottrell, M. T., and D. L. Kirchman (2000) Natural assemblages of marine proteobacteria and members of the *Cytophaga-Flavobacter* cluster consuming low- and high-molecular-weight dissolved organic matter, *Appl. Environ. Microbiol.*, **66**(4), 1692-1697.

Daims, H., A. Brühl, R. Amann, K. H. Schleifer, and M. Wagner (1999) The domain-specific probe EUB338 is insufficient for the detection of all bacteria: development and evaluation of a more comprehensive probe set, *Syst. Appl. Microbiol.*, **22**(3), 434-444.

Ito, T., J. L. Nielsen, S. Okabe, Y. Watanabe, and P. H. Nielsen (2002) Phylogenetic identification and substrate uptake patterns of sulfate-reducing bacteria inhabiting an oxic-anoxic sewer biofilm determined by combining microautoradiography and fluorescent in situ hybridization, *Appl. Environ. Microbiol.*, **68**(1), 356-364.

Lee, N., P. H. Nielsen, K. H. Andreasen, S. Juretschko, J. L. Nielsen, K. H. Schleifer, and M. Wagner (1999) Combination of fluorescent in situ hybridization and microautoradiography – a new tool for structure-function analyses in microbial ecology, *Appl. Environ. Microbiol.*, **65**(3), 1289-1297.

Manz W., R. Amann, W. Ludwig, M. Wagner, and K. H. Schleifer (1992) Phylogenetic oligodeoxynucleotide probes for the major subclasses of *Proteobacteria*: problems and solutions, *Syst. Appl. Microbiol.*, **15**(4), 593-600.

Manz W., R. Amann, W. Ludwig, M. Vancanneyt, and K. H. Schleifer (1996) Application of a suite of 16S rRNA-specific oligonucleotide probes designed to investigate bacteria of the phylum *cytophaga-flavobacter-bacteroides* in the natural environment, *Microbiol.*, **142**(5), 1097-1106.

Meier, H., R. Amann, W. Ludwig, and K. H. Schleifer (1999) Specific oligonucleotide probes for in situ detection of a major group of gram-positive bacteria with low DNA G+C content, *Syst. Appl. Microbiol.*, **22**(2), 186-196.

Neef, A. (1997) Anwendung der in situ einzelzell-identifizierung von bakterien zur populations analyse in komplexen mikrobiellen biozönosen, Doctoral thesis, Technische Universität München, Munich, Germany.

Nejidat, A., I. Saadi, and Z. Ronen (2004) Degradation of 2,4,6-tribromophenol by bacterial cells attached to chalk collected from a contaminated aquifer, *J. Appl. Microbiol.*, **96**(4), 844-852.

Ouverney, C. C., and J. A. Furhman (1999) Combined microautoradiography - 16S rRNA probe technique for determination of radioisotope uptake by specific microbial cell types in situ, *Appl. Environ. Microbiol.*, **65**(4), 1746-1752.

Roller, C., M. Wagner, R. Amann, W. Ludwig, and K. H. Schleifer (1994) In situ probing of Gram-positive bacteria with high DNA G+C content using 23S rRNA- targeted oligonucleotides, *Microbiol.*, **140**(10), 2849-2858. (Erratum in: *Microbiol.* (1995) **141**(5), 1267.)

Shimizu, Y., J. Takahashi, J. Matsubara, K. Ikeda, and S. Matsui (2002) Sorption of polycyclic aromatic hydrocarbons into liposomes (artificial cell membranes) and the effects of dissolved natural organic matter, *Lakes & Reservoirs: Research and Management*, **7**(4), 295–299.

Stahl, D. A., and R. Amann. (1991) Development and application of nucleic acid probes, in *Nucleic acid techniques in bacterial systematics*, E. Stackebrandt and M. Goodfellow (ed.), John Wiley & Sons Ltd., Chichester, England, 205-248.

Stringfellow, W. T., and L. Alvarez-Cohen (1999) Evaluating the relationship between the sorption of PAHs to bacterial biomass and biodegradation, *Water Res.*, **33**(11), 2535-2544.

Unge, A., R. Tombolini, L. Mølbak, and J. K. Jansson (1999) Simultaneous monitoring of cell number and metabolic activity of specific bacterial populations with a dual gfp-luxAB marker system, *Appl. Envir. Microbiol.*, **65**(2), 813-821.

Wallner, G., R. Amann, and W. Beisker (1993) Optimizing fluorescent in situ hybridization with rRNA-targeted oligonucleotide probes for flow cytometric identification of microorganisms, *Cytometry*, **14**(2), 136-143.

Table 5.1   **Properties of the coal-tar impacted aquifer sediments used in the study**

Property[a]	Value	Units
<u>**Grain Size Distribution:**</u>		
% Gravel	12.08	
% Sand	52.92	
% Silt	19.5	
% Clay	15.5	
Dry Bulk Density	1.69	$g \cdot cm^{-3}$
Organic Carbon Content (f_{oc})	0.0015 – 0.026	
Sample Depth	3.0 – 8.0	m bgs[b]
Phenanthrene	310	$mg \cdot kg^{-1}$ sediments
U.S. EPA Priority PAH	1530	$mg \cdot kg^{-1}$ sediments

a. Partially adapted from Biyani, 2002
b. m bgs = meters below ground surface

Table 5.2   **Target organisms and oligonucleotide probes**

Target Organisms	Probe	Oligonucleotide Sequence (5' – 3')	Fluor [b.]	Ref.
Archaea	ARCH915	GTG-CTC-CCC-CGC-CAA-TTC-CT	FITC	c
Bacteria	EUB338	GCT-GCC-TCC-CGT-AGG-AGT	TAM	d
	EUB338-II	GCA-GCC-ACC-CGT-AGG-TGT		e
	EUB338-III	GCT-GCC-ACC-CGT-AGG-TGT		e
α-Proteobacteria	ALF968	GGT-AAG-GTT-CTG-CGC-GTT	FITC	f
β-Proteobacteria	BET42a	GCC-TTC-CCA-CTT-CGT-TT	FITC	g
γ-Proteobacteria	GAM42a	GCC-TTC-CCA-CAT-GCT-TT	Cy3	g
Sulfate-Reducing Bacteria	SRB385	CGG-CGT-CGC-TGC-GTC-AGG	FAM	d
Actinobacteria	HGC69a	TAT-AGT-TAC-CAC-CGC-CGT	Cy3	h
Firmicutes	LGC354a	TGG-AAG-ATT-CCC-TAC-TGC	FITC	i
	LGC354b	CGG-AAG-ATT-CCC-TAC-TGC	FITC	i
	LGC354c	CCG-AAG-ATT-CCC-TAC-TGC	FITC	i
Bacteriodetes	CF319a	TGG-TCC-GTG-TCT-CAG-TAC	Cy3	j
Bacteriodes and *Prevotella* genera	BAC303	CCA-ATG-TGG-GGG-ACC-TT	FITC	j
Nonsense control	NONEUB	CGA-CGG-AGG-GCA-TCC-TCA	FITC	k

a. 16S or 23S rRNA position according to *Escherichia coli* numbering
b. Fluor = fluorochrome. Fluorescent markers were linked to the 5' end.
c. Stahl and Amann, 1991; d. Amann et al., 1990; e. Daims et al., 1999; f. Neef, 1997; g. Manz et al., 1992; h. Roller et al., 1994; i. Meier et al., 1999; j. Manz et al., 1996; k. Wallner et al., 1993

Table 5.3   **Microbial community structure of sediments *in-situ* and following MICRO-FISH with [9-^{14}C]phenanthrene.**

Taxa	Cells · g sediment $^{-1}$			
	Active Cells (relative to DAPI-stained cells)			
	Initial	**36 hours**	**96 hours**	**252 hours**
Total Direct DAPI	**44.1 ± 5.9**	**189 ± 22.7** *0.51 ± 0.34%*	**362 ± 33.8** *2.25 ± 0.73%*	**1290 ± 123** *6.2 ± 1.10%*
Bacteria	**36.1 ± 4.2**	**136 ± 25.6** *0.80 ± 0.90%*	**234 ± 29.9** *2.99 ± 2.44%*	**1260± 28.5** *11.4 ± 3.15%*
Archaea	**0.9 ± 0.7**	**0.6 ± 1.3** *ND*[b.]	**ND** *ND*	**ND** *ND*
"Proteobacteria"				
α - Proteobacteria	**0.6 ± 0.9**	**2.4 ± 4.6** *ND*	**2.6 ± 2.8** *ND*	**3.2± 4.4** *ND*
β - Proteobacteria	**3.5 ± 1.6**	**ND** *ND*	**39.1 ± 21.5** *ND*	**105 ± 59.1** *1.11 ± 0.03%*
γ - Proteobacteria	**12.0 ± 3.1**	**73.4 ± 16.4** *0.44 ± 0.58%*	**77.6 ± 24.5** *0.56 ± 060%*	**365 ± 87.8** *2.30 ± 1.11%*
Sulfate-Reducing Bacteria	**1.7 ± 1.3**	**2.4± 2.4** *ND*	**2.6 ± 2.8** *ND*	**3.2 ± 4.4** *ND*
Gram Positive Bacteria				
Actinobacteria	**12.5 ± 1.6**	**58.5 ± 18.2** *0.20 ± 0.40%*	**88.7 ± 30.0** *0.31 ± 0.41%*	**313 ± 101** *1.26 ± 0.95%*
Firmicutes	**2.7 ± 0.8**	**11.5 ± 4.8** *ND*	**1.7 ± 3.3** *ND*	**13.5 ± 13.8** *ND*
CFB Cluster				
Bacteriodetes	**1.7 ± 0.6**	**1.4 ± 1.9** *ND*	**3.0 ± 4.4** *ND*	**5.7± 7.7** *ND*
Bacteriodes and *Prevotella* *genera*	**0.7 ± 0.5**	**ND** *ND*	**0.7 ± 1.5** *ND*	**ND** *ND*

a. Reported as the **mean X 10^5** (±95% confidence interval),
b. ND = not detected
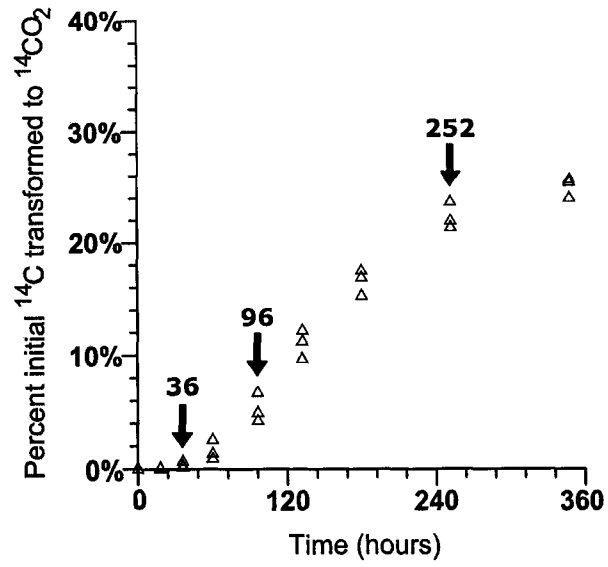
Figure 5.1   Evolution of $^{14}CO_2$ from mineralization of [9-^{14}C]phenanthrene in parallel aerobic incubations with site sediments.

168
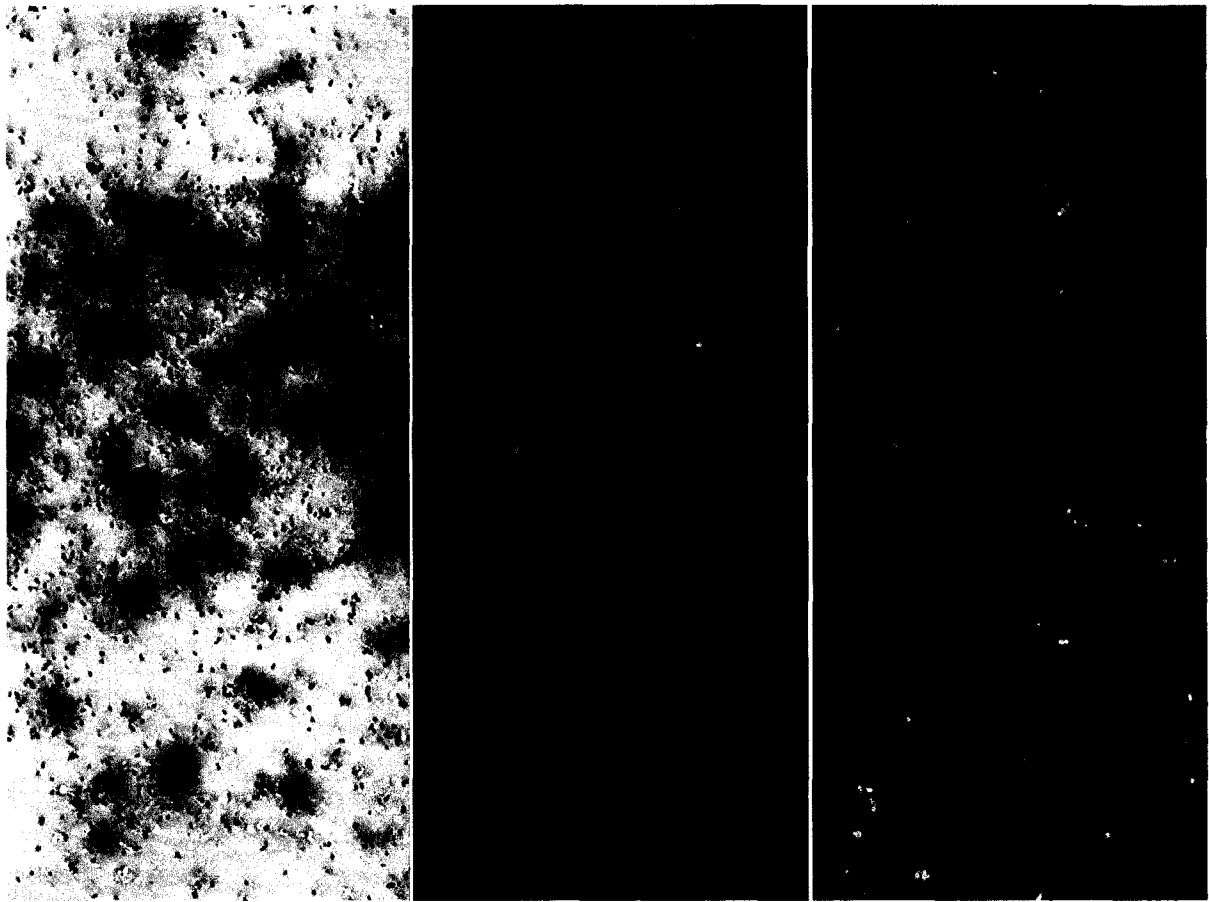
Figure 5.2   Fluorescence image and autoradiogram showing significant interference in the autoradiographic response due to sorption of [9-^{14}C]phenanthrene onto soil microorganisms: Blue cells represent DAPI-stained organisms. Cells hybridizing with the EUB338 probe set are colored red by image analysis. Silver grain formation indicates growth on [9-^{14}C] phenanthrene. Bar = 10 µm.
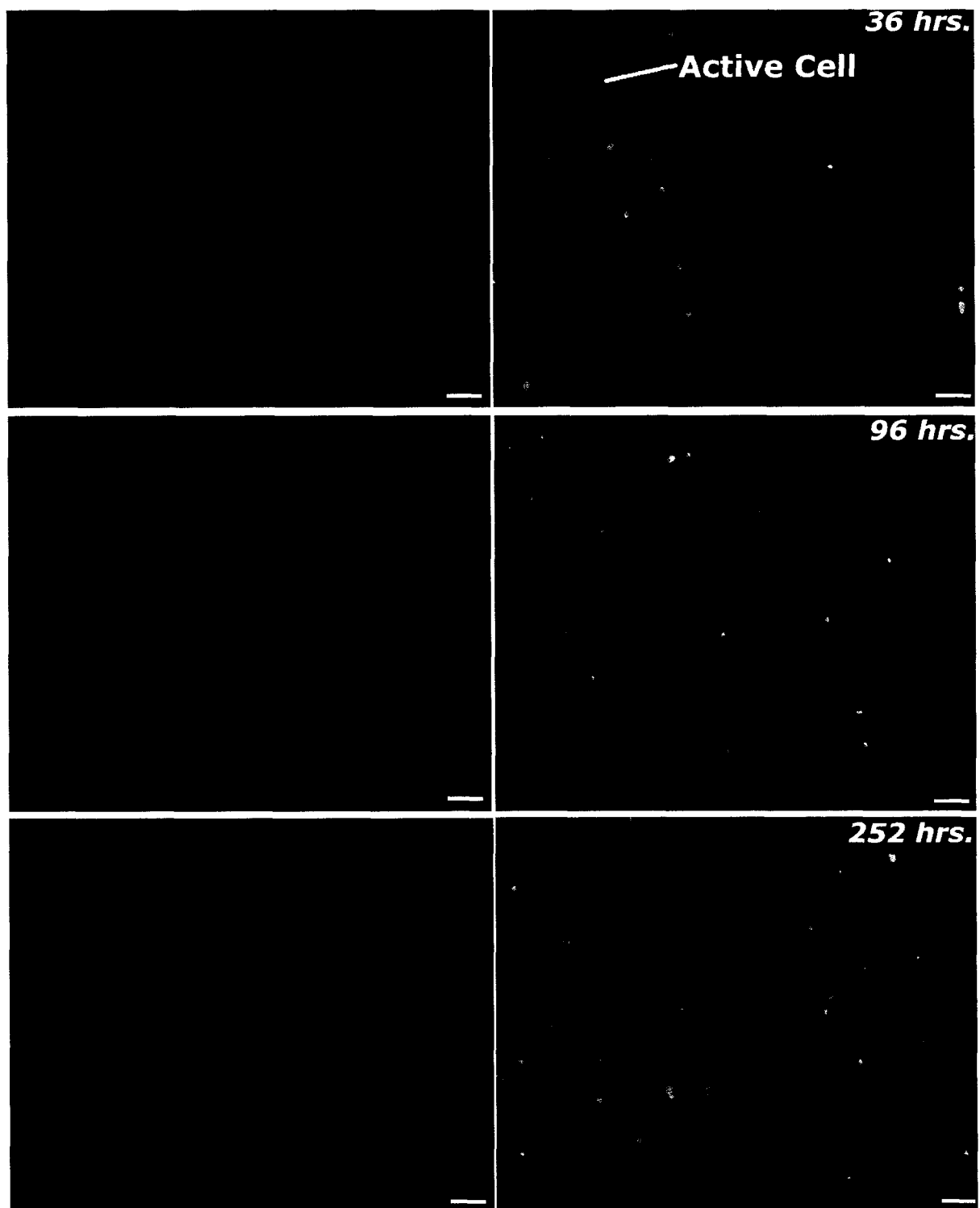
Figure 5.3   Fluorescence images and autoradiograms following MICRO-FISH assay with
coal-tar impacted aquifer sediments: *Bacteria*. Blue cells represent DAPI-
stained organisms. Cells hybridizing with the EUB338 probe set are colored red
by image analysis. Silver grain formation indicates growth on [9-^{14}C]
phenanthrene. Bar = 5 μm.

6. Application of Whole-cell Hybridizations and Microautoradiography to support 1ST-Order Biodegradation Rate Coefficients for Naphthalene and Phenanthrene Estimated with Analytical Plume-Scale Modeling

Shane W. Rogers, Say Kee Ong, and Thomas B. Moorman

6.1 Abstract

Whole-cell hybridizations with oligonucleotide probes specific to *Archaea* and several phyla of *Eubacteria* were used in conjunction with microautoradiography following brief incubations with radioisotopic naphthalene and phenanthrene to identify the spatial heterogeneity of specific microbial phylotypes degrading naphthalene and phenanthrene in coal-tar impacted aquifer sediments at a former manufactured gas plant site in northwestern Iowa. Microscopy revealed visible silver-grain density images in the autoradiograms that correlated well to the spatial locations of specific cell types identified by the whole-cell hybridization technique. Dominant phylotypes in the microbial community structures of sediments following aerobic incubation included *Actinobacteria*, *γ-Proteobacteria*, and *β-Proteobacteria*, and to a lesser extent *Bacteriodetes*, and *Firmicutes*. Detection of *α-Proteobacteria*, sulfate-reducing bacteria, and the *Bacteriodes* and *Prevotella* genera were variable following incubations. Microautoradiography indicated that the *β-Proteobacteria*, *γ-Proteobacteria*, and *Actinobacteria* were active in uptake of phenanthrene and naphthalene in these sediments, and that active cells comprised less than 5% of the total microbial community. However, the presence of the *β-Proteobacteria* in the in situ microbial community was overshadowed by that of the *Actinobacteria* and *γ-Proteobacteria*. Cell-specific biotransformation rates of naphthalene and phenanthrene were estimated based on specific contaminant uptake profiles of degrading cells as determined by whole-cell hybridizations and microautoradiography. The cell-specific biotransformation rates of naphthalene were determined to range from 4.7 to 97 pg·active cell^{-1}·d^{-1}, and compared favorably to rates estimated with first-order biodegradation rate coefficients from analytical plume-scale modeling (0.7 to 19 pg·active cell^{-1}·d^{-1}). Biotransformation rates for phenanthrene based on whole-cell hybridizations and microautoradiography in all sediment cores were between one and two orders of magnitude greater than model predicted values suggesting that

analytical modeling may have underestimated the intrinsic transformation rate of this PAH. Based on these results, the MICRO-FISH technique was shown to provide a strong tertiary line of evidence that can be quantitatively linked to the in-situ condition. However, specific issues such as appropriate incubation times, differences in bioavailability between intrinsic pollutants and inoculated hydrocarbons, and limited detections of substrate-active cells must be considered in data interpretation.

6.2 Introduction

Investigating natural attenuation of PAH compounds at former manufactured gas plant (FMGP) sites presents unique challenges due to the physiochemical properties of the primary coal-tar constituents including polycyclic aromatic hydrocarbons (PAHs). Many PAH compounds are sparingly soluble, typically exhibiting sorption nonlinearities and complex biodegradation patterns limited by the bioavailability of sorbed contaminant mass and complicated by the inhibitory and/or cometabolic effects of co-contaminating compounds in contaminated soils and sediments.

As most kinetic models of hydrocarbon biodegradation require physiological characteristics and population densities of the microorganisms carrying out the biodegradation process, modeling biodegradation of hydrocarbon compounds at contaminated sites may be limited by the ability to identify the populations actively involved in the degradation process and to determine their population amongst the overall ecology (Hanson et al., 1999). The use of pure cultures or enrichment techniques may not be directly appropriate to modeling contaminant depletion on the field-scale as they may poorly reflect the site biodiversity or underestimate ecosystem functioning. Perturbation in specific microbial phylotypes due to the presence of complex anthropogenic contaminant mixtures relative to the uncontaminated background ecology do not allow direct identification of substrate-specific activity or enumeration of the hydrocarbon degrading population as a subset of the overall microbial community structure (Dojka et al., 1998; Langworthy et al., 1998; McNaughton et al., 1999; Shi et al., 1999; Smit et al., 1997). Because of these difficulties, many researchers revert to plume-scale modeling approaches that rely on differences in aqueous concentrations measured at several monitoring locations, and which are subject to potential error associated with parameter fitting exercises. The accuracy of biodegradation rate coefficients for PAH compounds estimated in these types of plume-scale modeling approaches are difficult to reconcile with direct measures of biodegradation such as laboratory-scale bioassays, which typically result in exaggerated biodegradation rates compared to modeling estimates.

Molecular microbiological approaches are fast becoming popular tools for providing more detailed data sets valuable for investigations of natural attenuation at contaminated sites. One molecular tool, microautoradiography and epifluorescence microscopy (MAR-EM), was first used by Fliermans and Schmidt (1975), who stained autoradiographs with fluorescent antibodies to study the single-cell activity of *Nitrobacter*. Meyer-Reil (1978) further expanded the technique by combining acridine orange direct counts with MAR to link the number of actively metabolizing cells to the rate of uptake of glucose. Modifications of this technique have been used by several other researchers including Fuhrman and Azam (1982), who studied thymidine uptake and bacterioplankton growth in marine surface waters, and by Tabor and Neihof (1982, 1984), who studied structure-function relationships in waters from Chesapeake Bay (for a review of MAR-EM, see Nielsen et al., 1999).

The introduction of the fluorescent in situ hybridization (FISH) technique (DeLong et al., 1989) has greatly expanded the utility of MAR-EM. By combining microautoradiography with FISH, identification of substrate-active organisms can be done phylogenetically as opposed to morphologically, greatly increasing the accuracy of identification. In recent years, several researchers have employed combined FISH and microautoradiography to explore specific substrate uptake patterns in aqueous environmental samples (Lee et al.,1999; Ouverney and Fuhrman, 1999; Cottrell and Kirchman, 2000; Ito et al., 2002). In Chapter 5 of this work, it was shown that whole-cell hybridizations and microautoradiography (MICRO-FISH) could be effectively interfaced to identify phenanthrene-degrading organisms in complex coal-tar polluted sediments where the presence of the solid-phase and the hydrophobic nature of the substrate may greatly complicate the procedure. The unique data sets provided by this technique may yield a link between tertiary lines of evidence of natural attenuation such as laboratory-scale incubations and secondary lines of evidence such as plume-scale modeling and monitoring data.

In Chapter 3, plume-scale hydrogeological, contaminant, and geochemical data resulting from site characterization and monitoring activities were used to estimate first-order biodegradation rate coefficients for several PAH and BTEX compounds. In-situ biodegradation activity estimated in Chapter 3 was supported by an enrichment of PAH-degrading phylotypes associated with contaminated site sediments relative to nearby pristine conditions as well as biodegradation of select PAH compounds in laboratory-scale incubations with site sediments in Chapter 4. This work seeks to strengthen the case for natural attenuation of PAH compounds at the Cherokee FMGP site by interfacing the two data sets through expanded characterization of the microbial cell types active in the uptake of phenanthrene and naphthalene in situ. The objectives of this study are to (1) identify the spatial heterogeneity in microbial cell types growing on naphthalene and phenanthrene in the coal-tar

impacted aquifer underlying the Cherokee FMGP site, and (2) compare and contrast estimates of the in-situ biodegradation rates of naphthalene and phenanthrene based on molecular microbiological measurements to those of plume-scale analytical modeling approaches to evaluate the potential for molecular microbiological tools to support natural attenuation investigations as a third line of evidence. Interfacing molecular microbiological characterizations and cell-specific contaminant uptake profiles with plume-scale modeling and monitoring data is a new and untried technique for supporting plume-scale modeling approaches in support of natural attenuation investigations. The strengths and weaknesses of using these specific molecular modeling approaches are discussed.

6.3 Cell-specific mass transformation rates

Using molecular microbiological data collected in MICRO-FISH assays, cell-specific mass-transformation rates can be estimated. These rates can be compared to estimates from plume-scale model approaches considering measurements of the intrinsic microbial community structure presented in Chapter 4. In this manner, it is possible that tertiary lines of evidence, which are traditionally indirect measures of in-situ biodegradation potential, can be applied directly to support modeling and monitoring efforts.

Assuming no dead-end metabolite formation, the total PAH mass transformation in a short-term aerobic MICRO-FISH incubation is equal to the total PAH converted to CO_2 plus the total PAH converted to biomass. Considering that $^{14}CO_2$ evolution during the short incubation periods of the MICRO-FISH assays (24 to 42 hours) were approximately linear with time and assuming that microbial growth was similarly linear, the cell-specific radioactive mass transformation rate of PAH, $\frac{dm_{14C-PAH}}{dt}$, can be calculated from measurements of $^{14}CO_2$ production, radioactivity in the biomass, and microscopic counts of PAH-degrading bacteria based on MICRO-FISH, such that:

$$\frac{dm_{14C-PAH}}{dt} = -\frac{m_{14CO2} + m_{14C,B}}{t \cdot X_{active} \cdot M_S} \cdot \alpha_{14C-PAH} \qquad [1]$$

where m_{14CO2} and $m_{14C,B}$ are the total $^{14}CO_2$ evolved and total radioactivity of the biomass, respectively, following MICRO-FISH incubations (μCi), t is the incubation time (d), X_{active} represents active cells determined by microscopic counting of cells associated with silver grain cluster formation in corresponding autoradiograms (active cells · g sediment^{-1}), M_S is the mass of sediment in the assay

(g), and $\alpha_{14C\text{-}PAH}$ is the specific activity of the radioisotopic PAH (pg PAH $\cdot$ μCi^{-1}). This method assumes that only cells that yield positive autoradiograms in microautoradiography are active in biodegrading the hydrocarbon of interest.

MICRO-FISH incubations were performed with coal-tar impacted site sediments. Biodegradation of intrinsic contaminant mass during incubations (coal-tar DNAPLs and/or sorbed to aquifer solids) must be accounted for in the cell-specific microbial growth and respiration, but are not measured in $^{14}CO_2$ evolved or ^{14}C-biomass with liquid scintillation counting techniques. R is a factor that describes the ratio of the total bioavailable PAH in the MICRO-FISH incubation (^{14}C-amended PAH plus intrinsic bioavailable PAH) to the ^{14}C-amended PAH, such that:

$$R = \frac{M_{14CPAH} + C_{PAH}\psi \cdot M_S}{M_{14CPAH}} \qquad [2]$$

where M_{14CPAH} is the mass of radioisotopic PAH added to the assay, C_{PAH} is the concentration of PAH in the contaminated sediments (μg PAH $\cdot$ g sediment^{-1}), and ψ describes the fraction of PAH in the sediments that are bioavailable ($0 \leq \psi \leq 1$). To determine the total cell-specific PAH mass transformation rate from the cell-specific radioactive PAH mass transformation rate of equation 1, equation 1 should be multiplied by equation 2 to account for additional microbial growth and respiration at the expense of stable-carbon PAH intrinsic to the contaminated sediments:

$$\frac{dm_{14C\text{-}PAH}}{dt} = -\frac{m_{14CO2} + m_{14C,B}}{t \cdot X_{active} \cdot M_S} \cdot \alpha_{14C\text{-}PAH} \cdot R \qquad [3]$$

To simplify estimates of PAH uptake rates, it is assumed that there is no biological preference for either isotopic form of the PAH pollutant of interest.

The bioavailability of hydrophobic organic contaminants in aged soils and sediments may limit biodegradation rates and thus controls the value of R. There are no consistently reliable measures for bioavailability of specific hydrocarbon compounds in soils and sediments. However, there exists two extreme cases: all PAH is in the bioavailable form (ψ=1), or there is no bioavailable PAH (ψ=0). These extremes should provide a range of cell-specific mass transformation rates that bracket the actual value. Better methods for measuring bioavailability in different soil and sediment types would be helpful in providing more accurate calculations of the mass-transformation rates.

Radioisotopic PAHs inoculated into the MICRO-FISH assays are assumed to be completely bioavailable over the short periods of incubation.

In Chapter 3, a 2-D superimposed analytical solution to the fate and transport of PAHs at the Cherokee FMGP site was used to estimate first-order biodegradation rates (λ) for naphthalene (0.0058 d^{-1}) and phenanthrene (<0.0001 d^{-1}). The first-order biodegradation rates were based on the Monod model under the assumptions of no growth and a low substrate concentration. Considering these assumptions, the mass transformation rate (Chapter 3, Equation 7) is dependent on the mass of bioavailable PAH and intrinsic PAH-degrading microbial activity:

$$\frac{dM}{dt} = -\lambda(M_T) = -\frac{\mu_M \cdot B_{active,in-situ}}{Y \cdot K_S} \cdot M_T \qquad [4]$$

where M_T is the total mass of bioavailable PAH in the system of interest (pg), μ_M is the maximum specific growth rate of PAH-degrading cells (d^{-1}), $B_{active,in-situ}$ is the number of PAH-degrading cells in situ (cells · g sediment^{-1}), Y is the yield coefficient (PAH-degrading cells · pg PAH^{-1}), and K_S is the half-saturation constant (pg · g sediment^{-1}). Because the first-order rate coefficient was derived under field conditions assuming no microbial growth, the intrinsic PAH-degrading microbial population must be considered when estimating the cell-specific mass-transformation rate. The ratio of active to total cell populations per gram sediment in situ was assumed equal to that of the short-term MICRO-FISH assays. Based on equation 4, the in situ cell-specific mass transformation rate based on the plume-scale modeling rate coefficients, $\dfrac{dm_{in-situ}}{dt}$, can be estimated:

$$\frac{dm_{in-situ}}{dt} = -\frac{\lambda}{B_{active,in-situ} \cdot M_S} \cdot M_T = -\frac{\lambda}{B_{in-situ} \cdot M_S \cdot \left(\dfrac{X_{active}}{X_{total}}\right)} \cdot M_T = -\lambda' \cdot M_T \qquad [5]$$

where $B_{in-situ}$ is the total number of cells in situ (cells · g sediment^{-1}), X_{total} is the total number of cells in the MICRO-FISH incubations (cells · g sediment^{-1}), and λ' is the first-order cell-specific degradation rate estimated by plume-scale modeling. The measured cell-specific mass transformation rate calculated in equation 3 with MICRO-FISH incubation data can be directly compared to that estimated in equation 5 by allowing M_T in equation 5 to equal the total mass of PAH of interest in the MICRO-FISH assay such that:

$$M_T = M_{14CPAH} + C_{PAH}\psi \cdot M_S \qquad [6]$$

and:

$$\frac{dm_{in-situ}}{dt} = -\lambda' \cdot \left(M_{14CPAH} + C_{PAH}\psi \cdot M_S\right) \qquad [7]$$

Estimates made in this manner can be compared directly to the range of cell-specific mass-transformation rates estimated with molecular microbiological measurements using MICRO-FISH. It is important to note that zero-order rate coefficients are not being compared to first-order rate coefficients. Rather, mass transformation based on molecular microbiological measurements in MICRO-FISH is being compared to predicted mass transformation based on plume-scale modeling approaches on an equivalent mass PAH degraded per cell per time basis.

6.4 Materials and Methods

6.4.1 Microbial sampling

Sediments used in this study were extracted using percussion-probing direct push technology at the four locations shown in Figure 6.1. These locations were chosen for study as they represent the extent of naphthalene and phenanthrene contaminant plumes measured in situ. Detailed procedures on sampling and preservation of sediments are given in Chapter 4.

6.4.2 Aerobic incubations

Prior to use, the sediments were homogenized by passing through a #4 sieve to remove the gravel fraction. 2 g coal-tar contaminated sediments and 2 mL sterile basal salts medium (2 mM KH_2PO_4, 2 mM K_2HPO_4, 9.9 mM NH_4Cl, 0.5 mM $MgCl_2 \cdot 6H_2O$, 0.5 mM $CaCl_2 \cdot 2H_2O$, and 0.1 mM $FeCl_2 \cdot 4H_2O$, pH 7.1), which was sparged with air for 30 minutes, were added to 14 mL amber vials. 1.5 mL shell vials containing 1 mL of 2 N sodium hydroxide solution were carefully placed into the vials to serve as a trap for $^{14}CO_2$ evolved. The vials were carefully sealed with a butyl rubber stopper using an aluminum crimp cap. Approximately 0.18 µCi (400,000 dpm) [9-^{14}C]phenanthrene (specific

activity, 15 mCi/mmol; Sigma) or 0.079 µCi (175,000 dpm) [UL-14C]naphthalene (specific activity,

20 mCi/mmol; Sigma) was injected directly into the sediment-slurries through the butyl rubber septa,

and the vials carefully swirled by hand. All assay bottles were incubated at 20°C. $^{14}CO_2$ evolution

was monitored in the aerobic assays by sampling the 1 N NaOH solution via syringe through the

butyl rubber stoppers. The NaOH was added to 13 mL of Ultima Gold XR Liquid Scintillation

Cocktail (Packard Instrument Company, Perkin Elmer, Downers Grove, IL), and the amount of $^{14}CO_2$

evolved was determined by liquid scintillation counting.

MICRO-FISH assays were performed for phenanthrene with GPS 22, GPS 23, and GPS 25

sediments and for naphthalene on all sediments based on historical exposure history. MICRO-FISH

assays were constructed as described above, except they were amended with either 10 µCi

(22,200,000 dpm) [9-^{14}C]phenanthrene or 10 µCi (22,200,000 dpm) [UL-^{14}C]naphthalene and

contained no sodium hydroxide trap to minimize the potential for spillage into the assays. At 24 to 42

hours of incubation based on $^{14}CO_2$ evolution, individual MICRO-FISH assays were sacrificed by

directly injecting 10 mL 4% paraformaldehyde to the 14 mL vials. The vials were vortexed for three

minutes, placed in a 4°C refrigerator for 24 hours, and the microbes extracted from the sediments

using a modified method of Unge et al. (1999). Briefly, the preserved cell-sediment slurry was

transferred to a 50 mL sterile tube and brought up to 20 mL in 1X PBS (pH 7.2). 0.4 g of acid-

washed polyvinylpolypirollidone (PVPP) was added to each tube and vortexed for 3 minutes. Bulk

sediment and bound humic material was allowed to settle for twenty minutes and the supernatant was

poured into a sterile 50 mL tube. 10 mL of PBS was added to the original sediments and the tubes

vortexed again for 3 minutes. After another settling period of twenty minutes, the supernatant was

pooled with the original supernatant. This process was repeated one additional time, after which the

pooled supernatants were vortexed for one minute and centrifuged at 100 x g for 6 minutes.

Following centrifugation, the supernatants were poured into sterile 50 mL screw-cap tubes, washed

three times in 1X PBS (pH 7.2), and brought up to 20 mL in PBS.

6.4.3 Radiocarbon Distributions

Radiocarbon distributions between the $^{14}CO_2$, cell-interfaces, and biomass were measured by

liquid scintillation counting. $^{14}CO_2$ was measured in parallel bioassays as reported above, and percent

of the initial radiocarbon spike respired was assumed equal for the MICRO-FISH assays. To measure

the radiocarbon incorporated in to the biomass, 0.7 mL of cell-sediment suspension were washed

repeatedly in 50% ethanol-PBS until the wash solution indicated no further removal of ^{14}C (six

washes). The washed cell-sediment pellet was brought up to 0.7 mL in 1X PBS (pH 8.4) to aid in dispersion of the pellet, and transferred onto 0.8 mL Nycodenz (Nycomed) (density = 1.3 g/mL) in sterile 1.5 mL microcentrifuge tubes. The tubes were centrifuged at 10,000 x g for 15 minutes to pellet the remaining sediments. After centrifugation, the top 0.5 mL was discarded, and the next 0.5 mL (containing the banded microbial fraction) was measured by liquid scintillation counting. To determine the mass of sorbed radiocarbon (parent ^{14}C plus potential metabolites) 0.7 mL of the original cell-sediment suspension was transferred onto 0.8 mL Nycodenz and centrifuged as before to separate the cells from the remaining sediments. The banded microbial fraction was removed and the total ^{14}C associated with this fraction measured by liquid scintillation counting. The sorbed ^{14}C was assumed equal to the total unwashed cell-associated ^{14}C minus the total washed-cell-associated ^{14}C.

6.4.4   Oligonucleotide Probes and Stains

The DNA-intercalating dye 4',6-diamidino-2'-phenylindole (DAPI; Sigma, St. Louis, MO) was used to stain cells nonspecifically. DAPI was stored dry at -20 °C, and prior to use was reconstituted at 100 ng μL-1 in sterile, nanopure water. The oligonucleotide probes are shown in Table 6.1. The oligonucleotide probes were synthesized with either Cy 3 (Cy 3; Amersham, Zurich, Switzerland), TAM, or FITC reactive dye covalently bound to the 5'-end (Invitrogen Corp., Huntsville, AL). The dye-oligonucleotide conjugates (1:1) were lyophilized and stored dry in sterile microfuge tubes at -20 °C in the dark. Prior to use, the dry probes were reconstituted in TE buffer (10 mM Tris-HCl, 1 mM EDTA, pH 8.0), covered with aluminum foil, and stored at -20 °C.

6.4.5   Total cell counts

Total direct DAPI counts were used to identify the proper dilutions for whole-cell hybridizations. 0.7 mL cell suspension was transferred onto 0.8 mL Nycodenz (Nycomed) (density = 1.3 g/mL) in sterile 1.5 mL microcentrifuge tubes and centrifuged at 10,000 x g for 15 minutes to pellet the remaining sediments. After centrifugation, the top 0.5 mL was discarded, and the next 0.5 mL (containing the banded microbial fraction) was transferred to sterile 1.5 mL microcentrifuge tubes. The microbial fraction was supplemented with 20 μL of DAPI solution (100 ng μL^{-1}) and incubated for 7 minutes in the dark. Following incubation, the entire solution was transferred to a 15 mL vacuum filtration tower containing a pre-wetted 25 mm diameter polycarbonate filter (0.22 μm pore size) and 5 mL of sterile PBS (pH 7.2). The filter was washed three times under vacuum with 3

mL each of PBS. The filters were transferred onto slides, mounted with Citifluor mounting medium (Citifluor, Canterbury, UK), and examined under a Nikon Eclipse 400 microscope fitted with a digital imaging system, high pressure mercury lamp, and UV-2E/C filter. The cells were counted from duplicate slides at 600x magnification by randomly counting 20 fields on each slide covering an area of 0.0169 mm^2 each from a total area of 201 mm^2 per filter using Image-Pro Plus software (v. 4.5.1, Media Cybernetics, Silver Spring, MD).

6.4.6 MICRO-FISH

Nycodenz density gradient centrifugation of washed cell-sediment suspensions were used to separate soil microorganisms from the remaining sediments prior to MICRO-FISH as described above. The banded bacterial fractions were transferred to a 15 mL vacuum filtration tower containing a pre-wetted 25 mm diameter polycarbonate filter (0.22 μm pore size) and 5 mL PBS (pH 7.4). The filter was washed three times under vacuum with 3 mL each of PBS, transferred cell-side down onto a 22 mm square cover glass (No. 2) treated with a 4% solution of 3-aminopropyltriethoxysilane (Sigma, St. Louis, MO), clamped between two glass slides using binder clips, and placed in a 42°C oven for 1 hour, after which the filter was peeled away leaving the cells adhered to the cover glass. The cells were dehydrated using 50%, 80%, and 96% ethanol, respectively, three minutes each, and the cover glasses placed cell-size up on microscope slides. The cells were then brought into contact with a 30 μL drop of hybridization buffer (0.9 M NaCl, 20 mM Tris-HCl (pH 7.2), 2.5 mM EDTA, and 0.01% sodium dodecyl sulfate (SDS) in the presence of 20-35% formamide (ARCH915, BAC303, HGC69a, and SRB385 = 20%; EUB338 (I-III), BET42a, and GAM42a = 30%; ALF968, CF319a, LGC354(a,b,c) = 35%;NON338 = 20-35%)) containing 4 ng·$μL^{-1}$ of the relevant probe(s) and 4 ng·$μL^{-1}$ DAPI and covered with a Hybri-Slip (Sigma, St. Louis, MO). The slides were placed into 50 mL plastic tubes with ChemWipes® wetted with 2 mL of hybridization solution (humidity chambers) and hybridized at 46°C for 90 minutes. Following hybridization, the cover glasses were washed for 15 minutes at 48°C in the appropriate wash buffer (20 mM Tris-HCl (pH 7.2), 2.5 mM EDTA, 0.01% SDS, and either 308, 102, or 80 mM NaCl depending on the formamide concentration during hybridization (20%, 30%, or 35%, respectively)), then carefully dried under a stream of filtered air.

All autoradiographic procedures were performed in the dark using a method similar to Cottrell and Kirchman (2000). Briefly, the cover glasses were dipped in molten (43°C) Kodak NBT-2 autoradiographic emulsion diluted 2 parts emulsion and 1 part deionized water. After incubation at 4°C for 10 days, the slides were warmed to room temperature and developed using Kodak Dektol

developer, a deionized water stop bath, and Kodak fixer, as per manufacturer's instructions. The cover glasses were air dried, mounted on clean glass slides using Citifluor AF1 mounting medium (Citifluor Ltd., Canterbury, UK), and examined under a Nikon Eclipse 400 microscope using a G-2E/C filter for Cy3 and TAM-labeled cells, B-2E/C filter for FITC- and FAM-labeled cells, and UV-2E/C filter to determine the total direct DAPI count. Silver grain formation corresponding to hybridized cells was determined by switching between fluorescence and bright-field modes. Digital imaging analysis was performed using Image-Pro Plus (v. 4.5.1, Media Cybernetics, Inc., Silver Spring, MD).

6.5 Results

6.5.1 MICRO-FISH

Figures 6.2 to 6.4 show fluorescence images and autoradiograms resulting from the MICRO-FISH assays using GPS 25 sediments. Autoradiography resulted in visible silver-grain density images that correlated well to the spatial locations of specific cell types identified by the whole-cell hybridization technique. Active cells were identified as those that accumulated silver grain clusters.

Table 6.2 summarizes the total and active microbial community structure of sediments from all core locations for naphthalene and phenanthrene. Incubation resulted in growth of total DAPI-detected organisms from the in-situ condition presented in Chapter 4. Dominant phylotypes in the microbial communities included *Actinobacteria*, *γ-Proteobacteria*, and *β-Proteobacteria*, and to a lesser extent *Bacteriodetes*, and *Firmicutes*. Detection of *α-Proteobacteria*, sulfate-reducing bacteria, and the *Bacteriodes* and *Prevotella* genera were variable following incubations. Detections with the EUB338(I,II,III) probe set represented a larger portion of DAPI-detected cells than more specific probes for all sediments. The relatively lower detections with phylum- and subphylum-level probes may be due to the presence of bacteria not complimentary to the probe set used.

Microautoradiography indicated that the *β-Proteobacteria*, *γ-Proteobacteria*, and *Actinobacteria* were active in uptake of phenanthrene and naphthalene in these sediments. A variable number of active cells per microscopic field and the lack of active cells on some images resulted in relatively large confidence intervals about the mean probe-detected active cells. For instance, if 100 DAPI-stained cells per microscopic field are desired, an activity of a specific microbial phylotype of 0.3% of DAPI stained cells would result in approximately one detection per three microscopic fields. However, it can be said that in GPS 22 and GPS 23 sediments DAPI-detected organisms were more

active on naphthalene than on phenanthrene. The difference was quite distinct in GPS 22 sediments, where 3.76 ± 0.95% of DAPI-detected organisms were active on naphthalene versus 0.51 ± 0.34% on phenanthrene. The difference may be due to the competitive effects of alternative carbon sources in these highly contaminated sediments, as phenanthrene degradation was eventually observed (see Chapter 5). *β-Proteobacteria* did not assimilate radioisotopic phenanthrene in GPS 22 sediments but were active in the uptake of phenanthrene in GPS 23 sediments. Conversely, *γ-Proteobacteria* assimilated radioisotopic phenanthrene in GPS 22 sediments, but not in GPS 23 sediments. The reason for this difference is unclear. Active cells were less than 5% of the total microbial community following incubations in all cases.

6.5.2   Radiocarbon Distributions

Table 6.3 describes the fate of radiocarbons introduced into the MICRO-FISH assays. As can be seen in the Table 6.3, naphthalene mineralization ranged from 8.26% to 29.6% of the [UL-^{14}C]naphthalene added to the assays, accounting for 98.5% to 99.4% of the total naphthalene destruction (mineralized plus converted to biomass). Mineralization of phenanthrene was similar to naphthalene except in GPS 22 sediments, where phenanthrene mineralization exhibited a lag phase resulting in only 0.34% mineralization of added [9-^{14}C]phenanthrene over the 36 hour MICRO-FISH incubation reported in this study.

Sorption of the radioisotopic PAHs and potential metabolites of degradation to microbial cell surfaces was significant in all incubations, but followed no clear trend from one sediment location to another. Natural microbial communities may contain several bacterial types that exhibit significant heterogeneity in cell-surface hydrophobicity leading to differential sorption of hydrophobic organic contaminants. It has been posed that sorption of PAHs to the cell surface may pose a selective advantage for some organisms that use these compounds as growth substrates, and may be a phenotypic characteristic of several PAH-degrading microbial phylotypes such as *Actinobacteria* (Bastiens et al., 2002). However, there are no clear ways no measure differential sorption to cells in natural samples. Assuming that sorption was homogenous over the different cell types, the radioactivity per microbial cell associated with sorption of the radioisotopes reached on average as much as 51.6% of the radioactivity of active cells. This clearly highlights the need for microbial wash steps to remove sorbed radiocarbons that may interfere with the autoradiographic response (for more details, see Chapter 5).

The estimated radioactivity per active microbial cell based on liquid scintillation counting and total active cell counts ranged from 0.009 disintegrations per minute (dpm) to 0.094 dpm. This activity translates to approximately 0.26-0.50 pg radioisotopic PAH incorporated into each active microbial cell. By allowing for 10 days processing time for microautoradiography, 130 to 1350 disintegrations per active cell occurred. Higher activity cells generally resulted in larger silver grain clusters in the autoradiograms. The exception was in GPS 22 sediments that were incubated for 252 hours, potentially due to a combination of high cell densities on the microscope slides and large silver grain clusters that may have encompassed inactive cells (see Chapter 5).

To explore the effects of incubation time on radiocarbon distributions, a time series was performed for GPS 22 sediments with [9-^{14}C]phenanthrene. Sorption onto cells, incorporation of radiocarbon into biomass, and ^{14}CO$_2$ evolution increased with incubation time as expected. However, ^{14}CO$_2$ evolution accounted for a decreasing percentage of total destroyed [9-^{14}C]phenanthrene relative to total ^{14}CO$_2$ evolved plus ^{14}C incorporated into biomass. This may result from the shift in microbial cell phylotypes degrading the phenanthrene with time (see Table 5.3), a change in the microbial growth phase, or a combination of both. Incorporation of naphthalene and phenanthrene into biomass (relative to the total incorporated into biomass plus total ^{14}CO$_2$ evolved) was 0.37 to 1.53% and 0.84 to 5.56%, respectively, for all samples. This is much lower than would be expected for a more simple substrate such as glucose, and may reflect partial use of similar alternative carbon sources in the coal-tar contaminated sediments or specific bacterial strategies to degrading these toxic organic pollutants.

6.5.3   Cell-Specific Mass Transformation Rates

Radiocarbon distributions and the average specific contaminant uptake profiles of degrading cells were used in conjunction with measurements of the in-situ and MICRO-FISH microbial community structures to estimate cell-specific mass transformation rates (pg·d^{-1}·active cell^{-1}) as described in equations 1-7. PAH concentrations measured in the homogenized sediments from cores 22, 23, 25, and 26 are shown in Table 6.4. Also shown are the average in-situ total DAPI-direct counts for each sediment core as reported in Chapter 4, and the percent active cells based on the MICRO-FISH assays presented above. The number of degrading cells in situ was determined by multiplying the in-situ total direct DAPI-counted organisms in each core by the percent active cells determined using MICRO-FISH.

Table 6.4 shows the cell-specific mass transformation rates measured with the MICRO-FISH technique. The minimum values represent the case where all intrinsic naphthalene or phenanthrene

mass measured on the sediments were assumed not available for use as a carbon source by the PAH-degrading microbes (ψ=0). Therefore, these values represent the cell-specific mass transformation rates based solely on added radioisotopic PAH. The maximum values represent the case where all intrinsic naphthalene or phenanthrene mass measured on the sediments were assumed bioavailable (ψ=1). These values represent the maximum cell-specific mass transformation rates, in which measured cell-specific ^{14}C-PAH uptake rates were corrected to account for potential uptake of intrinsic (stable carbon) PAH compounds. A plume-scale first-order degradation rate coefficient (λ) for phenanthrene was set to 0.0001 d^{-1} to obtain cell-specific mass transformation rates as presented in equations 5 and 7 for comparison to results of the MICRO-FISH incubations.

As can be seen in Table 6.4, the ranges of cell-specific mass transformation rates measured for naphthalene agreed within an order of magnitude with rates estimated from plume-scale modeling approach of Chapter 3. Measured and predicted cell-specific mass transformation rates were most similar in sediments of cores GPS 25 and GPS 26. These cores were sampled from a region of the contaminated aquifer included in the analytical model of Chapter 3. GPS 22 and GPS 23 were sampled in the source region, outside the model boundary. In contrast, cell-specific mass transformation rates for phenanthrene based on MICRO-FISH in all sediment cores were approximately one to two orders of magnitude greater than predicted values. This reflects the discrepancy observed in the low in-situ biodegradation rate predicted by the analytical model in Chapter 3 versus the observation of phenanthrene degradation in bioassays presented in Chapter 4. The addition of a large mass of readily available PAH no doubt increased mass transformation rates to some extent over the in-situ condition. However, it is also likely that at least for the case of phenanthrene, the modeling approach used underestimated the mass transformation rate in situ. The true rate likely lies somewhere between the two values presented, and the plume-scale biodegradation rate would have to be adjusted accordingly to account for the difference and to yield more realistic modeling results. To apply the cell-specific contaminant uptake rates to a contaminant fate and transport models at the plume-scale, contaminant uptake rates would have to be adjusted to account for the difference in bioavailable PAH in the MICRO-FISH assays versus the bioavailable PAHs exhibited in situ.

6.6 Discussion

Naphthalene and phenanthrene-degrading bacteria were detected in all sediment cores analyzed with the MICRO-FISH technique. Phenanthrene-degrading organisms increased both in

number per gram sediment and as a fraction of the total microbial community structure as in-situ PAH concentrations decreased (lowest in GPS 22 sediments, highest in GPS 25 sediments). This suggests that phenanthrene degradation may be subject to some inhibiting factor related to total PAH contaminant concentration in situ such as product or substrate toxicity and or competitive inhibition. Naphthalene-degrading organisms display no clear trend as a percent of the microbial community structure or in numbers per gram sediments following incubations suggesting that these organisms are fairly ubiquitous in the contaminated aquifer sediments underlying the Cherokee FMGP site.

Actinobacteria were active in both naphthalene and phenanthrene degradation in all sediment cores tested. The activity of these bacteria in degrading PAH compounds in this coal-tar impacted aquifer is supported by their presence in-situ and relationship to previously characterized PAH-degrading bacteria, as reported in Chapter 4. Similarly, the *γ-Proteobacteria* were active in naphthalene and phenanthrene uptake in all sediments except GPS 23, where uptake of radioisotopic phenanthrene by *γ-Proteobacteria* was not detected. In most sediments *γ-Proteobacteria* dominated the uptake of naphthalene, expect at GPS 26 where *Actinobacteria* activity increased as a percent of the total DAPI-detected organisms. *γ-Proteobacteria* were the second-most commonly detected organisms in-situ. *β-Proteobacteria* activity was detected on both naphthalene and phenanthrene in all sediment cores, except for phenanthrene, GPS 22. This was interesting because the longer-term bioassays and MICRO-FISH studies of Chapter 4 indicated a dominating activity of *β-Proteobacteria* on phenanthrene. The enrichment effect discussed in Chapters 4 and 5 of long-term assays became very clear in these studies where short-term incubations were used. The studies of Chapter 4 revealed that *β-Proteobacteria* comprised only a small portion of the in-situ microbial community structure, except in GPS 22 core sediments. The importance of these bacteria in degrading naphthalene and phenanthrene in situ is overshadowed by that of the *Actinobacteria* and *γ-Proteobacteria*.

The goal of MICRO-FISH is to mimic in-situ conditions by using short incubations, but also to allow for enough incorporation of radiocarbon that cells can be detected using autoradiography. The 24 to 42 hour incubation times used in this study may be appropriate based on the works of others. Using a different isotopic technique to identify naphthalene degrading organisms in soils, stable isotope probing (SIP), Padmanabhan et al. (2003) noted the potential importance of short incubation times to limit perturbation in the intrinsic microbial community structure. These researchers used a 24 hour incubation time for naphthalene. However, for stable isotope probing, at least a doubling of active cells is required, as it relies on the construction of microbial DNA with carbon from an added ^{13}C-substrate. MICRO-FISH may require lower incubation times to yield positive autoradiograms than required by the SIP technique, as either growth or cell maintenance may

result in enough ^{14}C-uptake to elicit an autoradiographic response. One key aspect for successful application of MICRO-FISH may lie in finding the proper balance between incubation time to get a positive autoradiographic result but not to disturb the original microbial community structure. Exaggerated incubation times may also result in increased false-positive detections of "active" cells due to carbon cycling on metabolic byproducts or cellular decay. Large silver grain clusters in autoradiograms that spatially correspond to more than one cell may be a result of long incubation times as well, and highlight the importance of using proper dilutions and exposure times in performing the microautoradiography technique. Incubation times that are too short may result in a low and variable number of silver grain cluster detections per microscopic field making significant statistical interpretation difficult. For MICRO-FISH in aqueous environmental samples with compounds such as glucose, acetate, amino acids, proteins, chitin, proprionic acid, and formic acid, researchers have used incubation times ranging from 1 to 26 hours (Cottrell and Kirchman, 2000; Ouverney and Furhman, 1999; Lee et al., 1999; Ito et al, 2002).

In the ideal case, the final microbial community structure following MICRO-FISH will be very similar to the initial microbial community structure. Therefore, it follows that two assays ran with the same source materials but different radiocarbon compounds should still result in similar overall microbial community structures at termination of the assays. Similarities or differences in the degrading bacterial phylotypes should be revealed solely by microautoradiography. The final microbial community structures following MICRO-FISH incubations with radioisotopic naphthalene and phenanthrene were similar for GPS 22 sediments, except for a small difference in γ-Proteobacteria. In this case, DAPI-detected organisms only little more than doubled over the in-situ condition suggesting that the goal of little perturbation was attained. For GPS 23 sediments, large differences in most phylotypes were observed. In particular, β- and γ-Proteobacteria resulted in distinctly different activities as well as numbers. The R factors for these incubations were 1.20 and 1.16 for naphthalene and phenanthrene, respectively, when ψ was assumed equal to 1. The large mass of bioavailable radioisotope added to these incubations relative to the intrinsic phenanthrene and naphthalene mass may have resulted in differential perturbation of the microbial community structure. In comparison, the R-factors for naphthalene and phenanthrene in the GPS 22 MICRO-FISH assays (assuming ψ=1) were 9.0 and 6.7, respectively, indicating that the radiocarbon dose was much less significant relative to the intrinsic PAH mass.

Differences in final microbial community structures following short-term incubations highlight one difficulty in using MICRO-FISH in that it requires dosing large quantities of radiocarbon in a highly available form relative to the concentration of less available aged

hydrocarbons intrinsic to the contaminated sediments. Adding ^{14}C-PAH may increase cell-specific radiocarbon uptake rates and drive PAH-specific microbial growth leading to a divergence in measured mass transformation rates from the true in-situ condition. As the hydrophobicity of the substrate of interest increases and it becomes more recalcitrant in the site sediments, it could be expected that the error in measured cell-specific mass transformation rates resulting from large radiocarbon doses will increase. In such cases, MICRO-FISH may not provide highly reliable quantitative estimates of the in-situ mass transformation rates. The use of radioisotopes of larger specific activities could help alleviate some of these issues.

Cell-specific mass transformation rates based on MICRO-FISH incubations for naphthalene were surprisingly similar to plume-scale modeling estimates, especially in sediments corresponding to the modeled region (GPS 25 and GPS 26). For plume-scale cell-specific mass transformation rates to match that of MICRO-FISH in these sediments, the first-order plume-scale degradation rate coefficient for naphthalene (λ) would have had to have been between 0.0037d^{-1} and 0.0053d^{-1}. The first-order degradation rate coefficient for naphthalene from plume-scale modeling in Chapter 3 was 0.0058d^{-1}. Therefore in this instance, MICRO-FISH results support the plume-scale modeling observations. However, for plume-scale cell-specific mass transformation rates to match that of MICRO-FISH in the source sediments GPS 22 and GPS 23, the first-order plume-scale degradation rate coefficient for naphthalene would have had to have been between 0.033d^{-1} and 0.086 d^{-1}, which is still within a reasonable range based on the reported rates of others (see Chapter 2). The discrepancy between the two approaches may be a direct result of extending the use of model coefficients to sediments originating from outside the modeled region. A higher intrinsic activity may be present in source sediments, which are associated with rapid depletion of dissolved oxygen and nitrate, and the highest cell densities in situ. Least-squares biodegradation rates, if fitted to this region, would surely be higher than those fitted in the plume region. These discrepancies may also reflect limitations posed by the intrinsic bioavailability of specific PAHs, dissolved oxygen, and/or specific nutrients in situ relative to the optimized conditions in the MICRO-FISH incubations. The microbial community may not be transforming naphthalene to its fullest potential in situ. Therefore these results may suggest that addition of growth factors such as nutrients and/or bioventing/biosparging in the source region may enhance in situ transformation rates of naphthalene.

MICRO-FISH results suggest that the first-order biodegradation rate coefficient estimated for phenanthrene using plume-scale modeling may underestimate the actual biodegradation rate. Phenanthrene-degrading bacteria were active in all the sediment cores tested. However, the plume-scale modeling approach of Chapter 3 yielded a first-order degradation rate coefficient for

phenanthrene of less than 0.0001 d^{-1}. For plume-scale cell-specific mass transformation rates to match that of MICRO-FISH, the first-order degradation rate coefficient for phenanthrene would have to have been between 0.0024d^{-1} to 0.0082 d^{-1}. This is reasonable considering plume-scale estimates of others (see Chapter 2). The actual intrinsic degradation rate likely lies between the model fitted value of Chapter 3 and the MICRO-FISH value of this work. However, the activity of γ-Proteobacteria and Actinobacteria on naphthalene and phenanthrene in the MICRO-FISH assays reflect well the enrichment of these phylotypes in situ as presented in Chapter 4. Based on these results, the MICRO-FISH technique may provide a strong tertiary line of evidence that can be quantitatively linked to the in-situ condition.

6.7 Conclusions

In this study, whole-cell hybridizations and microautoradiography (MICRO-FISH) were effectively interfaced to identify the spatial heterogeneity in naphthalene- and phenanthrene-degrading organisms in the coal-tar impacted aquifer sediments underlying the Cherokee FMGP site. Although the overall microbial community structures were only slightly different all sediment cores tested, significant heterogeneity in total populations of PAH-degrading organisms and in phenanthrene-degrading bacterial phylotypes were observed. PAH-degrading bacteria identified with the MICRO-FISH technique comprised less than 5% of the total microbial community and were all of the Actinobacteria, β-Proteobacteria, and γ-Proteobacteria phylotypes. However, degradation of naphthalene by any specific phylotype did necessarily reflect the activity of those organisms in phenanthrene degradation for any particular sediment tested. The results of this study suggest that addressing the spatial heterogeneity in PAH-degrading organisms may be more effective for describing intrinsic biodegradation potential than investigating the overall microbial community structure relative to nearby pristine conditions at complex PAH-contaminated sites.

MICRO-FISH was shown to be a sensitive molecular marker for identifying and quantifying the cell-specific activity of naphthalene- and phenanthrene-degrading organisms, leading to estimates of cell-specific mass transformation rates that for naphthalene compared well to estimates based on plume-scale modeling approaches. However, molecular microbiological data suggested that plume-scale estimates of the degradation rate for phenanthrene may underestimate the actual rate of bioattenuation in situ. Modeling errors such as this may have significant implications when seeking regulatory approval for the use of natural attenuation as a remedial mechanism and highlights the potential usefulness of these molecular techniques. The positive identification of both naphthalene-

and phenanthrene-degrading bacteria in the coal-tar impacted sediments lends strong support for natural attenuation of at least low-ring PAH compounds in this coal-tar impacted aquifer. Based on the results presented herein, emerging molecular microbiological tools such as MICRO-FISH may yield valuable information useful for investigations of natural attenuation at hydrocarbon contaminated sites when carefully applied considering the field-scale microbial community structure.

6.8 References

Amann R. I., B. J. Binder, R. J. Olson, S. W. Chisholm, R. Devereux, and D. A. Stahl (1990) Combination of 16S rRNA-targeted oligonucleotide probes with flow cytometry for analyzing mixed microbial populations, *Appl. Environ. Microbiol.*, **56**(6), 1919-1925.

Bastiens, L., D. Springael, P. Wattiau, H. Harms, R. DeWatcher, H. Verachtert, and L. Diels (2000) Isolation of adherent polycyclic aromatic hydrocarbon (PAH)-degrading bacteria using PAH-sorbing carriers, *Appl. Environ. Microbiol.*, **66**(5), 1834-1843.

Cottrell, M. T., and D. L. Kirchman (2000) Natural assemblages of marine proteobacteria and members of the *Cytophaga-Flavobacter* cluster consuming low- and high-molecular-weight dissolved organic matter, *Appl. Environ. Microbiol.*, **66**(4), 1692-1697.

Daims, H., A. Brühl, R. Amann, K. H. Schleifer, and M. Wagner (1999) The domain-specific probe EUB338 is insufficient for the detection of all bacteria: development and evaluation of a more comprehensive probe set, *Syst. Appl. Microbiol.*, **22**(3), 434-444.

Delong, E. F., G. S. Wickham, and N. R. Pace (1989) Phylogenetic stains: ribosomal RNA-based probes for identification of single microbial cells, *Science*, **243**(4896), 1360-1363.

Dojka, M. A., P. Hugenholtz, S. K. Haack, and N. R. Pace (1998) Microbial diversity in a hydrocarbon- and chlorinated-solvent-contaminated aquifer undergoing intrinsic bioremediation, *Appl. Environ. Microbiol.*, **64**(10), 3869-3877.

Fliermans, C. B., and E. L. Schmidt (1975) Autoradiography and immunofluorescence combined for autecological study of single cell activity with nitrobacter as a model system, *Appl. Microbiol.*, **30**(4), 676-684.

Fuhrman, J. A. and F. Azam (1982) Thymidine incorporation as a measure of heterotrophic bacterioplankton production in marine surface waters: evaluation and field results, *Marine Biol.*, **66**(1), 109-120.

Hanson, J. R., J. L. Macalady, D. Harris, and K. M. Scow (1999) Linking toluene degradation with specific microbial populations in soil, *Appl. Environ. Microbiol.*, **65**(12), 5403-5408.

Ito, T., J. L. Nielsen, S. Okabe, Y. Watanabe, and P. H. Nielsen (2002) Phylogenetic identification and substrate uptake patterns of sulfate-reducing bacteria inhabiting an oxic-anoxic sewer biofilm determined by combining microautoradiography and fluorescent in situ hybridization, *Appl. Environ. Microbiol.*, **68**(1), 356-364.

Langworthy, D. E, R. D. Stapleton, G. S. Sayler, and R. H. Findlay (1998) Genotypic and phenotypic responses of a riverine microbial community to polycyclic aromatic hydrocarbon contamination, *Appl. Environ. Microbiol.*, **64**(9), 3422-3428.

Lee, N., P. H. Nielsen, K. H. Andreasen, S. Juretschko, J. L. Nielsen, K. H. Schleifer, and M. Wagner (1999) Combination of fluorescent in situ hybridization and microautoradiography – a new tool for structure-function analyses in microbial ecology, *Appl. Environ. Microbiol.*, **65**(3), 1289-1297.

MacNaughton, S. J., J. R. Stephen, A. D. Venosa, G. A. Davis, Y. J. Chang, and D. C. White (1999) Microbial population changes during bioremediation of an experimental oil spill, *Appl. Environ. Microbiol.*, **65**(8), 3566-3574.

Manz W., R. Amann, W. Ludwig, M. Wagner, and K. H. Schleifer (1992) Phylogenetic oligodeoxynucleotide probes for the major subclasses of *Proteobacteria*: problems and solutions, *Syst. Appl. Microbiol.*, **15**(4), 593-600.

Manz W., R. Amann, W. Ludwig, M. Vancanneyt, and K. H. Schleifer (1996) Application of a suite of 16S rRNA-specific oligonucleotide probes designed to investigate bacteria of the phylum *cytophaga-flavobacter-bacteroides* in the natural environment, *Microbiol.*, **142**(5), 1097-1106.

Meier, H., R. Amann, W. Ludwig, and K. H. Schleifer (1999) Specific oligonucleotide probes for in situ detection of a major group of gram-positive bacteria with low DNA G+C content, *Syst. Appl. Microbiol.*, **22**(2), 186-196.

Meyer-Reil, L. A. (1978) Autoradiography and epifluorescence microscopy combined for the determination of number and spectrum of actively metabolizing bacteria in natural waters, *Appl. Environ. Microbiol.*, **36**(3), 506-512.

Neef, A. (1997) Anwendung der in situ einzelzell-identifizierung von bakterien zur populations analyse in komplexen mikrobiellen biozönosen, Doctoral thesis, Technische Universität München, Munich, Germany.

Nielsen, P. H., K. Andreasen, N. Lee, and M. Wagner (1999) Use of microautoradiography and fluorescent in situ hybridization for characterization of microbial activity in activated sludge, *Water Sci. Technol.*, **39**(1), 1-9.

Ouverney, C. C., and J. A. Furhman (1999) Combined microautoradiography - 16S rRNA probe technique for determination of radioisotope uptake by specific microbial cell types in situ, *Appl. Environ. Microbiol.*, **65**(4), 1746-1752.

Padmanabhan, P., S. Padmanabhan, C. DeRito, A. Gray, D. Gannon, J. R. Snape, C. S. Tsai, W. Park, C. Jeon, and E. L. Madsen (2003) Respiration of 13C-labeled substrates added to soil in the field and subsequent 16S rRNA gene analysis of 13C-labeled soil DNA, *Appl. Environ. Microbiol.*, **69**(3), 1614-1622.

Roller, C., M. Wagner, R. Amann, W. Ludwig, and K. H. Schleifer (1994) In situ probing of Gram-positive bacteria with high DNA G+C content using 23S rRNA- targeted oligonucleotides, *Microbiol.*, **140**(10), 2849-2858. (Erratum in: *Microbiol.* (1995) **141**(5), 1267.)

Shi, Y., M. D. Zwolinski, M. E. Schreiber, J. M. Bahr, G. W. Sewell, and W. J. Hickey (1999) Molecular analysis of microbial community structures in pristine and contaminated aquifers: field and laboratory microcosm experiments, *Appl. Environ. Microbiol.*, **65**(5), 2143-2150.

Smit, E., P. Leeflang, and K. Wernars (1997) Detection of shifts in microbial community structure and diversity in soil caused by copper contamination using amplified ribosomal DNA restriction analysis, *FEMS Microbiol. Lett.*, **23**(2-3), 249-261.

Stahl, D. A., and R. Amann. (1991) Development and application of nucleic acid probes, in *Nucleic acid techniques in bacterial systematics*, E. Stackebrandt and M. Goodfellow (ed.), John Wiley & Sons Ltd., Chichester, England, 205-248.

Tabor, P. S., and R. A. Neihof (1982) Improved microautoradiographic method to determine individual microorganisms active in substrate uptake in natural waters, *Appl. Environ. Microbiol.*, **44**(4), 945-953.

Unge, A., R. Tombolini, L. Mølbak, and J. K. Jansson (1999) Simultaneous monitoring of cell number and metabolic activity of specific bacterial populations with a dual gfp-luxAB marker system, *Appl. Envir. Microbiol.*, **65**(2), 813-821.

Wallner, G., R. Amann, and W. Beisker (1993) Optimizing fluorescent in situ hybridization with rRNA-targeted oligonucleotide probes for flow cytometric identification of microorganisms, *Cytometry*, **14**(2), 136-143.

Table 6.1   Target organisms and oligonucleotide probes

Target Organisms	Probe	Oligonucleotide Sequence (5' – 3')	Fluor [a]	Reference
Domain-Level				
Archaea	ARCH915	GTG-CTC-CCC-CGC-CAA-TTC-CT	FITC	Stahl and Amann, 1991
Bacteria	EUB338	GCT-GCC-TCC-CGT-AGG-AGT	TAM	Amann et al., 1990
	EUB338-II	GCA-GCC-ACC-CGT-AGG-TGT		Daims et al., 1999
	EUB338-III	GCT-GCC-ACC-CGT-AGG-TGT		Daims et al., 1999
"Proteobacteria"				
α-Proteobacteria	ALF968	GGT-AAG-GTT-CTG-CGC-GTT	FITC	Neef, 1997
β-Proteobacteria	BET42a	GCC-TTC-CCA-CTT-CGT-TT	FITC	Manz et al., 1992
γ-Proteobacteria	GAM42a	GCC-TTC-CCA-CAT-GCT-TT	Cy3	Manz et al., 1992
Sulfate Reducing Bacteria	SRB385	CGG-CGT-CGC-TGC-GTC-AGG	FAM	Amann et al., 1990
Gram Positive Bacteria				
Actinobacteria	HGC69a	TAT-AGT-TAC-CAC-CGC-CGT	Cy3	Roller et al., 1994
Firmicutes	LGC354a	TGG-AAG-ATT-CCC-TAC-TGC	FITC	Meier et al., 1999
	LGC354b	CGG-AAG-ATT-CCC-TAC-TGC	FITC	Meier et al., 1999
	LGC354c	CCG-AAG-ATT-CCC-TAC-TGC	FITC	Meier et al., 1999
CFB Cluster				
Bacteriodetes	CF319a	TGG-TCC-GTG-TCT-CAG-TAC	Cy3	Manz et al., 1996
Bacteriodes and *Prevotella* genera	BAC303	CCA-ATG-TGG-GGG-ACC-TT	FITC	Manz et al., 1996
Negative Control Probe				
Nonsense	NONEUB	CGA-CGG-AGG-GCA-TCC-TCA	FITC	Wallner et al., 1993

a. Fluor = fluorochrome. Fluorescent markers were linked to the 5' end.

191

Table 6.2 Microbial community structure of sediments following MICRO-FISH with [UL-^{14}C]naphthalene and [9-^{14}C]phenanthrene.

Taxa	Cells · gm sediment^{-1}						
	Active Cells (relative to DAPI-stained cells)						
	GPS 22 [d.]		**GPS 23**		**GPS 25**		**GPS 26**
	Naphthalene	Phenanthrene	Naphthalene	Phenanthrene	Naphthalene	Phenanthrene	Naphthalene
Total Direct DAPI	181 ± 33.9 [a.]	189 ± 22.7	1110 ± 103	1080 ± 89.5	242 ± 20.7	541 ± 32.7	336 ± 50.4
	3.76 ± 0.95%	*0.51 ± 0.34%*	*1.92 ± 0.48%*	*1.01 ± 0.30%*	*4.78 ± 1.32%*	*3.98 ± 1.14%*	*3.14 ± 0.80%*
Bacteria	142 ± 16.6	136 ± 25.6	1050 ± 38.8	1050 ± 40.6	231 ± 12.4	532 ± 7.8	307 ± 20.3
	2.95 ± 1.35%	*0.80 ± 0.90%*	*2.43 ± 1.47%*	*0.96 ± 0.58%*	*3.15 ± 2.14%*	*1.00 ± 1.01%*	*4.52 ± 2.28%*
Archaea	4.1 ± 5.0	0.6 ± 1.3	ND	1.8 ± 1.7	0.5 ± 0.6	ND	ND
	ND [b.]	*ND* [b.]	*ND* [b.]	*ND* [b.]	*ND* [b.]	*ND* [b.]	*ND* [b.]
"Proteobacteria"							
α - *Proteobacteria*	4.4 ± 3.5	2.4 ± 4.6	ND	8.6 ± 13.7	ND	ND	ND
	ND	*ND*	*ND*	*ND*	*ND*	*ND*	*ND*
β - *Proteobacteria*	1.8 ± 1.9	ND	26.9 ± 34.2	165 ± 60.5	1.4 ± 1.8	4.4 ± 4.5	20.0 ± 9.5
	0.23 ± 0.01%	*ND*	*0.10 ± 0.01%*	*0.43 ± 0.02%*	*0.29 ± 0.02%*	*0.15 ± 0.01%*	*0.17 ± 0.01%*
γ - *Proteobacteria*	40.6 ± 11.8	73.4 ± 16.4	210 ± 74.3	116 ± 31.4	41.3 ± 13.1	69.9 ± 30.4	32.8 ± 7.1
	1.39 ± 1.39%	*0.44 ± 0.58%*	*1.15 ± 0.91%*	*ND*	*2.39 ± 2.09%*	*0.84 ± 0.89%*	*1.16 ± 0.73%*
δ - *Proteobacteria* [c.]	2.7 ± 2.5	2.4 ± 2.4	ND	1.6 ± 2.2	ND	ND	13.4 ± 7.0
	ND	*ND*	*ND*	*ND*	*ND*	*ND*	*ND*
Gram Positive Bacteria							
Actinobacteria	58.0 ± 15.6	58.5 ± 18.2	448 ± 64.0	468 ± 133	97.0 ± 24.0	131 ± 25.9	143 ± 26.7
	0.66 ± 0.44%	*0.20 ± 0.40%*	*0.46 ± 0.36%*	*0.37 ± 0.37%*	*0.19 ± 0.25%*	*0.19 ± 0.25%*	*1.59 ± 0.90%*
Firmicutes	8.4 ± 5.9	11.5 ± 4.8	0.9 ± 1.9	4.0 ± 6.6	0.9 ± 1.7	ND	3.3 ± 3.4
	ND	*ND*	*ND*	*ND*	*ND*	*ND*	*ND*
CFB Cluster							
Bacteriodetes	3.8 ± 2.8	1.4 ± 1.9	9.1 ± 10.3	46.0 ± 21.9	9.0 ± 8.4	20.5 ± 11.1	5.7 ± 5.1
	ND	*ND*	*ND*	*ND*	*ND*	*ND*	*ND*
Bacteriodes and	0.9 ± 0.9	ND	ND	ND	ND	ND	ND
Prevotella genera	*ND*	*ND*	*ND*	*ND*	*ND*	*ND*	*ND*

a. Reported as the **mean X 10^5** (±95% confidence interval),

b. ND = not detected

c. δ-*Proteobacteria* = SRB385-detected cells

d. GPS22 phenanthrene results reported for 36 hour incubation time

192

Table 6.3 Distribution of ^{14}C following MICRO-FISH with [UL-^{14}C]naphthalene and [9-^{14}C]phenanthrene.

Sediment Core	Radioisotope	Incubation Time *hours*	Radioactivity per Cell		Final distribution of radiocarbon			
			Sorbed [a.] *dpm*	Biomass [b.] *dpm*	$^{14}CO_2$ Evolved *μCi*	^{14}C on Cell Surfaces *μCi*	^{14}C in Biomass *μCi*	^{14}C remaining in Sediment Slurry *μCi*
GPS 22								
	Naphthalene	24	0.011	0.052	2.31 *22.5%*	0.212 *2.06%*	0.036 *0.35%*	7.71 *75.1%*
	Phenanthrene	36	0.006	0.070	0.032 *0.34%*	0.040 *0.43%*	0.002 *0.02%*	9.28 *99.2%*
		96	0.009	0.052	0.50 *5.31%*	0.096 *1.02%*	0.012 *0.13%*	8.75 *93.5%*
		252	0.016	0.031	2.09 *22.3%*	0.235 *2.51%*	0.031 *0.33%*	7.00 *74.8%*
GPS 23								
	Naphthalene	24	0.006	0.074	1.88 *18.3%*	0.124 *1.21%*	0.028 *0.28%*	8.24 *80.3%*
	Phenanthrene	36	0.008	0.094	1.22 *13.1%*	0.288 *3.08%*	0.035 *0.38%*	7.81 *83.5%*
GPS 25								
	Naphthalene	42	0.009	0.026	3.04 *29.6%*	0.075 *0.73%*	0.011 *0.11%*	7.14 *69.6%*
	Phenanthrene	42	0.030	0.067	2.66 *28.4%*	0.252 *2.69%*	0.023 *0.24%*	6.42 *68.6%*
GPS 26								
	Naphthalene	24	0.004	0.009	0.85 *8.26%*	0.071 *0.69%*	0.005 *0.05%*	9.34 *91.0%*

a. ^{14}C washed from cells prior to the MICRO-FISH technique. Sorption of ^{14}C assumed homogenous across all cell types. Radioactivity associated with ^{14}C in biomass not included.

b.   Active cells only

Table 6.4   Estimated cell-specific mass transformation rates based on MICRO-FISH and plume-scale modeling approaches.

Sediment Core	PAH	PAH Concentration	In-Situ Total Direct DAPI Count [a]	% Active Cells Based on MICRO-FISH	Cell-Specific Mass Transformation Rate $pg \cdot d^{-1} \cdot active\ cell^{-1}$			
					MICRO-FISH		Plume-Scale	
		$\mu g \cdot gm\ sediments^{-1}$	$Orgs. \cdot gm\ sediments^{-1}$		$\Psi = 0$	$\Psi = 1$	$\Psi = 0$	$\Psi = 1$
GPS 22								
	Naphthalene	293	74.5×10^5	3.76	9.8	97	0.68	6.8
	Phenanthrene	310	74.5×10^5	0.51	3.7	24	0.15	1.0
GPS 23								
	Naphthalene	6.47	39.6×10^5	1.92	14	17	2.5	3.0
	Phenanthrene	8.97	39.6×10^5	1.01	12	14	0.14	0.16
GPS 25								
	Naphthalene	0.64	2.11×10^5	4.78	12	12	19	19
	Phenanthrene	1.70	2.11×10^5	3.98	24	25	0.66	0.68
GPS 26								
	Naphthalene	0.09	11.2×10^5	3.14	4.7	4.8	5.4	5.5

a.   Average value measured in sediment core
b.   Active cells only

194
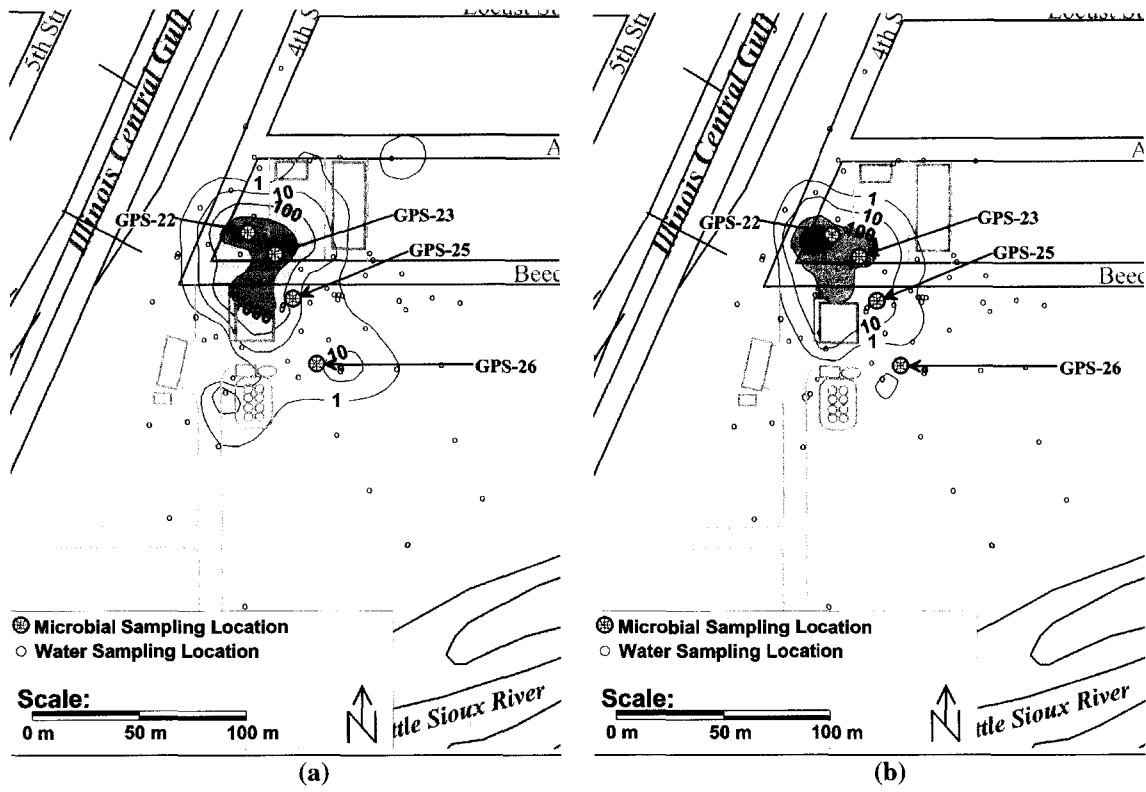
Figure 6.1   Cherokee FMGP site sediment core sampling locations and isoconcentration plots of (a) naphthalene and (b) phenanthrene.
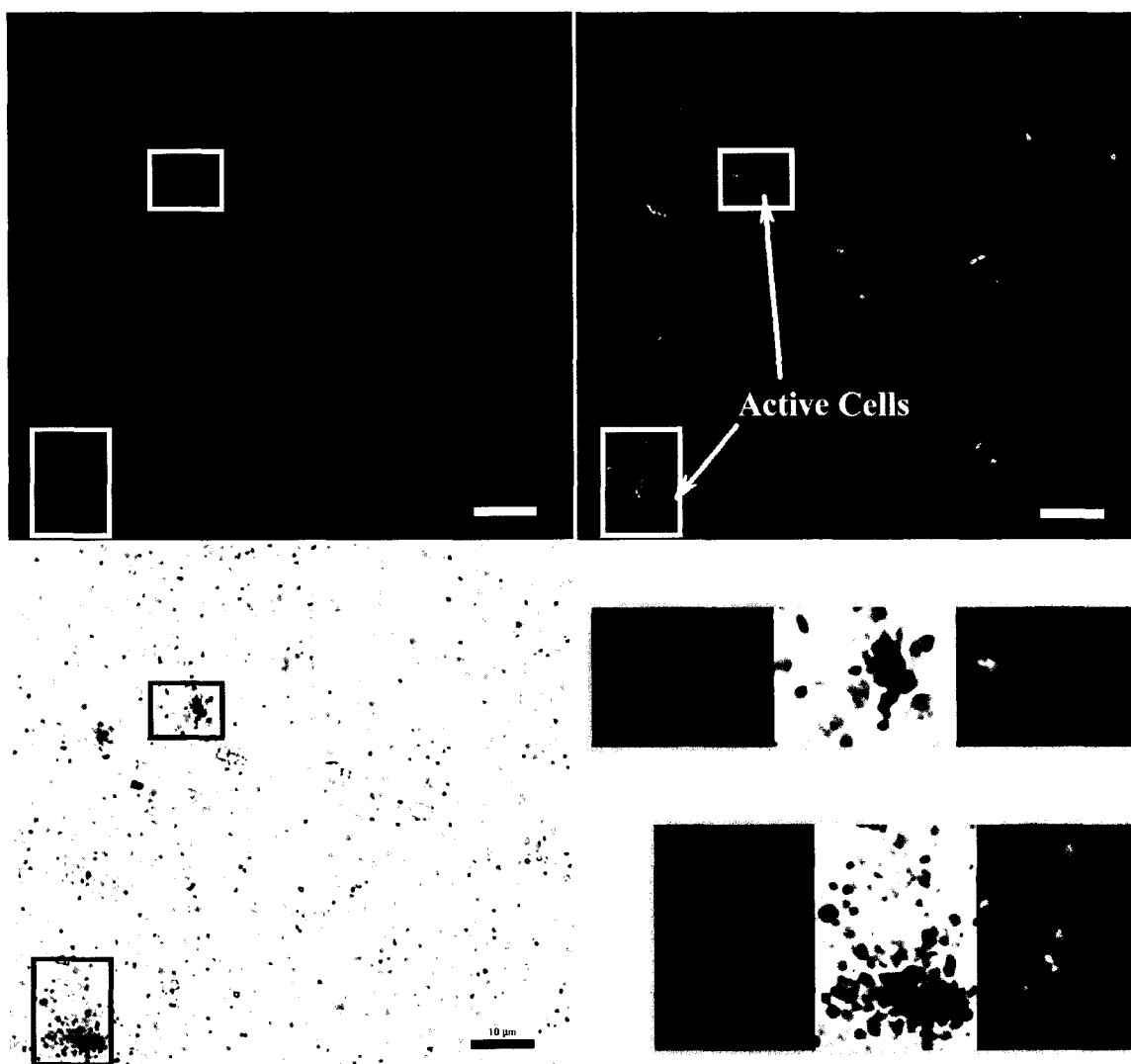
Figure 6.2   Fluorescence images and autoradiograms from GPS 25 sediments: *Bacteria*. Blue cells represent DAPI-stained organisms. Cells hybridizing with the EUB338 probe set are colored red by image analysis. Silver grain formation indicates growth on [9-^{14}C] phenanthrene. Bar = 10 μm.
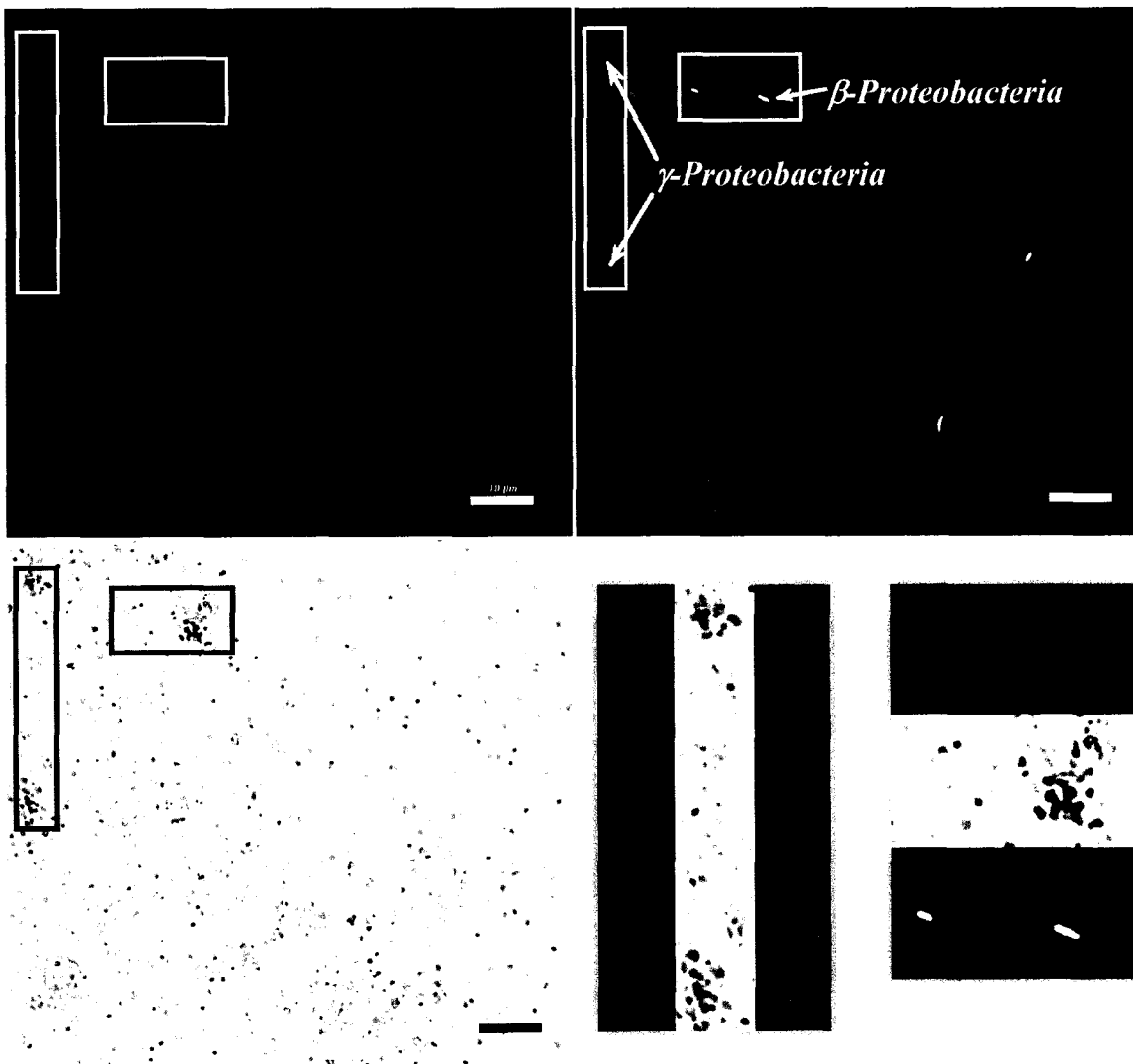
Figure 6.3   Fluorescence images and autoradiograms from GPS 25 sediments: β-
            Proteobacteria and γ*Proteobacteria*. Blue cells represent DAPI-stained
            organisms. Cells hybridizing with the GAM42a probe are colored red by image
            analysis. Cells hybridizing to the BET42a probe are colored green by image
            analysis. Silver grain formation indicates growth on [9-^{14}C] phenanthrene. Bar
            = 10 μm.
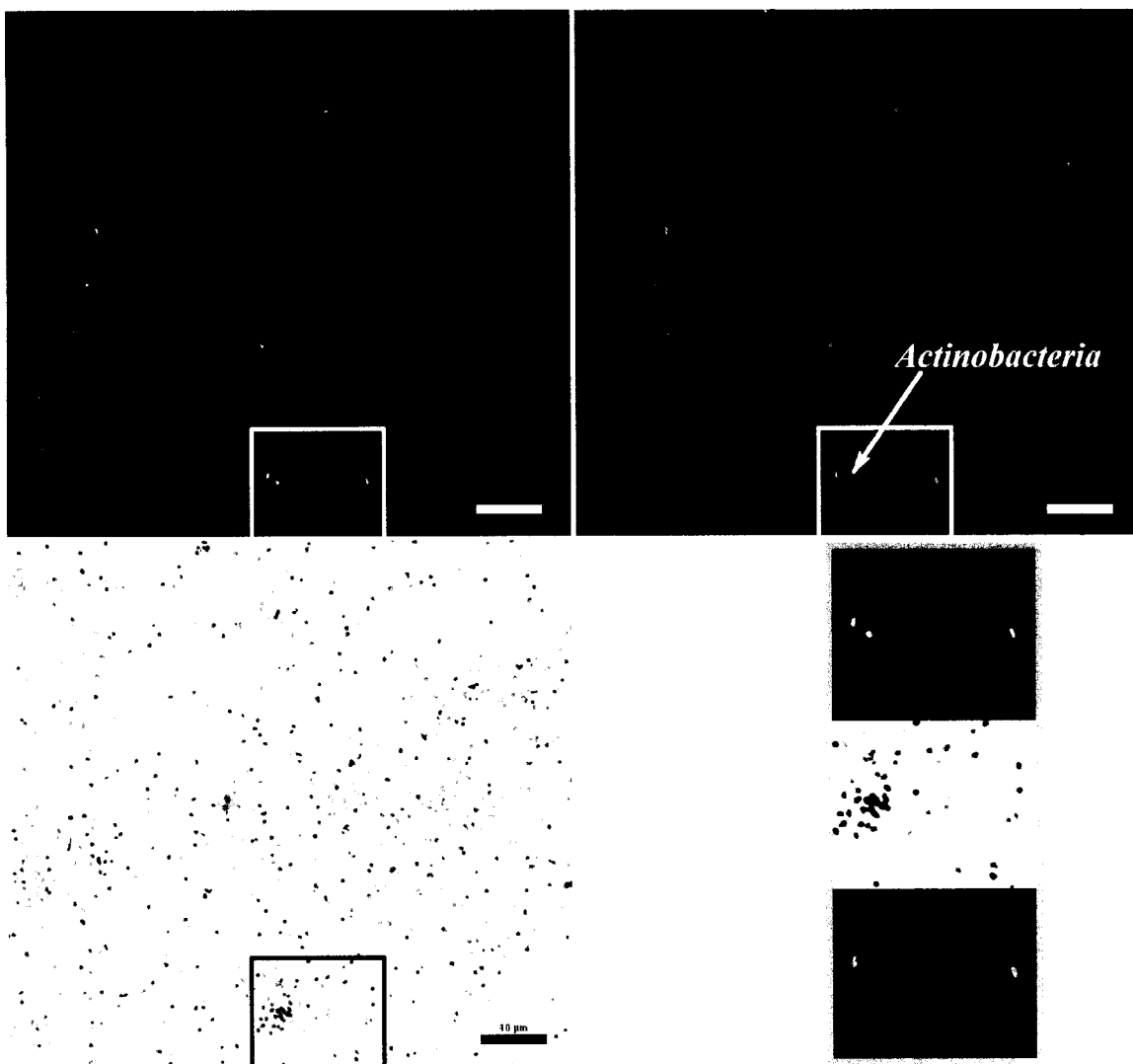
Figure 6.4   Fluorescence images and autoradiograms from GPS 25 sediments: *Archaea and Actinobacteria*. Blue cells represent DAPI-stained organisms. Cells hybridizing with the HGC69a probe are colored red by image analysis. Cells hybridizing with the ARCH915 probe are colored green by image analysis. Silver grain formation indicates growth on [9-^{14}C] phenanthrene. Bar = 10 μm.

7. CONCLUSIONS

7.1 Closing statements

Monitored natural attenuation has become an attractive remedial option at coal-tar impacted sites due to the difficulties associated with removal of residual coal-tar DNAPLs. However, there are relatively few published studies on natural attenuation of these sites. Modeling attenuation of PAH compounds typically involves several assumptions including steady-state plumes, linear and reversible sorption, and constant dissolution rates. Limitations imposed by these assumptions may preclude their usefulness as recent evidence has suggested that PAH sorption and desorption are highly non-linear and hysteric processes, and the strength of sorption can vary greatly with different geosorbents. Non-reversible sorption and phase change of PAH compounds would perfectly mimic biodegradation where plume-scale models are applied to aqueous-phase monitoring data, and may lead to incorrect conclusions regarding the fate of specific contaminants in situ. Poor estimates of lateral and transverse dispersivity could lead to gross error in estimating degradation rate coefficients.

There is evidence from published studies that alternate electron acceptors (other than dissolved oxygen) are being consumed in plumes emanating from coal-tar sources at various sites. However, most studies present little to no direct evidence that the exhibition of specific geochemical environments correlate with the biodegradation of PAH rather than co-contaminating compounds such as the monoaromatic hydrocarbons. Specific identification of PAH-degrading microbes is rarely performed. Most studies of natural attenuation of PAH compounds at coal-tar impacted sites have continued to regard natural microbial communities as a homogenous "black box". Natural microbial communities are dynamic in composition and activity in time and space, and therefore the microbial "black box" of these complex sites should not be assumed homogenous and consistent.

Tertiary lines of evidence may be necessary to support efforts of monitored natural attenuation at PAH contaminated sites. The classical approach is incubation of site sediments under specific redox conditions to "screen" the sediments for biodegradation potential. In many cases these studies affect the soil or sediment microbial community structure from that of the in situ condition, resulting in ambiguity regarding the applicability of laboratory results to modeling and monitoring efforts. Emerging molecular microbiological approaches may be well suited for bridging the gap between laboratory and field-scale studies.

In Chapter 3, analytical fate and transport and lumped hydrocarbon geochemical mass balance modeling were used to estimate biodegradation of select PAHs and monoaromatic

compounds. Both models produced mass degradation rates within the same order of magnitude mutually supporting their results. Biological activity in the contaminated aquifer was evidenced by standard heterotrophic plate counts in the contaminant source and plume region relative to background heterotrophic plate counts from nearby pristine groundwater samples. This work was significant in that it showed that it is possible to arrive at similar degradation rates predicted by a superposition of reactive transport analytical solutions with a terminal electron acceptor mass balance approach to estimate contaminant depletion in a hydrogeologically (variable groundwater flow direction) and chemically complex (commingled plumes) contaminated system, lending support to the intrinsic attenuation process.

In Chapter 4, the in situ microbial community structure and mineralization of select PAHs in aquifer sediments of the Cherokee FMGP site were investigated spatially using whole-cell hybridizations and incubations with site sediments under select redox conditions exhibited at the site level. Whole cell hybridizations revealed that *Actinobacteria*, *γ-Proteobacteria*, *Bacteriodetes*, and *β-Proteobacteria* were enriched in the contaminated aquifer and dominated the aerobic (>1 mg·L^{-1} dissolved oxygen) intrinsic microbial community structure. Anaerobic regions of the aquifer exhibiting elevated sulfide concentrations were enriched in sulfate-reducing bacteria, supporting the aqueous geochemical environments observed in groundwater monitoring. Laboratory-scale incubations with site sediments under aerobic conditions resulted in up to 61% mineralization of naphthalene and 42% mineralization of phenanthrene in all affected sediments tested. Mineralization of naphthalene in laboratory-scale incubations was observed in anaerobic nitrate-, sulfate- and iron(III)-amended incubations and corresponded to aqueous biogeochemical indicators measured in situ. Mineralization of phenanthrene in anaerobic iron-amended assays was also observed. Enrichment of *β-* and *γ-Proteobacteria* in the microbial communities following aerobic incubations indicated that bacteria of these sub-phyla were active in PAH degradation. Whole-cell hybridizations and microautoradiography confirmed these results but also indicated that *Actinobacteria* were active in the uptake of [9-^{14}C]phenanthrene, even though their populations declined in aerobic incubations. When compared to the in situ microbial community, it could be seen that three of the four enriched phylotypes observed in the aquifer correlated to organisms shown to be active on phenanthrene using whole-cell hybridizations and microautoradiography.

The results of the work in Chapter 4 have significant implications for studies that hypothesize that enrichment of specific microbial phylotypes in contaminated sediments relative to nearby pristine sediments can be used as a marker for pollutant-degrading microbes. In this study, the enrichment of *Bacteriodetes* could not be linked to the uptake of the model PAH, phenanthrene, even though they

were enriched in contaminated sediments in situ. More significantly, these results show conclusively that uptake of specific pollutants in laboratory-scale incubations may not be reflected well by enrichment of specific phylotypes following incubation in complex contaminated environmental media. Considering the activity of the *Actinobacteria* in the uptake of phenanthrene implied by whole-cell hybridizations and microautoradiography, these organisms could be of the most important PAH-degraders in situ, even though their populations declined in aerobic incubations.

Chapter 5 presents procedures for interfacing whole-cell hybridizations and microautoradiography (MICRO-FISH) to identify phylotypes active in specific PAH uptake in coal-tar DNAPL contaminated sediments. This work addressed potential interferences in microbial activity and false positive autoradiographic detections caused by extended incubation times or sorption of strongly hydrophobic radioisotopes to microbial cell walls. It was determined that extensive autoradiographic errors result when several washing steps with 50% ethanol-PBS to remove bound hydrophobic radiocarbon substrate and/or metabolites of degradation from microbial cells walls prior to performing MICRO-FISH were not performed. The choice of incubation time for the MICRO-FISH procedure was determined to be a trade-off between detection and relevance to in-situ conditions. Limited incubation times, even where a lag phase is exhibited in the laboratory-scale incubations, may be more appropriate for obtaining useful results for inference of the activity of specific microbial phylotypes in-situ. Longer incubation times may provide useful information regarding the presence and identification of potential pollutant degraders without cultivation, but may not accurately reflect the in-situ condition. This work presented a new and untried technique for tracking substrate-uptake to specific microbial types in complex contaminated environmental samples that may pose distinct advantages for investigating intrinsic remediation potential at several contaminated sites.

Chapter 6 describes the use of the MICRO-FISH technique in support of intrinsic degradation of PAH compounds at the Cherokee FMGP site. Through the use of this technique, naphthalene and/or phenanthrene-degrading *Actinobacteria, β-Proteobacteria*, and *γ-Proteobacteria* were detected in all sediment cores tested, but comprised less than 5% of the total intrinsic microbial communities. Phenanthrene-degrading bacterial activity was inversely proportional to contaminant concentrations in the site sediments suggesting that organisms of the phenanthrene-degrading phenotype may have been sensitive to product or substrate toxicity and/or competitive inhibition. Naphthalene-degrading organisms were determined to be fairly ubiquitous in the contaminated aquifer, representing a similar percent of the microbial community structure following MICRO-FISH assays at all locations tested.

In most sediments, *γ-Proteobacteria* dominated the uptake of PAHs. However, the studies presented in Chapter 4 indicated that *γ-Proteobacteria* were the second-most common organisms in-situ after the *Actinobacteria*. This suggests that alternative carbon sources had a strong impact on bacterial growth in MICRO-FISH incubations or that the *Actinobacteria* may posses some selective advantage for growth in the coal-tar impacted sediments in situ. *β-Proteobacteria* comprised only a small portion of the in-situ microbial community structure, except in GPS 22 core sediments. The importance of these bacteria in degrading naphthalene and phenanthrene in situ is overshadowed by that of the *Actinobacteria* and *γ-Proteobacteria*.

Cell-specific biotransformation rates of naphthalene were estimated based on MICRO-FISH and compared well to estimates based on the best-fit first-order degradation rate coefficients presented in Chapter 3. Cell-specific phenanthrene biotransformation rates estimated with best-fit first-order degradation rate coefficients from plume-scale modeling were one to two orders of magnitude lower than that measured in MICRO-FISH studies. This may suggest that plume-scale modeling provided overly conservative estimates of phenanthrene degradation rates. However, large doses of readily available ^{14}C-PAH in order to elicit an autoradiographic response may have increased cell-specific radiocarbon uptake rates in MICRO-FISH incubations leading to a divergence in measured mass transformation rates from the true in-situ condition. These discrepancies may also reflect limitations posed by the availability of specific growth factors in situ relative to the optimized conditions in the MICRO-FISH incubations. Thus, the in situ microbial community may not be transforming naphthalene and phenanthrene to its fullest potential. The results of this study suggest that specific engineered enhancements to the natural attenuation process such as addition of nutrients and/or bioventing/biosparging in the source region near sediment cores GPS 22 and GPS 23 may be effective for increasing biodegradation rates of coal-tar contaminants at this site.

7.2 Recommendations for future work

As the trend in natural attenuation policy shifts from merely displaying disappearance of contaminants at the field-scale to determining precisely the fate of the compounds (the definitive reasons for the depletion), the circumstantial evidences of attenuation processes will need to be supported by more direct evidence. Future studies will require a shift toward methods that better describe source releases and specifically track the fate and attenuation of PAH compounds from dilution, sorption, and biodegradation processes. These methods must have the capability of opening

the microbial "black-box" at contaminated sites and allow the study of the specific microbiological fate of contaminants under heterogeneous conditions.

Interfacing molecular microbiological characterizations and cell-specific contaminant uptake profiles with plume-scale modeling and monitoring data is a new and untried technique for supporting plume-scale modeling approaches in support of natural attenuation investigations. New approaches to determining structure-function relationships in environmental systems such as the coupled molecular approaches of this study provide more realistic identification of the activity of select microbial types on specific substrates of mixed systems necessary to improve modeling efforts at complex contaminated sites. Where successfully applied, the potential applications of this technology for investigating the biological fate of specific pollutants in engineered systems and the environment are vast. There are many thousands of contaminated aquifers, estuaries, rivers, and harbors with different pollutants that need to be restored. To advance the application of biotechnology for the remediation and restoration of these sites, specific information on pollutant uptakes are needed to further improve remedial technologies. Cataloging specific information regarding microbial communities populating extreme environments such as coal-tar polluted aquifers may lead to a better understanding of the relatedness of specific microorganisms involved in the degradation process globally. Investigations of intrinsic bioremediation potential of specific pollutants should use similar integrative approaches to link site-scale data to laboratory-scale data, thus validating conclusions drawn from field-scale studies.

From the results of this study, four primary areas of future research were identified:

1. A more detailed phylogenetic characterization of the microbial community structure using community profiling or cloning techniques should be performed in these coal-tar impacted sediments to:

    i. better identify known PAH-degrading phylotypes present in the microbial community, especially within the *Actinobacteria*, *β-Proteobacteria*, and *γ-Proteobacteria*

    ii. catalogue the microbial community profile for comparison to other PAH-degrading microbial communities

    iii. aid in developing more specific oligonucleotide probe sets relative to the dominant PAH-degrading bacteria that can be used as tools for future monitoring activities

2. The potential for anaerobic PAH degradation in these coal-tar impacted aquifer sediments should explored in further detail based on the potential for anaerobic transformation of

pollutant mass suggested by geochemical mass-balance modeling and mineralization of naphthalene and phenanthrene in anaerobic laboratory-scale incubations. In particular:

    i.   Anaerobic PAH degrading organisms in sediments of cores GPS 23, GPS 25, and GPS 27 should be cultivated and classified.

    ii.   Nitrate-reducing activity of anaerobic PAH-degrading isolates in GPS 23, iron-reducing activity in anaerobic PAH-degrading isolates of GPS 25, and sulfate-reducing activity in isolates of GPS 27 should be explored.

    iii.   The specific PAH uptake rates and potential for intrinsic remediation of coal-tar PAHs by these organisms in situ should be identified.

3.   Numerical and/or stochastic plume-scale models with the capability of integrating molecular microbiological data of the sort generated in this study should be constructed and evaluated in terms of the advantages and limitations in predicting contaminant plume behavior.

4.   Potential limitations and improved applications of the MICRO-FISH technique should be explored including:

    i.   Variability in cell-specific substrate-uptake profiles posed by varying radiocarbon doses for strongly hydrophobic compounds with low intrinsic bioavailable contaminant mass relative to dosed contaminant should be quantified.

    ii.   More detailed guidelines for obtaining statistically significant sample sizes with a relevant number of active microbial phylotypes for microscopic techniques should be established.

    iii.   Methods to quantify differential uptake rates of radioisotopic substrates to specific microbial phylotypes based on differences in the size of associated silver grain clusters should be established to improve estimates of the specific activity of different bacterial types in contaminated sediments.

    iv.   Coupled application of stable isotope probing and MICRO-FISH should be investigated to exploit the strengths of each technique. Stable isotope probing may provide detailed taxonomic characterizations of degrading microbial phylotypes that could be used to establish specific oligonucleotide probe sets for MICRO-FISH. MICRO-FISH could then be used to quantify the specific activity of individual PAH-degrading phylotypes to determine the relative importance of each in biodegradation activity. This level of detail may enhance data sets for environmental modeling and lead to specific oligonucleotide and/or PCR probe sets relevant to PAH-degrading organisms for future monitoring efforts.

APPENDIX A. GROUNDWATER SAMPLING DATA
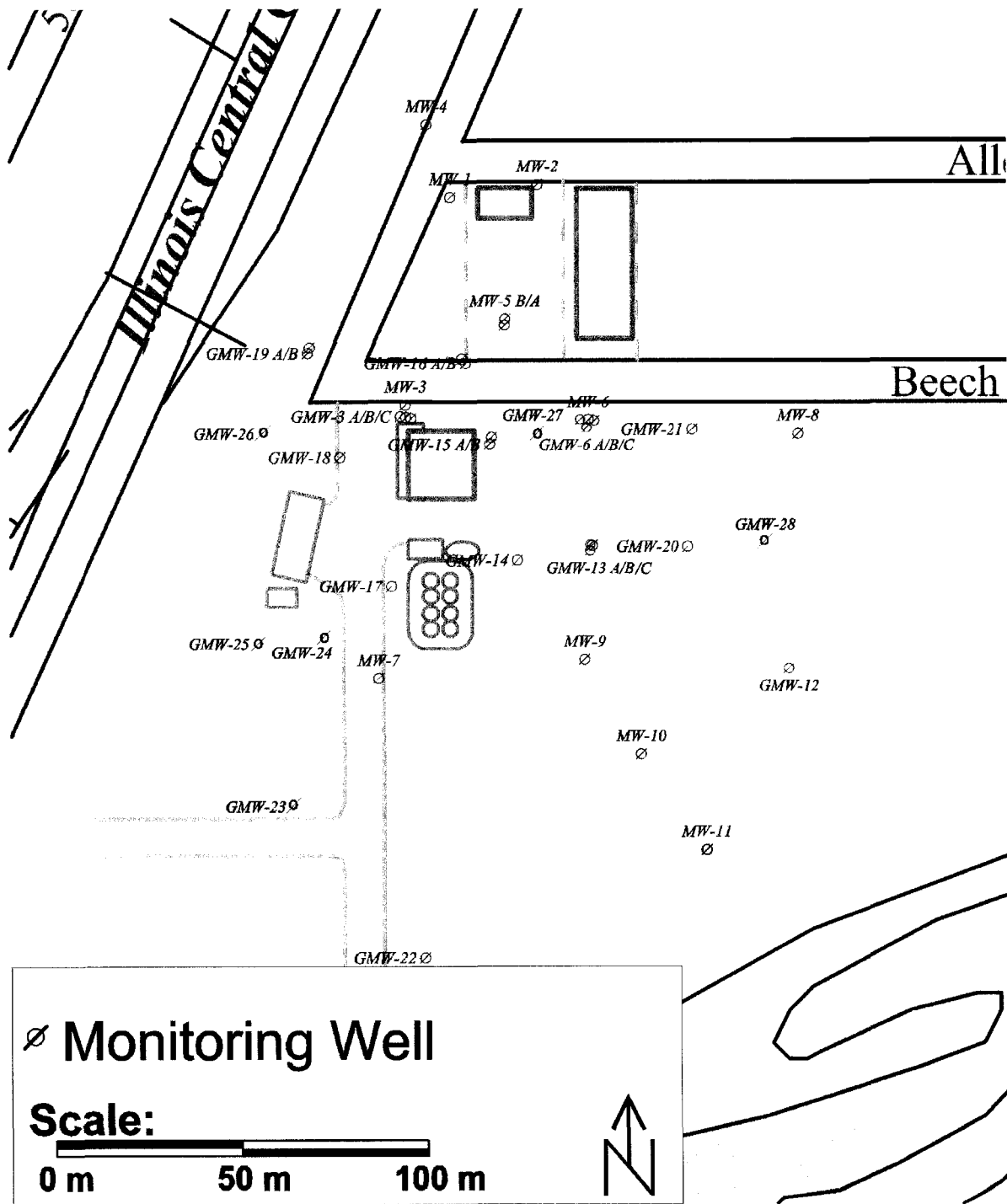
Figure A.1   **Monitoring well locations at the Cherokee FMGP Site**
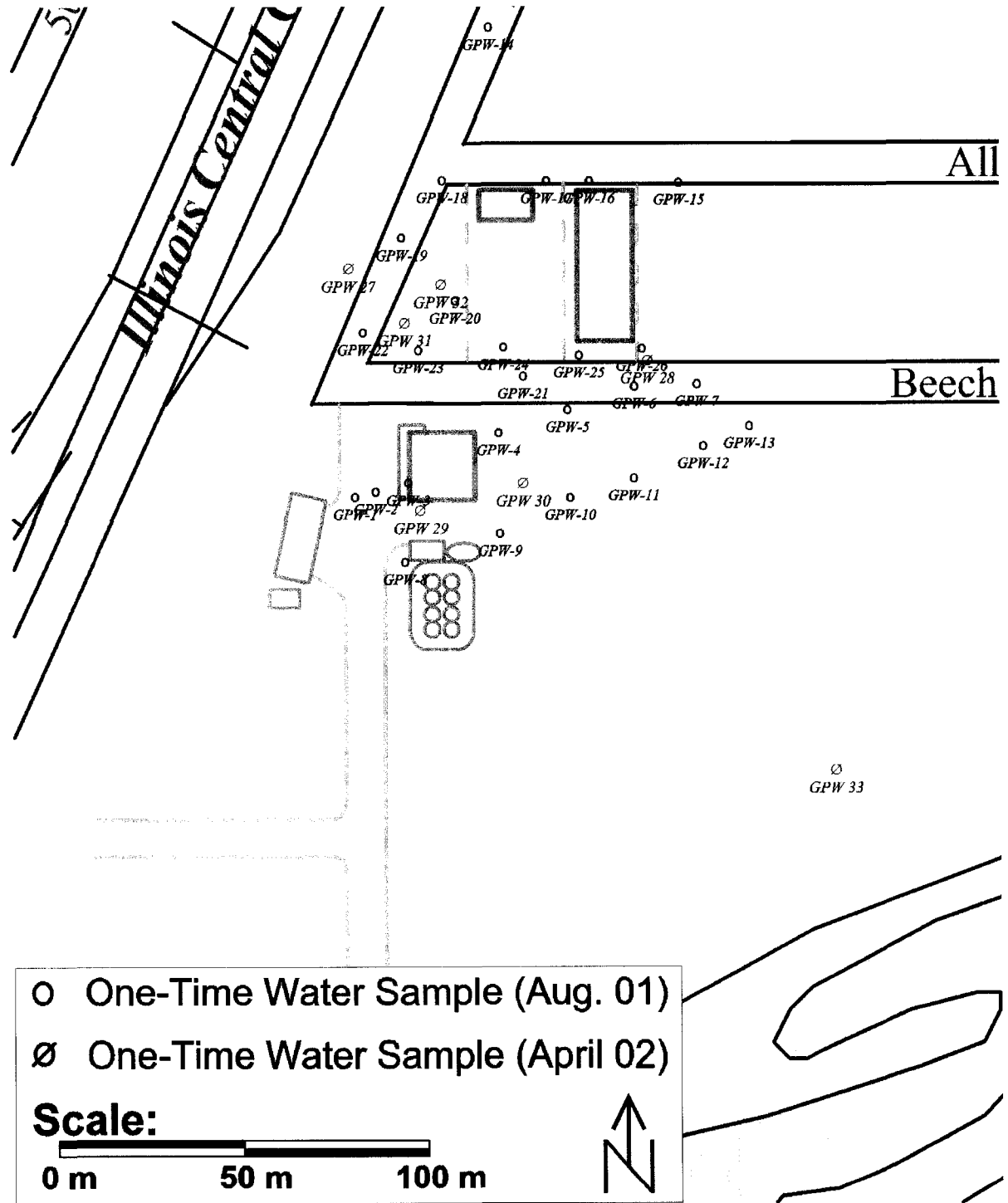
Figure A.2   One-time water sampling (direct push) locations at the Cherokee FMGP Site

Table A.1a   Measured aqueous geochemical characteristics at select monitoring locations

Analyte (Units)	MW 4[†] 3.05 m 354.84 m msl	GMW 19 1.22 m 356.8 m msl 355.7 m msl	GPW 18 0.61 m 356.0 m msl 352.4 m msl	GPW 14 0.61 m 356.3 m msl 353.2 m msl
Total Hardness (mg/L as CaCO₃)	586	504 583	- -	- -
Alkalinity (mg/L as CaCO₃)	298	330 403	- -	- -
Calcium (mg/L)	143, 150	150 170	196 193	138 168
Magnesium (mg/L)	37.7, 43	26 35	56.5 52.5	41.3 54.8
Sodium (mg/L)	52, 66	32 90	55 83.4	84.1 110
Potassium (mg/L)	3.9, 4.5	5.8 3.8	4.7 4.3	3.9 4
Ferrous Iron (mg/L)	ND, 0.02	0.01 ND	ND 0.2	0.09 0.1
Total Iron (mg/L)	0.01	ND, 0.02 ND, 0.01	0.16, 0.34 0.03, 0.31	ND, 0.23 0.18, 0.46
Total Manganese (mg/L)	ND	ND, 0.453 ND, 0.034	0.146 0.316	0.137 0.359
Chloride (mg/L)	122, 125	22.7 15.6	138 142	134 246
Sulfate (mg/L)	110, 160	140, 160 200, 210	100, 180 100, 220	110, 130 100, 150
Sulfide (mg/L)	0.002, 0.005	ND ND	0.014 0.002	ND 0.001
Nitrate+Nitrite (mg/L as N)	14.0, 16.5	2, 2.8 12, 14	1.8, 12 1.9, 11	3, 7.8 11, 14
Nitrite (mg/L as N)	0.005, 0.008	0.006 0.005	0.005 0.004	0.013 0.022
Ammonia (mg/L as N)	ND	ND ND	0.05 0.01	0.09 0.02
Total Phosphorus (mg/L)	ND	ND ND	- -	- -
Ortho-Phosphate (mg/L)	ND	- -	ND ND	ND ND
Dissolved Oxygen (mg/L)	6.1	0.7 4.43	- 4.4	- 5.6
Temperature (°C)	10.5, 13.2	10.9 10.6	- 14.6	- 16.9
pH	7.07	7.22 7.03	- -	- -
Electrical Conductivity (μS)	880, 1328	939 1286	- 1262	- 1327
Redox Potential (mV)	41, 91	33 57	- 40	- 73
Turbidity (NTU)	5.3	3.75 2.94	- -	- -
Plate Count (CFU/mL)	280, 63	3 1	- -	- -

† Monitoring well designation, screen length, and screen midpoint(s)

Table A.1b   Measured aqueous geochemical characteristics at select monitoring locations

Analyte (Units)	MW 11 1.52 m 345.34 m msl	GMW 22 1.22 m 347.55 m msl	MW 5 3.05 m 357.14 m msl 352.35 m msl	GMW 16 1.22 m 354.6 m msl 352.0 m msl
Total Hardness (mg/L as CaCO₃)	822	493	703 551	434 358
Alkalinity (mg/L as CaCO₃)	484	434	434 400	475 440
Calcium (mg/L)	200, 215	120	210, 228 160, 189	160 150
Magnesium (mg/L)	55, 57	34	38.0, 42.6 41.0, 47.5	38 39
Sodium (mg/L)	57.4, 62	81	26, 26.8 72, 82	48 85
Potassium (mg/L)	3.6, 3.7	ND	4.3, 5 3.4, 3.4	5.7 2.7
Ferrous Iron (mg/L)	0.03, 1.73	0.01	0.02, 0.11 0.90, 1.46	6.40 1.39
Total Iron (mg/L)	1.73, 1.8	0.03	0.02 1.13, 1.60	8.35 1.73
Total Manganese (mg/L)	1.00, 1.64	0.4, 0.61	1.15, 1.81 1.30, 2.25	0.23 1.25
Chloride (mg/L)	136, 136	48	26.6, 38 79.5, 173	36.5 92.8
Sulfate (mg/L)	160, 170	20, 64	185, 230 155, 160	95 136
Sulfide (mg/L)	ND, 0.001	ND	0.005, 0.012 0.002, 0.003	ND 0.008
Nitrate+Nitrite (mg/L as N)	0.3, 0.5	0.035	2.8, 4.2 3.3, 8.7	0.51 0.84
Nitrite (mg/L as N)	0.007, 0.025	0.005	0.012, 0.029 0.38, 0.78	0.008 0.287
Ammonia (mg/L as N)	ND, 0.12	ND	ND, 0.01 ND, 0.01	7.15 0.07
Total Phosphorus (mg/L)	0.12	0.12	ND ND	ND ND
Ortho-Phosphate (mg/L)	ND	-	ND ND	- -
Dissolved Oxygen (mg/L)	1.2	0.88	0.3 †	0.27 1.52
Temperature (°C)	10.5, 11.6	12.6	9.2, 14.2 †	10.9 11.7
pH	6.85	7.05	7.1 †	7.21 7.12
Electrical Conductivity (µS)	1080, 1564	1086	1050, 1262 †	1213 1361
Redox Potential (mV)	-6	2	-38, 44 †	-92 -73
Turbidity (NTU)	2.5	7.92	4.12 †	2.04 2.20
Plate Count (CFU/mL)	36, 11, 160	ND	7 4200, 6820	13 ND

Table A.1c   Measured aqueous geochemical characteristics at select monitoring locations

Analyte (Units)	GMW 15 1.22 m 354.1 m msl 352.3 m msl	GMW 14 1.22 m 349.6 m msl	GMW 13 1.22 m 353.0 m msl 350.2 m msl	GMW 20 1.22 m 348.8 m msl
Total Hardness (mg/L as CaCO₃)	627 526	483	850 273	522
Alkalinity (mg/L as CaCO₃)	405 428	504	802 287	514
Calcium (mg/L)	170 150	100	217, 190 85, 58	150
Magnesium (mg/L)	46 40	24	59, 53 24, 14	40
Sodium (mg/L)	48 100	170	304, 300 311, 150	220
Potassium (mg/L)	4.2 2.6	2.6	3.3, 3.0 2.7, 8.1	2.9
Ferrous Iron (mg/L)	0.31 2.28	0.26	0.85, 0.77 0.65, 0.08	0.34
Total Iron (mg/L)	0.35 2.29	0.25	1.39, 1.21 0.22, 0.46	0.48
Total Manganese (mg/L)	1.25 1.60	0.30	0.43, 0.26 0.27, 0.18	0.17
Chloride (mg/L)	83.2 141	47.4	311, 249 138, 61.3	177
Sulfate (mg/L)	175 138	175	110, 110 150, 130	145
Sulfide (mg/L)	0.005 0.003	0.52	0.001, ND 1.93, 0.073	0.65
Nitrate+Nitrite (mg/L as N)	0.31 0.20	0.91	0.51, 0.31 1.42, 0.61	0.60
Nitrite (mg/L as N)	0.005 0.005	0.006	0.005, 0.006 0.038, 0.013	0.006
Ammonia (mg/L as N)	0.05 0.03	0.16	0.38, 0.42 0.30, 0.41	0.62
Total Phosphorus (mg/L)	ND ND	ND	0.19 0.26	0.14
Ortho-Phosphate (mg/L)	- -	-	0 0.3	-
Dissolved Oxygen (mg/L)	0.25 0.26	0.49	0.6, 0.37 0.7	0.43
Temperature (°C)	10.1 10.9	10.4	14.2, 11.3 14.4	11.5
pH	6.96 7.16	7.04	7.02 -	7.16
Electrical Conductivity (µS)	1298 1421	1284	2050, 2440 1870	1848
Redox Potential (mV)	-17 -87	-194	-13, -18 -	-247
Turbidity (NTU)	13.7 14.2	28.5	4.8 -	2.08
Plate Count (CFU/mL)	ND 2	14	440 18000	34

Table A.2a   Average contaminant concentrations measured in monitoring wells at the Cherokee FMGP Site

Monitoring Well / Well Nest	Average Groundwater Concentrations (µg/L)						
	BTEX (1-Ring)				2-Ring PAH		
	Benzene	Toluene	Ethylbenzene	Xylenes	Naphthalene	1-Methylnaphthalene	2-Methylnaphthalene
MW-01	<1	<1	<1	<1	<0.1	<0.2	<0.2
MW-02	1.3	<1	<1	<1	2.2	<0.2	<0.2
MW-03	15.4	4.3	87.9	127	759	479	20.4
MW-04	<1	<1	<1	<1	<0.1	<0.2	<0.2
MW-05	293	74.2	176	232	790	124	98.3
MW-06	2.3	<1	2.0	7.7	0.5	8.3	<0.2
MW-07	<1	<1	<1	<3	<0.1	<0.2	<0.2
MW-08	<1	<1	<1	<3	<0.1	<0.2	<0.2
MW-09	<1	<1	<1	<3	<0.1	<0.2	<0.2
MW-10	<1	<1	<1	<3	<0.1	<0.2	<0.2
MW-11	<1	<1	<1	<3	<0.1	<0.2	<0.2
MW-12	<1	<1	<1	<3	<0.1	<0.2	<0.2
MW-13	29.8	<1	10.3	13.5	62.2	91.5	<0.2
MW-14	7.6	<1	5.54	20	1.7	10.4	<0.2
MW-15	544	48.9	553	376	2400	473	19.2
MW-16	831	213	754	689	3578	473	144
MW-17	5.0	<1	1.75	<3	42.2	29.4	0.5
MW-18	<1	<1	<1	<3	0.6	<0.2	<0.2
MW-19	<1	<1	<1	<3	0.1	<0.2	<0.2
MW-20	85.0	<1	22.4	16.6	2.0	1.2	<0.2
MW-21	<1	<1	<1	<3	<0.1	<0.2	<0.2
MW-22	<1	<1	<1	<3	<0.1	<0.2	<0.2
MW-23	<1	<1	<1	<3	<0.1	<0.2	<0.2
MW-24	<1	<1	<1	<3	<0.1	<0.2	<0.2
MW-25	<1	<1	<1	<3	<0.1	<0.2	<0.2
MW-26	<1	<1	<1	<3	<0.1	<0.2	<0.2
MW-27	41.0	<1	5.0	41.9	4.1	54.3	<0.2
MW-28	<1	<1	<1	<3	<0.1	<0.2	<0.2

Table A.2b   Average contaminant concentrations measured in monitoring wells at the Cherokee FMGP Site

Monitoring Well / Well Nest	Average Groundwater Concentrations (µg/L)								
	3-Ring PAH					4-Ring PAH			
	Acenaphthylene	Acenaphthene	Fluorene	Phenanthrene	Anthracene	Pyrene	Chrysene	Benzo(a) Anthracene	Fluoranthene
MW-01	<0.2	<0.2	<0.2	<0.1	<0.2	<0.2	<0.2	<0.2	<0.2
MW-02	<0.2	<0.2	<0.2	<0.1	<0.2	0.4	<0.2	<0.2	0.38
MW-03	479	59.2	114	76	12.7	0.4	0.22	<0.2	3.0
MW-04	<0.2	<0.2	<0.2	<0.1	<0.2	<0.2	<0.2	<0.2	<0.2
MW-05	124	19.3	52.9	61.9	14.1	16.5	1.5	1.2	7.8
MW-06	10.8	11.0	0.5	0.3	<0.2	<0.2	<0.2	<0.2	<0.2
MW-07	<0.2	<0.2	<0.2	<0.1	<0.2	<0.2	<0.2	<0.2	<0.2
MW-08	<0.2	<0.2	<0.2	0.19	<0.2	<0.2	<0.2	<0.2	<0.2
MW-09	<0.2	<0.2	<0.2	<0.1	<0.2	<0.2	<0.2	<0.2	<0.2
MW-10	<0.2	<0.2	<0.2	<0.1	0.24	0.2	<0.2	<0.2	<0.2
MW-11	<0.2	<0.2	<0.2	<0.1	<0.2	<0.2	<0.2	<0.2	<0.2
MW-12	<0.2	<0.2	<0.2	<0.1	<0.2	<0.2	<0.2	<0.2	<0.2
MW-13	32.1	55.2	1.0	<0.1	<0.2	<0.2	<0.2	<0.2	<0.2
MW-14	4.92	8.4	<0.2	0.4	<0.2	<0.2	<0.2	<0.2	<0.2
MW-15	56.9	309	34.8	62.6	9.9	4.8	<0.2	<0.2	1.0
MW-16	320	55.5	86.6	60.0	9.3	<0.2	<0.2	<0.2	2.1
MW-17	0.5	<0.2	0.7	0.2	<0.2	<0.2	<0.2	<0.2	0.3
MW-18	0.7	4.02	0.9	0.4	4.2	3.9	<0.2	<0.2	0.7
MW-19	<0.2	<0.2	<0.2	<0.1	<0.2	<0.2	<0.2	<0.2	<0.2
MW-20	<0.2	0.9	0.4	<0.1	<0.2	<0.2	<0.2	<0.2	<0.2
MW-21	<0.2	4.5	<0.2	<0.1	<0.2	<0.2	<0.2	<0.2	<0.2
MW-22	<0.2	<0.2	<0.2	<0.1	<0.2	<0.2	<0.2	<0.2	<0.2
MW-23	<0.2	<0.2	<0.2	<0.1	<0.2	<0.2	<0.2	<0.2	<0.2
MW-24	<0.2	<0.2	<0.2	<0.1	<0.2	<0.2	<0.2	<0.2	<0.2
MW-25	<0.2	<0.2	<0.2	<0.1	<0.2	<0.2	<0.2	<0.2	<0.2
MW-26	<0.2	<0.2	<0.2	<0.1	<0.2	<0.2	<0.2	<0.2	<0.2
MW-27	24.8	78.6	3.8	8.6	0.3	<0.2	<0.2	<0.2	<0.2
MW-28	<0.2	<0.2	<0.2	<0.1	<0.2	<0.2	<0.2	<0.2	<0.2

Table A.2c Average contaminant concentrations measured in monitoring wells at the Cherokee FMGP Site

Monitoring Well / Well Nest	Average Groundwater Concentrations (µg/L)					
	5-Ring PAH				6-Ring PAH	
	Benzo(b)fluoranthene	Benzo(k)fluoranthene	Benzo(a)pyrene	Dibenz(a,h)anthracene	Benzo(g,h,i)perylene	Indeno(1,2,3-c,d) pyrene
MW-01	<0.2	<0.2	<0.2	<0.2	<0.2	<0.2
MW-02	<0.2	<0.2	<0.2	<0.2	<0.2	<0.2
MW-03	<0.2	<0.2	<0.2	<0.2	<0.2	<0.2
MW-04	<0.2	<0.2	<0.2	<0.2	<0.2	<0.2
MW-05	0.6	0.7	<0.2	<0.2	<0.2	<0.2
MW-06	<0.2	<0.2	<0.2	<0.2	1.2	0.8
MW-07	<0.2	<0.2	<0.2	<0.2	<0.2	<0.2
MW-08	<0.2	<0.2	<0.2	<0.2	<0.2	<0.2
MW-09	<0.2	<0.2	<0.2	<0.2	<0.2	<0.2
MW-10	<0.2	<0.2	<0.2	<0.2	<0.2	<0.2
MW-11	<0.2	<0.2	<0.2	<0.2	<0.2	<0.2
MW-12	<0.2	<0.2	<0.2	<0.2	<0.2	<0.2
MW-13	<0.2	<0.2	<0.2	<0.2	<0.2	<0.2
MW-14	<0.2	<0.2	<0.2	<0.2	<0.2	<0.2
MW-15	<0.2	<0.2	<0.2	<0.2	<0.2	<0.2
MW-16	<0.2	<0.2	0.9	<0.2	<0.2	<0.2
MW-17	<0.2	<0.2	<0.2	<0.2	<0.2	<0.2
MW-18	<0.2	<0.2	<0.2	<0.2	<0.2	<0.2
MW-19	<0.2	<0.2	<0.2	<0.2	<0.2	<0.2
MW-20	<0.2	<0.2	<0.2	<0.2	<0.2	<0.2
MW-21	<0.2	<0.2	<0.2	<0.2	<0.2	<0.2
MW-22	<0.2	<0.2	<0.2	<0.2	<0.2	<0.2
MW-23	<0.2	<0.2	<0.2	<0.2	<0.2	<0.2
MW-24	<0.2	<0.2	<0.2	<0.2	<0.2	<0.2
MW-25	<0.2	<0.2	<0.2	<0.2	<0.2	<0.2
MW-26	<0.2	<0.2	<0.2	<0.2	<0.2	<0.2
MW-27	<0.2	<0.2	<0.2	<0.2	<0.2	<0.2
MW-28	<0.2	<0.2	<0.2	<0.2	<0.2	<0.2

APPENDIX B. **GROUNDWATER SAMPLING METHODS**

Table B.1   Analytical methods for groundwater sampling used in the study

Analyte [preservation method*]	Method	PQL[†] μg/L	Method Basis
On Site Analyses:			
Inorganics and Nutrients			
Total Hardness[A]	HACH #8213	10000	Titrimetric (EDTA)
Alkalinity[A]	HACH #8203	10000	Titrimetric (Phenolphthalein and Total)
Ammonium-N[A]	HACH #10023	10	Spectrophotometric, Salicylate
Nitrate-N[A]	HACH #8171	100	Spectrophotometric, Cadmium Reduction
Nitrite-N[A]	HACH #8507	10	Spectrophotometric, Diazotization
Ferrous Iron[A]	HACH #8146	10	Spectrophotometric, 1,10 Phenanthroline
Total Iron[A]	HACH #8008	10	Spectrophotometric, FerroVer
Total Manganese[A]	HACH #8034	100	Spectrophotometric, Periodate Oxidation
Sulfate[A]	HACH #8051	2000	Spectrophotometric, SulfaVer 4
Sulfide[A]	HACH #8131	10	Spectrophotometric, Methylene Blue
Water Quality Parameters			
Dissolved Oxygen[NA]	EPA 360.1	0.01 mgL[-1]	Electrode
Temperature[NA]	Probe	-5 – 50 °C	Electrode *(±0.1°C)*
pH[NA]	EPA 150.1	0.001	Electrode
Electrical Conductivity[NA]	EPA 120.1	0.1 μS/cm	Electrode
Redox Potential[NA]	SM 2580 B	±1600 mV	Electrode
Turbidity[NA]	SM 2130 B	0.01 NTU	Nephelometric
USEPA Certified Laboratory Analyses:			
Inorganics and Nutrients			
Calcium[B]	EPA-SW: 6010	5000	Inductively Coupled Plasma (ICP)
Magnesium[B]	EPA-SW: 6010	5000	ICP
Sodium[B]	EPA-SW: 6010	5000	ICP
Potassium[B]	EPA-SW: 6010	5000	ICP
Total Manganese[B]	EPA-SW: 6010	15	ICP
Total Iron[B]	EPA-SW: 6010	100	ICP
Chloride[C]	EPA-1: 325.3	1000	Titrimetric
Sulfate[I]	EPA-1: 375.4	2000	Turbidimetric
Sulfide[D]	EPA-1: 376.2	50	Spectrophotometric
Nitrate + Nitrite-N[E]	EPA-1: 353.1	1000	Reduction, Spectrophotometric
Ammonia-N[E]	EPA-1: 350.3	1000	Electrode
Total Phosphorus[B]	EPA-1: 365.2	100	Spectrophotometric
Ortho-Phosphorus[J]	EPA-1: 365.2	200	Spectrophotometric
Bacterial			
Het. Plate Count[F]	SM 9215	1 CFU/mL	Agar Pour Plate
Pollutants			
PAH[G]	EPA-SW: 8310	0.2	GC-MS
BTEX[H]	EPA-SW: 8021	1	GC-MS

*   A = Held at 4°C, analyzed on site within 2 hours, **B** = HNO_3 to pH<2, 4°C for a maximum of 6 months, **C** = 5 mL 1:1 HCl, 4°C for a maximum of 28 days, **D** = zinc acetate + NaOH to pH>9, 4°C for a maximum of 7 days, **E** = H_2SO_4 to pH<2, 4°C for a maximum of 28 days, **F** = 0.008% $Na_2S_2O_3$ in a sterile container, 4°C for a maximum of 24 hours, **G** = 0.008% $Na_2S_2O_3$ + HCl to pH<2, 4°C for a maximum of 14 days, **H** = 4°C for a maximum of 7 Days prior to liquid:liquid extraction, **I** = 4°C for a maximum of 28 days, **J** = 4°C for a maximum of 2 days, **NA** = Not Applicable

†   PQL = Practical Quantitation Limit